
Impacts of climate variability and climate change on renewable power generation

Inaugural-Dissertation

zur

Erlangung des Doktorgrades

der Mathematisch-Naturwissenschaftlichen Fakultät

der Universität zu Köln

vorgelegt von

Jan WOHLAND

aus Duisburg

Köln, 2019

Berichterstatter:

Prof. Dr. Dirk WITTHAUT
Prof. Dr. Andreas SCHADSCHNEIDER
Prof. Dr. David BRAYSHAW

*Vorsitzender der
Prüfungskommission:*

Prof. Dr. Thomas MICHELY

Tag der letzten mündlichen Prüfung: 12.06.2019

“The pessimist complains about the wind; the optimist expects it to change; the realist adjusts the sails.”

William Arthur Ward

“There is an urgent need to stop subsidizing the fossil fuel industry, dramatically reduce wasted energy, and significantly shift our power supplies from oil, coal and natural gas to wind, solar, geothermal, and other renewable energy sources.”

Bill McKibben

UNIVERSITY OF COLOGNE

*Abstract*Faculty of Mathematics and Natural Sciences
Department of Physics

Dr. rer. nat.

Impacts of climate variability and climate change on renewable power generation

by Jan WOHLAND

Anthropogenic climate change represents a major risk for human civilization and its mitigation requires reductions of greenhouse gas emissions. To stay consistent with the long-term temperature targets of international climate policy, global greenhouse gas emissions have to reach zero within a few decades. Such a dramatic transition towards sustainability in all sectors of human activity requires the decarbonization of power generation at an early stage. In absence of other viable technology choices and given the significant cost declines, renewable power generation forms the backbone of the decarbonization. In contrast to thermal power plants, most renewables are not dispatchable but their generation dynamics are governed by the weather.

This dissertation adds to the quantification of impacts of climate variability on wind power generation on different time scales. In particular, it shows that inter-annual wind power generation variability already today has a strong influence on congestion management costs in Germany. Understanding this variability as a normal system feature helps to prevent short-sighted reactions in legislation and power system design. Moreover, it is shown that relevant multi-decadal wind power generation variability exists. Owing to timescales of up to 50 years, these modes are not sufficiently sampled in any modern reanalysis (e.g., MERRA2 or ERA-Interim), which currently cover around 40 years. Consequently, power system assessments based on modern reanalyses may be flawed and should be complemented by multi-decadal assessments. In this context, I also show that 20th century reanalyses (ERA-20C, CERA20C, 20CRv2c) disagree strongly and systematically with respect to long-term wind speed trends. The discrepancy can be traced back to marine wind speed observations which also feature strong upward wind trends that are likely due to an evolving measurement technique. As a consequence, 20th century reanalyses should be employed with care and cross-validation of results is recommended.

Due to their weather dependency, renewables are potentially vulnerable to climate change. Indeed, I show that the benefits of large-scale transmission infrastructure in Europe shrink under strong climate change (RCP8.5). The effect is robust across a five member EUROCORDEX ensemble and can be solidified in a larger CMIP5 ensemble. It is rooted in more homogeneous wind conditions over Europe that lead to less smoothing effects via large scale spatial integration.

Lastly, the debate around negative emission technologies to enlarge the carbon budget currently focuses on land-based approaches such as Bioenergy with Carbon Capture and Storage. Based on a schematic integration of Direct Air Capture (DAC), we show that its flexibility complements renewable generation variability and can help to integrate large shares of renewables.

Zusammenfassung

Menschengemachter Klimawandel stellt ein substantielles Risiko für die menschliche Zivilisation dar und seine Begrenzung erfordert eine Reduktion des Ausstoßes von Treibhausgasen. Um mit den langfristigen Temperaturzielen des Pariser Klimaabkommens konsistent zu bleiben, müssen die globalen Treibhausgasemissionen in den nächsten Jahrzehnten auf Null reduziert werden. Ein solch tiefgreifender Übergang zu mehr Nachhaltigkeit in allen Sektoren menschlicher Aktivität erfordert die Dekarbonisierung des Strombereiches als einen der ersten Schritte. Angesichts mangelnder vielversprechender alternativer Technologieoptionen und aufgrund des starken Rückgangs der Kosten stellen erneuerbare Energien das Rückgrat dieser Dekarbonisierung dar. Im Gegensatz zu den meisten konventionellen Kraftwerken, sind Erneuerbare allerdings nicht direkt steuerbar. Stattdessen wird die Dynamik erneuerbarer Energieerzeugung vom Wetter diktiert.

Diese Dissertation trägt zur Quantifizierung von Einflüssen von Klimavariabilität auf Windenergieerzeugung bei und berücksichtigt dabei unterschiedliche Zeitskalen. Insbesondere zeigt sie auf, dass interannuale Variabilität von Windenergieerzeugung bereits heute einen starken Einfluss auf die Kosten von Engpassmanagement hat. Diese Variabilität als eine normale Eigenschaft des Systems zu verstehen hilft dabei kurzsichtige Reaktionen im Bereich der Gesetzgebung und dem Design des Stromsystems zu verhindern. Darüber hinaus wird gezeigt, dass es relevante multi-dekadische Windenergieerzeugungsvariabilität gibt. Da diese Moden Zeitskalen von bis zu 50 Jahren aufweisen sind sie in allen modernen Reanalysen (z.B. MERRA-2 oder ERA-interim) nicht ausreichend abgebildet, da moderne Reanalysen nur etwa die letzten 40 Jahre umfassen. Daraus folgt, dass Stromsystemanalysen, die auf modernen Reanalysen basieren, fehlerbehaftet sein können und mit multi-dekadischen Analysen ergänzt werden sollten. In diesem Zusammenhang zeige ich außerdem, dass Reanalysen des 20. Jahrhunderts (ERA20C, CERA20C, 20CRv2c) sich hinsichtlich langfristiger Windtrends deutlich und systematisch widersprechen. Der Widerspruch kann auf marine Windbeobachtungen, die ihrerseits bereits deutliche Aufwärtstrends beinhalten, zurückgeführt werden. Der Grund für die Trends ist wahrscheinlich eine sich entwickelnde Messtechnik, insbesondere eine systematische Verschiebung der Höhe der Messung. Es folgt, dass Reanalysen des 20. Jahrhunderts vorsichtig verwendet werden sollten und dass eine Validierung der Ergebnisse durch Vergleich mehrerer Datenquellen zu empfehlen ist.

Aufgrund ihrer Wetterabhängigkeit sind Erneuerbare potentiell gefährdet durch den Klimawandel. In der Tat zeigen wir, dass die Vorteile eines großskaligen Stromnetzes unter starkem Klimawandel (RCP8.5) reduziert werden. Der Effekt ist robust innerhalb eines EUROCORDEX Ensembles mit fünf Mitgliedern und kann weiter untermauert werden in einem größeren CMIP5 Ensemble. Der Effekt hat seinen Ursprung in gleichmäßigeren Windbedingungen über Europa, die weniger ausgleichende Effekte durch großskalige räumliche Integration ermöglichen.

Als letzter Themenbereich wird die Debatte um negative Emissionen aufgegriffen, die benötigt werden um das geringe verbleibende CO₂ Budget zu vergrößern. Diese Debatte konzentriert sich zum Großteil auf Bioenergie mit CO₂ Abscheidung und Speicherung. Wir zeigen mittels eines schematischen Ansatzes zur Integration von CO₂ Abscheidung aus der Luft (DAC), dass die Flexibilität von DAC und die Variabilität von Erneuerbaren sich ergänzen, sodass DAC helfen könnte große Anteile von Erneuerbaren in das Stromsystem zu integrieren.

Acknowledgements

This thesis would not have been possible without the continued support of many people. On the professional side, I want to thank JProf. Dr. Dirk Witthaut for countless valuable discussions, his general optimism and his willingness to interpret stupid regulations loosely. In the early phases of the thesis, Dr. Mark Reyers provided much support as did Prof. Dr. Noel Keenlyside and Dr. Nour-Eddine Omrani in the later parts. I also want to thank Noel for hosting me as a visiting PhD student at the Geophysical Institute in Bergen. I thank the Hitec Graduate School at Forschungszentrum Jülich, namely Marianne Feldmann and Maurice Nuys, for funding this visit. I owe gratitude to Dr. Carl-Friedrich Schleussner for a refreshing cooperation and Prof. Dr. Martin Greiner for feedback and support. Many thanks also go to my fellow PhD students for shared coffee breaks and laughs!

Even though not directly involved in the science, this thesis would have failed without loving support from Alicja. Thank you for sharing the ups and downs and supporting me in any phase!

On a similar note, I wouldn't have been able to write this dissertation without help from my parents Hans and Monika. In addition to their obvious contribution to my physical existence, they supported me during all steps that preceded this text and encouraged me to follow my own path. It goes without saying that the latter part also applies to my sister Anne who just never gives up.

Thank you all.

Contents

Abstract	vii
Zusammenfassung	ix
Acknowledgements	xi
Acronyms	xiv
1 Introduction	1
1.1 Climate change	1
1.1.1 Observed climate change	1
1.1.2 Future climate change	2
1.1.3 Safe climate change	3
The Paris Agreement and its carbon budgets	4
1.2 Climate variability	4
1.3 Tools and Datasets for climate assessment	5
1.3.1 Climate Models	5
Scenarios of atmospheric composition	6
1.3.2 Reanalyses	7
1.4 Energy transitions	7
1.4.1 Renewable power generation	8
1.5 Overview of the publications and their research questions	10
2 Methods	13
2.1 Spectral leakage in finite length time series	13
2.2 Multi-taper spectral analysis	14
2.2.1 Significance testing	15
3 Publications	17
3.1 Climate change	17
3.1.1 #1: Impacts on spatial balancing of wind power generation	17
Supplement	32
3.2 Inter-annual climate variability	43
3.2.1 #2: The impact of inter-annual wind variability on current German congestion management	43
Supplement	65
3.3 Multi-decadal climate variability	68
3.3.1 #3: Spurious long-term trends	68
Supplement	79
3.3.2 #4: Multi-decadal wind generation variability	84
3.4 Negative emissions	106
3.4.1 #5: Direct Air Capture	106
Supplement	112

4	Common discussion	125
4.1	The need for climate information in energy assessments	125
4.1.1	Uncertainties of climate data sources	126
4.1.2	Suitable metrics depend on context	127
4.1.3	The relative importance of forced changes versus multi-decadal climate variability for wind energy	128
4.2	Beyond wind	128
4.3	Multi-disciplinary approaches	129
4.4	Generation variability and the likely need for negative emissions . . .	129
4.5	New literature	130
4.5.1	Climate change impacts on the power system	130
	Karnauskas, Lundquist, and Zhang (2018)	130
	Schlott et al. (2018)	131
	Peter (2019)	132
	Jerez et al. (2019)	132
	Tobin et al. (2018)	133
	Behrens et al. (2017)	133
	Kozarcanin, Liu, and Andresen (2018)	134
4.5.2	Redispatch	134
4.5.3	DAC	136
4.5.4	Multi-decadal aspects	136
4.6	Conclusion	137
	Bibliography	139
A	Appendix	147
A.1	Own contribution	147
A.2	Erklärung (gemäß §4 Abs 1 Punkt 9 der Promotionsordnung)	148

Acronyms

20CR	NOAA's 20th century reanalysis
BECCS	Bio-energy with Carbon Capture and Storage
CERA20C	ECMWF's coupled atmosphere and ocean reanalysis of the 20th century
CMIP5	Climate Model Intercomparison Project Phase 5
CO ₂	Carbon Dioxide
COP	Conference of the Parties
CSP	Concentrating Solar Power
DAC	Direct Air Capture
DSO	Distribution System Operator
ECMWF	European Centre for Medium-Range Weather Forecasts
ERA20C	ECMWF's atmospheric reanalysis of the 20th century
ERA20CM	ECMWF's free model run of the 20th century
EUROCORDEX	Coordinated Downscaling Experiment - European Domain
GCM	General Circulation Model or Global Climate Model
GHG	Greenhouse Gas
IPCC	Intergovernmental Panel on Climate Change
MTM	Multi-Taper Method
NAO	North Atlantic Oscillation
NOAA	National Oceanic and Atmospheric Administration (USA)
PV	Photovoltaics
RCM	Regional Circulation Model or Regional Climate Model
RCP	Representative Concentration Pathway
ROC	Receiver-Operator Characteristics
TSO	Transmission System Operator
UNFCCC	United Nations Framework Convention on Climate Change

Chapter 1

Introduction

This dissertation touches two of the central challenges of the early 21st century: climate change and renewable energy. It also discusses the sometimes overlooked aspect of climate variability which deserves equal attention. It aims to shed light on their interactions in both expected and surprising ways using methods from time series analysis and statistics. Prior to the discussion of the research results, a few fundamentals are reviewed in the next sections to familiarize the reader with the relevant concepts in a straightforward manner. I start with a brief discussion of climate change, which is both one of the main reasons for the increased deployment of renewables and also a potential thread to highly renewable power systems. After a short review of climate variability which governs the dynamics of renewable power generation, I introduce the main tools and datasets that are used in the research section of this dissertation. The following subsection on energy transitions covers main aspects of renewable power generation and focuses on emissions and the property of dispatchability. The Introduction ends with an overview of the publications presented in this thesis. It is complemented by a Methods section that introduces an advanced spectral analysis tool that could only be briefly described in the corresponding publication.

1.1 Climate change

Human activity since the onset of industrialization has added substantial amounts of carbon dioxide (CO₂) and other greenhouse gases (GHGs) to the atmosphere as a byproduct of economic development. Current levels of atmospheric CO₂ exceed 400 parts per million (ppm), representing a 40% increase from a pre-industrial level of around 280 ppm. The current level of CO₂ in the atmosphere is unprecedented at least in the last 800 000 years (IPCC, 2013). This perturbation of atmospheric composition leads to an increased amount of longwave outgoing radiation that does not make its way to outer space but is absorbed and then partly re-emitted back towards the earth surface. This is commonly referred to as the greenhouse effect. The increase of atmospheric concentrations of GHGs induces a thermal disequilibrium of the planet which currently absorbs more energy than it emits. As compared to pre-industrial levels, global mean temperature has consequently risen by approximately 1 °C with a current rate of change of around 0.2°C per decade (IPCC, 2018).

1.1.1 Observed climate change

The responses to the thermal disequilibrium are not restricted to higher temperatures. Instead, they are many-fold and many of them pose a risk to human civilization and are therefore reasons for concern. The climate system consists of complex and interconnected components such as the atmosphere, the oceans, the cryosphere

(ice) and the biosphere. In many of these subsystems, impacts of anthropogenic climate change can already be detected today.

For example, global mean sea-level has risen by around 20cm over the 20th century mostly as a consequence of thermal expansion and shrinking glaciers (IPCC, 2013)¹. Other contributions come from mass losses of the Antarctic and Greenland ice sheet and land water storage. The rates of ice loss from Antarctica and Greenland have both increased from 1992-2001 to 2002-2011. Moreover, there has been an increasing number of extreme weather and climate events, such as more frequent warm days and nights, an increased frequency of heat waves in Europe, Asia and Australia and an increased area that is effected by heavy precipitation events. Even though individual extreme events can not be directly attributed to climate change for methodological reasons, their increased likelihood due to climate change can be documented in some cases (e.g., Wergen and Krug, 2010; Coumou and Rahmstorf, 2012; Wergen, Hense, and Krug, 2014). Parts of the emitted CO₂ are dissolved in the ocean, leading to ocean acidification and putting some marine habitats such as reefs at risk (Hoegh-Guldberg et al., 2007). Moreover, the climate systems features some self-amplifying feedbacks that can lead to tipping point behaviour. Once a system is perturbed sufficiently strongly (i.e., beyond its tipping point), it does not return to its initial state but transitions to another state following its internal dynamics. The transition to the new state may be accompanied by unusually high rates of change and it can feature hysteresis or irreversibility. Some of these tipping points may have already been crossed, as, for example, indicated by a weakening of the thermohaline circulation in the North Atlantic (Rahmstorf et al., 2015; Caesar et al., 2018) or a potentially triggered Marine Ice Sheet Instability in West Antarctica (Favier et al., 2014). Note that there is an ongoing debate about the stability of the thermohaline circulation in the North Atlantic. In a modeling study that was based on a large CMIP5 ensemble, Weaver et al. (2012) found a consistent reduction of the circulation strength but no evidence of a complete shutdown. A complete shutdown, as seen earlier in simpler models, might be prevented by stabilizing feedbacks between atmosphere and ocean processes that were not properly captured before (Buckley and Marshall, 2016). However, there is also concern that the current generation of climate models does not represent ocean freshwater transports correctly which could lead to an overestimation of stability. The question of whether or not the real circulation could feature tipping point behaviour thus remains an open one (Buckley and Marshall, 2016).

1.1.2 Future climate change

While some impacts of climate change can already be detected today, the bulk of it will occur in the future owing to the inertia of the climate system. The number one determinant of future climate change is the future evolution of GHG emissions and the resulting concentrations in the atmosphere. There is a large body of literature that investigates climate impacts under different GHG scenarios and the latest (and the upcoming) report of the Intergovernmental Panel of Climate Change (IPCC) is an excellent source to access this information (IPCC, 2013). This section does not aim to deliver a holistic overview of climate impacts. Instead, a few sea-level related examples are given in the following that shall illustrate the potential scale of climate impacts in the long run.

Even if global mean temperature was kept at its current value, roughly 1% of global land area will be below sea-level in 2000 years (Marzeion and Levermann,

¹the entire paragraph is based on this source unless another source is explicitly given

2014). While settlements may be easily relocated on this time scale, also 6% of world heritage sites will be effected. Moving them will prove more complicated. The numbers increase if higher levels of warming are assumed. In a 3°C warmer world, for example, 25-36 countries will lose more than 10% of their territory and some of them will see more than half of their land below sea level. Even in scenarios that are compatible with the long-term temperature goals of the Paris Agreement (see Sec. 1.1.3), sea-level rise in 2300 is expected to be at the order of one meter (Mengel et al., 2018). Critical infrastructure that is deliberately installed next to the coasts, such as some power plants, is particularly prone to sea-level related risks (Bierkandt, Auffhammer, and Levermann, 2015).

It has been mentioned earlier that parts of the West Antarctic Ice Sheet may have already entered a process called the Marine Ice Sheet Instability. This process requires a specific topography of the bedrock that the ice sheet rests upon. If looking upstream (i.e., towards the center of the ice sheet), the bedrock needs to slope downwards over some area. It has been shown that the destabilization of a part of the West Antarctic Ice Sheet is sufficient to trigger a process that culminates into its complete collapse (Feldmann and Levermann, 2015). This would lock in irreversible sea-level rise of around 3m in the next millenia. The same process could unfold in parts of East Antarctica, which has long been thought to be significantly more stable. If an ice volume that is equivalent to around 0.008m sea-level rise is melted via external forcing, ice dynamics can induce the discharge of ice equivalent of 3-4m sea-level rise (Mengel and Levermann, 2014). Sea-level rise in these orders of magnitude would require a fundamental reorganisation of infrastructures as many humans live next to the coasts.

Still more disastrous consequences are found if mankind was to use all fossil fuel resources that are currently considered available. The resulting forcing would trigger destabilization of the entire Antarctic ice sheet, ultimately releasing almost all of the ice that currently rests on the Antarctic continent (Winkelmann et al., 2015). The multi-millenia sea-level response would exceed 50m and the rate of change in the first millennium would exceed 3m per century.

1.1.3 Safe climate change

In light of potentially disastrous impacts of unmitigated climate change, the United Nations Framework Convention of Climate Change (UNFCCC) was founded in 1992. It's "ultimate objective (...) is to achieve (...) stabilization of greenhouse gas concentrations in the atmosphere at a level that would prevent dangerous anthropogenic interference with the climate system" (UNFCCC, 1992). This sentence implicitly assumes that there is a threshold separating non-dangerous and dangerous interference with the climate system. What is this threshold? At which point does climate change end being safe?

It is important to understand that the threshold can not be determined by science alone because it depends on moral judgments. Whether or not a certain impact of climate change is acceptable has to be answered outside the world of science. However, science can contribute to the debate by differentiating the expected climate impacts at distinct levels of climate change. While the literature has focused on separating impacts in a 2°C to 5°C warmer world in the earlier phase of this century (e.g., Bank, 2012; IPCC, 2013), the emphasis has shifted to compare impacts between 1.5°C and 2°C (e.g., Schleussner et al., 2016a; James et al., 2017; IPCC, 2018). This shift is rooted in a large consensus that climate change beyond 2°C can not be considered safe.

The Paris Agreement and its carbon budgets

At the end of the 21st UNFCCC Conference of the Parties (COP), a multi-lateral climate change mitigation agreement was adopted (UNFCCC, 2015). Named after the hosting city, the Paris Agreement contains ambitious goals for climate change mitigation and, at least in some sense, defines the threshold for dangerous interference. In the second half of the 21st century, it aims for "a balance between anthropogenic emissions by sources and removals by sinks" of GHG. This implies a net GHG neutral world economy within a few decades and constitutes a tremendous challenge. Regarding the long-term temperature goal, a compromise was found between countries that strongly argued in favour of limiting global warming to 1.5 °C and those that wanted to stick to the more conservative 2 °C target. The agreement contains both targets ("Holding the increase in the global average temperature to well below 2°C above pre-industrial levels and pursuing efforts to limit the temperature increase to 1.5 °C above pre-industrial levels") and calls for a special report of the IPCC on global warming of 1.5°C that was published in late 2018. The choice of the long-term temperature goal was welcomed by members of the scientific community (Schellnhuber, Rahmstorf, and Winkelmann, 2016).

An intuitive concept to illustrate the challenges in achieving the Paris Agreement's goals is a carbon budget (Messner et al., 2010). It relies on the assumption that climate impacts are determined by cumulative GHG emissions, irrespective of the actual timing of emissions. This assumption has been shown to be a justified simplification in many cases (Zickfeld et al., 2009) although it obviously collapses if irreversible processes are triggered. A carbon budget $B(T)$ is an amount of carbon B that leads to exceedance of a temperature limit T if emitted into the atmosphere (T is the global mean temperature averaged over a long time span of two or three decades such that natural temperature variability can be neglected). After the budget is depleted, net carbon emissions of all sectors need to equal zero. According to the IPCC Special Report on 1.5°C (IPCC, 2018), this budget is 550 GtCO₂ for a two-thirds chance to limit warming to 1.5°C. The budget estimate has a large uncertainty range of approximately ± 250 GtCO₂ dependent on non-CO₂ GHG mitigation and potentially -100 GtCO₂ to account for permafrost thawing and potential methane release plus another $\pm 50\%$ owing to a additional geophysical uncertainty due to non-CO₂ response. More details of the uncertainties of climate budgets are provided in Millar et al. (2017). This budget compares to current rates of carbon emissions of $\dot{B} \approx 35$ GtCO₂/y (Rogelj et al., 2015). If emissions remain constant, the entire budget of staying below 1.5 °C with a 66% chance will thus be used in the 2030s. The budget is larger for the less ambitious 2 ° goal which translates into more time until it is finally used up.

The small size of these budgets calls for fast and fundamental changes of all sectors that emit carbon (Rockstroem et al., 2017) which includes, but is not limited to, the energy sector (Rogelj et al., 2015). Current levels of ambitions are not sufficient to reach the targets of the Paris Agreement (Schleussner et al., 2016b; Rogelj et al., 2016).

1.2 Climate variability

Climate variability is often also referred to as natural or internal variability. It describes the dynamics of the climate system that would lead to climatic variations even in the absence of anthropogenic forcing. There are many different modes of climate variability with different temporal and spatial scales (e.g., Williams et al.,

2017). Some modes are very slow and effect the entire planet such as the variations in orbital parameters that have led to glaciation events in the past with periods of approximately 23, 41 and 100 thousand years (Imbrie et al., 1992). They can be safely ignored for the purpose of this thesis. However, some dominant modes of climate variability feature multi-decadal variability that stems from interactions of the troposphere with the ocean and the stratosphere (Keenlyside et al., 2015; Omrani et al., 2016). We will see in publication #4 that multi-decadal variability is important for wind power generation (Sec. 3.3.2). Some components of the climate system feature variability on short timescales that is restricted to small spatial areas such as wind gusts. Synoptic variability on timescales of a few days is one of the most important modes for the integration of renewables as passing weather systems can lead to fundamentally different generation characteristics. The long-term evolution of synoptic variability is thus highly relevant for power system design.

Climate variability generally prohibits the attribution of individual events to climate change and complicates the attribution of trends that are observed or modeled over relatively short timespans. One reason is that low-frequency climate variability (i.e. multi-decadal, centennial and beyond) can produce signals that feature statistically highly significant trends over timespans that are substantially shorter than their period. For example, if the available timeseries only samples parts of the natural variability, trends may be found in a period with an upward or downward tendency. Such trends are not representative for the entire process but only capture the dynamics over a short period. They can not be safely generalized.

There is a direct link between climate variability and renewable power generation because renewables depend on the weather. Wind parks remain idle without wind and solar panels require sunshine. The dependence of wind power generation on wind speeds is even non-linear, highlighting the importance of understanding wind speed dynamics to quantify wind power generation.

1.3 Tools and Datasets for climate assessment

1.3.1 Climate Models

The assessment of future climate requires numerical models and scenario assumptions regarding GHG concentrations. To this end, different Global Climate Models (GCMs) have been developed in climate modelling groups. They typically contain the most important climate subsystems and solve the underlying differential equations in discretized space and time. Their global coverage comes with the advantages that boundary effects are of minimum importance but also limits the obtainable resolution. For example, the GCM results from the Climate Modeling Intercomparison Phase 5 (CMIP5) that informed parts of the research reported in this study (see Sec. 3.1.1), have a typical resolution of around 1° , which is at the order of 100km (Taylor, Stouffer, and Meehl, 2011).

If higher resolution is needed, as it is the case for local assessments, Regional Climate Models (RCMs) can be used to downscale the GCM results (e.g., Giorgi and Gutowski, 2015). A RCM is a climate model with a limited spatial domain (e.g., Europe) but significantly higher spatial resolution. Per design, a RCM always needs boundary data such as heat and mass fluxes which are typically provided by a GCM. The combination of a driving GCM and a nested RCM is often referred to as a modeling chain and comes with some methodological weaknesses because uncertainties can propagate through the different steps of the chain.

Meaningful regional climate change assessments thus have to rely on ensembles of RCM-GCM combinations which allow to investigate the robustness of changes across models. An ensemble of different RCM-GCM combinations at high resolution is provided by the EUROCORDEX initiative (Jacob et al., 2014) and is used in our analysis (Sec. 3.1.1). Agreement of multiple models is considered indicative of the robustness of a result. Ideally, many GCMs should be used to drive many RCMs such that the effects of both modeling steps can be studied. This particularly includes an ensemble assessment of the GCM data which serves as an input to the RCMs. However, as climate models rely on high performance computers that are costly, sometimes compromises have to be made. For example, in our analysis of the effectiveness of European transmission infrastructure under strong climate change, we had to rely on a 5 member GCM-RCM ensemble in which the same RCM was used in all cases because a larger set was simply not available.

Alternative approaches to derive higher resolution data also exist. Main approaches are empirical-statistical downscaling (e.g., Hewitson et al., 2014) and statistical-dynamical downscaling (e.g., Reyers, Pinto, and Moemken, 2015). Both rely on the assumption that a relevant share of local-scale variability can be explained as a function of large-scale variability. In empirical-statistical downscaling, the mapping from large scale to local scale is established statistically. In statistical-dynamical downscaling, the mapping is calculated by running a RCM for a small set of typical configurations. Both methods allow for a computationally cheap downscaling of large datasets (e.g., GCM ensembles). In some cases, they are well suited to complement GCM-RCM modeling chains or to replace the usage of RCMs if computational costs are prohibitive. Both methods, however, may face serious methodological issues if the mapping is not stationary and/or if interannual to multi-decadal variability is not properly accounted for (Hewitson et al., 2014).

Scenarios of atmospheric composition

Human behaviour is not modeled in GCMs. This means that the addition of greenhouse gases to the atmosphere via combustion of fossil fuels is not captured by the climate models but has to be provided exogenously. This is done in the form of scenarios and the most recent set of those are called representative concentration pathways (RCPs) (Vuuren et al., 2011). To be precise, RCPs prescribe the evolution of greenhouse gases in the atmosphere rather than the fluxes of greenhouse gases into the atmosphere. This approach has been taken to enhance comparability in GCM ensembles. Owing to different parameterizations, for example, of the carbon cycle, the same amount of GHGs emitted into the atmosphere leads to different GHG concentrations and thus different radiative forcing in different GCMs.

In this thesis, the business as usual RCP8.5 scenario is investigated. It assumes no mitigation efforts and has been chosen to test the vulnerability of transmission infrastructure to climate change because it is a worst case scenario. The name stems from the amount of additional radiative forcing through increased levels of greenhouse gas concentrations which equals 8.5 W/m^2 in 2100 (Riahi et al., 2011). RCP8.5 causes a global mean temperature increase of around 3.6°C to 5.8°C in 2100 as compared to pre-industrial levels (IPCC, 2013). In studies other than sensitivity studies, scenario uncertainty is one of the major sources of uncertainty of climate projections in particular in the long run. For example, climate change impacts under the RCP2.6 scenario would be significantly different from those under RCP8.5 and nobody can forecast with certainty which emission trajectory will become reality. RCP2.6 includes climate change mitigation and is likely in line with the 2°C target. Other

sources of uncertainty are model uncertainty (e.g., the choice of parameterizations and numerical schemes) and internal variability (Hawkins and Sutton, 2009). A reduction of model uncertainty can be obtained through large ensembles of different models as explained in Sec. 1.3.1.

1.3.2 Reanalyses

Climate information is needed in many applications. In addition to future scenarios that are computed using climate models, data about the past is often needed. Such data can be obtained directly from observations. For example, the German Weather Service (DWD) operates a network of stations that measure climate variables. Similar services exist in most countries and the resulting station time series are typically readily available, for example, via web portals (Hewitson et al., 2017). However, the interpretation of station data is complicated. Among other reasons, this is due to the irregular sampling of stations in space, small-scale effects in the immediate vicinity of the stations, interruptions of operation, measurement errors and instrumental drifts. In many cases, reanalyses are a more suitable source of information than observations are.

Reanalysis datasets are a mixture of observations and modeling outputs. They provide gridded data that is internally consistent (i.e., respects fundamental laws of physics such as the conservation of mass) and that has minimum deviation from the observations. In contrast to observations, reanalyses typically have global coverage and are provided on a regular grid. They thus come in a format that allows for easy usage in many applications. They are particularly useful if observations are not available, sparse and/or available only over a short time period. Reanalyses are retrospective by design because they need observations as input. The reanalyses used in this thesis cover approximately the last 40 years (modern reanalyses) or the last 110 to 150 years (20th century reanalyses). The names of the reanalyses and their respective benefits and shortfalls are extensively discussed in Sec 3.

There are three important and fundamental differences between reanalyses and climate models that are relevant in the context of this thesis. First, climate models are generally not synchronized while reanalyses are. This means that it can not be expected that two different GCMs are in phase with respect to any mode of climate variability. In other words, there is no reason to assume that, for example, wind speeds in any location at any particular date are the same in two different GCMs. The situation is different for reanalyses because the assimilated observations are synchronized (or even identical). Consequently, the wind speeds at any given date in reanalysis 1 can be meaningfully compared to those in reanalyses 2. Second, reanalyses are generally more realistic because they are coupled to the real world through the assimilation of observations. This is particularly important if relevant processes are not captured in the models due to, for example, insufficient resolution or missing components such as the stratosphere. Third, the maximum timespan that can be covered by reanalyses is limited by the available observations while GCMs can be run for infinite periods (given infinite computational resources).

1.4 Energy transitions

As noted earlier, delivering on the Paris Agreement and avoiding dangerous climate change requires a zero emission world economy in a few decades. However, the evolution of global CO₂ emissions over the last decades points upwards rather than

downwards. For example, the global emissions from electricity and heat generation have risen from around 8 GtCO₂ in 1990 to almost 14 GtCO₂ in 2015 (IEA, 2017a). After global emissions had plateaued between 2014 and 2016, they increased by 1.6% (2%) in 2017 (2018) (Figueres et al., 2018). In other words, the peak of global emission still has not been reached.

In 2015, the largest fraction of CO₂ emissions originated from the generation of electricity and heat (42%) followed by the transport sector (24%) and industry (19%) (IEA, 2017a). These numbers illustrate that the decarbonization of power generation is not sufficient. Instead, emissions have to fall to zero in all sectors or remaining carbon emissions have to be offset by negative emission technologies. The prospects of one particular negative emission technology are discussed in Sec. 3.4.1.

Even though the transition to a fully renewable power system is not enough, it is a logical starting point. This is because renewable generation technologies (a) are available at scale (Brown et al., 2018a), (b) have minimum lifecycle GHG emissions (Pehl et al., 2017), and (c) electricity can be used to substitute fuels in transport and industry (Welder et al., 2018). Moreover, onshore wind and solar photovoltaics are least cost options for power generation already today (IEA and IRENA, 2017). Onshore wind even outperforms all other available types of generation in some locations in terms of levelized costs of electricity. Further cost reductions are anticipated (Creutzig et al., 2017). Technical renewable potentials are also significantly higher than current primary energy and electricity demand. Wind power alone could provide enough electricity to meet the global demand for electricity and the potential of solar power is even large enough to support multiples of the world's current primary energy demand (IPCC, 2014).

1.4.1 Renewable power generation

Renewable power generation means the utilization of self-replenishing resources to generate electricity. It includes these technologies: solar photovoltaics (PV), concentrating solar power (CSP), wind power, hydropower, bioenergy and a few others that only play niche roles (IEA, 2017b). Renewables are in contrast to conventional power generation that is based on burning fuels (e.g., coal, gas, oil, waste) or nuclear fission. Nuclear fusion will not become available in time to relevantly contribute to the initial decarbonization of power systems. Even the most optimistic scenarios reported by pro-fusion groups argue that "fusion can start market penetration around 2050 with up to 30% of electricity production by 2100" (EFD, 2012). Given that fundamental questions of reactor design are still not answered, these estimates are to be taken as highly speculative. However, even if fusion technology was available to be deployed at scale in 2050, it would have to be incorporated into a highly renewable system. This would require nuclear fusion to be operated flexibly, adding another massive design challenge. On top of this, the economic case for nuclear fusions remains unclear.

All types of power generation can be classified as either dispatchable or non-dispatchable. Wind and PV are non-dispatchable meaning that they can not be switched on when needed. Instead power generation from wind and PV is intermittent as it follows the weather. Conventional power generation is generally dispatchable although there are ramping constraints that need to be respected. CSP and hydropower are situated in between. While CSP generally is non-dispatchable, the addition of thermal storage can make it dispatchable on timescales of up to a few days (Pfenninger et al., 2014). Pumped hydropower is dispatchable as long

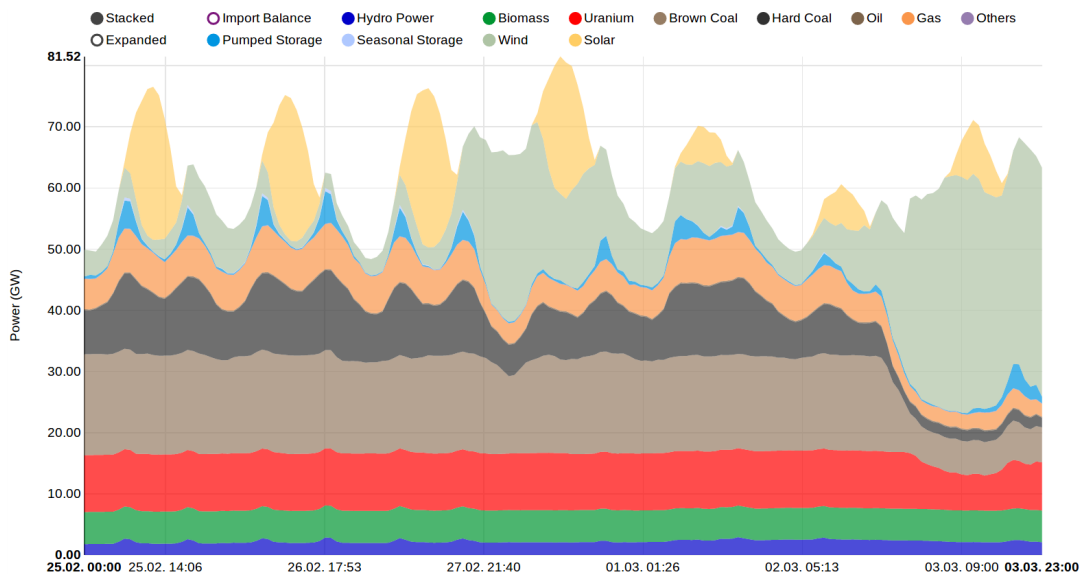


FIGURE 1.1: Power generation in Germany in one example week in early 2019. Different colors denote different generator technologies as defined in the legend. The illustration is taken from [energy-charts.de](#) on 26/03/2019 with kind permission from Bruno Burger (Fraunhofer ISE).

as constraints on its filling level are respected whereas run-off-river hydropower is generally non-dispatchable.

The German power generation during one example week in early 2019 is illustrated in Fig. 1.1. It displays different types of power generators and their variability. Solar photovoltaics only generates electricity during daytime. While it contributes relevantly on the first four days as can be seen from the first four peaks, the contribution on the remaining days is small. The pattern of wind generation is different and partly complementary. Wind plays a minor role until the evening of the third day when wind power generation strongly increases. Following a period of medium contribution, feed-in from wind power is dominant over the last day. Hydropower plays a minor role. Of the dispatchable generators, brown coal, uranium and biomass are operated in baseload mode (i.e., constantly) for almost the entire week. Hard coal and gas are used flexibly to respond to changes in wind and solar generation.

The non-dispatchability of wind and PV constitutes the main challenge of building highly to fully renewable power systems because a stable and reliable power supply is considered a necessity in many parts of the world. While it requires new thinking and new infrastructures, there is evidence that this challenge can be solved. The main strategies to integrate high shares of renewables are well understood. They all share the idea of optimizing the energy system in light of renewable generation variability and thus require accurate representations of climate variability. The main strategies are:

1. Averaging over large areas using transmission infrastructure (e.g., Rodriguez et al., 2014; Rodriguez, Becker, and Greiner, 2015; Rodriguez, 2014; Andresen et al., 2012; Becker et al., 2014; Schlachtberger et al., 2017; Santos-Alamillos et al., 2017; Grams et al., 2017)

2. Averaging over time using storage infrastructure (e.g., Beaudin et al., 2010; Díaz-González et al., 2012; Toledo, Oliveira Filho, and Diniz, 2010; Kittner, Lill, and Kammen, 2017; Pleßmann et al., 2014; Luo et al., 2015; Reuß et al., 2017)
3. Increased flexibility on the demand side and combination of different sectors, such as heat and electricity (e.g., Brown et al., 2018b; Huber, Dimkova, and Hamacher, 2014; Kondziella and Bruckner, 2016)

Flexible conventional power generation from backup infrastructure will be needed during the transition. In fact, Schlach Berger et al. (2016) argue that even relatively inflexible generators can contribute beneficially in the early steps towards fully renewable systems.

1.5 Overview of the publications and their research questions

All publications in Sec. 3 contribute to the research field outlined above. They all use climate information to quantitatively assess energy related questions and make use of time series analysis and statistics. The focus is always on wind energy even though system wide effects are also studied in some cases.

In publication #1 (Wohland et al., 2017), we investigate the impact of climate change on the smoothing effects of a continental transmission system in Europe. As explained in Sec. 1.4.1, large scale transmission infrastructure smooths the generation timeseries. This is because large areas are rarely affected by the same weather pattern simultaneously. Instead, below average wind generation in some countries often coincides with above average generation in others. In the paper, we address whether the benefits of large scale transmission are affected by strong climate change. We show that the effectiveness of transmission is robustly compromised under strong climate change at the end of the 21st century. The effect is rooted in more homogeneous wind conditions that imply higher synchrony of over generation and generation shortfalls across Europe. Albeit robust, the effect has a maximum amplitude of around 7% and is thus small enough not to prohibit highly renewable power system even under strong climate change.

Publication #2 (Wohland et al., 2018) addresses congestion management and associated costs in the German electricity system. Due to transmission line constraints and a spatial mismatch of power generation and consumption, regulatory interventions to secure stable supply are sometimes needed. We focus on a measure called redispatch that has been used more extensively over the last years. Redispatch comes with annual costs at the order of a few hundred million Euros per year and is regularly discussed in the media. We contextualize an unexpected cost drop from 2015 to 2016 by comparison with expected inter-annual variability. The results highlight the importance of a proper inclusion of natural wind variability into energy policy and energy system design.

Publications #3 and #4 (Wohland et al., 2019a; Wohland et al., 2019b) both deal with multi-decadal wind assessments. They are based on 20th century reanalyses and aim to quantify whether any important modes of wind variability are missed in modern reanalysis. Owing to the methodological differences in approaches of the two providing centers of 20th century reanalyses, massive discrepancies in wind speed trends are reported in publication #3. Very strong upward trends are found over a large fraction of the planet in one family of reanalyses. We can trace back the

discrepancy to the assimilated wind speeds in the reanalyses that are provided by the European Centre for Medium-Range Weather Forecasts (ECMWF). Furthermore, based on a comparison with the literature and due to known issues with marine wind observations, we conclude that the upward trends in one family of datasets is likely spurious. After subtraction of the trends, agreement between the dataset is good as shown in publication #4. The corrected datasets feature significant multi-decadal modes of wind power generation averaged over the typical lifetime of a wind park. In particular, the ratio of winter to summer generation varies strongly ($\pm 15\%$) which has direct implications for optimum technology choices.

In the last publication #5 (Wohland, Witthaut, and Schleussner, 2018), we focus on a negative emission technology called direct air capture (DAC). Almost all scenarios that are compatible with the Paris Agreement require negative emissions to compensate exceedence of the carbon budget. In many models, negative emissions are reached via Bio-energy with Carbon Capture and Storage (BECCS), even though BECCS raises sustainability concerns owing to its large water and land footprint and resource competition with food production. We argue that DAC is a promising candidate for negative emissions because it can be used flexibly and therefore complements renewable generation variability. We run a simple European power model to illustrate potentials of DAC for negative emissions and discuss co-benefits of storage and DAC.

During my PhD I also contributed to Weber et al. (2018) which is not discussed here. Moreover, another publication that I contributed to was accepted and published during the course of my PhD (Hewitson et al., 2017).

Chapter 2

Methods

The objective of this thesis is to distill robust information about impacts of climate variability and climate change on renewable power generation with a focus on wind energy. To this end, I use methods from time series analysis, statistics and uncertainty estimation based on cross-validation of suitable datasets. In general, all methods are introduced and discussed in the respective publication. They will not be repeated here for the sake of brevity. However, as the format of article #4 (Sec. 3.3.2) did not allow to introduce the multi-taper method (MTM) in sufficient detail, additional information about MTM is given below. It starts with an introduction of spectral leakage which provides the motivation to use MTM.

2.1 Spectral leakage in finite length time series

In this section, we consider a univariate and discrete time series $X(t)$ of finite length $t = 1, \dots, N$ and time steps ΔT . Often, the underlying dynamics of the timeseries are unknown (or too complex to be solved exactly). In such cases, a standard tool to investigate the properties of the time series is spectral analysis. Its easiest form is a discrete Fourier transform which is defined as

$$F\{X\}(\omega) = \sum_{t=-\infty}^{\infty} X(t)e^{-i2\pi\omega t}, \quad (2.1)$$

where ω is referred to as frequency (e.g., Storch and Zwiers, 1999).

As a trivial example, we know that the Fourier transform of a sinusoid

$$X_{\text{example}}(t) = \cos(2\pi\omega_{\text{example}}t), \quad (2.2)$$

defined over an infinite period ($t = -\infty, \dots, \infty$), has a single peak at frequency ω_{example} :

$$F\{X_{\text{example}}\} = \delta(\omega - \omega_{\text{example}}). \quad (2.3)$$

In real applications, however, time series are never of infinite length and rarely sufficiently long to justify the assumption of infinite length. For example in the climate context discussed in publication #4, we know that the length of the time series (110 years) only poorly samples the multi-decadal mode of a climatic process known as the North Atlantic Oscillation.

A finite length timeseries $X_{\text{example}}^{\text{finite}}(t)$ can be considered as a combination of an infinite length timeseries $X_{\text{example}}(t)$ and a windowing function $W(t)$:

$$X_{\text{example}}^{\text{finite}}(t) = X_{\text{example}}(t) \cdot W(t). \quad (2.4)$$

The windowing function could, again following the easiest case, be a box:

$$W(t) = \begin{cases} 1, & \text{if } t \in [t_s, t_e] \\ 0, & \text{otherwise} \end{cases} \quad (2.5)$$

Such a box could represent measurements over a finite period of time from t_s to t_e of an infinite process. The Fourier transform of the finite length time series, assuming the special case $\omega_{\text{example}} = 0$ for illustration, is

$$F\{X_{\text{example}}^{\text{finite}}(t)\} = F\{X_{\text{example}}(t) \cdot W(t)\} = F\{\underbrace{\cos(2\pi 0t)}_{=1} \cdot W(t)\} = F\{W(t)\}. \quad (2.6)$$

The Fourier transform of the finite length timeseries is thus directly effected by the window (cf. equations 2.3 and 2.6). While in this simple example, the Fourier transform of the finite length timeseries is even identical to the Fourier transform of the window, the exact influence of the windowing function on the spectra in more realistic cases cannot be seen as simply. However, from eq. 2.6, it follows that

$$F\{X_{\text{example}}^{\text{finite}}(t)\} \neq F\{X_{\text{example}}(t)\} \quad (2.7)$$

for most windows $W(t)$. This effect of the windowing function on the spectrum is called spectral leakage and the multi-taper method is one approach to minimize the effects of spectral leakage in finite time series.

2.2 Multi-taper spectral analysis

The entire section is based on Ghil (2002) unless stated otherwise. MTM consists of three steps.

First, a set of tapers (also referred to as windowing functions)

$$w_k(t), \quad (2.8)$$

is calculated, and the total number of tapers is set by the user: $k = 1, \dots, K$. The tapers are a discrete set of eigenfunctions that solve the variational problem to minimize spectral leakage outside a frequency band with half bandwidth $p \cdot f_R$, where $f_R = \frac{1}{N \cdot \Delta T}$ is the Rayleigh frequency and p is another parameter. The definition of the tapers via the minimization problem implies that it is less heuristic than traditional techniques. The set of eigenfunctions is referred to as discrete prolate spheroidal sequences [Slepian, 1992].

In a second step, the tapers are multiplied with the time series

$$X_k(t) = X(t)w_k(t) \quad (2.9)$$

and the discrete Fourier transform $Y_k(f)$ of $X_k(t)$ is calculated. Consequently, the spectral estimate for each taper is defined as

$$\hat{S}_k(f) = |Y_k(f)|^2. \quad (2.10)$$

Lastly, the multi-taper spectrum $S_r(f)$ is defined as a weighted sum of the spectra \hat{S}_k :

$$S_r(f) = \frac{\sum_{k=1}^K \mu_k \hat{S}_k}{\sum_{k=1}^K \mu_k}, \quad (2.11)$$

where μ_k denotes the weights that are deduced from the fractional leakage associated with the k th data taper. However, there is some flexibility regarding the choice of the weights and alternative versions of eq. 2.11 have been developed (see Appendix A1 of Mann and Lees (1996)). Through averaging over K different spectra, the variance of the spectral estimate is reduced thereby enhancing the signal-to-noise ratio. This happens at the cost of reduced spectral resolution.

2.2.1 Significance testing

Maxima in the spectrum $S_r(f)$ can occur by chance or due to a real process with an oscillatory component. To allow meaningful usage of the MTM, both cases need to distinguished. To this end, we adopt a method developed by Mann and Lees (1996).

They suggest a procedure that is referred to as *robust* background estimation. It assumes that the background noise is red and is generated by a an auto-regressive process of first order AR(1):

$$X(t) = \rho X(t-1) + w(t), \quad (2.12)$$

where ρ is the lag-one autocorrelation that describes the memory of the process and $w(t)$ is a Gaussian white noise sequence with variance σ^2 . In the case $\rho = 0$, the AR(1) process collapses to an AR(0) process. The assumption of an underlying AR(1) or AR(0) process is plausible in climatic contexts because atmosphere dynamics is to first order white (Wunsch, 1999) and ocean-atmosphere interactions have been shown to add memory to the coupled system (Mecking, Keenlyside, and Greatbatch, 2015).

The power spectrum of an AR(1) process has two degrees of freedom and reads:

$$S_{\text{AR1}}(f) = S_0 \frac{1 - \rho^2}{1 - 2\rho \cdot \cos(\pi f / f_N) + \rho^2}, \quad (2.13)$$

where S_0 is the average value of the power system and depends on the white noise variance σ^2 as $S_0 = \frac{\sigma^2}{(1-\rho^2)}$ and the Nyquist frequency $f_N = \frac{1}{2\Delta T}$ is the highest frequency that can be resolved. The parameters in eq. 2.13 can be determined via least squares fitting to an observed spectrum.

Instead of fitting eq. 2.13 to the observed spectrum immediately, Mann and Lees (1996) suggest to apply a median smoothing to the raw spectrum first. As a consequence, individual peaks that are considered signal rather than background have less effect of the background spectrum and subsequent significance estimation. The added value of the approach is documented in applications to synthetic and climate

examples (Mann and Lees, 1996). It is particularly helpful in preventing unjustifiably high background floors at low frequencies if low-frequency variability is present. The smoothing width is chosen as

$$\Delta f = \min \left(\frac{f_N}{4}, 2pf_R \right), \quad (2.14)$$

where p is the parameter defined above. Note that this choice is heuristic. It combines two ideas and defines the smoothing frequency either as a function of the highest frequency that can be resolved, or as a function of the MTM spectral resolution. More precisely, if $\frac{f_N}{4} < 2pf_R$, the first expression $\frac{f_N}{4}$ secures sufficient sampling as the smoothing frequency is chosen to be one fourth of the highest frequency that can be resolved (f_N). If $\frac{f_N}{4} > 2pf_R$, the second expression ensures that the smoothing width equals the spectral resolution of the MTM (see also eq. 2.8 and subsequent explanation).

The median smoothed spectrum $S_{ms}(f)$ is then defined by replacing the initial spectrum estimate at each frequency with the median value in a moving window centered at this frequency. Near the edges, the window is truncated such that the median smoothed spectrum is defined over the same frequency interval as the initial spectrum.

Significance testing is performed by comparison of the MTM spectrum $S_r(f)$ with the median smoothed spectrum $S_{ms}(f)$. The MTM spectrum has 2 degrees of freedom per taper, that is 2K degrees of freedom in total. It is furthermore assumed that the ratio of power

$$ROP(f) = \frac{|S_r(f)|^2}{|S_{ms}(f)|^2} \quad (2.15)$$

is distributed as $\chi^2/2K$, following the argumentation and numerical validation reported in Mann and Lees (1996). A peak in the spectrum $S_r(f)$ at frequency f' is thus considered significant at a confidence level c if

$$ROP(f') \geq \chi^2(c, 2K), \quad (2.16)$$

where $\chi^2(c, 2K)$ denotes the chi square distribution with 2K degrees of freedom at confidence level c .

Chapter 3

Publications

3.1 Climate change

3.1.1 #1: Impacts on spatial balancing of wind power generation



More homogeneous wind conditions under strong climate change decrease the potential for inter-state balancing of electricity in Europe

Jan Wohland^{1,2}, Mark Reyers³, Juliane Weber^{1,2}, and Dirk Witthaut^{1,2}

¹Forschungszentrum Jülich, Institute for Energy and Climate Research (IEK-STE), 52428 Jülich, Germany

²Institute for Theoretical Physics, University of Cologne, 50937 Cologne, Germany

³Institute for Geophysics and Meteorology, University of Cologne, Cologne, Germany

Correspondence to: Jan Wohland (j.wohland@fz-juelich.de)

Received: 19 May 2017 – Discussion started: 24 May 2017

Revised: 19 September 2017 – Accepted: 19 October 2017 – Published: 29 November 2017

Abstract. Limiting anthropogenic climate change requires the fast decarbonization of the electricity system. Renewable electricity generation is determined by the weather and is hence subject to climate change. We simulate the operation of a coarse-scale fully renewable European electricity system based on downscaled high-resolution climate data from EURO-CORDEX. Following a high-emission pathway (RCP8.5), we find a robust but modest increase (up to 7 %) of backup energy in Europe through the end of the 21st century. The absolute increase in the backup energy is almost independent of potential grid expansion, leading to the paradoxical effect that relative impacts of climate change increase in a highly interconnected European system. The increase is rooted in more homogeneous wind conditions over Europe resulting in intensified simultaneous generation shortfalls. Individual country contributions to European generation shortfall increase by up to 9 TWh yr⁻¹, reflecting an increase of up to 4 %. Our results are strengthened by comparison with a large CMIP5 ensemble using an approach based on circulation weather types.

1 Introduction

Massive reductions of greenhouse gas emissions are needed in order to reach the temperature goals defined in the Paris Agreement (UNFCCC, 2015; Schleussner et al., 2016b). With a share of around 35 % of current emissions being caused by the electricity system (Bruckner et al., 2014), its decarbonization is the key to any mitigation strategy. However, today's pledges are not yet sufficient to limit warming to below 2 °C, not to mention 1.5 °C (Rogelj et al., 2016).

In addition to the need of mitigating carbon emissions, a second interaction between the energy system and the climate system exists and becomes increasingly important with higher penetrations of renewable energies. Volatile renewable energy generation is driven by weather conditions which are subject to climate change. Large backup facilities are needed to guarantee a stable supply of electricity during periods of low wind and solar power genera-

tion (Rodriguez et al., 2014). Furthermore, climate change affects the demand for electric power (Auffhammer et al., 2017) as well as the operation conditions for thermoelectric and hydroelectric power plants which serve as backup (van Vliet et al., 2016, 2012). However, feedback effects of large-scale wind fleets on atmospheric flows are limited (Vautard et al., 2014).

In line with the Paris Agreement, the scientific community is increasingly interested in differentiating climate impacts at 1.5 and 2 °C (Schleussner et al., 2016a; James et al., 2017) and the IPCC is currently preparing a special report on 1.5 °C. However, many low-carbon pathways rely on negative emissions during the second half of this century (Rogelj et al., 2015; van Vuuren et al., 2016), although their feasibility at scale remains debated (Anderson and Peters, 2016). Future emissions from existing CO₂-emitting infrastructure (Davis et al., 2010) and current political developments in the US (Trump,

2017), among other things, might impede fast decarbonization. Different climatic futures are hence plausible and mitigation strategies need to work in all of them. Therefore, we are led to the question of how sensitive a fully renewable electric power system is to climate change, and, in particular, how severely could strong climate change impact such a system.

Anthropogenic climate change affects the large-scale atmospheric flow and thus the operation conditions for renewable power generation. State-of-the-art global climate models reveal that changes in zonal wind depend on the temperature structure of the lower atmosphere (Haarsma et al., 2013) and that zonal-mean zonal wind and eddy kinetic energy decline almost linearly in time due to polar amplification (Coumou et al., 2015). There are also natural sources of variability at up to decadal timescales. Some of them originate from ocean–atmosphere interactions in the Atlantic and are potentially predictable (Haekkinen et al., 2011; Peings and Magnusdottir, 2014). The North Atlantic Oscillation has been shown to directly influence the operation of inter-connected renewable electricity systems (Ely et al., 2013). Predictability of such natural variations is of great interest for system integration and efforts are undertaken to assess and improve forecasting skills (Moemken et al., 2016).

To assess the impact of climate change on the operation of renewable power systems, downscaled climate model output is needed. It comes at a high temporal and spatial resolution and is better suited than global model output to capture local features such as land–sea transitions or mountains (Rummukainen, 2016). Temporal resolutions at the sub-daily scale are needed since electricity consumption varies strongly during the day. Changes in wind energy yields and capacity factors have been assessed based on dynamical (Tobin et al., 2015, 2016) and statistical–dynamical downscaling outputs (Reyers et al., 2015, 2016). Tobin et al. (2016) evaluate the EURO-CORDEX data archive and find that changes in the annual wind energy yield across Europe are of the order of 5 % and models do not agree on the sign of change. Following a different approach that allows for the inclusion of the output of 22 global climate models, Reyers et al. (2016) report an increasing intra-annual gradient between winter and summer wind generation and different trends in northern and central Europe as compared to southern Europe.

Assessing changes in solar power generation is arguably more difficult due to, among other things, unresolved processes in relatively coarse climate models and uncertain parameterizations (e.g., Chiacchio et al., 2015; Herwehe et al., 2014). Acknowledging this difficulty and associated uncertainties, an evaluation of the EURO-CORDEX data finds limited impacts of climate change on solar photovoltaic (PV) potentials (Jerez et al., 2015). Southern Europe, having the highest potential for PV, sees only small changes, as an increase in downwelling irradiation is counteracted by a decreasing efficiency due to warming. In contrast, the output of concentrated solar power systems (CSPs) is expected to

increase by around 10 % because the efficiency of CSP increases with temperature (Crook et al., 2011).

While wind and solar power sources have shown remarkable development in the last decades, system integration remains a huge challenge (Huber et al., 2014). In a highly renewable power system the timing of generation events becomes crucial. Even in an European electricity system that is on average fed by 100 % renewables, roughly one-quarter of the energy is produced at the wrong time and has to be curtailed (Rodriguez et al., 2014, 2015a).

It is thus necessary to consider indicators such as the variability and synchronicity of generation in addition to total energy yields (Monforti et al., 2016; Bruckner et al., 2014; Bloomfield et al., 2016). Several validated time series of renewable generation based on reanalysis data are available to assess the power system operation (Pfenninger and Staffell, 2016; Staffell and Pfenninger, 2016; Gonzalez Aparicio et al., 2016). However, these data sets are restricted to current climatic conditions and might thus be misleading for long-term planning of the electricity system.

In this article we study the impact of climate change on the operation conditions for future fully renewable power systems. We combine the analysis and simulation of power systems with high-resolution regional climate modeling results to quantify changes in wind power generation. We adopt a coarse-scale view on the power system to uncover the large-scale impacts of climate change. The coarse-scale perspective neglects details that are irrelevant for the balancing of demand with wind generation such as supply of reactive power or different voltage levels in the grid. The focus of this study is to address the potential of transnational power transmission to cover local balancing needs.

Our results reveal the sensitivity of fully renewable power systems to climate change. They should not be mistaken with a forecast and rather be considered a thought experiment to assess potential risks and to answer the following question: what happens to a fully renewable electricity system if mitigation actions are ineffective or come too late?

2 Methods

Modeling the operation of a fully renewable power system under climate change

To assess the impact of strong climate change, we simulate the operation of a fully renewable power system making use of high-resolution climate projections. We use the EURO-CORDEX ensemble containing output of global circulation models (GCMs) which has been dynamically down-scaled to a finer resolution (Jacob et al., 2014) to quantify changes in wind power generation. The ensemble contains five GCMs (HadGEM2-ES, CNRM-CM5, EC-EARTH, CM5A-MR and MPI-ESM-LR) which are all downscaled by the regional climate model RCA4 (Strandberg et al., 2015). The GCM output is part of the Climate Model In-

tercomparison Project Phase 5 (CMIP5) and publicly available (Taylor et al., 2011). We use near-surface wind speeds at 0.11° spatial and 3 h temporal resolution and hence capture intra-day effects. In the spirit of a sensitivity analysis, we evaluate the representative concentration pathway RCP8.5. It describes atmospheric greenhouse gas concentrations following a business-as-usual strategy and leads to approximately 4.3°C warming at the end of the century as compared to pre-industrial values (Stocker et al., 2013). In view of inter-model spread and other uncertainties, a strong climate change scenario bears the advantage of high signal-to-noise ratios.

The approach used in this study is illustrated in Fig. 1. The climate data is used to calculate the aggregated wind power generation time series for each country in the interconnected European power grid (grey circles in Fig. 1a). Near-surface wind speeds are scaled up to hub height (80 m) based on a power law and a standard power curve is used to obtain the power generation of the wind turbines, both as in Tobin et al. (2016; see also Supplement S1). The power curve assumes a cut-in velocity of 3.5 m s^{-1} , a rated velocity of 12 m s^{-1} and a cut-out velocity of 25 m s^{-1} . Wake losses are not accounted for. The country-wise aggregated wind power is obtained by summing the generation of 100 MW wind parks until the system is fully renewable on average. The wind park size was chosen as a compromise between increasing turbine capacities (Wiser et al., 2016) and the need for a sufficient amount of distinct parks. Wind parks are deployed semi-randomly following the approach of Monforti et al. (2016). In order to single out climate-change-induced alterations, we fix the technological parameters such as hub heights or turbine efficiencies, and we do not account for changes in the consumption such as load shifting or sector coupling throughout the 21st century. Tests including validated historical PV time series (Pfenninger and Staffell, 2016) reveal that the inclusion of PV does not change the overall results (see Supplement S2). For the sake of simplicity, we thus decide to restrict the analysis to wind-driven power systems in this paper.

Wind power generation strongly fluctuates over various timescales as shown in Fig. 1c. In periods of scarcity, energy has to be imported from other countries or generated from local dispatchable power plants. We refer to the latter as backup energy. In the situation depicted in Fig. 1a, scarcity in southern Europe can mainly be compensated for by imports from northern Europe. Transnational balancing of this kind often requires large transmission capacities. Moreover, the import of electric energy requires a respective exporter which has a surplus at the same time. Backup energy in future renewable power systems is thus essentially determined by the temporal and spatial heterogeneity of wind and solar power throughout the system.

In addition to enhanced spatial balancing via imports and exports, an extension of storage facilities will reduce backup energy (Rasmussen et al., 2012). However, storage assets are more costly than grid expansion (Schlachtberger et al., 2017;

Brown et al., 2016). Since a cost-optimal solution will thus favor grid expansion, we focus on spatial effects and transnational balancing. An assessment of climate change effects on storage following a similar approach is presented by Weber et al. (2017).

To quantify backup energy, we adopt a coarse-scale view of the transmission system (see, e.g., Rodriguez et al., 2015a, 2014). We consider each country i to be a node in the European transmission network and define a nodal mismatch for each point in time $t = 1, 2, \dots$ as

$$M_i(t) = P_i(t) - D_i(t), \quad (1)$$

where $P_i(t)$ is intermittent renewable generation and $D_i(t)$ is the load (here hourly data for 2015 averaged over 3 h time steps from ENTSO-E; European Network of Transmission System Operators for Electricity, 2015). The assumption of a fully renewable system means that all countries generate as much electricity as needed on average ($\int_{t_s}^{t_e} M_i(t) dt = 0$). The assumption of a fully renewable system means that all countries generate as much electricity as needed on average (integral), where t_s and t_e are defined in Table 1. Furthermore, we assume all countries to run a loss-free and unlimited transmission network within their borders.

If a country has a negative mismatch ($M_i < 0$, red circles in Fig. 1d), it tries to import energy. If it has a positive mismatch ($M_i > 0$, green circles in Fig. 1d), it tries to export energy. For each country i the power balance must be satisfied:

$$M_i(t) + B_i(t) + F_i(t) = C_i(t). \quad (2)$$

The mismatch M_i can be compensated for either by power generation from conventional backup power plants ($B_i \geq 0$), the curtailment of renewable power generation ($C_i \geq 0$) or by imports ($F_i > 0$) or exports ($F_i < 0$). To utilize renewable generation in an optimal way, countries will first try to balance power using imports and exports. However, a perfect balancing of all nodes is impossible if there is a continent-wide shortage or overproduction. Furthermore, cross-border flows along lines are bound by the directional net transfer capacities (NTCs; see Supplement S1 for details), which may also impede balancing for some nodes. Power balance must then be satisfied by local means: in the case of a shortage, power must be backed up by conventional generators ($B_i > 0$). Similarly, if excess power can not be exported, it has to be curtailed ($C_i > 0$). We recognize that the technical details of backup generation often matter for implementation (Schlachtberger et al., 2016), but we focus on gross electricity needs in this study.

For each time step we determine the system operation which minimizes backup power and thus macroeconomic costs as well as greenhouse gas emissions. To assess the impact of climate change, we compare future backup energy to historical values. Time frames are chosen to contain 20 years in order to capture natural variability of the climate system on

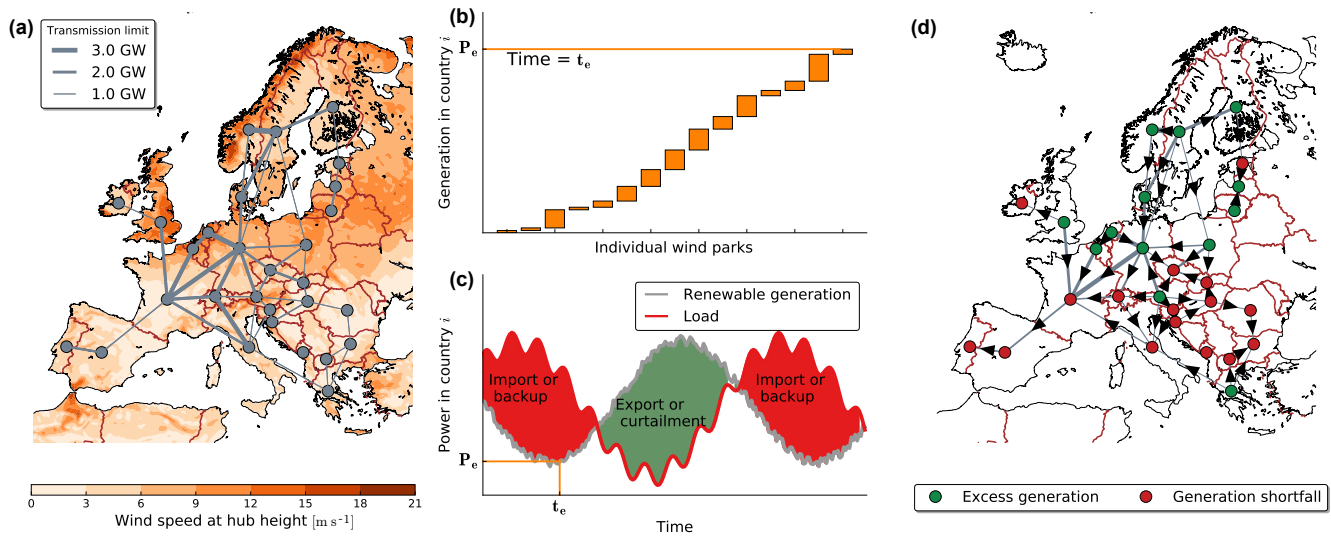


Figure 1. Approach of the study. (a) Wind fields from high-resolution climate models and the 2010/2011 net transfer capacities are used as input to the model. (b) The wind speeds are first translated into generation of individual wind parks using local wind fields and then aggregated to a national level for each country. (c) In combination with country-specific load data, the nodal mismatch for every country and time step is computed. If generation exceeds the load (green area), countries can export energy until lines reach their transmission capacity. Remaining energy has to be curtailed (dumped). If generation is lower than load, electricity will be imported. If importing is not an option due to transmission limits or lack of available excess energy in other countries, backup energy has to be provided by dispatchable power plants. (d) A minimization of the total backup energy of all countries then yields a flow pattern in Europe.

a multi-year timescale while still ensuring that elapsed time between periods is long enough to consider them distinctly (see Table 1). Since GCMs do not reproduce natural variations synchronously (Farneti, 2017), robust signals found in the ensemble are very unlikely to be rooted in natural variations with a recurrence time of a couple of decades (such as the Atlantic Meridional Oscillation or the North Atlantic Oscillation; see Peings and Magnúsdóttir, 2014, for a discussion of their role in mediating atmospheric conditions). The backup energy E_B per period is defined as the sum over all backup powers in a given period:

$$E_B(\text{period}) = \sum_{t \in \text{period}} \min_i \sum_i B_i(t), \quad (3)$$

such that Eq. (2) is satisfied for all countries i and the line limits are respected.

The European amount of backup energy is identical to the amount of curtailment over a full period. This is a direct consequence of the assumptions made and can be formally derived by summing Eq. (2) over all countries and integrating over an entire period. Since $\int_{t_s}^{t_e} M_i(t) dt = 0$ (each country is fully renewable on average) and $\sum_i F_i = 0$ (all imports to one country $F_j = c$ are exports from another $F_k = -c$), it follows that

$$\int_{t_s}^{t_e} \sum_i B_i(t) dt = \int_{t_s}^{t_e} \sum_i C_i(t) dt. \quad (4)$$

A change of the backup energy thus directly implies a change in total curtailment.

We use climate model ensembles to account for model uncertainties. Interpreting the ensemble output by means of the ensemble mean can be misleading as a single model might dominate the ensemble. In such cases, the model mean would be in disarray with the majority of models and hence would not be representative of the ensemble. We thus assess the robustness of changes by means of inter-model agreement. We label a signal “robust” if all models agree on the sign of change and use “high agreement” if all but one model agree. In the evaluation of the large CMIP5 ensemble we adopt language defined for the latest IPCC report and label a change “likely” if at least 66 % of models agree (Mastrandrea et al., 2010).

A variety of studies have analyzed transmission and backup energy in future renewable power systems and cost-optimal transition pathways in a similar way (Rodríguez et al., 2015a, 2014, 2015b; Becker et al., 2014; Rasmussen et al., 2012; Schlachtberger et al., 2016; Hagspiel et al., 2014). However, the potentially crucial role of changes in climatic conditions have not yet been assessed in this context. The remainder of this article focuses on the quantification of impacts to the power system, a correlation analysis of wind resources and an assessment of the larger CMIP5 ensemble to contextualize our findings.

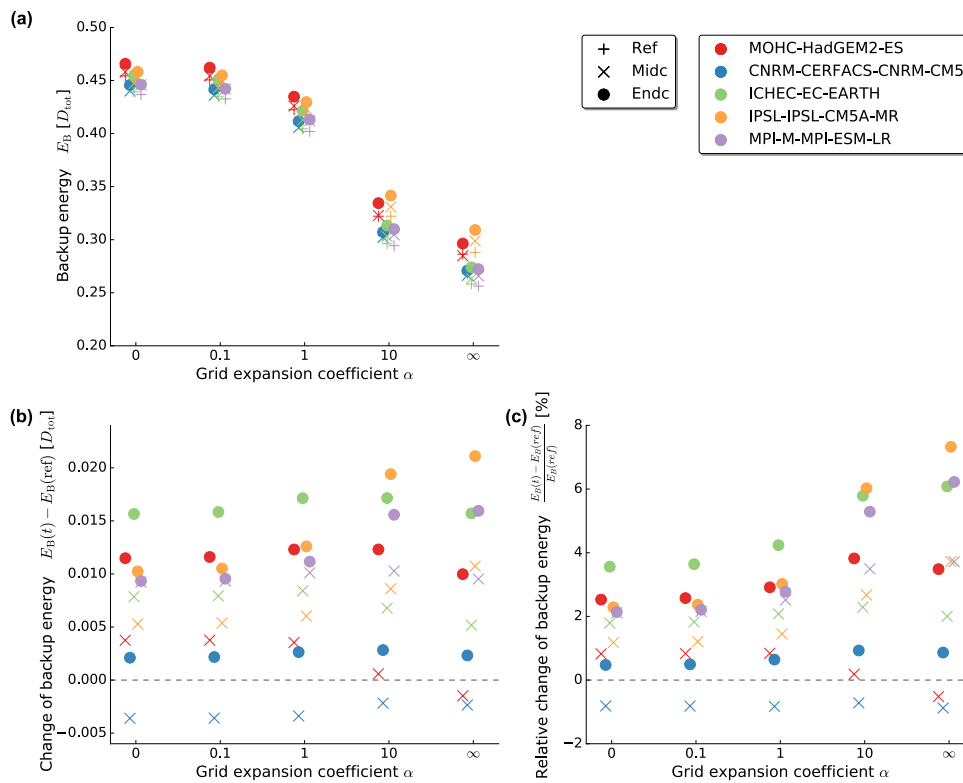


Figure 2. The impact of climate change on backup energy under different grid expansion scenarios. Different realizations of the European inter-state grid expansion are given by the grid expansion coefficient α . While $\alpha = 0$ denotes the isolated case without an inter-country transmission network, $\alpha = 1$ reproduces the configuration as of today and $\alpha = \infty$ represents unlimited European transmission. Different markers refer to distinct 20-year time periods (see Table 1), and colors denote different climate models. (a) Backup energy as a function of grid expansion expressed in units of the total European load $D_{\text{tot}} = \int \sum_i D_i(t) dt$. (b) Absolute change of backup energy by the end of the century. (c) Relative change of backup energy by the end of the century.

Table 1. Periods used in this study. The reference period ref ends before 2005 because GCMs in CMIP5 are driven by historic emissions only until this date and follow different representative concentration scenarios afterwards.

Period name	t_{start}	t_{end}
ref	1985	2004
midc	2040	2059
endc	2080	2099

3 Results and discussion

3.1 Energy: increasing backup energy

A cost-efficient way of power balancing is given by transnational imports and exports. Remarkably, we find that strong climate change impedes the potential of this balancing measure in most of Europe (see Fig. 2). We report that backup energy in Europe increases under strong climate change by the end of the century. This finding is robust across all EURO-CORDEX ensemble members. Since we consider a scenario

where 100 % of electricity is generated from renewables on average, an increase in backup energy is accompanied by an increase in excess energy which has to be curtailed.

To uncover this effect we simulate backup energy for different scenarios of the development of the transnational grid quantified by the NTCs. We allow for a homogeneous scaling of transmission capacity by multiplying NTCs by a factor α . Without any grid ($\alpha = 0$), approximately 45 % of the wind-energy is produced at the wrong time and thus has to be curtailed and backed up later on. Strong grid extension ($\alpha \gg 1$) clearly reduces backup energy to about 27 % (see Fig. 2a). However, all models report an increase in backup energy at the end of the century. The effect of climate change is almost independent of a grid extension: the absolute increase in backup energy until end of century is largely independent of the expansion coefficient α for three out of five models (see Fig. 2b). Hence, the relative increase in backup energy paradoxically becomes even more pronounced for a strongly interconnected Europe (see Fig. 2c). Highly connected systems can suffer from an increase in backup energy of up to 7 %. There is considerable inter-model spread regarding the

magnitude of change which varies by up to 1 order of magnitude depending on the climate model (see Fig. 2b, $\alpha = \infty$). In particular, changes for CNRM are generally weak and HadGEM2 features only a slight overall increase with grid expansion. However, remarkably, all models agree on the sign of change at the end of the century such that we consider the direction of change very likely.

In conclusion, we find that the effectiveness of transnational balancing decreases due to climate change. This decrease is due to more homogeneous wind generation as we will show in the climate section of this paper. Moreover, a control simulation including PV generation from Pfenninger and Staffell (2016) yields similar results although the magnitude of change is reduced by roughly a factor of 2 and only four out of five models agree on the sign of change (see Supplement S2). Results are barely sensitive to changes in the load time series as an assessment using constant loads reveals (see Supplement S3).

Spatial distribution of mismatch contributions

To obtain a more detailed view, we evaluate transnational balancing potentials separately for each country. We calculate the likeliness that a given country has a local scarcity ($M_i < 0$) while Europe as a whole suffers from a lack of generation ($\sum_j M_j < 0$). This corresponds to events where a country would favor importing electricity but can not due to a continent-wide scarcity. These events require conventional backup even in the case of unlimited transmission infrastructure and thus give a lower bound for backup energy. The approach allows us to identify those countries which are most responsible for overall scarcity. Mathematically speaking, we restrict our analysis to time steps T_i with local and Europe-wide scarcity:

$$T_i = \left\{ t : \left(\sum_j M_j(t) < 0 \text{ and } M_i(t) < 0 \right) \right\}. \quad (5)$$

The negative mismatch contribution occurrence ν_i corresponds to the joint probability of country i and Europe experiencing generation shortfall at the same time:

$$\nu_i = \frac{\sum_{t \in T_i} 1}{N_T}, \quad (6)$$

where N_T is the number of time steps. We define the annual energy that is lacking (i.e., generation shortfall) in country i during European scarcity as

$$L_i = \frac{\sum_{t \in T_i} |M_i(t)|}{20y}, \quad (7)$$

where we chose the absolute value of M_i for convenience of interpretation. L_i is given in TWh yr^{-1} . A high value

of L_i characterizes a country which would favor importing a large quantity of energy during European scarcity, whereas a low value of L_i indicates a country whose generation shortfall can often be balanced by imports. In order to compare values of L_i with loads, we provide country values for D_i in the Supplement S5. The European sum is $\sum_i D_i \approx 3100 \text{ TWh yr}^{-1}$.

Values for ν and L during the reference period are shown in Fig. 3a, b. Large consumers like Germany and France are also the dominant contributors to European scarcity in terms of missing energy (see Fig. 3a). The German contribution corresponds to approximately 8 % of the European annual load of 3100 TWh. However, the role of these countries, for example, in comparison to eastern Europe or Benelux, is less pronounced if only the occurrence of negative mismatch events ν is considered (see Fig. 3b). The reason for their strong impact on L is thus primarily rooted in the high absolute values of their mismatches rather than their frequency. Moreover, a large consumer also has a bigger influence on the Europe-wide mismatches which implies that the conditions in Eq. (5) are not independent. For example, the European mismatch can be negative because of an elevated German mismatch and in such a situation a high contribution to L would be observed. Interestingly, there is considerable spread regarding ν in different countries (Fig. 3b). Greece and Norway contribute the least often to European scarcity (less than 40 %) while central Europe contributes around 50–60 % of the time.

Next, we focus on changes until the end of the 21st century:

$$\Delta \nu_i = \nu_i|_{\text{endc}} - \nu_i|_{\text{ref}} \text{ and } \Delta L_i = L_i|_{\text{endc}} - L_i|_{\text{ref}}. \quad (8)$$

In France, Benelux, Scandinavia, the UK, Ireland and most countries in central Europe the negative mismatch contribution occurrence ν and the respective negative energy contribution L increase (see Fig. 3c, d). In these countries it becomes more likely that a Europe-wide scarcity coincides with a local scarcity and the amount of required backup energy increases. In turn, these countries can not alleviate the overall shortage by exporting excess generation. This points to a stronger homogeneity of wind power generation in central Europe which is discussed in more detail below. An increase in the occurrence ν can also be observed for eastern and southeastern Europe, excluding Greece, with high inter-model agreement (see Fig. 3d). However, these increases are weak in terms of energy contributions (see Fig. 3c).

An opposite trend is observed in Spain, where transnational balancing is facilitated as negative mismatch contributions L become weaker (see Fig. 3c). At the same time, models generally disagree on the sign of change regarding $\Delta \nu$ (see Fig. 3d). Combined, this indicates weaker but not less frequent negative contributions of Spain. Moreover, Greece shows favorable changes for the European system in terms of energy contributions and occurrences with a high inter-model agreement (see Fig. 3c, d). This finding is particularly

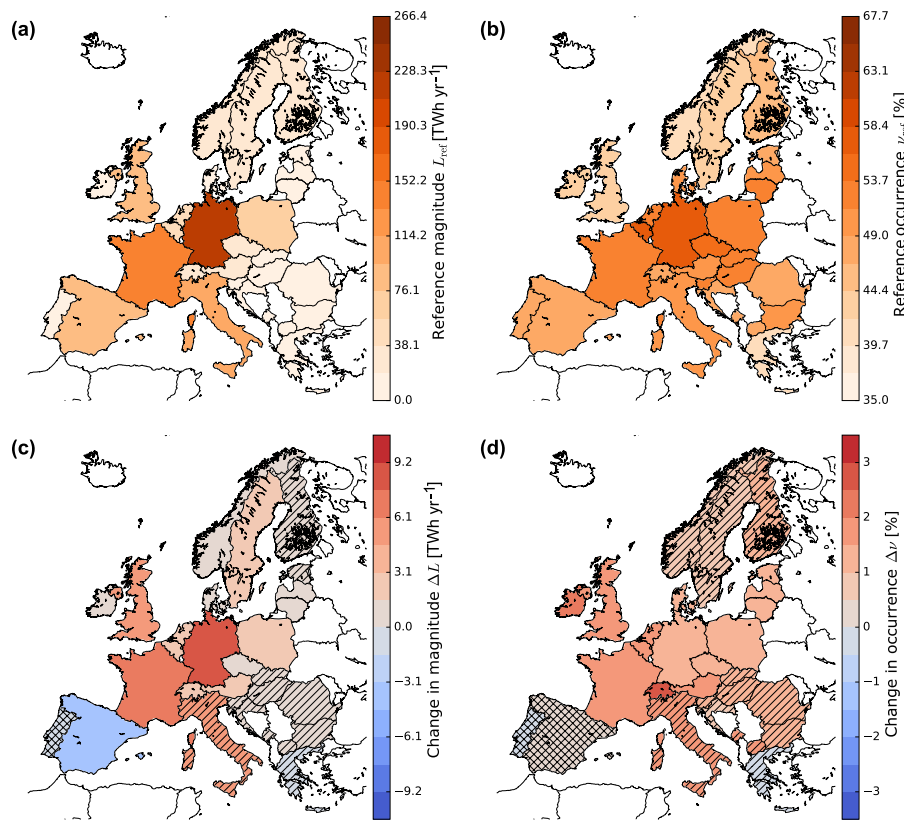


Figure 3. Country contributions in times of overall and local generation shortfall and their change until end of century. Values denote the inter-model mean. Shading indicates inter-model agreement as follows: no hatches indicate perfect agreement on sign of change; striped: four out of five models agree; hatching: less than four agree. **(a)** Lacking energy L_{ref} during local and overall scarcity in the reference period (see Eq. 7). **(b)** Simultaneous occurrence of local and overall generation shortfall v_{ref} (see Eq. 6). **(c, d)** Changes of the quantities given in **(a, b)** until end of century (see Eq. 8). Red colors denote unfavorable changes (stronger or more frequent contribution of a country to overall scarcity) while blue colors denote favorable changes.

interesting as Grams et al. (2017) show that a combination of wind parks allocated in the North Sea and the Balkans allows for substantial reduction in volatility under current climatic conditions. Based on our results, this positive effect from incorporating the Balkans would further be enhanced under strong climate change.

We stress that our findings do not refute the efficiency of transmission grid expansions in general. In any case backup energy decreases monotonously with the grid expansion, but the magnitude of the decrease is subject to climatic conditions. Furthermore, we assume a homogeneous expansion of the grid, although an optimal system design will probably lead to heterogeneous grid expansions and heterogeneous allocations of generation capacities. Our results suggest that such an optimal system will include stronger interconnections to Spain and Greece to reduce backup energy. Also, on a country level, certain extensions can be incentivized while others are downgraded. For instance, for France it can become more favorable to extend the connections to Spain rather than to Germany (see Fig. 3c). Despite this, and in

light of regulatory and powerful social acceptance issues, regarding grid extensions (Battaglini et al., 2012), we consider a future grid which resembles the current one in its fundamental characteristics a reasonable first guess.

3.2 Climate: increasing correlations of wind resources

As reported above, we find an increase in backup energy due to strong climate change in a wind-powered electricity system. This increase is solely rooted in changes of wind resources since all other parameters are kept constant.

For the identification of changes in the spatial wind patterns, we perform a correlation analysis over 20-year time spans of wind speeds (see Table 1). We use Pearson correlation on the highest spatial scale; i.e., we correlate every grid point to all others instead of aggregating the wind fields first. Hence, the full spatial detail of the downscaled climate data is taken into consideration. In order to visualize results, correlation values are averaged on country level in the next step. To highlight long-term trends, we only show correlation changes between 2080–2099 (endc) and 1985–2004 (ref):

$$\Delta R_{\text{endc}}(A,B) = R_{\text{endc}}(A,B) - R_{\text{ref}}(A,B), \quad (9)$$

where $R_{\text{period}}(A,B)$ denotes the average of all point-to-point correlations between country A and country B in a given period. The computation is repeated for all possible combinations (A,B). We calculate $\Delta R_{\text{endc}}(A,B)$ for each climate model separately and show the model mean if not stated otherwise.

To reveal general patterns, we first consider the average correlation change of a fixed country A by averaging Eq. (9) over all countries B excluding A (see Fig. 4). There is a general tendency towards higher correlations of wind speeds for central Europe in the ensemble mean. This change is most pronounced in Germany, Switzerland, Benelux and Ireland. Decreasing correlations only occur at the fringes of the continent and they are strongest in Portugal and Greece. Positive correlation changes occur in most countries and the maximum positive change is approximately 3 times larger in magnitude than the maximum negative change. Interestingly, the overall pattern is similar to the mismatch contribution analysis (see Fig. 3). This similarity is not a trivial finding since the mismatch contribution analysis accounts for the nonlinear turbine power curve and the collective behavior of the entire electricity grid while the correlation analysis is solely based on wind speeds. Summarizing, we find more homogeneous wind conditions over most of the continent while the fringes decouple slightly. Results for mid-century are weaker but clearly similar (see Supplement Fig. S5).

Assessing pairwise correlation changes between countries, we find that the correlation increase over central Europe has at least a high agreement in the EURO-CORDEX ensemble (see Fig. 5). Some country combinations (e.g., DE–CZ, FR–CZ, BE–UK, FR–NL) even show robust trends. For example, in Germany the correlations to all neighboring countries plus the UK, Ireland and eastern Europe increase with high agreement. The importance of this finding is strengthened by the fact that central Europe plays an important role for the power system: Germany, France, the United Kingdom, Poland and Benelux account for more than half of the European load. Correlations between Germany and Greece decrease with high model agreement. In contrast, changes between Germany and the Iberian Peninsula, Italy and Norway are uncertain.

The decoupling of Portugal and Greece which is found in the aggregated plot (Fig. 4) is only robust in a few country combinations and models disagree regarding some important pairs (e.g., PT–DE, PT–FR, PT–UK; GR–IT, GR–UK; and ES–FR, ES–DE). The uncertainty with respect to the correlation changes between these countries is thus high.

However, a robust trend is found in Scandinavia, where Norway, Finland and Sweden become more highly correlated. This change also partly holds for the Baltic region. At the same time Scandinavia decouples robustly from some

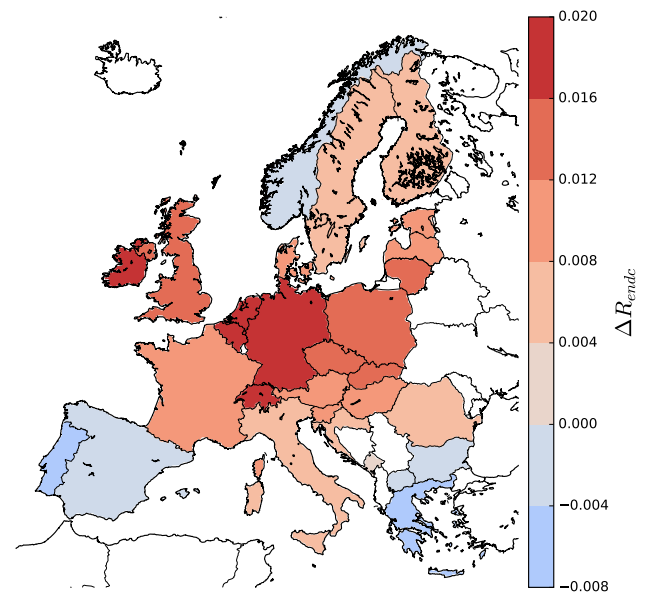


Figure 4. Correlation changes of wind time series averaged over all models (difference between end of century and reference correlations). A more detailed assessment, which in particular addresses inter-model spread, is shown in Fig. 5.

parts of southern Europe (e.g., SE–GR, NO–ES). In the context of large-scale European grid expansions, these alterations might enhance the value of high-voltage direct current (HVDC) lines between these distinct regions.

Correlation increases in Scandinavia are also robust in the middle of the century (see Supplement Fig. S6). However, inter-model agreement for correlation increases in central Europe is lower although the overall pattern is still conceivable. The decoupling of Portugal and Greece can be seen in the inter-model mean, while agreement across models is rare.

3.3 Climate: complementing EURO-CORDEX with CMIP5 using circulation weather types

The EURO-CORDEX data set includes only a five-member subset of all CMIP5 GCMs and might thus not be representative of the entire CMIP5 ensemble. Moreover, subgroups of GCMs can be biased in the same way since they did not develop separately, but along the same lines. The most drastic example is the sharing of code by CNRM and EC-EARTH, which are both part of the EURO-CORDEX ensemble and run the same atmosphere module (Knutti et al., 2013).

Uncertainty in climate projections has been argued to stem from three main sources: (1) natural variability, (2) model uncertainty and (3) scenario uncertainty (Hawkins and Sutton, 2009). In some situations the choice of initial conditions also contributes substantially (Hawkins et al., 2016). We neglect scenario uncertainty by design of this study since we only focus on the sensitivity to strong climate change (RCP8.5). As the importance of natural variability decreases with the time

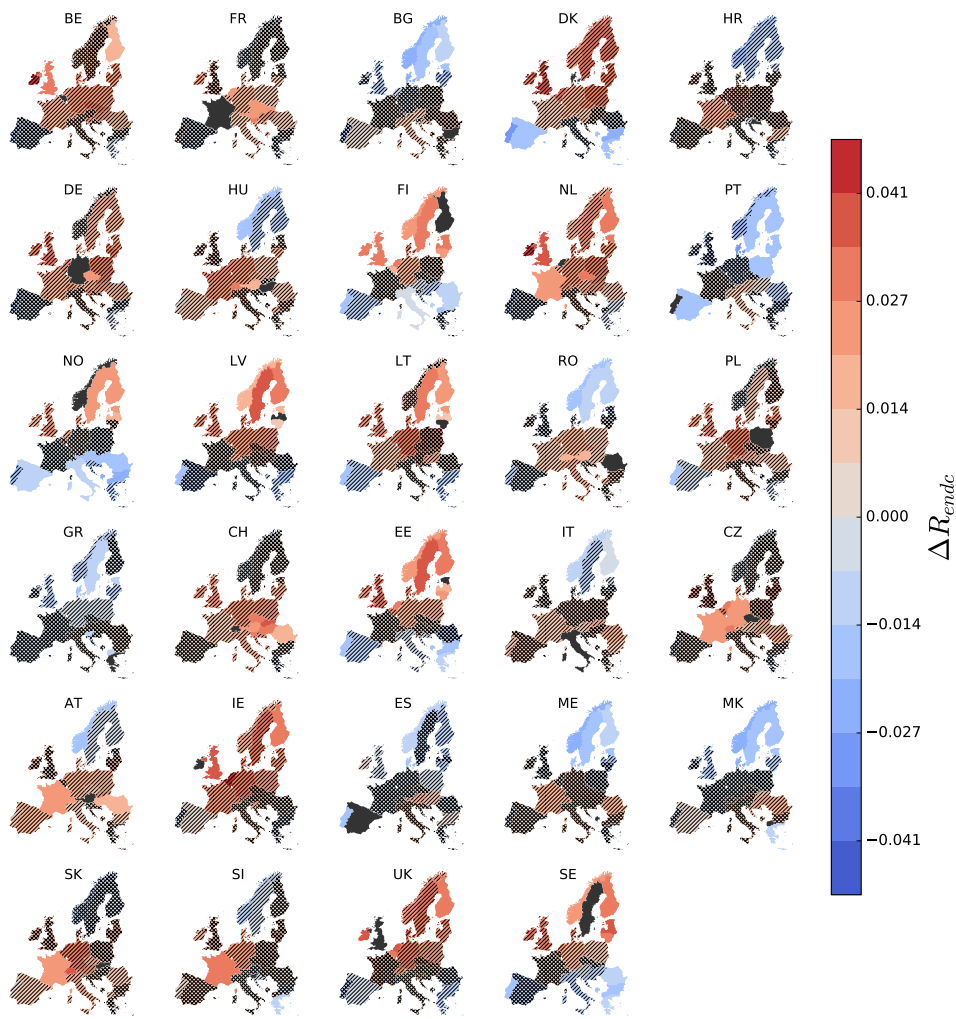


Figure 5. Country-specific change of wind speed correlations at the end of the 21st century including inter-model agreement. Colors denote the model-average correlation change of a country to the reference country (highlighted in black and given in the respective heading). Shading indicates inter-model agreement as follows: no hatches indicate perfect agreement on sign of change; striped: four out of five models agree; hatching: less than four agree.

intervals averaged over, model uncertainty is likely to be the dominant source of uncertainty here.

In order to rule out the possibility that our findings are biased due to the (arbitrary) choice of GCMs that were scaled down for EURO-CORDEX, we follow a statistical–dynamical approach which was developed by Reyers et al. (2015, 2016) to downscale a large CMIP5 ensemble for wind energy applications. This approach is based on a circulation weather type (CWT) classification methodology (Jones et al., 1993). Daily mean sea level pressure (MSLP) values at 16 GCM grid points around a central point located in Germany are used to assign the near-surface atmospheric flow over Europe to either a directional flow (north, northeast, east, etc.) or a rotational flow (anticyclonic, cyclonic). Aside from the direction of the atmospheric flow a f parameter is calculated, which is representative of the instantaneous pressure gradient

and thus for the general wind speed conditions over Germany and the surrounding countries:

$$f = \sqrt{dP_z^2 + dP_m^2}, \tag{10}$$

where dP_z is the mean pressure gradient in east–west direction (zonal component) and dP_m is the mean pressure gradient in north–south direction (meridional component). f parameter values from below 5 hPa per 1000 km (weak MSLP gradient and thus low wind speed conditions) up to 45 hPa per 1000 km (strong MSLP gradients and thus high wind speed conditions) were found. Reyers et al. (2016) demonstrated that such a CWT classification provides a suitable and effective basis for wind energy applications on the regional scale and therefore enables the consideration of a large CMIP5 ensemble in future projections.

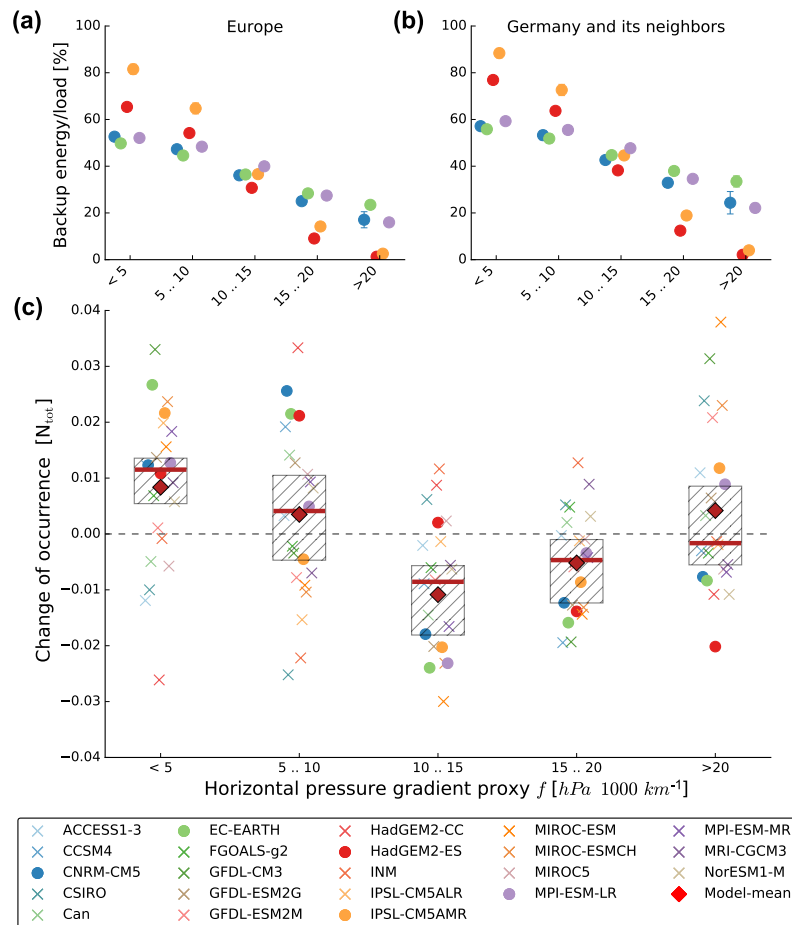


Figure 6. Backup energy and change of occurrence as a function of the f parameter. **(a)** Backup energy versus f parameter for the entire domain. Circles denote the mean over the three considered periods for each model and error bars indicate the standard deviation thereof. Error bars are, however, most often smaller than the circle size. **(b)** Same as **(a)** but restricted to Germany and its neighbors. **(c)** Change of occurrence of different f parameter values. The change of occurrence is computed as the difference between end of century and the reference period and is given in units of the total number of time steps N_{tot} . Red diamonds denote the ensemble mean, red lines the ensemble median and hatched boxes indicate the 33rd to 67th percentile. If a box lies completely above/below zero, the sign of the change can be considered as likely.

Analyzing the five individual GCMs contributing to the EURO-CORDEX ensemble reveals a link between the CWTs and the backup energy derived from dynamically downscaled data (see Eqs. 1, 2, 3). We find that backup energy decreases monotonously with increasing f parameter values (see Fig. 6a, b). All models in the EURO-CORDEX ensemble agree on this result which is also physically plausible as the pressure gradient drives the atmospheric circulation. This statement holds for Germany and its neighbors and for Europe as a whole. We see this as evidence that the CWT analyses in this particular case can be applied to the entire continent in the sense that the f parameter is a reasonable proxy for the European backup energy.

The majority of CMIP5 models (16 out of 22) predict an increase in events with low f parameter values by the end of the century (see Fig. 6c). Following the likelihood

classification developed for the latest IPCC report (Masrandrea et al., 2010), it is thus likely that low f parameter values become more abundant. This trend originates mainly from more frequent anticyclonic pressure configurations (see Fig. 7). For this CWT, spatial homogeneity of wind resources is higher as compared to all other CWTs (see Supplement Fig. S7). In such a homogeneous situation, it is plausible that backup energy is elevated since countries are more likely to experience shortfall of generation simultaneously. In contrast, medium ($10 \leq f[\text{hPa}/1000\text{km}] \leq 15$) and high ($15 \leq f[\text{hPa}/1000\text{km}] \leq 20$) f parameters are likely to occur less frequently since 17 models agree on these signals. We thus conclude that the majority of CMIP5 models agree with the main finding of increasing backup energy.

The larger CMIP5 ensemble also allows for an assessment of the EURO-CORDEX ensemble input data. We re-

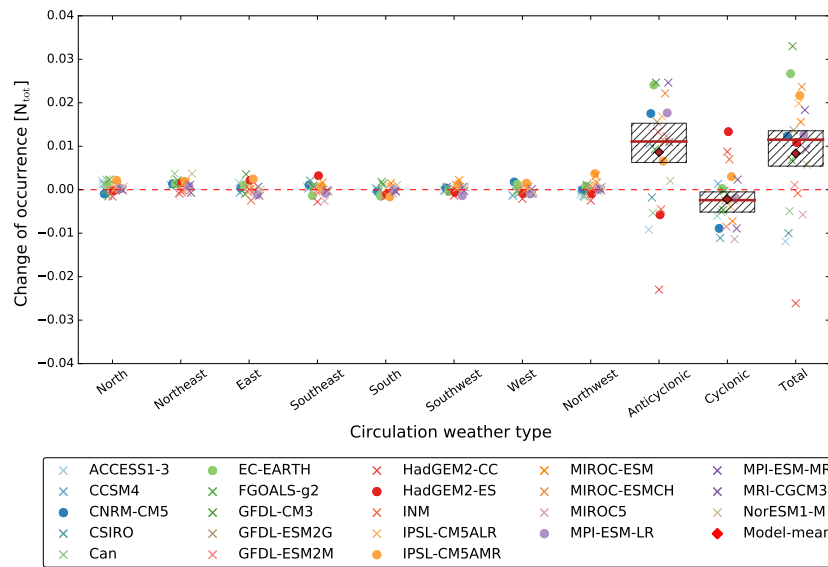


Figure 7. Changes of relative occurrence of primary CWTs with low f parameter values ($f \leq 5$ hPa/1000 km). Changes are differences in occurrence between end of century and the reference period and are given in units of the total number of time steps N_{tot} . Boxes indicate the 33rd to 67th percentile and are only shown if changes are substantial. Red diamonds denote the ensemble mean and red lines denote the ensemble median.

port that the GCMs contributing to EURO-CORDEX are within the spread of the remaining CMIP5 ensemble (except for HadGEM with very strong f parameters) and are thus generally representative of the larger ensemble (see Fig. 6). However, they also show comparably strong changes in the occurrence of specific f parameters. The CMIP5 overall projection regarding backup energy might thus be lower than results reported in this paper. In order to test this speculative hypothesis, a consistent downscaling of all CMIP5 models would be necessary, which is far beyond the scope of this article but should be tackled in future works.

4 Conclusions

A future highly renewable electricity system will be governed by weather conditions. If mankind fails to reduce carbon emissions fast, climate change will impede the operation of a wind-driven system in Europe. This conclusion is based on three separate lines of evidence.

1. A coarse-scale electricity model fed with EURO-CORDEX climate data shows robust increases in backup energy.
2. Spatial correlations in wind time series in EURO-CORDEX data across central Europe are found to increase. Countries are thus more likely to experience generation shortfall simultaneously.
3. Building upon a statistical–dynamical downscaling technique and a 22-member CMIP5 ensemble we find a likely increase in circulation weather types with low

f parameters values. They are associated with low Europe-wide wind generation.

It has to be stressed that results are for the end of the 21st century and based on a strong climate change scenario (RCP8.5). They should be thought of as a sensitivity test. While the increases of backup energy are robust, they are also restricted to relative increases of 7% (see Fig. 2). A fully renewable electricity system will hence not become unfeasible due to catastrophic changes.

In the emerging field of linking energy and climate research, many additional questions are to be addressed in order to deliver a more holistic assessment. We simulated a wind-driven electricity system and performed a control simulation with a fixed share of PV. Time series for the latter were taken from a validated data set based on reanalysis data (Pfenninger and Staffell, 2016). Ideally, future works would assess the combined effects of climate change on wind and solar generation. They could also include concentrated solar power since this technology bears advantages for system integration (Pfenninger et al., 2014). Load shifting, sector coupling and storage are further topics for more detailed assessments.

In terms of climate modeling output, a larger high-resolution ensemble which contains multiple regional climate models (RCMs) is particularly desirable. The next generation of CORDEX is planned to deliver such data (Gutowski Jr. et al., 2016) and will hence allow for an inclusion of RCM spread in future assessments. It will also facilitate similar assessment for other world regions as spatial extent is expanded.

Data availability. The climate data (EUROCORDEX and CMIP5) are accessible via the ESGF: <https://esgf-data.dkrz.de/search/cordex-dkrz/>. Hourly load data are provided by the European Network of Transmission System Operators for Electricity at <https://www.entsoe.eu/db-query/consumption/mh1v-all-countries-for-a-specific-month>. The current net transfer capacities for Europe are made available by the same body at https://www.entsoe.eu/fileadmin/user_upload/_library/ntc/archive/NTC-Values-Winter-2010-2011.pdf.

The Supplement related to this article is available online at <https://doi.org/10.5194/esd-8-1047-2017-supplement>.

Author contributions. JaW performed the simulations, analyzed the data, produced all figures and wrote most of the manuscript. DW conceived and supervised the research and contributed to the writing, in particular regarding the electricity system. MR supplied the CWT analysis and wrote parts of the CWT chapter. All authors contributed ideas, gave feedback and helped to improve the manuscript.

Competing interests. The authors declare that they have no conflict of interest.

Acknowledgements. We thank Martin Greiner, Gorm Bruun Andresen, Smail Kozarcanin, Tom Brown, David Schlachtberger and Christoph Ball for stimulating discussions. We owe Julia Brugger gratitude for checking the final manuscript. We also acknowledge the World Climate Research Programme's Working Group on Regional Climate, and the Working Group on Coupled Modeling, former coordinating body of CORDEX and responsible panel for CMIP5. We thank the climate modeling groups for producing and making available their model output. We acknowledge the Earth System Grid Federation infrastructure an international effort led by the U.S. Department of Energy's Program for Climate Model Diagnosis and Intercomparison, the European Network for Earth System Modelling and other partners in the Global Organization for Earth System Science Portals (GO-ESSP). The authors gratefully acknowledge the computing time granted by the JARA-HPC Vergabegremium on the supercomputer JURECA (Jülich Supercomputing Centre, 2016) at Forschungszentrum Jülich. We gratefully acknowledge support from the Helmholtz Association (via the joint initiative "Energy System 2050 – A Contribution of the Research Field Energy" and the grant no. VH-NG-1025 to Dirk Witthaut).

The article processing charges for this open-access publication were covered by a Research Centre of the Helmholtz Association.

Edited by: Somnath Baidya Roy

Reviewed by: two anonymous referees

References

- Anderson, K. and Peters, G.: The trouble with negative emissions, *Science*, 354, 182–183, 2016.
- Auffhammer, M., Baylis, P., and Hausman, C. H.: Climate change is projected to have severe impacts on the frequency and intensity of peak electricity demand across the United States, *P. Natl. Acad. Sci. USA*, 114, 1886–1891, <https://doi.org/10.1073/pnas.1613193114>, 2017.
- Battaglini, A., Komendantova, N., Brtnik, P., and Patt, A.: Perception of barriers for expansion of electricity grids in the European Union, *Energy Policy*, 47, 254–259, <https://doi.org/10.1016/j.enpol.2012.04.065>, 2012.
- Becker, S., Rodriguez, R., Andresen, G., Schramm, S., and Greiner, M.: Transmission grid extensions during the build-up of a fully renewable pan-European electricity supply, *Energy*, 64, 404–418, <https://doi.org/10.1016/j.energy.2013.10.010>, 2014.
- Bloomfield, H. C., Brayshaw, D. J., Shaffrey, L. C., Coker, P. J., and Thornton, H. E.: Quantifying the increasing sensitivity of power systems to climate variability, *Environ. Res. Lett.*, 11, 124025, <https://doi.org/10.1088/1748-9326/11/12/124025>, 2016.
- Brown, T., Schierhorn, P.-P., Troester, E., and Ackermann, T.: Optimising the European transmission system for 77 % renewable electricity by 2030, *IET Renew. Power Gen.*, 10, 3–9, <https://doi.org/10.1049/iet-rpg.2015.0135>, 2016.
- Bruckner, T., Bashmakov, I. A., Mulugeta, Y., Chum, H., de la Vega Navarro, A., Edmonds, J., Faaij, A., Functammasan, B., Garg, A., Hertwich, E., Honnery, D., Infield, D., Kainuma, M., Khenas, S., Kim, S., Nimir, H. B., Riahi, K., Strachan, N., Wiser, R., and Zhang, X.: Energy Systems, in: *Climate Change 2014: Mitigation of Climate Change. Contribution of Working Group III to the Fifth Assessment Report of the Intergovernmental Panel on Climate Change*, edited by: Edenhofer, O., Pichs-Madruga, R., Sokona, Y., Farahani, E., Kadner, S., Seyboth, K., Adler, A., Baum, I., Brunner, S., Eickemeier, P., Kriemann, B., Savolainen, J., Schlömer, S., von Stechow, C., Zwickel, T., and Minx, J. C., Cambridge University Press, Cambridge, UK and New York, NY, USA, 2014.
- Chiacchio, M., Solmon, F., Giorgi, F., Stackhouse, P., and Wild, M.: Evaluation of the radiation budget with a regional climate model over Europe and inspection of dimming and brightening: Evaluation of the radiation budget, *J. Geophys. Res.-Atmos.*, 120, 1951–1971, <https://doi.org/10.1002/2014JD022497>, 2015.
- Coumou, D., Lehmann, J., and Beckmann, J.: The weakening summer circulation in the Northern Hemisphere mid-latitudes, *Science*, 348, 324–327, 2015.
- Crook, J. A., Jones, L. A., Forster, P. M., and Crook, R.: Climate change impacts on future photovoltaic and concentrated solar power energy output, *Energy Environ. Sci.*, 4, 3101, <https://doi.org/10.1039/c1ee01495a>, 2011.
- Davis, S. J., Caldeira, K., and Matthews, H. D.: Future CO₂ Emissions and Climate Change from Existing Energy Infrastructure, *Science*, 329, 1330–1333, <https://doi.org/10.1126/science.1194210>, 2010.
- Ely, C. R., Brayshaw, D. J., Methven, J., Cox, J., and Pearce, O.: Implications of the North Atlantic Oscillation for a UK–Norway Renewable power system, *Energy Policy*, 62, 1420–1427, <https://doi.org/10.1016/j.enpol.2013.06.037>, 2013.

- European Network of Transmission System Operators for Electricity: Hourly load values for all countries for a specific month (in MW), available at: <https://www.entsoe.eu/db-query/consumption/mhlv-all-countries-for-a-specific-month> (last access: 21 November 2016), 2015.
- Farneti, R.: Modelling interdecadal climate variability and the role of the ocean, *Wiley Interdisciplinary Reviews: Climate Change*, 8, e441, <https://doi.org/10.1002/wcc.441>, 2017.
- Gonzalez Aparicio, I., Zucker, A., Careri, F., Monforti, F., Huld, T., and Badger, J.: EMHIRE dataset; Part 1: Wind power generation, Tech. Rep. EUR 28171 EN, Joint Research Center, 2016.
- Grams, C. M., Beerli, R., Pfenninger, S., Staffell, I., and Wernli, H.: Balancing Europe's wind-power output through spatial deployment informed by weather regimes, *Nature Climate Change*, 7, 557–562, <https://doi.org/10.1038/nclimate3338>, 2017.
- Gutowski Jr., W. J., Giorgi, F., Timbal, B., Frigon, A., Jacob, D., Kang, H.-S., Raghavan, K., Lee, B., Lennard, C., Nikulin, G., O'Rourke, E., Rixen, M., Solman, S., Stephenson, T., and Tangang, F.: WCRP COordinated Regional Downscaling EXperiment (CORDEX): a diagnostic MIP for CMIP6, *Geosci. Model Dev.*, 9, 4087–4095, <https://doi.org/10.5194/gmd-9-4087-2016>, 2016.
- Haarsma, R. J., Selten, F., and van Oldenborgh, G. J.: Anthropogenic changes of the thermal and zonal flow structure over Western Europe and Eastern North Atlantic in CMIP3 and CMIP5 models, *Clim. Dynam.*, 41, 2577–2588, <https://doi.org/10.1007/s00382-013-1734-8>, 2013.
- Haekkinen, S., Rhines, P. B., and Worthen, D. L.: Atmospheric Blocking and Atlantic Multidecadal Ocean Variability, *Science*, 334, 655–659, 2011.
- Hagspiel, S., Jaegemann, C., Lindenberger, D., Brown, T., Chervatskiy, S., and Troester, E.: Cost-optimal power system extension under flow-based market coupling, *Energy*, 66, 654–666, <https://doi.org/10.1016/j.energy.2014.01.025>, 2014.
- Hawkins, E. and Sutton, R.: The potential to narrow uncertainty in regional climate predictions, *B. Am. Meteorol. Soc.*, 90, 1095–1107, <https://doi.org/10.1175/2009BAMS2607.1>, 2009.
- Hawkins, E., Smith, R. S., Gregory, J. M., and Stainforth, D. A.: Irreducible uncertainty in near-term climate projections, *Clim. Dynam.*, 46, 3807–3819, <https://doi.org/10.1007/s00382-015-2806-8>, 2016.
- Herwehe, J. A., Alapaty, K., Spero, T. L., and Nolte, C. G.: Increasing the credibility of regional climate simulations by introducing subgrid-scale cloud-radiation interactions, *J. Geophys. Res.-Atmos.*, 119, 5317–5330, <https://doi.org/10.1002/2014JD021504>, 2014.
- Huber, M., Dimkova, D., and Hamacher, T.: Integration of wind and solar power in Europe: Assessment of flexibility requirements, *Energy*, 69, 236–246, <https://doi.org/10.1016/j.energy.2014.02.109>, 2014.
- Jacob, D., Petersen, J., Eggert, B., Alias, A., Christensen, O. B., Bouwer, L. M., Braun, A., Colette, A., Déqué, M., Georgievski, G., Georgopoulou, E., Gobiet, A., Menut, L., Nikulin, G., Haensler, A., Hempelmann, N., Jones, C., Keuler, K., Kovats, S., Kröner, N., Kotlarski, S., Kriegsmann, A., Martin, E., van Meijgaard, E., Moseley, C., Pfeifer, S., Preuschmann, S., Radermacher, C., Radtke, K., Rechid, D., Rounsevell, M., Samuelsson, P., Somot, S., Soussana, J.-F., Teichmann, C., Valentini, R., Vautard, R., Weber, B., and Yiou, P.: EURO-
- CORDEX: new high-resolution climate change projections for European impact research, *Reg. Environ. Change*, 14, 563–578, <https://doi.org/10.1007/s10113-013-0499-2>, 2014.
- James, R., Washington, R., Schleussner, C.-F., Rogelj, J., and Conway, D.: Characterizing half-a-degree difference: a review of methods for identifying regional climate responses to global warming targets: Characterizing half-a-degree difference, *Wiley Interdisciplinary Reviews: Climate Change*, 8, e457, <https://doi.org/10.1002/wcc.457>, 2017.
- Jerez, S., Tobin, I., Vautard, R., Montávez, J. P., López-Romero, J. M., Thais, F., Bartok, B., Christensen, O. B., Colette, A., Déqué, M., Nikulin, G., Kotlarski, S., van Meijgaard, E., Teichmann, C., and Wild, M.: The impact of climate change on photovoltaic power generation in Europe, *Nat. Commun.*, 6, 10014, <https://doi.org/10.1038/ncomms10014>, 2015.
- Jones, P. D., Hulme, M., and Briffa, K. R.: A comparison of Lamb circulation types with an objective classification scheme, *Int. J. Climatol.*, 13, 655–663, 1993.
- Jülich Supercomputing Centre: JURECA: General-purpose supercomputer at Jülich Supercomputing Centre, *Journal of Large-Scale Research Facilities*, 2, A62, <https://doi.org/10.17815/jlsrf-2-121>, 2016.
- Knutti, R., Masson, D., and Gettelman, A.: Climate model genealogy: Generation CMIP5 and how we got there, *Geophys. Res. Lett.*, 40, 1194–1199, <https://doi.org/10.1002/grl.50256>, 2013.
- Mastrandrea, M. D., Field, C. B., Stocker, T. F., Edenhofer, O., Ebi, K. L., Frame, D. J., Held, H., Kriegler, E., Mach, K. J., Matschoss, P. R., Plattner, G.-K., Yohe, G. W., and Zwiers, F. W.: Guidance note for lead authors of the IPCC fifth assessment report on consistent treatment of uncertainties, available at: <http://pubman.mpdl.mpg.de/pubman/item/escidoc:2147184/component/escidoc:2147185/uncertainty-guidance-note.pdf> (last access: 13 April 2017), 2010.
- Moemken, J., Reyers, M., Buldmann, B., and Pinto, J. G.: Decadal predictability of regional scale wind speed and wind energy potentials over Central Europe, *Tellus A*, 68, 29199, <https://doi.org/10.3402/tellusa.v68.29199>, 2016.
- Monforti, F., Gaetani, M., and Vignati, E.: How synchronous is wind energy production among European countries?, *Renewable and Sustainable Energy Reviews*, 59, 1622–1638, <https://doi.org/10.1016/j.rser.2015.12.318>, 2016.
- Peings, Y. and Magnusdottir, G.: Forcing of the wintertime atmospheric circulation by the multidecadal fluctuations of the North Atlantic ocean, *Environ. Res. Lett.*, 9, 034018, <https://doi.org/10.1088/1748-9326/9/3/034018>, 2014.
- Pfenninger, S. and Staffell, I.: Long-term patterns of European PV output using 30 years of validated hourly reanalysis and satellite data, *Energy*, 114, 1251–1265, <https://doi.org/10.1016/j.energy.2016.08.060>, 2016.
- Pfenninger, S., Gauché, P., Lilliestam, J., Damerau, K., Wagner, F., and Patt, A.: Potential for concentrating solar power to provide baseload and dispatchable power, *Nature Climate Change*, 4, 689–692, <https://doi.org/10.1038/nclimate2276>, 2014.
- Rasmussen, M. G., Andresen, G. B., and Greiner, M.: Storage and balancing synergies in a fully or highly renewable pan-European power system, *Energy Policy*, 51, 642–651, <https://doi.org/10.1016/j.enpol.2012.09.009>, 2012.
- Reyers, M., Pinto, J. G., and Moemken, J.: Statistical-dynamical downscaling for wind energy potentials: evaluation and applica-

- tions to decadal hindcasts and climate change projections, *Int. J. Climatol.*, 35, 229–244, <https://doi.org/10.1002/joc.3975>, 2015.
- Reyers, M., Moemken, J., and Pinto, J. G.: Future changes of wind energy potentials over Europe in a large CMIP5 multi-model ensemble, *Int. J. Climatol.*, 36, 783–796, <https://doi.org/10.1002/joc.4382>, 2016.
- Rodriguez, R. A., Becker, S., Andresen, G. B., Heide, D., and Greiner, M.: Transmission needs across a fully renewable European power system, *Renew. Energ.*, 63, 467–476, <https://doi.org/10.1016/j.renene.2013.10.005>, 2014.
- Rodriguez, R. A., Becker, S., and Greiner, M.: Cost-optimal design of a simplified, highly renewable pan-European electricity system, *Energy*, 83, 658–668, <https://doi.org/10.1016/j.energy.2015.02.066>, 2015a.
- Rodriguez, R. A., Dahl, M., Becker, S., and Greiner, M.: Localized vs. synchronized exports across a highly renewable pan-European transmission network, *Energy, Sustainability and Society*, 5, 21, <https://doi.org/10.1186/s13705-015-0048-6>, 2015b.
- Rogelj, J., Luderer, G., Pietzcker, R. C., Kriegler, E., Schaeffer, M., Krey, V., and Riahi, K.: Energy system transformations for limiting end-of-century warming to below 1.5 °C, *Nature Climate Change*, 5, 519–527, <https://doi.org/10.1038/nclimate2572>, 2015.
- Rogelj, J., den Elzen, M., Hoehne, N., Fransen, T., Fekete, H., Winkler, H., Schaeffer, R., Sha, F., Riahi, K., and Meinshausen, M.: Paris Agreement climate proposals need a boost to keep warming well below 2 °C, *Nature*, 534, 631–639, <https://doi.org/10.1038/nature18307>, 2016.
- Rummukainen, M.: Added value in regional climate modeling, *Wiley Interdisciplinary Reviews: Climate Change*, 7, 145–159, <https://doi.org/10.1002/wcc.378>, 2016.
- Schlachtberger, D., Becker, S., Schramm, S., and Greiner, M.: Backup flexibility classes in emerging large-scale renewable electricity systems, *Energ. Convers. Manage.*, 125, 336–346, <https://doi.org/10.1016/j.enconman.2016.04.020>, 2016.
- Schlachtberger, D., Brown, T., Schramm, S., and Greiner, M.: The benefits of cooperation in a highly renewable European electricity network, *Energy*, 134, 469–481, <https://doi.org/10.1016/j.energy.2017.06.004>, 2017.
- Schleussner, C.-F., Lissner, T. K., Fischer, E. M., Wohland, J., Perrette, M., Golly, A., Rogelj, J., Childers, K., Schewe, J., Frieler, K., Mengel, M., Hare, W., and Schaeffer, M.: Differential climate impacts for policy-relevant limits to global warming: the case of 1.5 °C and 2 °C, *Earth Syst. Dynam.*, 7, 327–351, <https://doi.org/10.5194/esd-7-327-2016>, 2016a.
- Schleussner, C.-F., Rogelj, J., Schaeffer, M., Lissner, T., Licker, R., Fischer, E. M., Knutti, R., Levermann, A., Frieler, K., and Hare, W.: Science and policy characteristics of the Paris Agreement temperature goal, *Nature Climate Change*, 6, 827–835, <https://doi.org/10.1038/nclimate3096>, 2016b.
- Staffell, I. and Pfenninger, S.: Using bias-corrected reanalysis to simulate current and future wind power output, *Energy*, 114, 1224–1239, <https://doi.org/10.1016/j.energy.2016.08.068>, 2016.
- Stocker, T. F., Qin, D., Plattner, G.-K., et al.: Technical summary, in: *Climate Change 2013: The Physical Science Basis. Contribution of Working Group I to the Fifth Assessment Report of the Intergovernmental Panel on Climate Change*, 33–115, Cambridge University Press, available at: http://pubman.mpdl.mpg.de/pubman/item/escidoc:1977530/component/escidoc:1977527/WG1AR5_TS_FINAL.pdf (last access: 3 March 2017), 2013.
- Strandberg, G., Barring, L., Hansson, U., Jansson, C., Jones, C., Kjellström, E., Kolax, M., Kupiainen, M., Nikulin, G., Samuelsson, P., Ullerstig, A., and Wang, S.: CORDEX scenarios for Europe from the Rossby Centre regional climate model RCA4, SMHI, Sveriges Meteorologiska och Hydrologiska Institut, 2015.
- Taylor, K. E., Stouffer, R. J., and Meehl, G. A.: An Overview of CMIP5 and the Experiment Design, *B. Am. Meteorol. Soc.*, 93, 485–498, 2011.
- Tobin, I., Vautard, R., Balog, I., Bréon, F.-M., Jerez, S., Ruti, P. M., Thais, F., Vrac, M., and Yiou, P.: Assessing climate change impacts on European wind energy from ENSEMBLES high-resolution climate projections, *Climatic Change*, 128, 99–112, <https://doi.org/10.1007/s10584-014-1291-0>, 2015.
- Tobin, I., Jerez, S., Vautard, R., Thais, F., van Meijgaard, E., Prein, A., Deque, M., Kotlarski, S., Maule, C. F., Nikulin, G., Noel, T., and Teichmann, C.: Climate change impacts on the power generation potential of a European mid-century wind farms scenario, *Environ. Res. Lett.*, 11, 034013, <https://doi.org/10.1088/1748-9326/11/3/034013>, 2016.
- Trump, D. J.: Presidential Executive Order on Promoting Energy Independence and Economic Growth, available at: <https://www.whitehouse.gov/the-press-office/2017/03/28/presidential-executive-order-promoting-energy-independence-and-economy-1> (last access: 4 June 2017), 2017.
- UNFCCC: Adoption of the Paris Agreement, *FCCC/CP/2015/10/Add.1*, 2015.
- van Vliet, M. T. H., Yearsley, J. R., Ludwig, F., Voegele, S., Lettenmaier, D. P., and Kabat, P.: Vulnerability of US and European electricity supply to climate change, *Nature Climate Change*, 2, 676–681, <https://doi.org/10.1038/nclimate1546>, 2012.
- van Vliet, M. T. H., Wiberg, D., Leduc, S., and Riahi, K.: Power-generation system vulnerability and adaptation to changes in climate and water resources, *Nature Climate Change*, 6, 375–380, <https://doi.org/10.1038/nclimate2903>, 2016.
- van Vuuren, D. P., van Soest, H., Riahi, K., Clarke, L., Krey, V., Kriegler, E., Rogelj, J., Schaeffer, M., and Tavoni, M.: Carbon budgets and energy transition pathways, *Environ. Res. Lett.*, 11, 075002, <https://doi.org/10.1088/1748-9326/11/7/075002>, 2016.
- Vautard, R., Thais, F., Tobin, I., Bréon, F.-M., de Lavergne, J.-G. D., Colette, A., Yiou, P., and Ruti, P. M.: Regional climate model simulations indicate limited climatic impacts by operational and planned European wind farms, *Nat. Commun.*, 5, 3196, <https://doi.org/10.1038/ncomms4196>, 2014.
- Weber, J., Wohland, J., Reyers, M., Moemken, J., Hoppe, C., Pinto, J. G., and Witthaut, D.: Impact of climate change on backup and storage needs in a wind-dominated European power system, in review, 2017.
- Wiser, R., Bolinger, M., Barbose, G., Darghouth, N., Hoen, B., Mills, A., Rand, J., Millstein, D., Porter, K., and Widiss, R.: 2015 Wind Technologies Market Report, available at: <https://pubarchive.lbl.gov/islandora/object/ir%3A1005951/data%stream/PDF/download/citation.pdf> (last access: 28 August 2017), 2016.

Supplement

Supplement of Earth Syst. Dynam., 8, 1047–1060, 2017
<https://doi.org/10.5194/esd-8-1047-2017-supplement>
© Author(s) 2017. This work is distributed under
the Creative Commons Attribution 3.0 License.



Supplement of

More homogeneous wind conditions under strong climate change decrease the potential for inter-state balancing of electricity in Europe

Jan Wohland et al.

Correspondence to: Jan Wohland (j.wohland@fz-juelich.de)

The copyright of individual parts of the supplement might differ from the CC BY 3.0 License.

Supplementary Material

655 S1) Detailed methodology

Adopting the approach of Tobin et al. (2016), we use near-surface wind speeds 10 meters above the ground. Assuming a power-law relationship for the vertical wind profile, the velocity at hub height H is obtained as

$$v_H = v_{10m} \cdot \left(\frac{H}{10} \right)^{\frac{1}{7}} \quad (\text{S1})$$

660 and we chose $H = 80\text{m}$.

The conversion of wind speeds into renewable generation is performed using a simple power curve

$$P(v_H) = P_0 \begin{cases} 0, & \text{if } v_H < v_i \text{ or } v_H > v_0 \\ \frac{v_H^3 - v_i^3}{v_R^3 - v_i^3}, & \text{if } v_i \leq v_H < v_R \\ 1, & \text{if } v_R \leq v_H < v_0 \end{cases} \quad (\text{S2})$$

where v_H denotes wind velocity at hub height and $v_i = 3.5$ m/s, $v_R = 12$ m/s, $v_0 = 25$ m/s denote the cut-in, rated and cut-out velocity of the wind turbine, respectively. We assume that every
665 wind park has a capacity $P_0 = 0.1$ GW.

If the number of wind parks per grid cell $N_{\text{wind}}(x, y)$ is known, the renewable generation in a country with area A_i is given by

$$P_i(t) = \sum_{x, y \in A_i} N_{\text{wind}}(x, y) \cdot P(v_H(x, y, t)). \quad (\text{S3})$$

Note that we assume a stationary configuration of wind parks throughout every 20 year period.
670 Moreover, we assume that each country generates as much energy from renewables as is needed in a 20 year period ranging from t_{start} to t_{end}

$$\int_{t_{\text{start}}}^{t_{\text{end}}} P_i(t) dt = \int_{t_{\text{start}}}^{t_{\text{end}}} D_i(t) dt \quad (\text{S4})$$

Since all variables except from N_{wind} are used as input to the model, and hence are known, equations (S3) and (S4) can be used to determine N_{wind} . However, the solution is degenerate. In order to
675 single out one solution, we adopt the strategy of Monforti et al. (2016) who distribute wind parks randomly at those places where the temporal average of renewable generation P is above average. Performing a Monte Carlo analysis for the deployment of wind parks, Monforti et al. found that the sensitivity of this partially random allocation procedure to changes in the actual configuration of N_{wind} is small.

680 **Transmission**

The imports/exports F_i of a country i (see Eq. (2)) depend on the incidence matrix

$$K_{i,l} = \begin{cases} 1, & \text{if line } l \text{ starts in country } i \\ -1 & \text{if line } l \text{ ends in country } i \\ 0 & \text{otherwise} \end{cases} \quad (S5)$$

and the flows \hat{F}_l along a line l

$$F_i = - \sum_l K_{i,l} \hat{F}_l, \quad (S6)$$

685 where the minus sign stems from the (arbitrary) choice that $F_i > 0$ means imports. The flow along a line l is bound by

$$\alpha \cdot \text{NTC}_{l-} \leq \hat{F}_l \leq \alpha \cdot \text{NTC}_{l+}, \quad (S7)$$

where α denotes grid expansion. The line limits $\text{NTC}_{l+} \geq 0$ and $\text{NTC}_{l-} \leq 0$ are direction dependent and the former refers to the line limit in the direction of line l as defined via the incidence matrix (S5).

690 Line limits are directional winter Net Transfer Capacities published by ENTSO-E for 2010/2011 (European Network of Transmission System Operators for Electricity, 2011).

Inclusion of PV generation

We use PV generation timeseries from Pfenninger and Staffell (2016) which is more complete than other open source datasets like Open Power System Data¹. The data set is bias corrected and vali-
695 dated at around 1000 locations. We favored to use the part of the dataset which is based on MERRA over SARAH because the latter is lacking data in the first years.

We average over 30 years of data to compute a representative PV generation timeseris $PV_i(t)$ for every country i . Using a representative year is not an ideal approach since inter-year variations are artificially muted. However, the PV generation timeseries only exists for the historical period. If
700 one was to combine PV generations from one year with wind generations from another, the result is likely to be unrealistic because the corresponding state of the climate system belonging to either the PV or wind generation would be out of phase. We thus consider our approach to be the most suitable one in this assessment.

In order to incorporate PV generation into the model, we replace the original load $D_i(t)$ in Eq. (1)
705 with the residual load after PV generation is subtracted as

¹ <http://www.open-power-system-data.org/>

$$D_i(t) \rightarrow D_i(t) - \gamma \cdot PV_i(t), \quad (\text{S8})$$

where γ is chosen such that 29% of the overall generation is contributed by PV. This share has been found to be the European optimum in terms of minimizing backup energy in a similar setup (Rodriguez et al., 2014). The load $D_i(t)$ now represents the residual load which has to be satisfied
 710 by wind, im-/exports or dispatchable power plants. Results including PV are shown in Supplement B.

Sensitivity to load timeseries

We repeat our analysis assuming constant loads

$$D_i(t) \rightarrow \langle \hat{D}_i(t) \rangle_t, \quad (\text{S9})$$

715 where $\hat{D}_i(t)$ denotes monthly load data from ENTSO-E and $\langle \cdot \rangle_t$ denotes the temporal average. The goal of muting the time dependency of the load is to test for the influence of the load timeseries on our modelling outcomes. Results for constant loads are shown in Supplement C.

S2) Energy results including PV

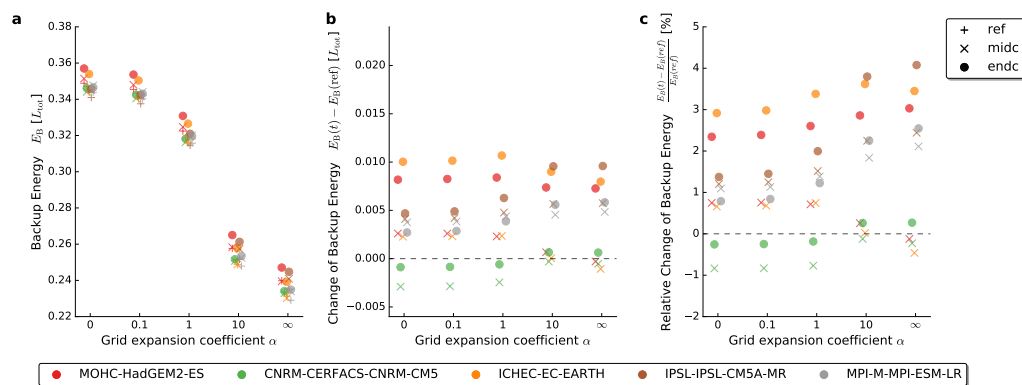


Figure S1. Same as Fig. 2, but including PV from Pfenninger and Staffell (2016).

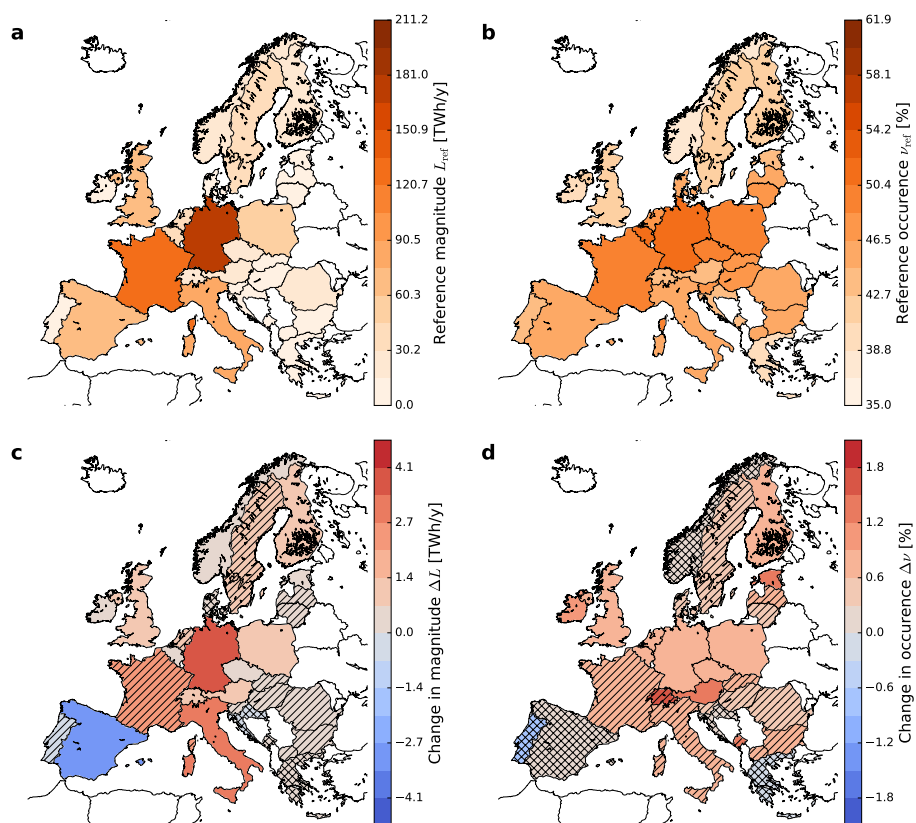


Figure S2. Same as Fig. 3 but including PV from Pfenninger and Staffell (2016).

S3) Energy results assuming constant loads

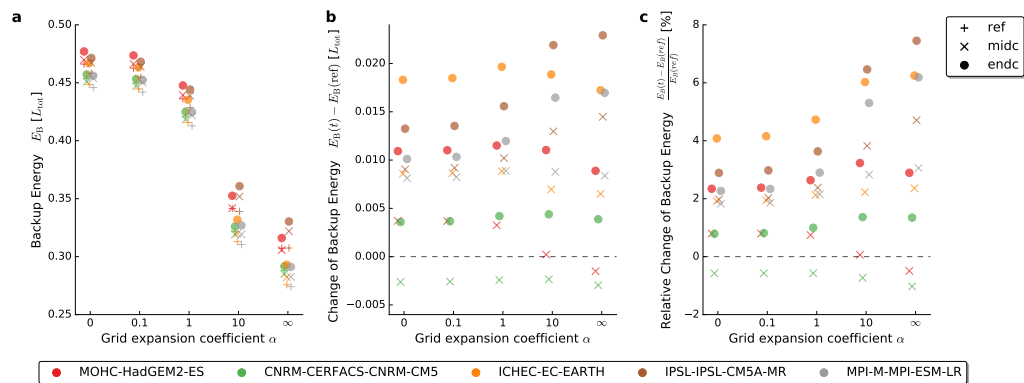


Figure S3. Same as Fig. 2, but with constant load.

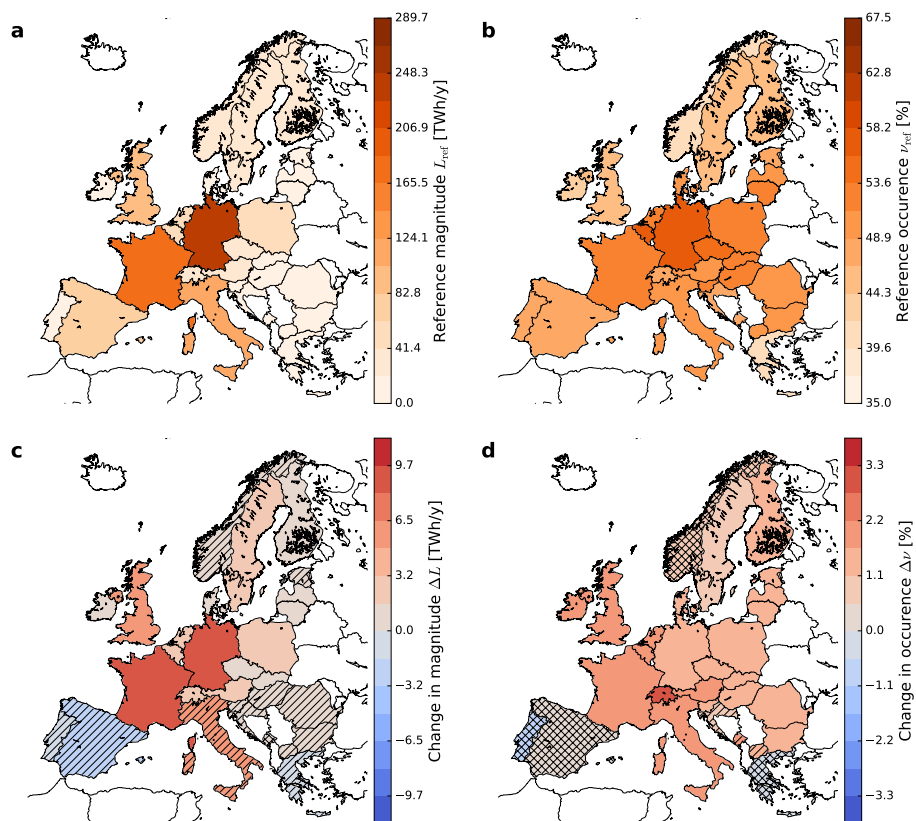


Figure S4. Same as Fig. 3 but assuming constant load.

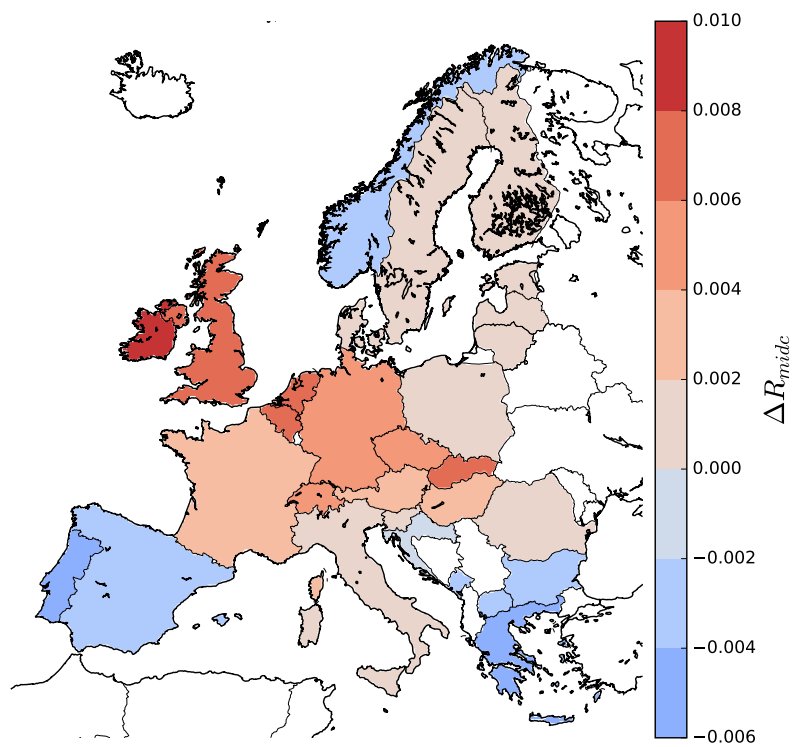


Figure S5. Same as Fig. 4 but for mid century.

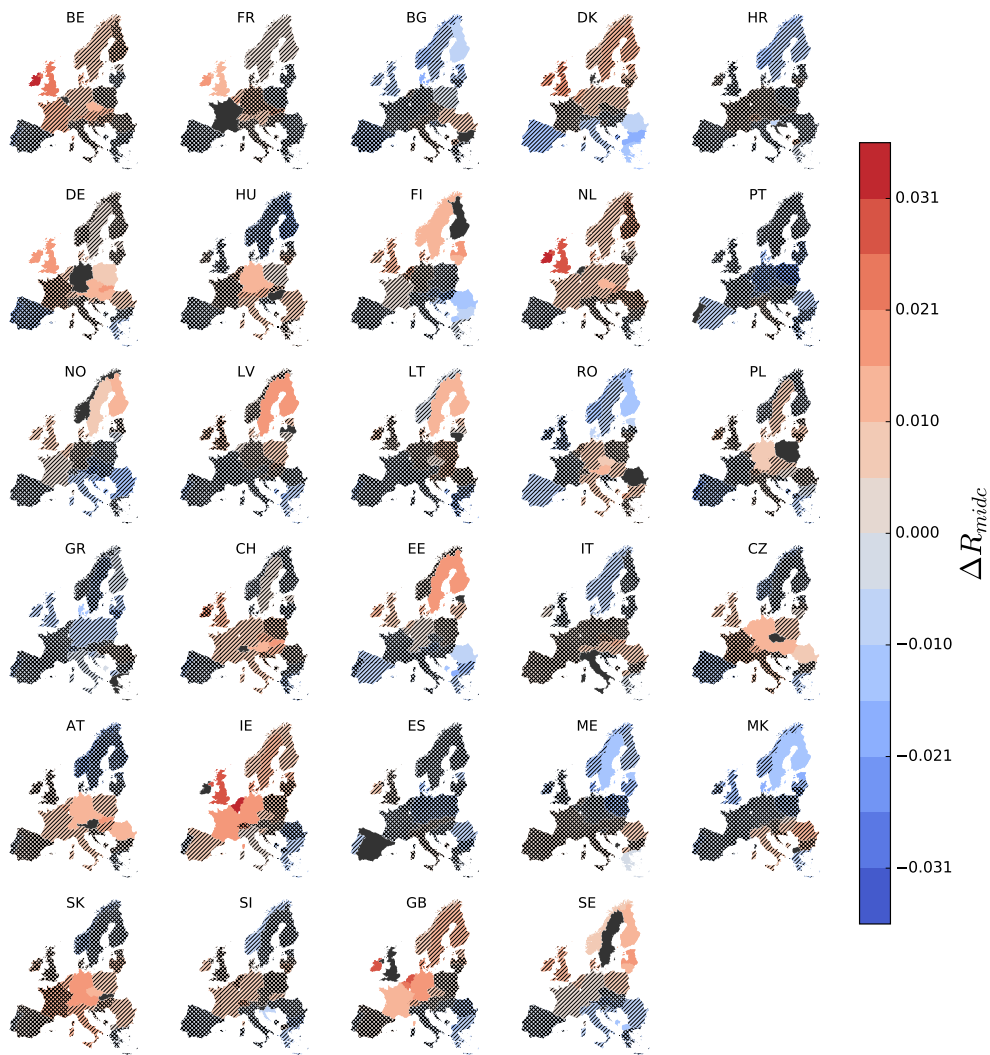


Figure S6. Same as Fig. 5 but for mid century.

S5) Spatial homogeneity and CWTs

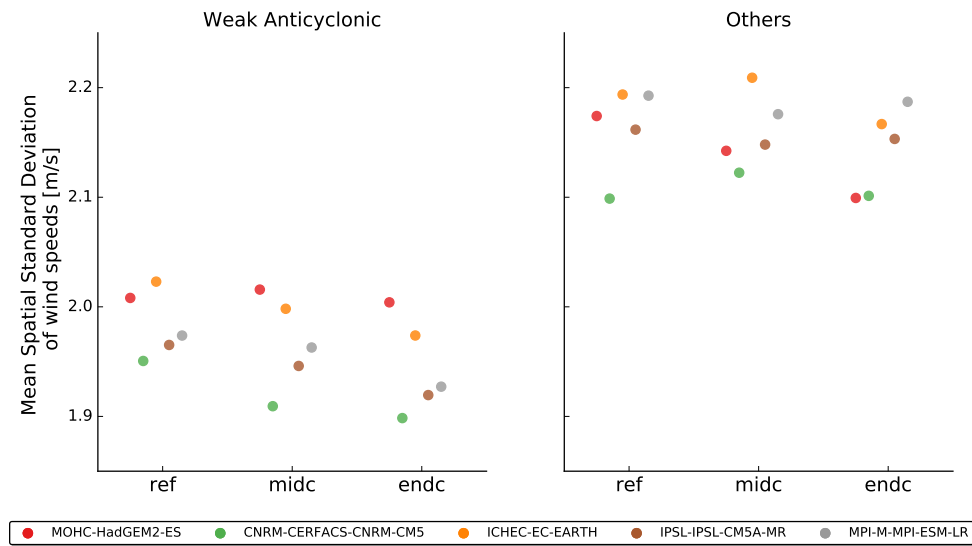


Figure S7. Mean spatial standard deviation of wind speeds over all 28 countries considered in the energy assessment. The standard deviation is calculated for each grid point separately. The weak anticyclonic CWT has a distinctly smaller spatial standard deviation than all other situations considered together. Hence, it is characterized by more homogeneous wind fields.

S6) Annual load values on country level

Table S1. Annual sums of country electricity consumption based on hourly 2015 data provided by the European Network of Transmission System Operators for Electricity (2015).

country	country code	Annual load [TWh]
Austria	AT	69.62
Belgium	BE	85.22
Bulgaria	BG	38.62
Switzerland	CH	62.06
Czech Republic	CZ	63.53
Germany	DE	505.27
Denmark	DK	33.9
Estonia	EE	7.93
Spain	ES	248.5
Finland	FI	82.5
France	FR	471.26
Great Britain	GB	282.19
Greece	GR	51.4
Croatia	HR	17.19
Hungary	HU	40.75
Ireland	IE	26.57
Italy	IT	314.35
Lithuania	LT	10.86
Latvia	LV	7.07
Montenegro	ME	3.42
Macedonia	MK	7.84
Netherlands	NL	113.25
Norway	NO	128.65
Poland	PL	149.96
Portugal	PT	48.93
Romania	RO	52.31
Sweden	SE	135.93
Slovenia	SI	13.65
Slovakia	SK	28.21
Total		3100.94

3.2 Inter-annual climate variability

3.2.1 #2: The impact of inter-annual wind variability on current German congestion management

RESEARCH ARTICLE

Natural wind variability triggered drop in German redispatch volume and costs from 2015 to 2016

Jan Wohland^{1,2*}, Mark Reyers³, Carolin Märker¹, Dirk Witthaut^{1,2}

1 Institute for Energy and Climate Research (IEK-STE), Forschungszentrum Jülich, Jülich, Germany, **2** Institute for Theoretical Physics, University of Cologne, Cologne, Germany, **3** Institute for Geophysics and Meteorology, University of Cologne, Cologne, Germany

* j.wohland@fz-juelich.de



Abstract

Avoiding dangerous climate change necessitates the decarbonization of electricity systems within the next few decades. In Germany, this decarbonization is based on an increased exploitation of variable renewable electricity sources such as wind and solar power. While system security has remained constantly high, the integration of renewables causes additional costs. In 2015, the costs of grid management saw an all time high of about € 1 billion. Despite the addition of renewable capacity, these costs dropped substantially in 2016. We thus investigate the effect of natural climate variability on grid management costs in this study. We show that the decline is triggered by natural wind variability focusing on redispatch as a main cost driver. In particular, we find that 2016 was a weak year in terms of wind generation averages and the occurrence of westerly circulation weather types. Moreover, we show that a simple model based on the wind generation time series is skillful in detecting redispatch events on timescales of weeks and beyond. As a consequence, alterations in annual redispatch costs in the order of hundreds of millions of euros need to be understood and communicated as a normal feature of the current system due to natural wind variability.

OPEN ACCESS

Citation: Wohland J, Reyers M, Märker C, Witthaut D (2018) Natural wind variability triggered drop in German redispatch volume and costs from 2015 to 2016. PLoS ONE 13(1): e0190707. <https://doi.org/10.1371/journal.pone.0190707>

Editor: Bruno Merk, University of Liverpool, UNITED KINGDOM

Received: September 28, 2017

Accepted: December 19, 2017

Published: January 12, 2018

Copyright: © 2018 Wohland et al. This is an open access article distributed under the terms of the [Creative Commons Attribution License](https://creativecommons.org/licenses/by/4.0/), which permits unrestricted use, distribution, and reproduction in any medium, provided the original author and source are credited.

Data Availability Statement: The study is based on publicly available data. ERAINT reanalysis can, for example, be downloaded from the ECMWF webpage. All other data sources (i.e. redispatch timeseries, wind park locations and renewable ninja PV and wind timeseries) are explicitly given in the manuscript. We furthermore provide our wind generation timeseries as Supplementary Material to the manuscript.

Funding: This work was supported by the Helmholtz Association (via the joint initiative "Energy System 2050 - A Contribution of the

Introduction

In the last years renewable generation capacity has grown strongly while costs have decreased substantially [1]. Since 1990, electricity generation in the OECD from wind has increased by a factor of 158 (to 600 TWh in 2016) and photovoltaic generation has increased by a factor of 11500 (to 218 TWh in 2016) [2]. The energy portfolio has thus changed substantially since the first publication of evidence for anthropogenic climate change by the Intergovernmental Panel of Climate Change [3].

In Germany, for example, the relative contribution of renewables to overall electricity generation reached roughly 33% in 2016 [4] and it is planned to increase further. Installed capacity in the German wind sector alone totalled roughly 50 GW in 2016. To give an impression of scale, this implies that electricity demand could theoretically be balanced by wind generation on a windy Saturday. Since consumption is higher during the week, current installed wind

Research Field Energy” and the grant no. VH-NG-1025 to D. Witthaut. The funders had no role in study design, data collection and analysis, decision to publish, or preparation of the manuscript.

Competing interests: The authors have declared that no competing interests exist.

capacities are not yet sufficient to cover weekday consumption entirely. However, this will likely be the case in a few years time. Onshore wind energy is widely considered a least-cost energy source and photovoltaic (PV) cells are about to enter this domain as well [5]. Additionally, in April 2017, a major German offshore wind park won acceptance of its bid without any subsidy at all which indicates the economic viability of the technology [6]. The relative attractiveness of wind and solar power plants in contrast to conventional power plants would still increase if large pre-tax subsidies for coal were included in the economic assessment [7].

This development is promising in the sense that fast decarbonization of the electricity system is economically feasible. A carbon-neutral electricity system is a fundamental ingredient in restricting climate change in line with the Paris Agreement which aims to avoid dangerous interference with the climate system [8, 9]. In order to reach the ambitious Paris goals, however, decarbonization needs to be accelerated and extended to sectors other than electricity [10–12]. Recent research has revealed that sector coupling and the usage of flexible loads allows the creation of functional and cost-efficient energy systems fueled by renewables only [13–16].

However, non-dispatchable and intermittent renewable electricity generation poses a challenge for grid integration. This challenge expands as renewable penetration increases and regulatory means to ensure system stability are needed (e.g., [17]). In Germany, renewable generation is given priority for grid feed-in. As the centers of, in particular, wind generation and electricity demand are spatially separated, large amounts of electricity need to be transmitted across the country. The north-south gradient of wind park allocations is presented in Fig 1. Since the transmission system has not been initially designed to serve this purpose, overloading and congestion in times of high renewable generation occurs (e.g., [18]). Adaption of the grid via new or enlarged transmission lines is planned, yet involves timescales of multiple years to decades.

According to the German Energy Act (‘Energiewirtschaftsgesetz’), Transmission System Operators (TSOs) and Distribution System Operators (DSOs) are in charge of maintaining energy system stability at all times [19]. In order to achieve this, four strategies can be applied: redispatch (shifting conventional generation in space by increasing and decreasing generation of conventional power plants in comparison to the initial market-based dispatch), usage of reserve plants (ramping up conventional power plants from a specific pool of plants, ‘Netzreserve’), feed-in management (reducing renewable generation, ‘Einspeisemanagement’) and lastly adaption measures (emergency measure to reduce generation, ‘Anpassungsmassnahmen’). These measures increase overall system costs because plant operators are compensated for having to reduce generation which is in addition to the costs of increasing generation elsewhere. As an exception, the adaption measures are not paid for since they are used in emergency cases only.

Germany saw a large increase in redispatch and feed-in management in 2015. Redispatch (sum of reductions and increases) was used to control about 15.4 TWh of electricity at a total cost of € 412 million, reflecting a threefold increase as compared to the previous year. Both the usage of reserve plants and feed-in management increased substantially as well [20]. The federal network agency for electricity, gas, telecommunications, post and railway (Bundesnetzagentur) lists a couple of reasons for these sharp increases: Besides the strong increase in wind capacity on land, the commissioning of two conventional power plants in the north and decommissioning of one nuclear power plant in the south added to the spatial mismatch of generation and load. This mismatch was exacerbated by substantial electricity exports to Austria. Moreover, grid extensions required temporal shutdown of grid elements and grid expansion in general was lagging behind schedule. As an aside, there is disagreement as to whether

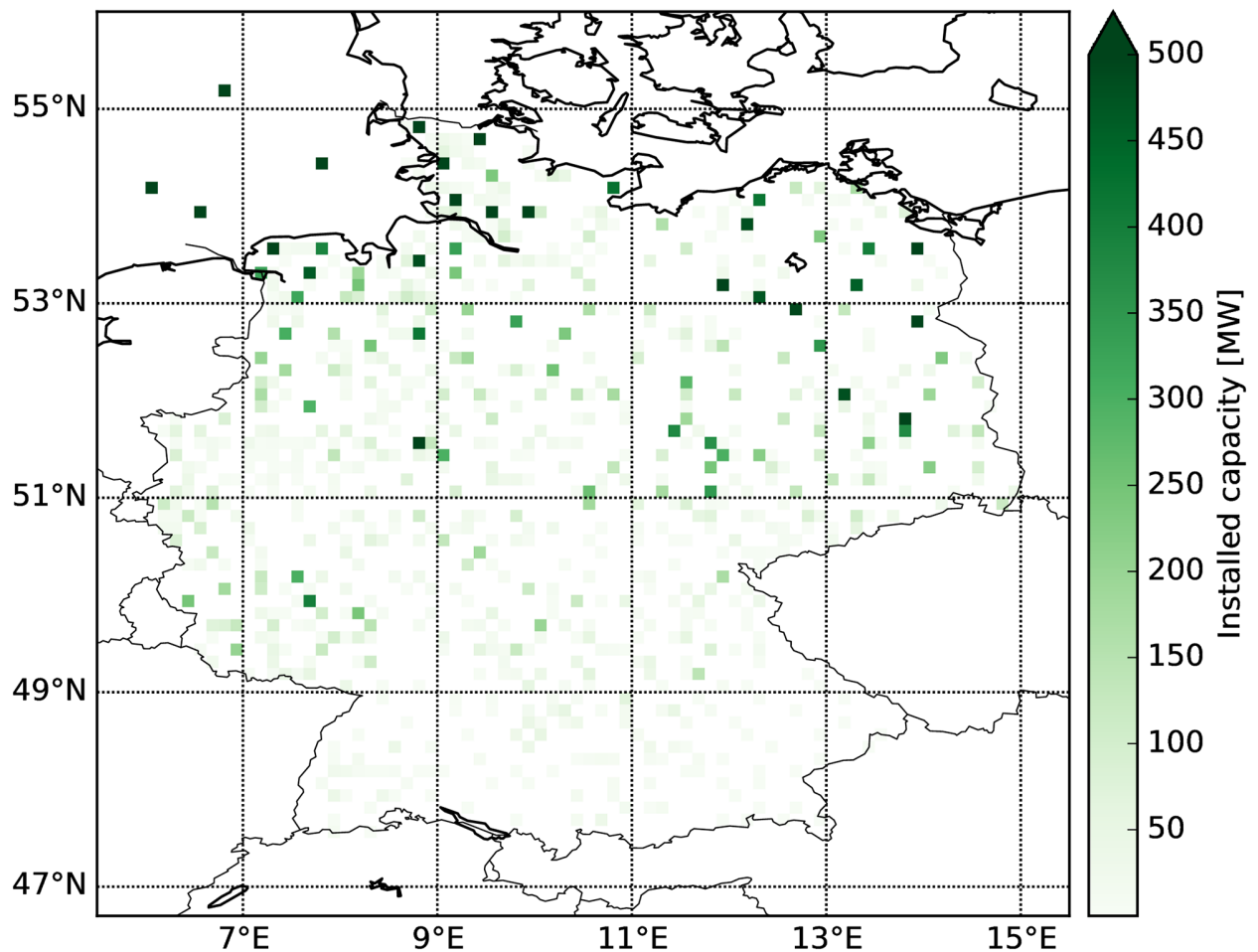


Fig 1. Allocation of wind parks used in this study. Note that an upper bound of 500 MW is set for the colorbar to ensure visibility of smaller parks. The biggest installed capacity per grid cell is around 1.4 GW. Wind park data is taken from the OPSD database for end of 2016 [53]. Offshore wind parks are not georeferenced in the input data and they are equally distributed to the four biggest operational offshore wind parks (Bard, Borkum Riffgrund, Amrumbank West, Sandbank).

<https://doi.org/10.1371/journal.pone.0190707.g001>

the grid is currently limiting the progress of the energy transition or whether it just sets a limit to exporting electricity from cheap coal-fired plants [21].

The issue of escalating grid management costs, including redispatch, even entered the public debate, particularly in late 2015 and January 2016, as numerous newspaper articles show (e.g., [22–25]). Since redispatch costs contribute to overall grid fees which accounted for around one fifth of the electricity price in 2016, they directly influence the energy costs of consumers [26]. This might have influenced the timing and content of modifications made to the Renewable Energy Act (“Erneuerbare Energien Gesetz”, EEG) in July 2016 [27]. The main goals of the modifications are to reduce subsidies via competition between investors and to provide a steering mechanism which controls the siting of new projects and also limits installed capacities. In particular, it includes a restriction for onshore wind parks in regions with a high probability of congestion while system-friendly installations are incentivized [27]. In other words, the allocation of new parks is regulated in order to reduce future increases of grid management costs. This part of the EEG reform can be seen as an attempt to reduce

redispatch costs by synchronizing the expansion of grids and renewable energy sources. Since the reform only entered into force in early 2017, it cannot have influenced the 2016 figures.

Unexpectedly, redispatch and feed-in management substantially decreased in 2016. The redispatch volume dropped to 11.5 TWh (25% reduction) at a cost of € 220 million (46% reduction). Although there was a small increase in reserve plant usage from 0.6 TWh to 1.2 TWh at the same time, it cannot explain the stronger change in redispatch because of its small magnitude.

What caused the substantial drop in redispatch costs? What does a likely evolution for the years ahead look like? In this paper, we address these questions based on the hypothesis that natural interannual variations of the wind resource caused the drop. There is a multitude of other potential reasons for redispatch. For example, other volatile types of renewable generation, namely solar photovoltaics, could lead to redispatch during times of high generation. Since the German electricity grid is currently being expanded in order to meet the changing needs, temporal shutdown of grid elements during this expansion might also contribute to redispatch. Moreover, electricity exports to neighboring countries can increase the loads and thereby exacerbate congestion. Scheduled downtimes of conventional plants for maintenance might have also played a role. All of these other reasons do not depend directly on the wind resource and are hence not dominant if our hypothesis can be validated. In contrast, if natural variability dominates the redispatch variability, it also has a strong impact on the technological and economic aspects of the energy transition. It would follow that more attention should be paid to assessing and dealing with climate-induced uncertainty. Therefore, the interplay of energy and climate in general would need further investigation. This is especially true since installed wind capacities will continue to increase.

Background

Wind fluctuates naturally on timescales from seconds to multiple years and so does wind power generation (e.g., [28–32]). In addition to understanding the variations themselves, it is important to quantify their impact on the power system and the associated costs. This is partly because the costs for renewable power generation are intrinsically linked to system costs [33, 34]. Focusing on the US, [34] found that installation and maintenance costs are not sufficient to characterize the actual costs of renewables if the renewable gross share exceeds around 30%. Instead, system costs from balancing mismatches between volatile generation and load need to be incorporated. Interestingly, 2015 was the first year during which renewables contributed more than 30% to German electricity production.

In principle, there are well-known options to reduce the vulnerability of the power system to wind variability. For example, wind fluctuations can be compensated by PV fluctuations thus smoothing the renewable generation time series [35]. Storage and intercountry balancing facilitate system stability [36–38]. Moreover, a multinational optimization of future wind park allocations would allow for a substantial reduction of volatility [39]. This effect is amplified under strong climate change due to changes in wind correlations [40]. In this context, it is also important to study the co-evolution of renewable generation and electricity consumption. In places where a substantial fraction of heating (or cooling) is provided by electricity, a strong annual cycle of electricity consumption is expected. [41] found that wind generation generally decreases synchronously with increasing consumption in winter in Great Britain, which implies that wind power is not well suited to cover winter demands there. However, as an exception to this tendency, they also report that the wind power generation partly recovers at the highest consumption events. Moreover, [42] identified a spatial shift in electricity consumption as a consequence of climate change. Its amplitude increases with the level of

greenhouse gas concentrations in the atmosphere. If carbon emissions continue to rise in the future, this effect will thus have to be accounted for in long-term energy system planning.

We expect wind generation to trigger redispatch events because it features a substantial spatial mismatch between generation and consumption in Germany. This is in contrast to PV, which is strongly deployed in the south and thus closer to major industries [18]. Moreover, the diurnal cycle of solar generation resembles the daily load profile in principle and is thus rather system friendly (at current levels of installed capacities). Wind power generation also varies stronger with wind speeds (cubic dependency within a certain range) than PV generation varies with incoming irradiance (linear dependency) [43]. We thus investigate the interrelation between redispatch and wind generation here.

Methods and data

Generally speaking, we used high-resolution weather data to calculate wind generation and investigate its relationship to the redispatch time series of 2015–2016. High-resolution weather data, in contrast to ex post generation data, has the advantage that long time series of multiple decades exist and thus natural climatic variability can be accounted for. Moreover, it isolates the impact of weather, which is masked by increases in capacity in ex post data.

Wind generation based on ERAINT

More precisely, we calculate wind generation $G_{\text{Wind}}(t)$ based on the ERAINT reanalysis on 0.11° angular resolution (roughly 12km) and 6 hour time steps [44]. ERAINT has a native grid spacing of 0.75° and the increase in resolution to 0.11° is achieved via bilinear interpolation done by the climate modelers. The dataset is available from 1979 and is regularly updated. In particular, the years 2015 and 2016 are included. Reanalysis data combines the advantages of model results and measurements in the sense that it (a) gives data on regular grids which (b) is also based on observations. It is for this reason that reanalyses have already been widely used for energy-related assessments [45–52].

The ERAINT reanalysis provides near-surface wind speeds. In order to calculate wind generation from near-surface wind speeds, a couple of assumptions are made. These assumptions are later justified by comparison with measured wind generation data (see Fig 2). Following the approach described in [40], we first assume a power-law vertical wind profile with a fixed exponent ($v(z) = v(z = 10\text{m}) \cdot \left(\frac{z}{10\text{m}}\right)^{\frac{1}{7}}$) and thereby neglect different stability regimes. Surface roughness is also neglected such that land cover and land-sea differences are not incorporated in the vertical scaling. They are, however, included in the derivation of the ERAINT dataset itself. Second, all wind turbines are assumed to be of the same kind and have a constant hub height of 80m. Third, wind park locations and sizes are assumed to be constant during the two-year period and taken as the end-2016 values from the Open Power System Database [53], see Fig 1. Keeping the installed wind capacities fixed allows us to isolate the effect of meteorological changes on wind power generation. Given that almost 10% new wind capacity was added in Germany during each of the last two years, the assumption of a steady state may seem crude. However, it is a well-accepted approach to assess non-stationary systems by studying steady-state cases first and include perturbations in time in a second step. Nevertheless, this approach can only be applied to relatively short periods of measured data. If the analysis was extended from a two-year measured time series to, for example, a ten-year series, the evolution of the wind parks became dominant and would have to be accounted for.

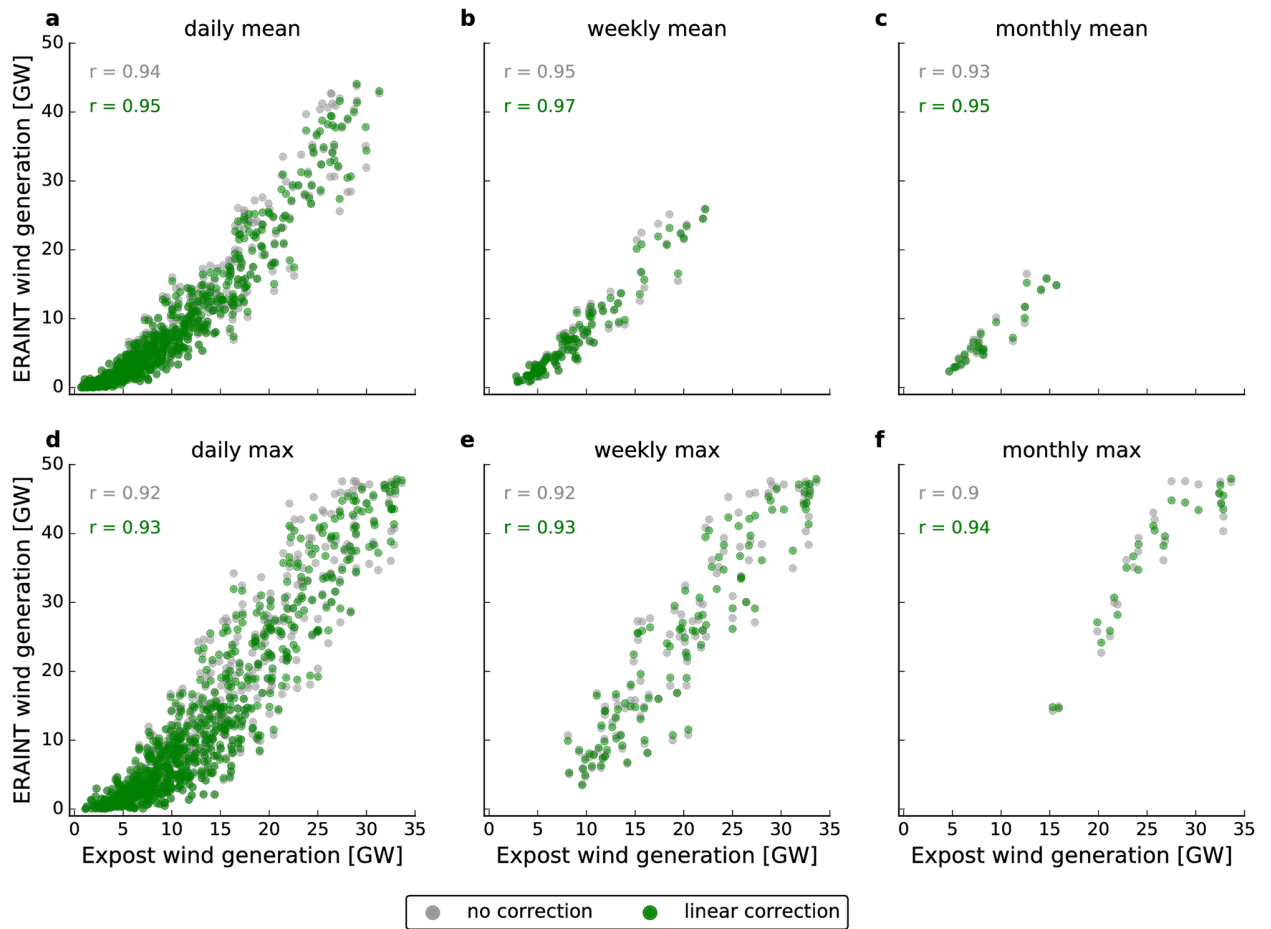


Fig 2. Scatter plots of ERAINT-based wind generation derived in this study versus expost wind generation as reported by German TSOs. Gray colors indicate ERAINT-based data that completely neglects capacity extension. Green denotes data that has been linearly adjusted for capacity increases. The Pearson correlation is given in the upper left area of each subplot. Columns represent different temporal aggregation levels ranging from daily (a,d) to weekly (b,e) and monthly (c,f) data. The upper line (a-c) shows mean values over the given interval while the lower line (d-f) represents maxima. All values are Germany-wide aggregates.

<https://doi.org/10.1371/journal.pone.0190707.g002>

Again following [40], wind speeds at hub height are translated into wind generation using a simple power curve:

$$P(v_H) = P_0 \begin{cases} 0, & \text{if } v_H < v_I \text{ or } v_H > v_0 \\ \frac{v_H^3 - v_I^3}{v_R^3 - v_I^3}, & \text{if } v_I \leq v_H < v_R \\ 1, & \text{if } v_R \leq v_H < v_0 \end{cases} \quad (1)$$

where v_H denotes wind velocity at hub height and $v_I = 3.5$ m/s, $v_R = 12$ m/s, $v_0 = 25$ m/s denote the cut-in, rated and cut-out velocity of the wind turbine, respectively. P_0 is the installed capacity in the grid cell.

Validation of generation timeseries

The validity of our approach is proven by comparison with measured data. In Fig 2, scatter plots of our wind generation time series from ERAINT versus ex post wind generation as reported by the four German TSOs are given. The ex post data was preprocessed by Open Power System Data and is freely available online [54]. It contains hourly German wind generation starting in summer 2009. However, we only use 2015 and 2016 here as these years are the focus of this investigation. We consider both different temporal sampling (from daily to monthly) and different sampling methods (mean or max values during the sampling period). Pearson correlations are always at least $r = 0.9$ and we hence conclude that our model captures the behavior of the real system sufficiently well. A linear correction of the ERAINT wind generation time series to include the effect of added capacities (given in green) further increases the correlations. For example, the correlation of daily means (Fig 2a) increases from $r = 0.94$ to $r = 0.95$. As correlations are already high without this correction, the remainder of this study is based on the uncorrected wind generation data. Furthermore, we observe a systematic deviation for small values of the ERAINT wind generation, where ex post data is higher. The direction of this mismatch can be explained by the spatial and temporal averaging in ERAINT: wind speeds within a 6-hour interval (or within a grid box) can well be above the cut-in velocity of the wind turbines even if the 6-hour (or grid box) average is lower. In fact, it is the very task of wind park planners to identify locations with above-average yields due to small scale effects (e.g. channeling or land-sea circulations). Wind turbines with a larger hub height and/or lower cut-in velocity further add to this mismatch. In contrast, in the realm of high generation, our approach yields higher values than the ex post analysis. Given that the ex post data accounts for curtailed generation that could not be fed into the grid (while our approach neglects curtailment), we expect such a tendency. In conclusion, we consider our approach well suited to capture system-wide effects and long-term developments while we also acknowledge the existence of systematic deviations of limited magnitude.

Redispatch data

The redispatch time series is published by the German TSOs and it is available through a transparency platform [55]. They have hourly resolution and we utilize the 2015 and 2016 data. We refer to the redispatch timeseries as $R(t)$. Although spatial information is included (such as the grid region that is affected or the plant that had to ramp up/down its generation), we consider the German aggregate only because we are interested in system-wide effects. In principle, redispatch can be subdivided into voltage-induced and current-induced redispatch. The latter is responsible for the majority of redispatch events. However, we found that our results are largely insensitive to restriction to current-induced redispatch and hence decided to evaluate all redispatch events. Moreover, the present analysis is based on redispatch *reduction* measures. In order to maintain the energy balance, a redispatch reduction measure requires ramping up plants elsewhere. Ramping up can be realized via redispatch increases or via reserve plants. As the latter strategy proved to be more efficient, the relative contribution of reserve plants increased during the period under investigation [56]. In focusing on reduction measures, we circumvent these regulatory changes. Redispatch events are associated with the point in time (day or week or month) when they were started.

Receiver operating characteristics (ROC)

The scope of this paper is to analyze the dependency of redispatch and wind generation on different time scales using both standard correlation measures and a binary performance measure. We employ the binary measure because it seems plausible that there is a threshold-like

behavior of the redispatch. If no wind park generates electricity, no wind-induced redispatch is expected. While wind speeds increase, parks ramp up their generation. As long as generation is small, no congestion in the grid occurs and hence there is still no redispatch. But once a certain level of wind power generation is exceeded, system stability would be affected and redispatch measures begin.

In order to test this hypothesis, we define a binary classifier R_{pred} as

$$R_{pred}(t) = \begin{cases} 1, & \text{if } G_{Wind}(t) \geq \sigma \\ 0, & \text{if } G_{Wind}(t) < \sigma \end{cases} \quad (2)$$

where $G_{Wind}(t)$ is ERAINT-based wind generation at time t (see above) and $\sigma \in [0, \max(G_{Wind}(t))]$ is a threshold value. Similarly, we define a binary redispatch time series $R_{bin}(t)$ as

$$R_{bin}(t) = \begin{cases} 1, & \text{if } R(t) \geq \theta \\ 0, & \text{if } R(t) < \theta \end{cases} \quad (3)$$

where θ is another threshold value and $R(t)$ denotes redispatch reduction at time t (see above). We choose θ such that a given percentage of $R(t)$ is considered an event in R_{bin} (i.e. $R_{bin} = 1$). This formulation allows for an assessment of, for example, the 75th percentile (i.e. 25% strongest redispatch events).

We assess the capability of the model (Eq 2) to reconstruct the binary redispatch time series (Eq 3) using ROC analysis [57]. In a ROC curve, the true positive rate (TPR) is plotted against the false positive rate (FPR). TPR is defined as the number of correctly identified redispatch events (TP, true positives) divided by the number of redispatch events (P, positives):

$$TPR = \frac{TP}{P}, \quad (4)$$

where

$$TP = \sum_t \begin{cases} 1, & \text{if } R_{pred}(t) = 1 \text{ and } R_{bin}(t) = 1 \\ 0, & \text{otherwise} \end{cases} \quad (5)$$

and

$$P = \sum_t R_{bin}(t). \quad (6)$$

Similarly, FPR is defined as the number of erroneously predicted redispatch events (FP, false positives) divided by the number of non-redispatch events (N, negatives):

$$FPR = \frac{FP}{N}, \quad (7)$$

where

$$FP = \sum_t \begin{cases} 1, & \text{if } R_{pred}(t) = 1 \text{ and } R_{bin}(t) = 0 \\ 0, & \text{otherwise} \end{cases} \quad (8)$$

and

$$N = \sum_t \begin{cases} 1, & \text{if } R_{\text{bin}}(t) = 0 \\ 0, & \text{otherwise} \end{cases} \quad (9)$$

A random classifier would create values along the diagonal, whereas a perfect classifier is given by a true positive rate of 1 and a false positive rate of 0. As a scalar performance measure, we calculate the area under the curve (AUC) which can be identified with ‘the possibility that the classifier will rank a randomly chosen positive instance higher than a randomly chosen negative instance’ [57]. The question we ask is: Given a certain redispatch threshold θ , how much of the binary redispatch time series can be explained based on the wind time series? Note that θ is predefined by us, while different values of σ are used to construct the ROC curve.

Circulation weather types (CWTs)

This approach allows us to relate our findings to large-scale meteorologic conditions. In order to study the connection of redispatch variability and wind generation variability, we investigate the dependency of redispatch on different typical pressure regimes over Germany. The approach is based on a CWT classification [58] of the ERAINT dataset. The classification is centered over Germany, is representative for Central Europe and comes with a daily temporal resolution. The method separates eight directional CWTs (North:N, Northeast:NE, East:E etc.) and four non-directional ones (Cyclonic:C, Mixed Cyclonic:Mixed C, Anticyclonic:AC, Mixed Anticyclonic:Mixed AC). Further explanations can be found in [59]. The methodology has repeatedly been applied for energy-related purposes [31, 40, 60, 61].

Results

Natural variability of wind generation

Fig 3 shows the time series of annual wind generation based on ERAINT. For validation purposes, it also includes version 1.1 wind generation data from renewables.ninja [45]. The renewables.ninja dataset starts in 1980 such that 1979 is only covered in our calculations. In Fig 3, renewables.ninja data is normalized such that its 2016 value coincides exactly with the ERAINT-based 2016 relative wind generation. There is quasi-perfect agreement between both time series in terms of the direction of changes between years. However, the magnitude of interannual changes in renewables.ninja is generally smaller. This may be due to differences in resolution. The underlying MERRA-2 reanalysis [62] has a fivefold coarser resolution than the ERAINT output used here, resulting in 25 ERAINT grid boxes per MERRA-2 grid box and thus a less realistic representation of spatial variability. This effect is, however, weakened or compensated for since [45] interpolated wind speeds to the wind park locations. However, the MERRA-2 reanalysis has a sixfold higher temporal resolution (hourly) such that a more realistic representation of fast changes is expected. Other differences in the approaches include that [45] accounted for different turbine types, interpolated vertically by fitting a logarithmic wind profile, applied a bias correction and used the wind park configuration of 2015.

Based on a detailed representation of the end-2015 wind parks, [50] followed a different approach to handle the coarse resolution of the MERRA reanalysis in deriving the EMHIRES dataset. They applied statistical downscaling over land to account for small-scale effects like complex topography and reported enhanced agreement with measured data. Over the ocean, no downscaling was applied because ocean surface conditions are sufficiently homogeneous.

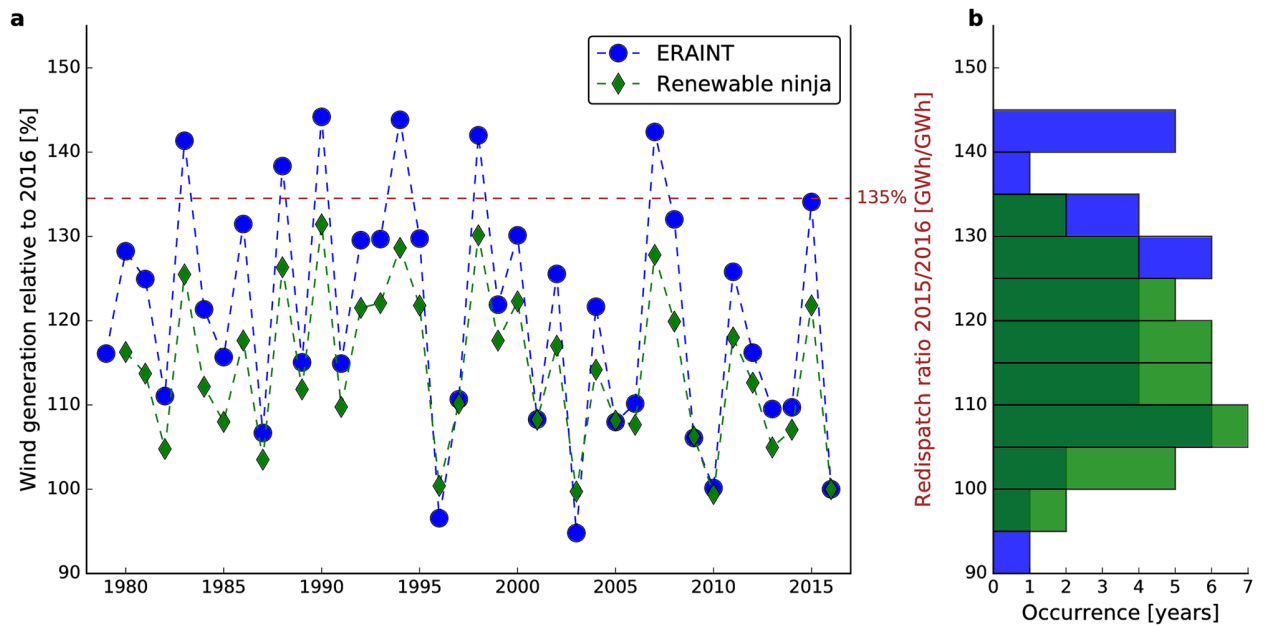


Fig 3. Natural variability of wind generation relative to 2016 in Germany. Time series of wind generation (a) and its distribution (b). Wind park configuration is kept constant throughout the entire timespan such that variations are solely rooted in wind variability. Blue denotes our own calculations and green indicates the renewables.ninja dataset [45]. The dashed brown line shows the ratio of 2015 to 2016 redispatch volume.

<https://doi.org/10.1371/journal.pone.0190707.g003>

The energy generated from the end-2016 German wind fleet fluctuates strongly in time (see Fig 3). In comparison to the weakest years, an additional 40% wind energy can be generated in the strongest years (30% based on renewables.ninja). In particular, there was substantially less wind generation in 2016 compared to 2015. This agrees perfectly with elevated redispatch costs in 2015: the ratio of 2015 to 2016 redispatch volume is given as a dashed brown line and fits extremely well with the ratio of 2015 to 2016 wind generation. Although the closeness of the agreement is likely a coincidence, it shows that both the direction of change and magnitude of ERAINT-based wind generation and measured redispatch volumes are in agreement.

Moreover, it is evident that 2016 was at the lower edge of all years covered in both datasets. If no regulatory changes were made to the system, an increase in redispatch would hence be very likely in 2017 (yet not guaranteed) and the TSO TenneT has already reported an increase of costs in spring 2017 [63]. Based on the historical record, the increase could even be higher than the drop from 2015 to 2016. However, this obviously depends on the actual characteristics of 2017 wind fields which we do not claim to forecast here.

Extent to which redispatch can be traced back to wind generation

In the following subsections, we quantify the dependency between redispatch energy and wind generation based on correlations and receiver operator characteristics. Furthermore, we investigate the underlying meteorological variability by means of circulation weather types.

Correlation analysis. We compare the wind generation and redispatch time series by evaluating three different correlation measures in Fig 4. They are the linear Pearson correlation, the non-linear Spearman's rank and Kendall's rank correlation (e.g., [64]). We assess different levels of temporal aggregation from daily to monthly. Within the resampling window, we either use the mean or the maximum value for both time series. This yields four possible combinations of averaging procedures as presented in the subplots (Fig 4a–4d).

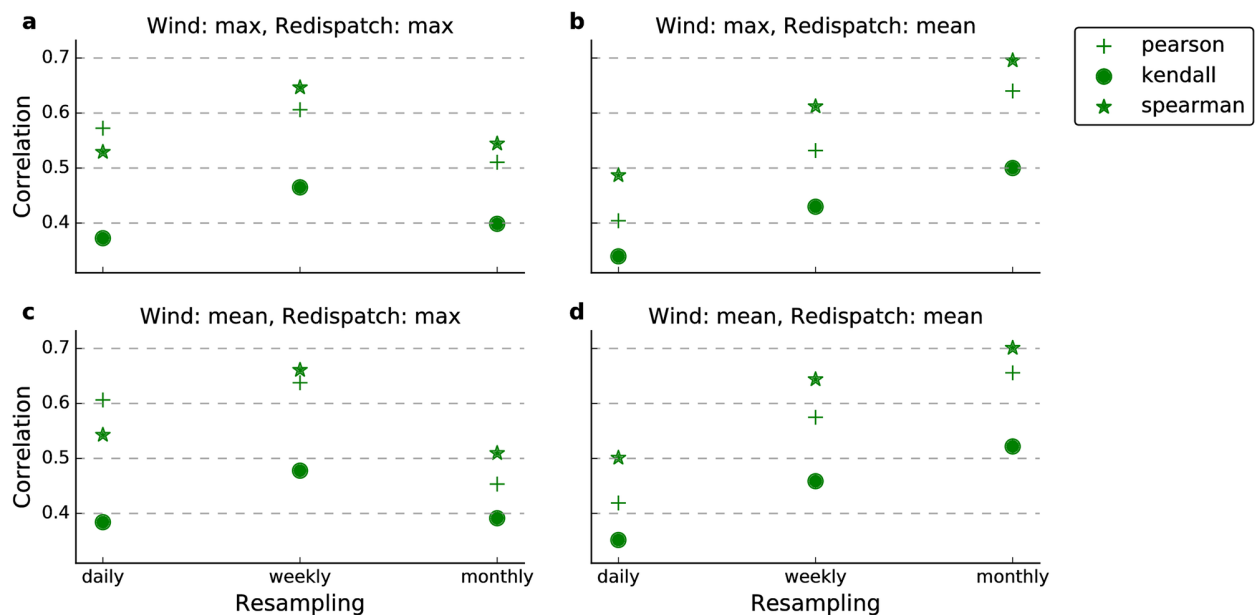


Fig 4. Correlation measures between wind generation and redispatch timeseries. Different panels show different temporal sampling methods. The upper line (a,b) uses maximum values of the wind generation time series, while the lower one (c,d) uses the mean. The left column (a,c) employs maximum values for redispatch resampling, while the right (b,d) is based on the mean. Markers denote the correlation measure employed (Kendall's τ , Spearman's ρ or the Pearson correlation coefficient r). Horizontal dashed lines are given for ease of interpretation.

<https://doi.org/10.1371/journal.pone.0190707.g004>

Generally, we report moderate to strong positive correlations. This statement holds for the linear Pearson measure as well as for the non-linear Spearman's and Kendall's rank correlations. The mean redispatch volume follows wind generation better if averaged over long periods (i.e. weeks or months) and reaches values of around 0.7 (Fig 4b and 4d). This tendency is in agreement with the results of the receiver operating characteristics (cf. below). In contrast, model performance for the redispatch maxima deteriorates on a monthly level (Fig 4a and 4c) indicating that the maximum redispatch events within a month are not strongly connected to the monthly wind generation. However, we want to highlight the monotonous increase in correlations for the mean redispatch and mean wind (Fig 4d) because it shows that mean wind generation can be translated into mean redispatch. Due to this monotony, we expect the seasonal and annual values to be even higher than the monthly values. We are thus confident that average wind generation has good predictive skill for average redispatch on a seasonal and annual basis.

Receiver operating characteristic (ROC) analysis. Based on a ROC analysis (see [Methods and data](#)), we report that the wind generation time series can partly explain redispatch as shown in Fig 5. Both the redispatch and the wind generation time series were resampled using the mean over a time interval (day or week) here. The analysis reveals that the classifier performs reasonably for daily values (Fig 5a). Showing AUC of 0.75 ± 0.02 , it is distinctly better than a random classification ($AUC = 0.5$) and hence there is clearly a signal of the wind generation in the daily series. On a weekly basis, the model performance is distinctly better (Fig 5b). This could be indicative of redispatch measures being scattered around the meteorological events causing them. Sometimes a redispatch is scheduled prior to the strong wind event, sometimes it lags behind. This scattering might be caused by uncertainties regarding the timing of strong wind events and it could also be affected by inertia of the conventional power system (such as long ramping times which require system operators to act well ahead of

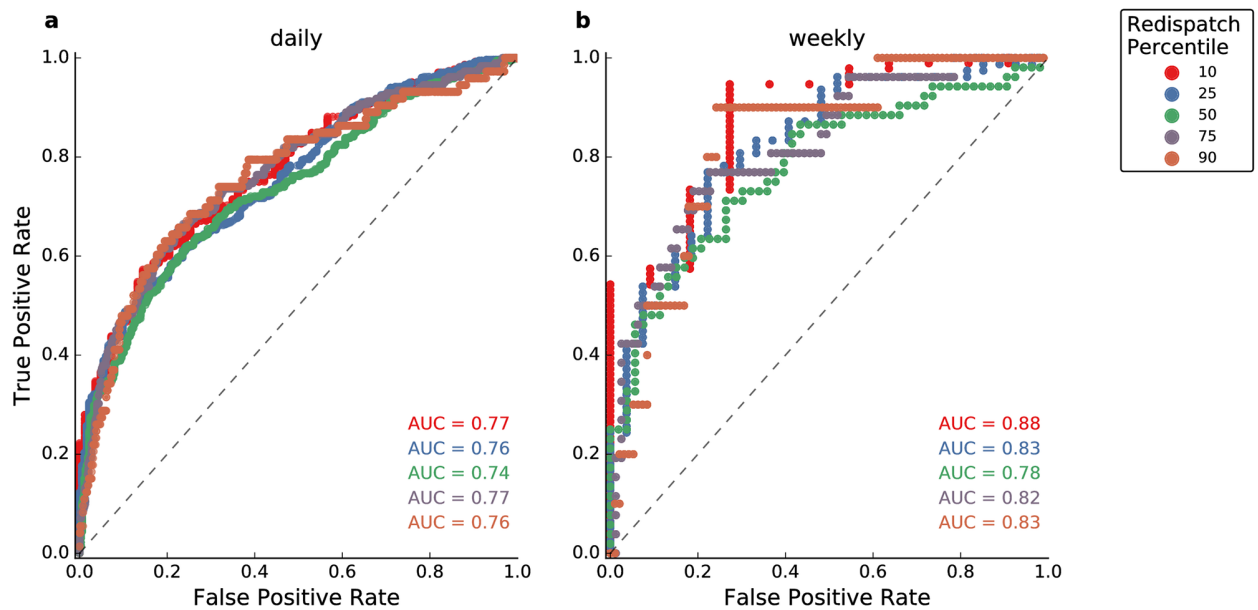


Fig 5. Receiver operator characteristic curve testing the performance of wind generation as a binary classifier for redispatch. Both wind and redispatch timeseries were resampled based on daily means (a) and weekly means (b).

<https://doi.org/10.1371/journal.pone.0190707.g005>

the actual event). While a mis-association of events on a daily basis follows, the coarser consideration based on weeks weakens this effect.

On the weekly basis, the classifier performs very well in separating the 10th percentile (AUC = 0.88). This means that we can isolate low redispatch weeks well. Very high redispatch weeks can also be separated well (AUC = 0.83 for the 90th percentile and AUC = 0.82 for the 75th percentile). Separating the 50th percentile, however, is not quite as reliable (AUC = 0.78).

The ROC analysis was also performed for resampling methods other than the mean (see [S1 File](#)). The results are mostly insensitive to changes in the sampling method with one interesting exception: the mean and max wind time series are skillful in determining the 90th percentile of max redispatch events on a daily basis (AUC = 0.89 and AUC = 0.88). In other words, the highest single redispatch event on a daily level can be attributed well to high wind generation, independent of the resampling method of the wind time series.

Variability of weather patterns. In the two preceding subsections, we showed that redispatch is related to the natural variability of near-surface wind conditions. Wind patterns over Europe in turn are associated with large-scale weather types. We therefore investigate the dependency of redispatch on CWTs (see [Methods and data](#)) by calculating the relative contributions of individual CWTs to overall redispatch.

CWTs of type southwest (SW), west (W) and northwest (NW) are characterized by high levels of redispatch (see [Fig 6](#)) and we refer to them collectively as westerly CWTs. 27.7% of redispatch happened during such westerly CWTs although they only occurred during 19.1% of the time. From a meteorological point of view, this finding is plausible since westerly CWTs are typically accompanied by relatively large pressure gradients and strong winds. The largest contributors to redispatch in absolute terms are anticyclonic (AC, 24.6%) and mixed anticyclonic (Mixed AC, 24.6%) configurations but they also occur most often (27.9% and 20.5%, respectively). Therefore, they are less redispatch-intense than westerly CWTs. Furthermore, the 95th percentile is highest for the western (W) CWT, indicating that the strongest

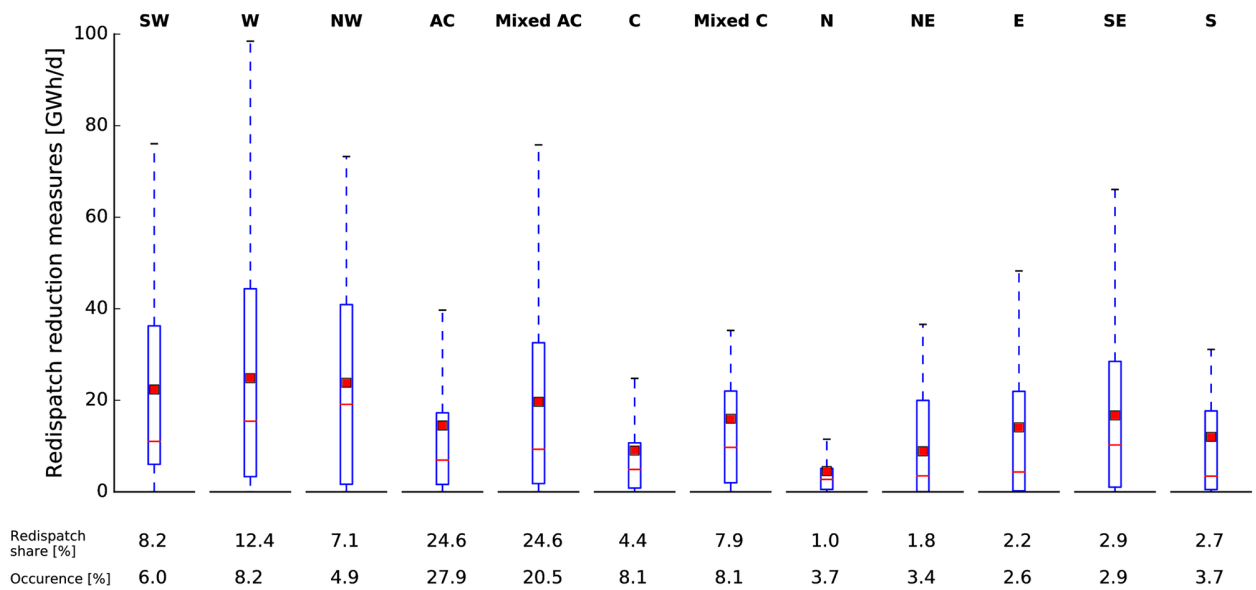


Fig 6. Daily redispatch decomposition for different CWTs. Each boxplot shows the statistics of 2015 to 2016 daily redispatch data differentiating between the CWT prevalent on the respective day. Blue boxes indicate the 25th to 75th percentile and error bars indicate the 5th to 95th percentile. A red thin line denotes the median while the mean is given as a red thick line. Below the plot, the share of redispatch and the relative occurrence of each CWT are given. Abbreviations denote the different CWTs. In addition to the directional CWTs (e.g. southwest, SW), there are anticyclonic (AC) and cyclonic (C) CWTs and also mixed versions of them.

<https://doi.org/10.1371/journal.pone.0190707.g006>

redispatch events occur during this CWT. Weak redispatch is to be expected under CWTs of type cyclonic (C), north (N), northeast (NE), east (E) and south (S). Interestingly, all distributions of redispatch reduction measures given a certain CWT have positive skewness since the average is always greater than the median.

Having found that westerly CWTs are characterized by elevated levels of redispatch, an assessment of their variability is insightful. Fig 7 shows that westerly CWTs prevail between 16% and 27% of the year in ERAINT, indicating a similar range of variability as for wind generation (cf. Fig 3). With respect to the last two years, it is clearly visible that 2015 had more westerly CWTs than 2016 in line with the downward shift of redispatch volume. Moreover, 2016 is among the lowest years on record in terms of westerly CWT occurrence. Only 1996 lies below and 1991 shows an almost identical value. The remaining 34 years on the record are characterized by higher values. Hence, 2016 has an exceptionally low occurrence of westerly CWTs.

Discussion

As outlined in the Results section, we assessed the variability of annual wind energy generation due to natural climatic variability. We found annual variability to be substantial and argue that it is an important characteristic of power systems with a high share of wind generation, in agreement with the literature (e.g., [65–67]). Capturing this variability does not necessarily introduce the need to use extensive time series of volatile renewable generation directly. Instead, a high level of the fluctuations can be reproduced by representative days based on a hierarchical clustering algorithm [68]. Representative days can reduce the computational costs substantially, although the required number of representative days depends on the question to be answered. [69] argued that benefits from more realistic time resolutions dominate over

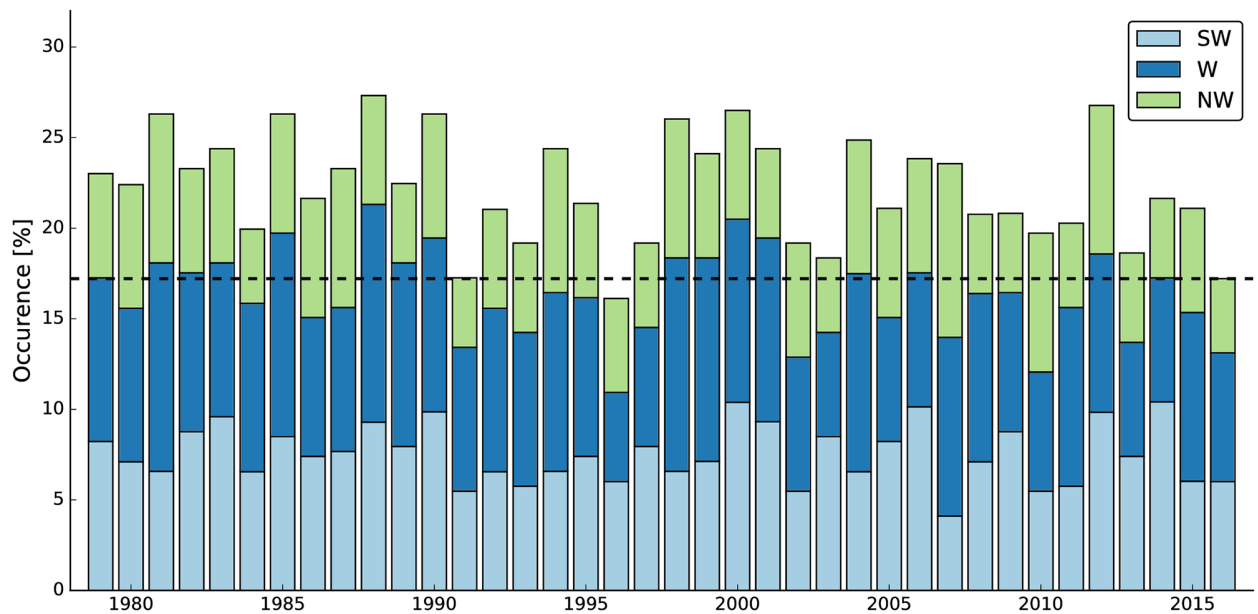


Fig 7. Variability of westerly CWTs. The occurrence is given in percent and is based on a daily CWT classification. The horizontal dashed line indicates the 2016 value and is plotted for convenience.

<https://doi.org/10.1371/journal.pone.0190707.g007>

benefits from the inclusion of techno-economic details. They thus advocate that model developers should aim at improving the temporal resolution.

In this context, it appears problematic that some state-of-the-art integrated assessment models [70, 71] and policy-relevant studies on a national level (e.g., [72]) still use single or representative weather years as input for their calculations. By ignoring interannual generation variability in the analysis, results can be biased. For example, Elsner et al. [72] use 2008 weather data although this particular year was above average in terms of mean wind generation (see Fig 3).

Moreover, in a climate system away from equilibrium, interannual wind variability may well change in the future. [31] showed that the climate change impact on interannual variability is subject to large inter-model spread in a large climate model ensemble (CMIP 5) and is hence substantially uncertain. However, the increase of inter-annual wind variability over Germany in downscaled climate projections can be as high as 30% under strong climate change at the end of the 21st century [73]. In a study aiming to establish a framework for economic assessments of climate change impacts on electricity generation, [74] also covered potential changes of inter-annual variability.

Supporting our results, a previous, non-peer-reviewed study, also found wind generation and redispatch to be substantially correlated [75]. Based on daily ex post data, they reported a Pearson correlation coefficient of 0.65 in the period April 2013 to March 2017. In comparison to our values, their correlation coefficient is generally higher, although we obtain comparable Pearson correlations for some sampling methods (see Fig 4a and 4c). This slight discrepancy is not surprising as the considered time intervals differ.

The relatively high correlations motivate a linear model of the redispatch

$$R(t) = a \cdot G_{\text{wind}}(t) + b, \tag{10}$$

where $R(t)$ is redispatch at time t , $G_{\text{wind}}(t)$ is wind generation, a and b are constants. Similar to

the correlations themselves, the skill will increase with coarser resampling and we expect good skill at monthly or even annual resampling.

In addition, Fig 3 shows that a 35% increase in annual wind generation translates into a 35% increase in the annual redispatch energy from 2016 to 2015:

$$\frac{R(2015)}{R(2016)} = \frac{G_{\text{Wind}}(2015)}{G_{\text{Wind}}(2016)}. \quad (11)$$

A combination of Eqs 10 and 11 yields $b = 0$. The ratio of redispatch between two weather years y_1 and y_2 is hence identical to the ratio of wind generation

$$\frac{R(y_1)}{R(y_2)} = \frac{a \cdot G_{\text{Wind}}(y_1) + b}{a \cdot G_{\text{Wind}}(y_2) + b} = \frac{a \cdot G_{\text{Wind}}(y_1)}{a \cdot G_{\text{Wind}}(y_2)} = \frac{G_{\text{Wind}}(y_1)}{G_{\text{Wind}}(y_2)}. \quad (12)$$

As a consequence, the range of variability of wind generation is identical to the range of redispatch variability. Fig 3 thus allows the latter to be quantified as between 95% and 145% of the 2016 values for the entire period covered by ERAINT. Admittedly, a stringent test of this statement would require freezing the electricity system as of today and studying its evolution in different weather years forever. This is obviously not feasible, leaving us with incomplete knowledge and leading to a standard verification dilemma of numerical models in the earth sciences [76]. Despite this and in line with [76], we argue that our finding provides a useful heuristic. It is furthermore obvious that this linear model is no longer valid after substantial changes are made to the current system, for example via transmission line extension or modifications of the guiding principle of the dispatch.

The CWT analysis revealed that redispatch is particularly high during westerly flows in line with meteorological intuition. In terms of planning, this finding could be employed beneficially for the overall system performance. For example, the addition of wind parks that are optimized to yield maximum output under non-westerly CWTs will have a substantially smaller effect on redispatch energy. However, the challenge here lies in the identification of suitable locations which still have sufficiently high capacity factors to prove economically viable.

It is furthermore interesting to note that the stochasticity of the wind generation signal can have a large influence on public perception. For example, the high redispatch costs in 2015 led to extensive media coverage across the entire spectrum from tabloids [77], online-only [78] and weekly magazines [23] to standard newspapers [22, 79, 80]. The language in the articles is heated, for example, it is stressed repeatedly that wind park operators are paid for idleness [24, 25] and the word ‘battle’ (‘Kampf’) is used in some headlines [78, 80]. During this public debate, the German minister for economics and energy, Sigmar Gabriel, is cited expecting a further 50% increase in overall grid-management costs to € 1.5 billion in 2016 [79]. In light of the lively public debate with respect to costs, it seems plausible that the strong wind year 2015 had an impact on policy making. In particular, it is questionable whether the 2016 EEG reform [27] would have been the same, had 2015 been a rather calm wind year.

Conclusion and policy implications

The German power system is undergoing a fast and drastic transition towards renewables. As an unpleasant side-effect, redispatch measures which aim at securing stability of the power grid have been used more extensively and reached an annual cost of around € 400 million in 2015. The subsequent year was characterized by a sharp decline of these costs. We report that much of this decline is rooted in natural climatic phenomena and is hence stochastic. Our

confidence in this finding is very high since our argumentation is based on multiple lines of evidence.

First, 2015 was a strong wind year in terms of annual wind power generation and 2016 was a weak one compared to a 37-year reanalysis time series. Second, ROC analysis suggests that mean wind generations are a suitable classifier to determine redispatch on long time scales (i.e. weeks and beyond). On these time scales there is even a considerable linear and rank correlation between the wind generation time series and the redispatch time series. Hence, a weak wind year translates into a low redispatch year. Third, redispatch is found to be high during westerly CWTs and those were more abundant in 2015 than in 2016.

Over the 37 years covered by the ERAINT dataset, we found annual wind generation variability ranging from 95% to 145% of the 2016 values. Following a simple linear model calibrated by the 2015 and 2016 redispatch energy, this also implies variability of redispatch energy in the same range.

It should be noted that all these conclusions are bound to the current power system. This is true both in terms of physical constraints and management aspects. While the physical constraints, such as transmission limits or locations of generators, are hard facts (i.e. evolve on long time scales of multiple years to decades), system management is, amongst others, subject to laws, regulations and economic incentives. Given political will, the latter can be adapted faster than the physical system. For example, including limited transmission capacities in deriving the dispatch would clearly be a game changer and may have the potential to reduce redispatch dramatically. This is because the current guiding principle of the dispatch is based on the assumption that its outcome is mostly compatible with transmission grid constraints. Conflicts with these constraints are assumed to be minor. If they occur, the redispatch will ensure system stability. However, given the continued addition of renewables, and the relatively slow pace of transmission line extensions, this assumption is challenged as congestion becomes more important. As a consequence, the minimization of power generation costs does not necessarily coincide with optimum operation of the power system. Instead of solving dispatch problems via the redispatch, it thus may be favorable to include the physical constraints into the dispatch as in optimal power flow algorithms (e.g., [81]). More generally, reducing the time window of the dispatch may have a positive effect due to less uncertain forecasts. Also, efficient carbon pricing may make gas plants economically superior to coal plants and hence decrease average ramping times in the dispatch.

In order to understand redispatch more precisely, a possible next step would be to resolve the national grid explicitly. This would allow congestion owing to renewable generation to be simulated and subsequently compared to the redispatch energy reported by TSOs. It would also be interesting to expand the assessment to the time series of the feed-in management and the grid reserve. Moreover, the role of electricity exports could be assessed. As hypothesized earlier, redispatch could be exacerbated by exports that introduce additional loads to the electricity grid in times of high renewable generation.

Independent of the exact design of the future power system, variability will be a fundamental property of it. This is true for any power system based on renewables and by no means limited to the German example studied here. Therefore, we suggest a stronger consideration of uncertainty and natural variability in any assessment of the current energy system. As public perception can be affected strongly by single events like the 2015 peak in redispatch costs, short-sighted reactions might follow. They are to be avoided because hectic weakening of renewable expansion in times of high redispatch years and strengthening of renewable expansion during low redispatch years may substantially harm the energy transition. This is because renewable energy companies need stable ground to build on [82]. There is hence a requirement for robust decision making [83] incorporating interannual variability of the wind

resources. In order for science to be helpful in this, research should aim at better understanding and quantifying climate-induced variability on different time scales including years and decades. Additionally, closer collaboration between energy and climate modelers is urgently needed.

Supporting information

S1 File. ROC analyses under different resampling methods.
(PDF)

S2 File. Wind generation time series.
(CSV)

Acknowledgments

We thank Ju. Weber for valuable comments and her effort in proofreading the manuscript.

Funding: This work was supported by the Helmholtz Association (via the joint initiative “Energy System 2050—A Contribution of the Research Field Energy” and the grant no. VH-NG-1025 to D. W.).

Author Contributions

Conceptualization: Jan Wohland, Dirk Witthaut.

Formal analysis: Jan Wohland.

Investigation: Jan Wohland, Mark Reyers, Carolin Märker.

Methodology: Jan Wohland, Dirk Witthaut.

Resources: Mark Reyers.

Software: Jan Wohland.

Supervision: Dirk Witthaut.

Visualization: Jan Wohland.

Writing – original draft: Jan Wohland.

Writing – review & editing: Jan Wohland, Mark Reyers, Carolin Märker, Dirk Witthaut.

References

1. Lazard. Lazard’s leveled costs of energy analysis—version 10.0; 2016.
2. IEA. Renewables Information: Overview. International Energy Agency; 2017.
3. IPCC. CLIMATE CHANGE—The IPCC Scientific Assessment. Bracknell (UK): Intergovernmental Panel on Climate Change; 1990.
4. Fraunhofer ISE. Jaehrlicher Anteil erneuerbarer Energien an der Stromerzeugung in Deutschland, https://www.energy-charts.de/ren_share_de.htm?source=ren-share&period=annual&year=all (assessed on 20/07/17); 2017. Available from: https://www.energy-charts.de/ren_share_de.htm?source=ren-share&period=annual&year=all.
5. Milligan M, Frew B, Kirby B, Schuerger M, Clark K, Lew D, et al. Alternatives No More: Wind and Solar Power Are Mainstays of a Clean, Reliable, Affordable Grid. *IEEE Power and Energy Magazine*. 2015; 13(6):78–87. <https://doi.org/10.1109/MPE.2015.2462311>
6. Bundesnetzagentur. WindSeeG—1. Ausschreibung fuer bestehende Projekte nach § 26 WindSeeG. Bonn: Bundesnetzagentur; 2017.
7. Coady DP, Parry I, Sears L, Shang B. How large are global energy subsidies? IMF Working Paper. 2015;WP/15/105.

8. UNFCCC. Adoption of the Paris Agreement. 2015;FCCC/CP/2015/10/Add.1.
9. Schlessner CF, Rogelj J, Schaeffer M, Lissner T, Licker R, Fischer EM, et al. Science and policy characteristics of the Paris Agreement temperature goal. *Nature Climate Change*. 2016; 6(9):827–835. <https://doi.org/10.1038/nclimate3096>
10. Rockstroem J, Gaffney O, Rogelj J, Meinshausen M, Nakicenovic N, Schellnhuber HJ. A roadmap for rapid decarbonization. *Science*. 2017; 355(6331):1269. <https://doi.org/10.1126/science.aah3443>
11. Rogelj J, den Elzen M, Hoehne N, Fransen T, Fekete H, Winkler H, et al. Paris Agreement climate proposals need a boost to keep warming well below 2 degree C. *Nature*. 2016; 534(7609):631–639. <https://doi.org/10.1038/nature18307> PMID: 27357792
12. Rogelj J, Luderer G, Pietzcker RC, Kriegler E, Schaeffer M, Krey V, et al. Energy system transformations for limiting end-of-century warming to below 1.5°C. *Nature Climate Change*. 2015; 5(6):519–527. <https://doi.org/10.1038/nclimate2572>
13. Gerhardt N, Boettger D, Trost T, Scholz A, Pape C, Gerlach AK, et al. Analyse eines europäischen -95%-Klimaszenarios über mehrere Wetterjahre. Kassel: Fraunhofer IWES; 2017.
14. Jacobson MZ, Delucchi MA, Cameron MA, Frew BA. Low-cost solution to the grid reliability problem with 100% penetration of intermittent wind, water, and solar for all purposes. *Proceedings of the National Academy of Sciences*. 2015; 112(49):15060–15065. <https://doi.org/10.1073/pnas.1510028112>
15. Barbosa LdSNS, Bogdanov D, Vainikka P, Breyer C. Hydro, wind and solar power as a base for a 100% Renewable Energy supply for South and Central America. *PloS one*. 2017; 12(3):e0173820. <https://doi.org/10.1371/journal.pone.0173820> PMID: 28329023
16. Gulagi A, Choudhary P, Bogdanov D, Breyer C. Electricity system based on 100% renewable energy for India and SAARC. *PLOS ONE*. 2017; 12(7):1–27. <https://doi.org/10.1371/journal.pone.0180611>
17. Huber M, Dimkova D, Hamacher T. Integration of wind and solar power in Europe: Assessment of flexibility requirements. *Energy*. 2014; 69:236–246. <https://doi.org/10.1016/j.energy.2014.02.109>
18. Pesch T, Allelein HJ, Hake JF. Impacts of the transformation of the German energy system on the transmission grid. *The European Physical Journal Special Topics*. 2014; 223(12):2561–2575. <https://doi.org/10.1140/epjst/e2014-02214-y>
19. EnWG. Energiewirtschaftsgesetz vom 7. Juli 2005 (BGBl. I S. 1970, 3621), das zuletzt durch Artikel 2 Absatz 6 des Gesetzes vom 20. Juli 2017 (BGBl. I S. 2808) geändert worden ist; 2005.
20. Bundesnetzagentur. 3. Quartalsbericht 2015 zu Netz- und Systemsicherheitsmaßnahmen. Bonn: Bundesnetzagentur; 2016.
21. Kemfert C, Gerbaulet C, Hirschhausen Cv. Stromnetze und Speichertechnologien fuer die Energiewende eine Analyse mit Bezug zur Diskussion des EEG 2016; Gutachten im Auftrag der Hermann-Scheer-Stiftung. Berlin: DIW Berlin, Deutsches Institut fuer Wirtschaftsforschung; 2016. Available from: <http://hdl.handle.net/10419/142790>.
22. Welt. Kunden zahlen fuer Troedel-Energiewende kraeftig drauf. <https://www.welt.de/wirtschaft/article148012515/Kunden-zahlen-fuer-Troedel-Energiewende-kraeftig-drauf.html> (published 25/10/15); 2015.
23. Focus Money. Sigmar Gabriel hat Energiewende-Kosten nicht im Griff. http://www.focus.de/finanzen/news/wirtschaftsticker/industrie-gabriel-hat-energiewende-kosten-nicht-im-griff_id_5016090.html (published on 15/10/2015); 2015.
24. Welt. Stromkunden zahlen Millionen fuer Phantom-Energie. <https://www.welt.de/wirtschaft/article148700408/Stromkunden-zahlen-Millionen-fuer-Phantom-Energie.html> (published on 10/11/15); 2015.
25. Handelsblatt. Es geht um Milliarden. <http://www.cdu-fuchs.de/presse/detailansicht/datum/2016/januar/12/artikel/michael-fuchs-es-geht-um-milliarden.html> (published 12.01.2016); 2016.
26. Bundesnetzagentur. Monitoringbericht 2016. Bonn: Bundesnetzagentur; 2016.
27. Bundestag. Entwurf eines Gesetzes zur Einfuehrung von Ausschreibungen fuer Strom aus erneuerbaren Energien und zu weiteren Aenderungen des Rechts der erneuerbaren Energien; 2016.
28. Milan P, Waechter M, Peinke J. Turbulent Character of Wind Energy. *Physical Review Letters*. 2013; 110(13). <https://doi.org/10.1103/PhysRevLett.110.138701> PMID: 23581387
29. Peings Y, Magnusdottir G. Forcing of the wintertime atmospheric circulation by the multidecadal fluctuations of the North Atlantic ocean. *Environmental Research Letters*. 2014; 9(3):034018. <https://doi.org/10.1088/1748-9326/9/3/034018>
30. Farneti R. Modelling interdecadal climate variability and the role of the ocean. *Wiley Interdisciplinary Reviews: Climate Change*. 2017; 8(1):e441.

31. Reyers M, Moemken J, Pinto JG. Future changes of wind energy potentials over Europe in a large CMIP5 multi-model ensemble. *International Journal of Climatology*. 2016; 36(2):783–796. <https://doi.org/10.1002/joc.4382>
32. Weber J, Zachow C, Witthaut D. Modeling long correlation times using additive binary Markov chains: applications to wind generation time series. *arXiv preprint arXiv:171103294*. 2017.
33. Ueckerdt F, Hirth L, Luderer G, Edenhofer O. System LCOE: What are the costs of variable renewables? *Energy*. 2013; 63:61–75. <https://doi.org/10.1016/j.energy.2013.10.072>
34. Becker S, Frew BA, Andresen GB, Jacobson MZ, Schramm S, Greiner M. Renewable build-up pathways for the US: Generation costs are not system costs. *Energy*. 2015; 81:437–445. <https://doi.org/10.1016/j.energy.2014.12.056>
35. Becker S, Frew BA, Andresen GB, Zeyer T, Schramm S, Greiner M, et al. Features of a fully renewable US electricity system: Optimized mixes of wind and solar PV and transmission grid extensions. *Energy*. 2014; 72:443–458. <https://doi.org/10.1016/j.energy.2014.05.067>
36. Schlachtberger DP, Brown T, Schramm S, Greiner M. The benefits of cooperation in a highly renewable European electricity network. *Energy*. 2017; 134:469–481. <https://doi.org/10.1016/j.energy.2017.06.004>
37. Weitemeyer S, Kleinhans D, Vogt T, Agert C. Integration of Renewable Energy Sources in future power systems: The role of storage. *Renewable Energy*. 2015; 75:14–20. <https://doi.org/10.1016/j.renene.2014.09.028>
38. Rasmussen MG, Andresen GB, Greiner M. Storage and balancing synergies in a fully or highly renewable pan-European power system. *Energy Policy*. 2012; 51:642–651. <https://doi.org/10.1016/j.enpol.2012.09.009>
39. Grams CM, Beerli R, Pfenninger S, Staffell I, Wernli H. Balancing Europe's wind-power output through spatial deployment informed by weather regimes. *Nature Climate Change*. 2017; <https://doi.org/10.1038/nclimate3338> PMID: 28781614
40. Wohland J, Reyers M, Weber J, Witthaut D. More homogeneous wind conditions under strong climate change decrease the potential for inter-state balancing of electricity in Europe. *Earth System Dynamics*. 2017; 8(4):1047–1060. <https://doi.org/10.5194/esd-8-1047-2017>
41. Thornton HE, Scaife AA, Hoskins BJ, Brayshaw DJ. The relationship between wind power, electricity demand and winter weather patterns in Great Britain. *Environmental Research Letters*. 2017; 12(6):064017. <https://doi.org/10.1088/1748-9326/aa69c6>
42. Wenz L, Levermann A, Auffhammer M. North—south polarization of European electricity consumption under future warming. *Proceedings of the National Academy of Sciences*. 2017; 114(38):E7910–E7918. <https://doi.org/10.1073/pnas.1704339114>
43. Mavromatakis F, Makrides G, Georghiou G, Pothrakis A, Franghiadakis Y, Drakakis E, et al. Modeling the photovoltaic potential of a site. *Renewable Energy*. 2010; 35(7):1387–1390. <https://doi.org/10.1016/j.renene.2009.11.010>
44. Dee DP, Uppala SM, Simmons AJ, Berrisford P, Poli P, Kobayashi S, et al. The ERA-Interim reanalysis: configuration and performance of the data assimilation system. *Quarterly Journal of the Royal Meteorological Society*. 2011; 137(656):553–597. <https://doi.org/10.1002/qj.828>
45. Staffell I, Pfenninger S. Using bias-corrected reanalysis to simulate current and future wind power output. *Energy*. 2016; 114:1224–1239. <https://doi.org/10.1016/j.energy.2016.08.068>
46. Andresen GB, Søndergaard AA, Greiner M. Validation of Danish wind time series from a new global renewable energy atlas for energy system analysis. *Energy*. 2015; 93:1074–1088.
47. Pfenninger S, Gauché P, Lilliestam J, Damerou K, Wagner F, Patt A. Potential for concentrating solar power to provide baseload and dispatchable power. *Nature Climate Change*. 2014; 4(8):689–692. <https://doi.org/10.1038/nclimate2276>
48. Jerez S, Trigo RM, Sarsa A, Lorente-Plazas R, Pozo-Vázquez D, Montávez JP. Spatio-temporal Complementarity between Solar and Wind Power in the Iberian Peninsula. *Energy Procedia*. 2013; 40:48–57. <https://doi.org/10.1016/j.egypro.2013.08.007>
49. Jerez S, Trigo RM, Vicente-Serrano SM, Pozo-Vázquez D, Lorente-Plazas R, Lorenzo-Lacruz J, et al. The Impact of the North Atlantic Oscillation on Renewable Energy Resources in Southwestern Europe. *Journal of Applied Meteorology and Climatology*. 2013; 52(10):2204–2225. <https://doi.org/10.1175/JAMC-D-12-0257.1>
50. González-Aparicio I, Monforti F, Volker P, Zucker A, Careri F, Huld T, et al. Simulating European wind power generation applying statistical downscaling to reanalysis data. *Applied Energy*. 2017; 199:155–168. <https://doi.org/10.1016/j.apenergy.2017.04.066>

51. Ely CR, Brayshaw DJ, Methven J, Cox J, Pearce O. Implications of the North Atlantic Oscillation for a UK-Norway Renewable power system. *Energy Policy*. 2013; 62:1420–1427. <https://doi.org/10.1016/j.enpol.2013.06.037>
52. Cannon DJ, Brayshaw DJ, Methven J, Coker PJ, Lenaghan D. Using reanalysis data to quantify extreme wind power generation statistics: A 33 year case study in Great Britain. *Renewable Energy*. 2015; 75:767–778. <https://doi.org/10.1016/j.renene.2014.10.024>
53. OPSD. Renewable power plants, https://data.open-power-system-data.org/renewable_power_plants/ (version 16/02/17); 2017.
54. OPSD. Data Platform—Time series, https://data.open-power-system-data.org/time_series/2017-07-09/ (accessed 18/07/17); 2017.
55. Netztransparenz. Netztransparenz Redispatch, <https://www.netztransparenz.de/EnWG/Redispatch> (accessed 02/06/17); 2017.
56. Bundesnetzagentur. Quartalsbericht zu Netz- und Systemsicherheitsmaßnahmen - Viertes Quartal und Gesamtjahr 2016. Bonn: Bundesnetzagentur; 2017.
57. Fawcett T. An introduction to ROC analysis. *Pattern Recognition Letters*. 2006; 27(8):861–874. <https://doi.org/10.1016/j.patrec.2005.10.010>
58. Jones PD, Hulme M, Briffa KR. A comparison of Lamb circulation types with an objective classification scheme. *International Journal of Climatology*. 1993; 13(6):655–663. <https://doi.org/10.1002/joc.3370130606>
59. Reyers M, Pinto JG, Moemken J. Statistical-dynamical downscaling for wind energy potentials: evaluation and applications to decadal hindcasts and climate change projections. *International Journal of Climatology*. 2015; 35(2):229–244. <https://doi.org/10.1002/joc.3975>
60. Moemken J, Reyers M, Buldmann B, Pinto JG. Decadal predictability of regional scale wind speed and wind energy potentials over Central Europe. *Tellus A: Dynamic Meteorology and Oceanography*. 2016; 68(1):29199. <https://doi.org/10.3402/tellusa.v68.29199>
61. Weber J, Wohland J, Reyers M, Moemken J, Hoppe C, Pinto JG, et al. Impact of climate change on backup and storage needs in a wind-dominated European power system. *arXiv preprint arXiv:1711.05569*. 2017.
62. Molod A, Takacs L, Suarez M, Bacmeister J. Development of the GEOS-5 atmospheric general circulation model: evolution from MERRA to MERRA2. *Geoscientific Model Development*. 2015; 8(5):1339–1356. <https://doi.org/10.5194/gmd-8-1339-2015>
63. Heise. Deutlich hoehere Kosten fuer Noteingriffe ins Stromnetz. <https://www.heise.de/newsticker/meldung/Deutlich-hoehere-Kosten-fuer-Noteingriffe-ins-Stromnetz-3755090.html> (published on 24/06/17); 2017.
64. Roenz B, Foerster E. Regressions- und Korrelationsanalyse: Grundlagen, Methoden, Beispiele. Wiesbaden: Gabler; 1992.
65. Pfenninger S. Dealing with multiple decades of hourly wind and PV time series in energy models: A comparison of methods to reduce time resolution and the planning implications of inter-annual variability. *Applied Energy*. 2017; 197:1–13. <https://doi.org/10.1016/j.apenergy.2017.03.051>
66. Bloomfield HC, Brayshaw DJ, Shaffrey LC, Coker PJ, Thornton HE. Quantifying the increasing sensitivity of power systems to climate variability. *Environmental Research Letters*. 2016; 11(12):124025. <https://doi.org/10.1088/1748-9326/11/12/124025>
67. Rodriguez RA, Becker S, Andresen GB, Heide D, Greiner M. Transmission needs across a fully renewable European power system. *Renewable Energy*. 2014; 63:467–476. <https://doi.org/10.1016/j.renene.2013.10.005>
68. Nahmacher P, Schmid E, Hirth L, Knopf B. Carpe diem: A novel approach to select representative days for long-term power system modeling. *Energy*. 2016; 112:430–442. <https://doi.org/10.1016/j.energy.2016.06.081>
69. Poncelet K, Delarue E, Six D, Duerinck J, D'haeseleer W. Impact of the level of temporal and operational detail in energy-system planning models. *Applied Energy*. 2016; 162:631–643. <https://doi.org/10.1016/j.apenergy.2015.10.100>
70. Ueckerdt F, Pietzcker R, Scholz Y, Stetter D, Giannousakis A, Luderer G. Decarbonizing global power supply under region-specific consideration of challenges and options of integrating variable renewables in the REMIND model. *Energy Economics*. 2017; 64:665–684. <https://doi.org/10.1016/j.eneco.2016.05.012>
71. Pietzcker RC, Ueckerdt F, Carrara S, de Boer HS, Després J, Fujimori S, et al. System integration of wind and solar power in integrated assessment models: A cross-model evaluation of new approaches. *Energy Economics*. 2017; 64:583–599. <https://doi.org/10.1016/j.eneco.2016.11.018>

72. Elsner P, Fishedick M, Sauer DU, editors. Flexibilitaetskonzepte fuer die Stromversorgung 2050: Technologien—Szenarien—Systemzusammenhänge. Schriftenreihe Energiesysteme der Zukunft. Muenchen: acatech - Deutsche Akademie der Technikwissenschaften e. V; 2015.
73. Moemken J, Reyers M, Feldmann H, Pinto JG. Wind speed and wind energy potentials in EURO-CORDEX ensemble simulations: evaluation and future changes. submitted. 2017.
74. Hdidouan D, Staffell I. The impact of climate change on the levelised cost of wind energy. *Renewable Energy*. 2017; 101:575–592. <https://doi.org/10.1016/j.renene.2016.09.003>
75. BDEW. Redispatch in Deutschland—Auswertung der Transparenzdaten. Berlin: Bundesverband der Energie und Wasserwirtschaft; 2017.
76. Oreskes N, Shrader-Frechette K, Belitz K, others. Verification, validation, and confirmation of numerical models in the earth sciences. *Science*. 1994; 263(5147):641–646. <https://doi.org/10.1126/science.263.5147.641> PMID: 17747657
77. Bild. Energie Irrsinn: Warum wir mehr fuer Strom zahlen, den wir nicht nutzen. <http://www.bild.de/politik/inland/strompreis/mehr-zahlen-fuer-ungenutzen-strom-45590608.bild.html> (published 29/04/16); 2016.
78. Heise. Kampf gegen Stromnetz-Blackout: Rekordkosten von einer Milliarde Euro. <https://www.heise.de/newsticker/meldung/Kampf-gegen-Stromnetz-Blackout-Rekordkosten-von-einer-Milliarde-Euro-3072872.html> (published 17.01.2016); 2016.
79. Handelsblatt. Hochspannung im Stromnetz. <http://www.handelsblatt.com/unternehmen/energie/handelsblatt-energietagung-hochspannung-im-stromnetz/12862992.html> (published 21/01/16); 2016.
80. FAZ. Kampf gegen Stromausfaelle so teuer wie noch nie. <http://www.faz.net/aktuell/wirtschaft/energiepolitik/kampf-gegen-stromausfaelle-so-teuer-wie-noch-nie-14018769.html> (published 17/01/16); 2016.
81. Hoersch J, Ronellenfitch H, Witthaut D, Brown T. Linear Optimal Power Flow Using Cycle Flows. arXiv preprint arXiv:17041881. 2017.
82. Smith Stegen K, Seel M. The winds of change: How wind firms assess Germany's energy transition. *Energy Policy*. 2013; 61:1481–1489. <https://doi.org/10.1016/j.enpol.2013.06.130>
83. Lempert RJ, Popper SW, Bankes SC. Robust decision making: coping with uncertainty. *The Futurist*. 2010; 44(1):47.

Supplement

S1: ROC analyses under different resampling methods

Supporting information to "Natural wind variability triggered drop in German redispatch volume and costs from 2015 to 2016" by Wohland et al.

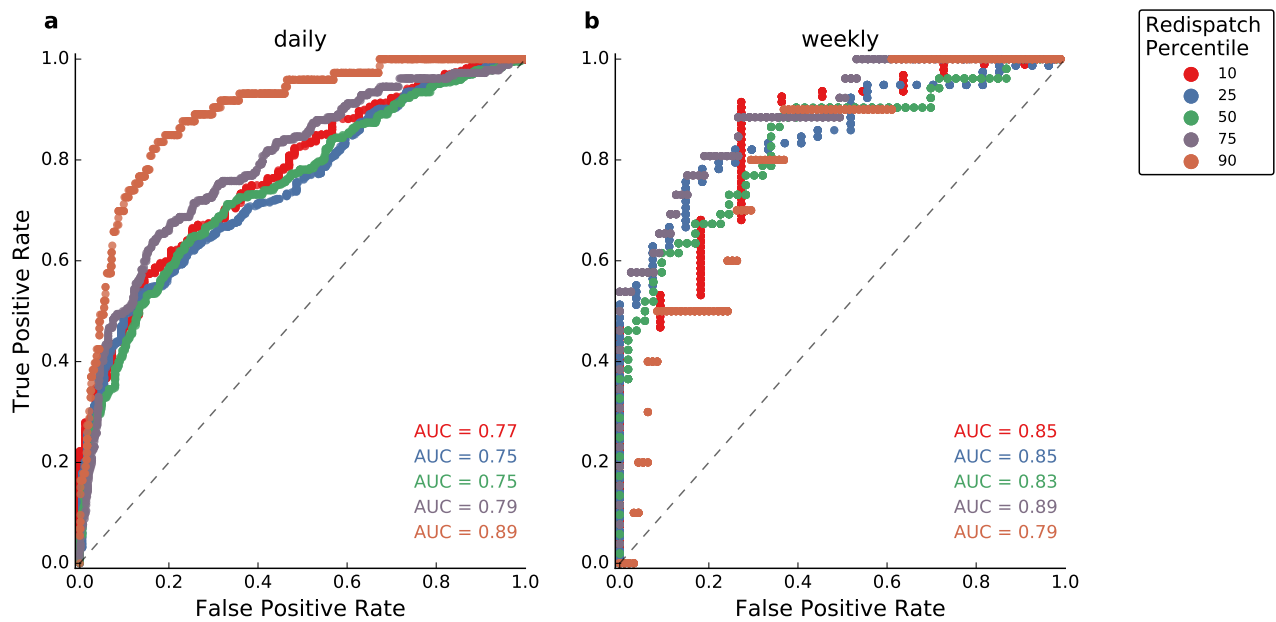


Figure S1: Same as Fig. 5 in the manuscript but for mean resampling of wind and max resampling of redispatch.

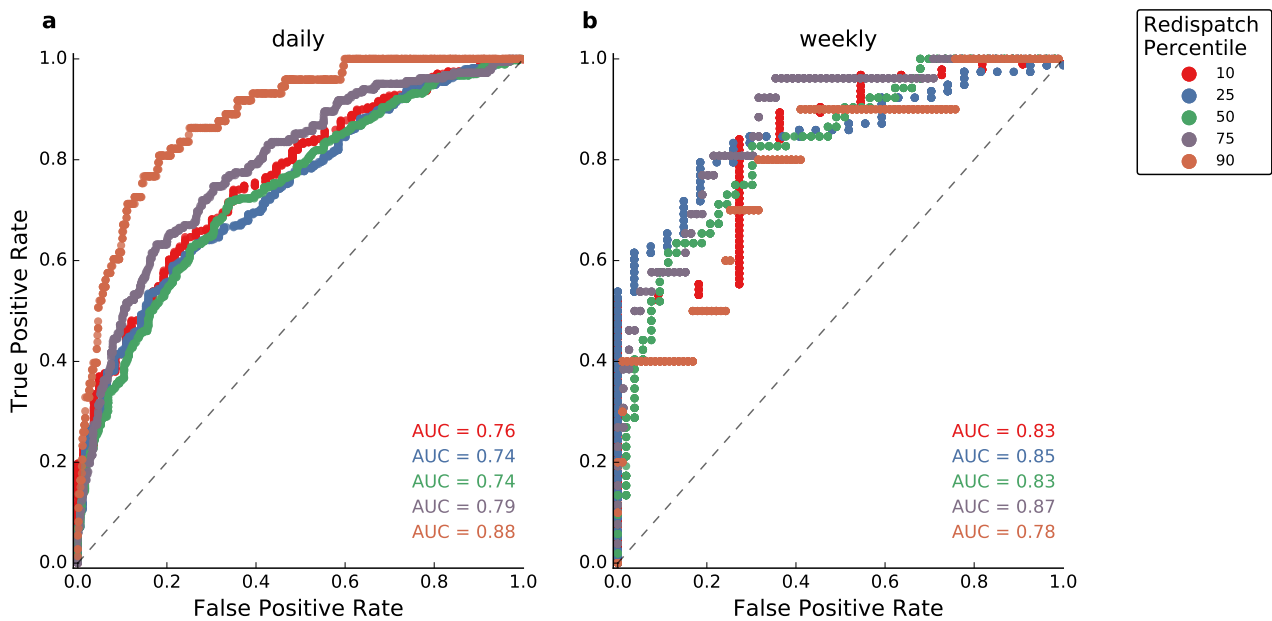


Figure S2: Same as Fig. 5 in the manuscript but for max resampling of wind and max resampling of redispatch.

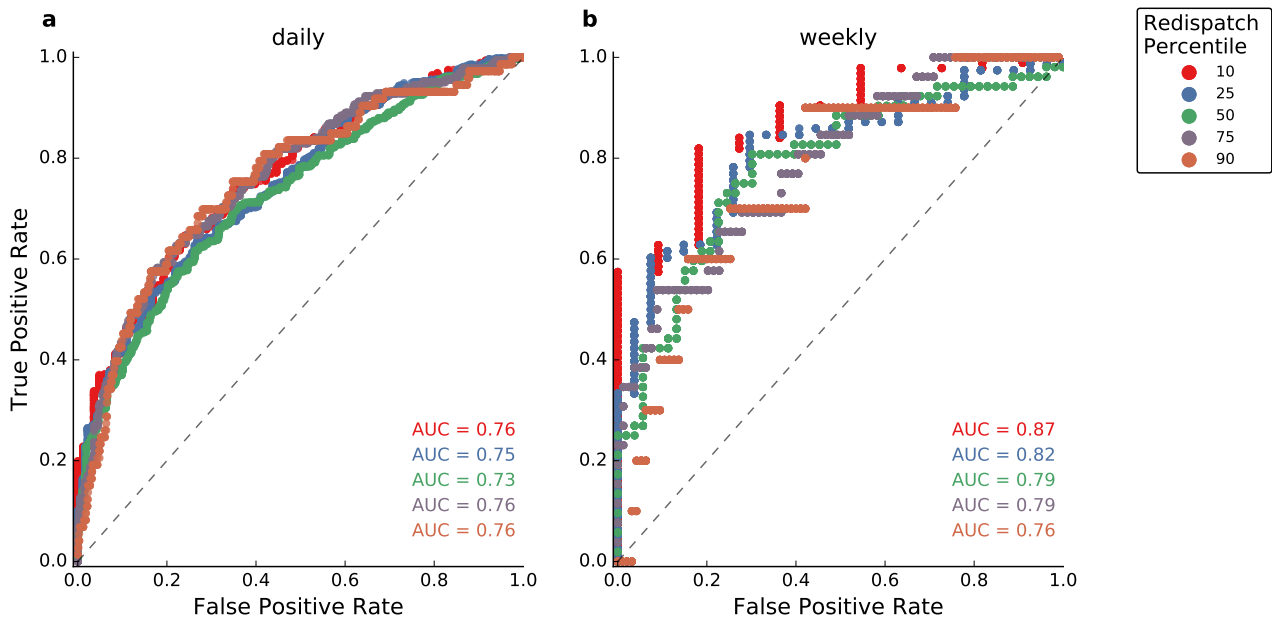


Figure S3: Same as Fig. 5 in the manuscript but for max resampling of wind and mean resampling of redispatch.

3.3 Multi-decadal climate variability

3.3.1 #3: Spurious long-term trends



RESEARCH ARTICLE

10.1029/2018JD030083

Inconsistent Wind Speed Trends in Current Twentieth Century Reanalyses

Jan Wohland^{1,2} , Nour-Eddine Omrani³, Dirk Witthaut^{1,2} , and Noel S. Keenlyside³

¹Institute for Energy and Climate Research–Systems Analysis and Technology Evaluation, Forschungszentrum Jülich, Jülich, Germany, ²Institute for Theoretical Physics, University of Cologne, Cologne, Germany, ³Geophysical Institute and Bjerknes Centre for Climate Research, University of Bergen, Bergen, Norway

Key Points:

- ECMWFs twentieth century reanalyses show strong upward wind speed trends
- The trends are also found in the assimilated wind speed data from ICOADS
- There is no equivalent trend in the NOAA 20CR reanalysis indicating large disagreement

Supporting Information:

- Supporting Information S1

Correspondence to:

J. Wohland,
j.wohland@fz-juelich.de

Citation:

Wohland, J., Omrani, N.-E., Witthaut, D., & Keenlyside, N. S. (2019). Inconsistent wind speed trends in current twentieth century reanalyses. *Journal of Geophysical Research: Atmospheres*, 124. <https://doi.org/10.1029/2018JD030083>

Received 29 NOV 2018

Accepted 25 JAN 2019

Accepted article online 3 FEB 2019

Author Contributions

Conceptualization: Jan Wohland, Nour-Eddine Omrani, Dirk Witthaut, Noel S. Keenlyside

Funding Acquisition: Jan Wohland, Dirk Witthaut

Methodology: Jan Wohland, Nour-Eddine Omrani, Dirk Witthaut, Noel S. Keenlyside

Writing - Original Draft: Jan Wohland

Formal Analysis: Jan Wohland

Investigation: Jan Wohland, Nour-Eddine Omrani, Dirk Witthaut

Resources: Dirk Witthaut, Noel S. Keenlyside

Supervision: Dirk Witthaut, Noel S. Keenlyside

Visualization: Jan Wohland

Writing - review & editing: Jan Wohland, Nour-Eddine Omrani, Dirk Witthaut, Noel S. Keenlyside

©2019. The Authors.

This is an open access article under the terms of the Creative Commons Attribution-NonCommercial-NoDerivs License, which permits use and distribution in any medium, provided the original work is properly cited, the use is non-commercial and no modifications or adaptations are made.

Abstract Reanalysis data underpin much research in atmospheric and related sciences. While most reanalysis only cover the last couple of decades, National Oceanic and Atmospheric Administration (20CR) and European Centre for Medium-Range Weather Forecasts (ERA20C and CERA20C) also developed reanalyses for the entire twentieth century that theoretically allow investigation of multidecadal variability. However, the approaches adopted to handle the massively evolving number of observations can cause spurious signals. Here we focus on wind speeds, as its assimilation is a key difference among these two products. We show that ERA20C and CERA20C feature significant trends in the North Atlantic and North Pacific wind speeds of up to 3 m/s per century. We show that there is a good relation between the trends in the reanalysis and assimilated wind speeds. In contrast, 20CR and the European Centre for Medium-Range Weather Forecasts free model run ERA20CM do not show positive trends in the same regions. As a consequence, conclusions drawn from any single twentieth century reanalysis should be treated cautiously in particular in sectors with a strong wind dependency (e.g., wind energy).

Plain Language Summary Many areas of human activity are directly influenced by the climate, and an enhanced understanding of its variability is hence beneficial for the society. We need long-term climate data sets in order to quantify and understand climate variability better. As of today, there are two centers that provide gridded climate data sets for the last century (so called twentieth century reanalysis). Deriving these data sets is intricate because the number and quality of observations has changed dramatically during the period of interest. In our study, we show that the data sets disagree strongly with respect to long-term wind speed trends. As the climate system is highly coupled, other climatic variables are likely also affected. We analyze the underlying observational data, and we can show that the upward trends in one data set also exist in the observations. Furthermore, we can rule out that the model itself created the trends. By comparison with earlier studies, we argue that the trends are likely spurious (i.e., not real) but some uncertainty remains. We recommend that climate impact assessments should be based on data from both centers. In future research projects, attempts must be made to resolve the strong discrepancy between the data sets.

1. Introduction

The climate system shows variability on various time scales in many interconnected components, for example, the atmosphere (Williams et al., 2017) and the oceans (Keenlyside et al., 2015). Improved understanding of these variations is essential for climate assessment, in particular regarding the identification of dominant modes of variability and for the separation of natural climate variability and anthropogenic climate change. It is also highly relevant because of the impacts of climate variability on society. For example, the design and management of energy infrastructure is directly affected by climate variability (e.g., Bloomfield et al., 2016; Conway et al., 2017; Wohland et al., 2018) and climate change (Schlott et al., 2018; Wohland et al., 2017). Incorporating climate variability into transmission system design (e.g., Kempton et al., 2010) and wind park siting (e.g., Grams et al., 2017) facilitates integration of wind energy. Relevant temporal scales range from subseconds (e.g., Schäfer et al., 2018), over diurnal, synoptic and interannual (e.g., Zubiate et al., 2017), up to multidecadal and centennial timescales (Bett et al., 2017). The last two have received relatively little attention and are therefore the focus of this study.

A meaningful quantification of climate variability requires sufficiently long data sets. Reanalysis data sets are often considered an ideal compromise between nongridded observations and gridded model output. They typically provide climate variables on regular grids and time intervals, and that follow available observations (taking into account the uncertainties). An introduction to the concept of data assimilation is given in Carrassi et al. (2018). Most reanalyses cover only a couple of decades as they rely on a large number of observations that are not available for a longer time span. Driven by the demand from end users and operational centers, the National Oceanic and Atmospheric Administration (NOAA) in the United States and the European Centre for Medium-Range Weather Forecasts (ECMWF) developed centennial reanalyses based on the relatively sparse data coverage. However, discrepancies among reanalyses can be large when data are scarce, because of the differences in models and data assimilation. Given the extensive usage of these reanalyses across and beyond the geosciences, such discrepancies would have major impacts on scientific results.

In this paper we address the issue of disagreeing wind speed trends in current twentieth century reanalyses. Our aim is to investigate wind speed trends in the different reanalysis products, to understand these trends in the context of the assimilated observations, and to comment on their trustworthiness. We show that the disagreement is linked to the assimilation of marine surface winds, which is only performed in the ECMWF reanalyses. Our results have implication beyond wind applications and may explain several issues identified in previous analysis, such as reported drifts and discontinuities of ocean heat content (Laloyaux et al., 2016), trends in Arctic mean sea level pressure (MSLP; Bloomfield et al., 2018), and disagreeing long-term trends in cyclones and wind storms (Befort et al., 2016). Moreover, trends in wind speeds are expected to impact other societally relevant fields such as energy, the water cycle (McVicar et al., 2012), and food chains in the oceans (Kahru et al., 2010). We seek to raise awareness among users and provide feedback for the developers of the data set since “reanalysis is an ongoing activity that should never be regarded as completed” (Laloyaux et al., 2016).

2. Data and Methods

2.1. Ensemble of Twentieth Century Reanalyses

We base our assessment on the full set of currently available reanalyses that span at least the period from 1900–2010. The set consists of the NOAA 20CR data set (Compo et al., 2011) and three different products from ECMWF, namely, ERA20CM (Hersbach et al., 2015a), ERA20C (Poli et al., 2016), and CERA20C (Laloyaux et al., 2018). All of them are widely used. Throughout the manuscript, we use (C)ERA20C to refer to ERA20C and CERA20C. 20CR and ERA20C are atmospheric reanalyses that take ocean variables as boundary conditions, whereas CERA20C is a coupled reanalysis that explicitly resolves the oceans (and other components of the climate system such as sea ice). ERA20CM, in contrast, is a free model run of the same atmospheric model used for ERA20C and constraint by the same boundary conditions. We include ERA20CM even though it is not a reanalysis because a comparison between ERA20C and ERA20CM allows to isolate the effects of data assimilation.

All reanalyses have been shown to be able to reproduce important modes of climate variability. 20CR agrees well with ERA-Interim (Dee et al., 2011) in terms of representing the North Atlantic Oscillation (NAO) and the Pacific Walker Circulation. It has also been shown that ERA20C has skill to reproduce, for example, NAO in the recent past (Poli et al., 2016). Its successor CERA20C is reported to feature significant improvements in the troposphere as compared to both ERA20C and 20CR (Laloyaux et al., 2018).

The assimilation strategy behind 20CR and (C)ERA20C differs substantially. While 20CR assimilates surface pressures only, both ERA20C and CERA20C also assimilate marine wind measurements. The number of pressure observations is capped in 20CR to minimize spurious effects of the increasing observation density. As a consequence of these main differences, Poli and National Center for Atmospheric Research Staff (2017) argue that 20CR is better suited in scarcely sampled regions, while ERA20C is believed to be superior in “well observed areas (...) where the assimilation of winds also assists to better represent synoptic systems.” In addition, CERA20C includes subsurface ocean temperature measurements and salinity profiles. The assimilated wind speeds are made available in an Observation Feedback Archive (OFA, Hersbach et al., 2015b).

Another difference lies in the ensemble size, which is large for 20CR (58) and smaller for ERA20CM and CERA20C (both 10). The smaller ensemble size for the ECMWF product could mean that the ensemble

spread is not well suited to quantify uncertainty. In fact, Laloyaux et al. (2018) report that the CERA20C ensemble spread for wind speeds is too low to quantify the uncertainty by a factor of 2 to 3. This issue is exacerbated for ERA20C that is deterministic and hence has no ensemble.

All ECMWF products share the same resolution of roughly $1.125^\circ \cdot 1.125^\circ$ (T159). The resolution of the older 20CR data set is coarser (roughly $1.875^\circ \cdot 1.875^\circ$, T62). Local topographic features such as individual mountains or the precise location of the coastline cannot be captured, potentially leading to massive uncertainties over small continental regions. In large areas over the oceans, however, the negligence of spatial details is likely of minor importance.

It is noteworthy that the ECMWF products are not independent and errors can hence propagate through the modeling chain. Both ERA20C and CERA20C make use of the ECMWF Integrated Forecast System (IFS). While ERA20C uses IFS CY38r1, CERA20C is based on the newer version IFS CY41R2, which allows for bidirectional interactions between the atmosphere and the ocean and thereby enables to capture dynamic feedbacks (Laloyaux et al., 2018; Poli et al., 2016). In both cases, a 24-hr assimilation window is applied. In addition, ERA20C uses background errors that are based on the ERA20CM ensemble and the 10-year CERA20C streams are in turn initialized from ERA20C data. All three ECMWF products are thus directly and indirectly connected. Nevertheless, there are also substantial differences. For example, the CERA20C background errors do not stem from the free model run ERA20CM as for ERA20C but are generated internally and are better suited to adapt to an evolving observational density by assigning flow-dependent background errors.

We base this study on the monthly mean 10-m wind speeds as the assimilation of wind speeds is one major difference between the data sets. For ERA20CM, unfortunately, the monthly average wind speeds have not been computed and archived (K. Hennermann, personal communication, March 2nd, 2018). We will therefore use the euclidean norm of the monthly mean wind components as a proxy for the wind speed. This leads to lower values because positive and negative values during a month can cancel each other out. We consider this approach justified because we focus on trends rather than absolute values.

2.2. Trend Assessment (1901–2010)

We perform linear least squares regressions for the annual and seasonal wind speed averages in Python based on the `scipy.stats.linregress` function. We consider a trend significant if a Wald Test yields a p value of less than 0.01 for the Null Hypothesis of no trend (i.e., 99% confidence level). For ERA20CM and CERA20C, we report the ensemble mean trend if at least 9 out of 10 ensemble members show significant trends of the same sign. Since ERA20C is deterministic, an ensemble assessment is not feasible. Although 20CR comes with a large ensemble, we restrict the analysis to the ensemble mean here. There can be trends in the ensemble mean that are not robust across the ensemble and such trends would be rejected if the full set of information was considered. As a consequence, the trends reported for 20CR are to be considered an upper bound in the sense that some of them could become nonsignificant if ensemble agreement in 20CR was accounted for. However, as we will see later, the main difference between the reanalyses is that (C)ERA20C features upward trends where 20CR either shows no or negative trends. This disparity can not be resolved by including the full 20CR ensemble because the more stringent trend condition will neither make nonsignificant trends significant nor will it flip signs of trends. Another reason to focus on the ensemble mean for 20CR is that we did not intend to repeat the assessment of Bett et al. (2017). Focusing on Europe, they find weak to no trends in the 20CR data set.

We define two focus regions in which the temporal evolution of the relationship between the observations and (C)ERA20C is studied in detail. They are referred to as North Atlantic ($25\text{--}55^\circ\text{N}$, $50\text{--}20^\circ\text{W}$) and North Pacific ($35\text{--}50^\circ\text{N}$, $180\text{--}130^\circ\text{W}$) and are displayed in Figure 1b. In a sensitivity test, we have also shifted the North Atlantic box northeastward by 10° ($35\text{--}65^\circ\text{N}$, $40\text{--}10^\circ\text{W}$). Boxes are defined to be of similar size while capturing the most pronounced trends seen in the global maps. The trends are homogeneous inside the boxes in ERA20C such that the averaging procedure does not average out distinct spatial features (see Figure 1b). Within the boxes, annual time series of wind speed measurements are derived from the ship-based measurements that are assimilated into (C)ERA20C. To ensure that the entire annual cycle is sufficiently sampled, we only consider years with at least four measurements in all months. Without this constraint, increasing annual values could be rooted in an expansion of shipping activities into the winter months, an effect that has occurred over the twentieth century following technological innovations.

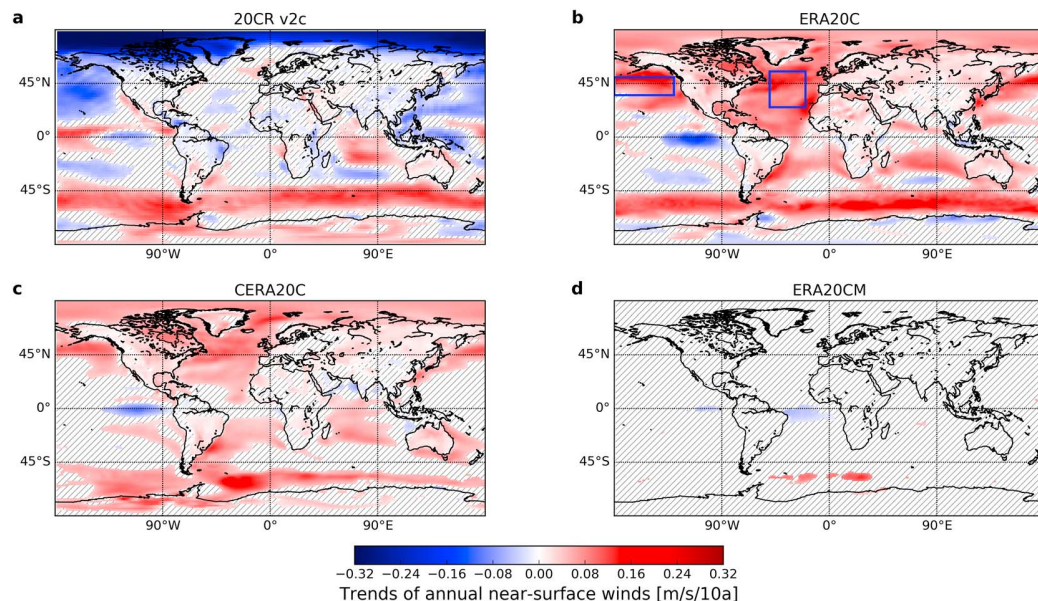


Figure 1. Maps of 10-m annual wind speed trends calculated from 1901 to 2010 for the different datasets (a–d). Colors denote trends that are statistically significant at the 99% level, and white-hatched regions mask out regions without statistically significant trends. In the case of ERA20CM and CERA20C, the ensemble mean trend is plotted if there is agreement across the ensemble with respect to the sign of change (9 out of 10). Focus regions for further assessment are given as blue boxes in (b) and are denoted as North Pacific and North Atlantic.

Lastly, we provide a gridded version of the trends of annual wind speeds in the observations. The measurements are projected onto the ERA20C grid by assigning each measurement to the nearest grid box. In addition to a required significance level of 99%, we only report trends if data in a grid box covers at least 60 years, begins no later than 1920, and ends no earlier than 2000, allowing for interruptions. This approach focuses on well-sampled regions and limits the effect of expanding shipping routes, while regions with occasionally missing data (e.g., due to World War 2) are not excluded. To quantify the relation between trends in the observations and the reanalysis, we compute four different measures. First, we calculate the pattern correlation p between trends in the observations and the reanalysis, considering only grid boxes where observations and model show significant trends: If $\text{trend}_{\text{OFA}}$ ($\text{trend}_{\text{REA}}$) denotes the trend in the OFA (reanalysis) and the index i samples all boxes that feature trends in OFA and the reanalysis, we define the pattern correlation as

$$p = r(\text{trend}_{\text{OFA}}, \text{trend}_{\text{REA}}), \quad (1)$$

where $r()$ denotes the Pearson correlation. Second, we define a binary classifier that predicts the sign of a trend in the reanalysis to be identical to the sign of the trend in the OFA for all boxes where the OFA shows a significant trend. The true positive rate (TPR) of this classifier is then computed as the number of correct predictions divided by the number of trends in OFA. Third, we quantify the fraction of grid boxes that feature trends in OFA but not in the reanalysis (NANR). Fourth, the total error rate is computed as the fraction of significant trends with opposing sign in OFA and the reanalysis.

3. Results

3.1. Disagreement of Wind Speed Trends in (C)ERA20C and 20CR (1901–2010)

In the ensemble mean of the 20CR reanalysis, we find decreasing centennial trends in the annual mean wind speeds over the North Pacific and the Arctic and increasing trends in the Southern Ocean (see Figure 1a). Over land, trends are largely absent. In particular, there are no trends in continental Europe and relatively weak trends west of Great Britain; this is in agreement with two earlier studies (Bett et al., 2013, 2017).

In contrast to 20CR, ERA20C and CERA20C both show strong centennial upward trends in annual mean wind speeds over much of the globe (see Figures 1b and 1c). They are most pronounced over the oceans, particularly in the North Atlantic, the northern North Pacific, and the Southern Oceans. Albeit weaker, trends are also found over large parts of all continents. A comparison between the CERA20C and ERA20C

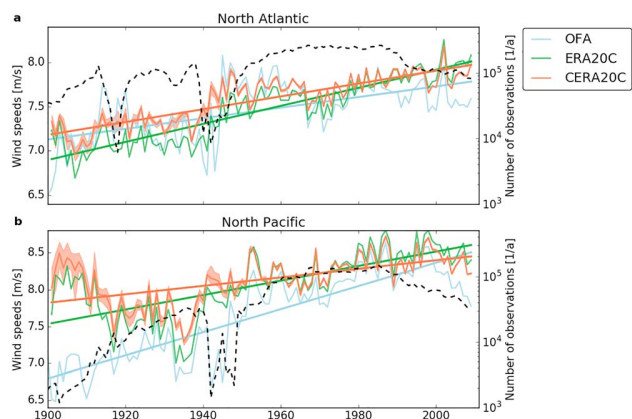


Figure 2. Wind speed trends over boxes in the North Atlantic and North Pacific for the assimilated observations (Observation Feedback Archive, OFA) and both European Centre for Medium-Range Weather Forecasts twentieth century reanalyses. CERA20C shading represents the full ensemble range while the line denotes the ensemble mean. The black dashed line represents the number of observations displayed on a logarithmic scale.

trends reveals that the magnitude of changes is reduced in the coupled reanalysis. This might hint to a dampening effect of the ocean or could be caused by the assimilation of subsurface ocean measurements. The overall pattern, however, remains unchanged.

Trends are absent almost everywhere in the free model runs ERA20CM (see Figure 1d), indicating that the trends are not a feature of the model or stem from the boundary conditions. Instead, they likely originate from the assimilation of wind speeds and/or sea level pressure data.

An assessment of the seasonal trends yields mostly the same results (see supporting information Figures S1–S4). In particular, (C)ERA20C feature upward trends in the North Atlantic and the North Pacific in all seasons although the December, January, and February trend in CERA20C is relatively weak. In 20CR, the North Pacific downward trend is seen in all seasons except of December, January, and February and no season features widespread trends in the North Atlantic, although there are a few patches of upward and downward trends in June, July, and August. As for the annual values, the free model run ERA20CM is almost completely trend free for all seasons.

While 20CR and (C)ERA20C agree on the centennial trends of annual means in the Southern Ocean and the El Niño–Southern Oscillation region, there is considerable disagreement in most other areas. In partic-

ular, trends of opposite sign are reported for the Northern North Pacific. Similarly, in the North Atlantic (C)ERA20C shows a very clear upward trend, while 20CR does not feature significant trends. We will therefore investigate these two regions more closely. Since the assimilation of marine winds is one of the most important differences between 20CR and ERA20C, we will focus on the assimilated wind speeds in (C)ERA20C in the remainder of this paper.

3.2. Trends Also Present in Assimilated Wind Speeds

To test the hypothesis that wind assimilation is responsible for the disagreement between (C)ERA20C and 20CR over the North Atlantic and the North Pacific, we display time series of these two regions in Figure 2. In addition to the reanalysis wind speeds, the assimilated wind speeds from the ERA20C OFA are reported. For both regions, all three data sets show a significant upward trend between 1900 and 2010. The spread of the CERA20C ensemble is small at the beginning of the twentieth century (≈ 0.2 m/s) and decays to practically zero from 1950 onward. In the highly sampled North Atlantic, CERA20C and ERA20C follow the assimilated wind speeds very closely throughout the entire twentieth century. The results are large scale and do not depend on the precise location of the grid box as very similar results are found using a northeasterly shifted box (see supporting information Figure S6). In the North Pacific, the reanalyses deviate substantially from the OFA in the early twentieth century and around World War II. During these periods of sparse measurements, the observed wind speeds are distinctly lower than the reanalysis. This suggests that the wind speed assimilation pulls the models toward lower wind speeds in the first half of the century if the number of observations is high. If the data coverage in the early decades was higher, the reanalysis trends would thus likely be as high as the OFA trends. After WW2 and approximately between 1920 and 1935, the reanalyses are close to the assimilated wind speed observations also in the North Pacific. No significant trends are found in ERA20CM (not shown).

If the twentieth century is split in two parts, pre- and post-WW2, the trend assessment yields different results (see supporting information Figure S1). No significant trends are found in the North Atlantic OFA for either period. However, there is a substantial jump of wind speeds during WW2 and we are not aware of any physical justification of such a jump. Significant upward trends are still found for CERA20C (both periods) and for ERA20C (after WW2). The observational record indicates significant upward trends in the North Pacific for both periods. They are paralleled by the reanalyses after WW2. In the first decades of the twentieth century, significant downward trends are found in the reanalyses. They are most likely rooted in the exponential increase of observations between 1900 and 1930 (see Figure 2).

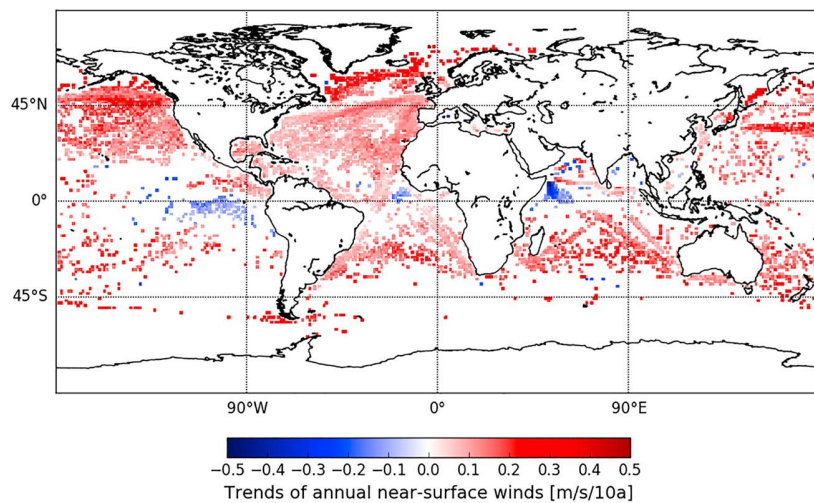


Figure 3. Trends in ship-based wind speed measurements that are assimilated in (C)ERA20C (projected onto the ERA20C grid). Trends are only displayed if significant at the 99% level and if the observations at each individual grid box fulfill these criteria: first measurement no later than 1920, last measurement not earlier than 2000, and at least 60 years of data.

Moreover, the gridded OFA wind speed trends (see Figure 3) show remarkable similarity with the (C)ERA20C trends (cf. Figure 1). In particular, there is a strong upward signal in the North Atlantic and the North Pacific and a downward trend in the eastern equatorial Pacific. Compared to the large extent of these areas, the error induced through gridding of the observations is negligible. The general dominance of positive over negative trends is supported by the OFA data. However, there are also some slight discrepancies, for example, off the Somalian coast in Eastern Africa. A quantitative analysis (see Table 1) reveals that positive trends in an OFA grid box translate into a positive trend in ERA20C (CERA20C) in at least 73% (60%) of the cases. More stringent data requirement in terms of minimum years of available observations lead to higher True Positive Rates, reaching up to 86% (74%). This substantiates a very strong relationship between the trends in OFA and the reanalysis output. The generally weaker agreement between OFA and CERA20C is due to fewer significant trends in CERA20C. For example, for 80 years of observations, the share of grid boxes that feature a trend in OFA but not in CERA20C (i.e., NANR) is 27% as compared to 12% in ERA20C. The higher share in CERA20C as compared to ERA20C can stem from disagreement across the ensemble or from the assimilation of ocean observations in CERA20C among others. The total error rate, interestingly, never deviates by more than 2% between ERA20C and CERA20C, highlighting that the increased share of grid boxes that feature a trend in OFA but not in CERA20C balances the decreased True Positive Rate. The main difference is thus fewer significant trends in CERA20C. Note that the share of grid boxes that feature a trend in OFA but not in the reanalyses decays with more stringent data requirements, which means that the best sampled trends in OFA are more often mirrored by trends in the reanalyses.

While OFA is a good predictor for the sign of trends in the reanalysis, there is only a mediocre pattern correlation between them ($0.37 \leq p \leq 0.48$) indicating a weak linear relationship. Since the models used

Table 1
Quantitative Assessment of Relationship Between OFA and Reanalysis Trends for Different Minimum Years of Available Observations

Years of observations	Pattern correlation p	TPR (%)	NANR (%)	TER (%)
60	0.39/0.45	73/60	12/27	15/13
80	0.45/0.48	75/62	12/27	13/11
100	0.42/0.37	86/74	6/19	8/7

Note. TPR is the true positive rate of a simple binary classifier as defined in section 2, NANR is the fraction of grid boxes with significant trends in the Observation Feedback Archive (OFA) and without trends in the reanalysis, and TER is the total error rate. Data are given for both reanalyses as ERA20C/CERA20C.

in the reanalyses are based on nonlinear dynamics and ensure fundamental principles of physics, such as the conservation of mass, reanalysis wind speeds cannot be expected to be a local linear function of OFA wind speeds. Instead, the precise wind speed value in any box is affected by the atmospheric dynamics in a larger region. The relatively small correlation values thus do not conflict with our basic argument that the reanalysis trends stem from the OFA trends.

4. Discussion—Are These Trends Real?

In light of the strong disagreement between data sets, we list known issues and findings that might help to judge the reanalyses' trustworthiness in the following paragraphs. To start with, there is a substantial amount of literature about spurious trends in wind speed measurements that arise due to changes in measurement techniques (e.g., Cardone et al., 1990; The WASA Group, 1998; Ward, 1992; Ward & Hoskins, 1996). Main aspects are increasing anemometer heights and the transition from estimated to measured wind speeds. Thomas et al. (2008) argue that trends in the ICOADS data set disappear if known biases are accounted for. Unfortunately, their analysis does not cover the entire twentieth century and they also report remaining trends in the period 1982–2002, which are still unexplained. Even though Cardone et al. (1990) report weaker wind speeds prior to 1950 after correction, they are still critical about the credibility of these trends. They argue that the changes may be due to a lack of standardization in measurements which is not captured by their correction. Apart from changes in the measurement technique, the sampling has also evolved considerably (see Figure 2).

Moreover, focusing on the Arctic Oscillation, a recent study finds that the ERA20C Arctic MSLP disagrees with the HadSLP2 observational data set (Bloomfield et al., 2018). While no trend is found in the observations, ERA20C features a significant downward trend in the Arctic, which increases the meridional pressure gradient over large parts of the Atlantic and the northern North Pacific. In other words, ERA20C features a MSLP trend that is consistent with the assimilated winds while being inconsistent with MSLP observations. In conclusion, it seems that the assimilated wind speed and MSLP observation disagree with each other. In order to reproduce the wind speed observations, unobserved MSLP trends are generated.

Over the Northern Hemisphere's continents, decreasing wind speeds are found since around 1980 with a rate of change of -0.7 m/s in 50 years (McVicar et al., 2012). This decrease is termed stilling and has been largely attributed to an increasing surface roughness (Vautard et al., 2010). It is likely that ECMWF has decided not to assimilate land-based wind measurements to avoid spurious downward trends in its reanalyses. Marine wind speeds are not affected via this process due to a very limited number of infrastructure projects at the ocean surface. Stilling seems to be inconsistent with the upward (C)ERA20C trends over land (see Figures 1b and 1c). However, surface roughness is virtually unchanged in all twentieth century reanalyses and (C)ERA20C is therefore not expected to feature stilling. In the real world, the downward trends due to surface roughness changes would be superimposed on the upward trend found in (C)ERA20C and the above mentioned studies would report the net effect.

In light of potential impacts of climate change on the wind energy sector, a couple of studies have looked into changing wind energy potentials over land. These studies are typically based on CMIP5 (Taylor et al., 2011) or downscaled projects such as EUROCORDEX (Jacob et al., 2014) and generally find small signals even under strong climate change scenarios. For example, Tobin et al. (2016) report changes of $\pm 5\%$ of European wind farm yields under the RCP4.5 and RCP8.5 scenarios based on EUROCORDEX. Based on statistical-dynamical downscaling of a large CMIP5 ensemble, Reyers et al. (2015) also report uncertain signs of changes in wind energy yields. The strong (C)ERA20C trends are hence unrealistic if the CMIP5 ensemble is considered trustworthy.

However, there are also reasons not to reject the (C)ERA20C trends as unrealistic. While the wind speed measurement technique has evolved dramatically over the last century, the method to estimate significant wave heights has changed less. Gulev and Grigorieva (2004) find significant long-term trends in wave heights in the North Pacific, which supports the wind speed trends reported here. In the North Atlantic they report significant changes for the second half of the last century only. In an effort to combine wind and wave height measurements, Tokinaga and Xie (2011) provide a corrected data set for the period 1950–2008. They adjust for increasing anemometer heights, employ Lindau's equivalent wind scale, and correct for known disparities in the daily cycle of visual observations. While these adjustments reduce the trends in wind speeds

by roughly a factor of four as compared to the unadjusted ICOADS data set, a significant trend remains in the globally averaged wind speeds.

Moreover, Torralba et al. (2017) compare wind speed trends in modern reanalyses in 1980–2015. They report a few locations where significant trends occur in ERA-Interim, MERRA2, and JRA55. They are mostly located over the oceans and dominantly show upward trends. Apart from a section of the Southern Ocean, the trends generally do not agree with our results. In particular, they do not find a robust signal over the North Atlantic or the Northern North Pacific. However, in light of multidecadal variability, the short considered time span might prohibit assessments of long-term trends. For example, Siegmund and Schrum (2001) reported a strong upward trend in the North Sea based on the National Centers for Atmospheric Prediction/National Center for Atmospheric Research reanalysis between 1958 and 1997, which largely disappears if an extended period 1948 to 2014 is used as input (Stendel et al., 2016). The reason that these two studies estimate different trends may well be connected to low-frequency variability of the NAO (e.g., Hurrell et al., 2001). The biggest positive NAO trends associated with its multidecadal fluctuations were observed between 1960 and 1995 (Omriani et al., 2014), and the expansion of the period to 1948–2014 will counteract the positive NAO trend due to the recent negative NAO trend since 1990s. The significance of these NAO fluctuations is supported by studies showing that the decadal variations in seasonal forecast skill are linked to it (Scaife et al., 2014; Weisheimer et al., 2017). The long-term trends in winds identified here are not likely caused by the multidecadal variability: the trend has much larger amplitude than expected from the multidecadal variations (see Figure 2). Furthermore, the 110-year period considered in this study reduces the aliasing affect of multidecadal variability on the estimation of long-term trends.

Overall, aspects that challenge the trustworthiness of the (C)ERA20C trends dominate. They come from independent lines of evidence including highly trusted sea level pressure measurements, an evolving measurement technique of marine wind speeds, land-based wind speed measurements, and climate models. Nevertheless, there is no strict proof that the trends are wrong and even some indications that they might be right. The trends can thus not be refuted with certainty at the moment.

5. Conclusion

We report strong upward wind speed trends in the ERA20C and CERA20C reanalyses that generally do not agree with trends in 20CR. Similar trends are not found in the free model runs ERA20CM. We show that there is a close agreement between the presence of the wind speed trends and the assimilated wind speed data in ERA20C and CERA20C. Therefore, the trends in the reanalyses most likely originate from the assimilated wind speeds.

The trends may be spurious and due to evolving wind measurement techniques. Moreover, Bloomfield et al. (2018) report a spurious MSLP trend over the Arctic, which hints to a disagreement between the assimilated MSLP and wind speed data. The trends also disagree with land-based wind measurements, which feature downward trends in the last couple of decades. However, visual wave height estimations independently support some of the wind trends such that they cannot be fully ruled out as unrealistic.

Since the Earth system is interconnected in many ways, the trends in wind speeds will likely impact other climatic variables. We thus conclude that assessments of historical long-term trends or low-frequency variability from any single twentieth century reanalysis may be boldly misleading. We stress that it is important to recognize the great uncertainties in long-term wind trends and that more work is required to resolve this issue. For the time being, we suggest that any long-term impact assessment ought to be based on an ensemble of twentieth century reanalysis that at least consists of one member of 20CR and either ERA20C or CERA20C.

References

- Befort, D. J., Wild, S., Kruschke, T., Ulbrich, U., & Leckebusch, G. C. (2016). Different long-term trends of extra-tropical cyclones and windstorms in ERA-20C and NOAA-20CR reanalyses: Extra-tropical cyclones and windstorms in 20th century reanalyses. *Atmospheric Science Letters*, 17(11), 586–595. <https://doi.org/10.1002/asl.694>
- Bett, P. E., Thornton, H. E., & Clark, R. T. (2013). European wind variability over 140 yr. *Advances in Science and Research*, 10, 51–58. <https://doi.org/10.5194/asr-10-51-2013>
- Bett, P. E., Thornton, H. E., & Clark, R. T. (2017). Using the twentieth century reanalysis to assess climate variability for the european wind industry. *Theoretical and Applied Climatology*, 127(1-2), 61–80. <https://doi.org/10.1007/s00704-015-1591-y>

Acknowledgments

We thank Idar Barstad and Joachim Reuder for stimulating discussions. We thank ECMWF for making ERA20CM, ERA20C, and CERA20C publicly available as well as publishing the underlying wind speeds observations in the OFA. ECMWF data were downloaded from the website (<https://apps.ecmwf.int/datasets/>). We thank NOAA for making 20CRv2c available, which was downloaded from the website (https://www.esrl.noaa.gov/psd/data/gridded/data.20thC_ReanV2c.html). J. W. thanks the Hitec graduate school at Forschungszentrum Jülich for a travel grant. J. W. and D. W. are funded by the Helmholtz Association through the joint initiative “Energy System 2050—A Contribution of the Research Field Energy and the grant VH-NG-1025 to Dirk Witthaut.

- Bloomfield, H. C., Brayshaw, D. J., Shaffrey, L. C., Coker, P. J., & Thornton, H. E. (2016). Quantifying the increasing sensitivity of power systems to climate variability. *Environmental Research Letters*, *11*(12), 124025. <https://doi.org/10.1088/1748-9326/11/12/124025>
- Bloomfield, H., Shaffrey, L., Hodges, K. I., & Vidale, P. L. (2018). A critical assessment of the long term changes in the wintertime surface arctic oscillation and northern hemisphere storminess in the ERA20C reanalysis. *Environmental Research Letters*, *13*, 94004. <https://doi.org/10.1088/1748-9326/aad5c5>
- Cardone, V. J., Greenwood, J. G., & Cane, M. A. (1990). On trends in historical marine wind data. *Journal of Climate*, *3*(1), 113–127.
- Carrassi, A., Bocquet, M., Bertino, L., & Evensen, G. (2018). Data assimilation in the geosciences: An overview on methods, issues and perspectives. *Wiley Interdisciplinary Reviews: Climate Change*, *9*(5), e535. <https://doi.org/10.1002/wcc.535>
- Compo, G. P., Whitaker, J. S., Sardeshmukh, P. D., Matsui, N., Allan, R. J., Yin, X., et al. (2011). The twentieth century reanalysis project. *Quarterly Journal of the Royal Meteorological Society*, *137*(654), 1–28. <https://doi.org/10.1002/qj.776>
- Conway, D., Dalin, C., Landman, W. A., & Osborn, T. J. (2017). Hydropower plans in eastern and southern Africa increase risk of concurrent climate-related electricity supply disruption. *Nature Energy*, *2*(12), 946–953. <https://doi.org/10.1038/s41560-017-0037-4>
- Dee, D. P., Uppala, S. M., Simmons, A. J., Berrisford, P., Poli, P., Kobayashi, S., et al. (2011). The ERA-Interim reanalysis: Configuration and performance of the data assimilation system. *Quarterly Journal of the Royal Meteorological Society*, *137*(656), 553–597. <https://doi.org/10.1002/qj.828>
- Grams, C. M., Beerli, R., Pfenninger, S., Staffell, I., & Wernli, H. (2017). Balancing Europe's wind-power output through spatial deployment informed by weather regimes. *Nature Climate Change*, *7*, 557–562. <https://doi.org/10.1038/nclimate3338>
- Gulev, S. K., & Grigorieva, V. (2004). Last century changes in ocean wind wave height from global visual wave data. *Geophysical Research Letters*, *31*, L24302. <https://doi.org/10.1029/2004GL021040>
- Hersbach, H., Peubey, C., Simmons, A., Berrisford, P., Poli, P., & Dee, D. (2015a). ERA20CM: A twentieth-century atmospheric model ensemble. *Quarterly Journal of the Royal Meteorological Society*, *141*(691), 2350–2375.
- Hersbach, H., Poli, P., & Dee, D. P. (2015b). The observation feedback archive for the ICOADS and ISPD data sets, 18. Shinfield Park, Reading: ECMWF.
- Hurrell, J. W., Kushnir, Y., & Visbeck, M. (2001). The North Atlantic Oscillation. *Science*, *291*(5504), 603–605. <https://doi.org/10.1126/science.1058761>
- Jacob, D., Petersen, J., Eggert, B., Alias, A., Christensen, O. B., Bouwer, L. M., et al. (2014). EURO-CORDEX: New high-resolution climate change projections for European impact research. *Regional Environmental Change*, *14*(2), 563–578. <https://doi.org/10.1007/s10113-013-0499-2>
- Kahru, M., Gille, S. T., Murtugudde, R., Strutton, P. G., Manzano-Sarabia, M., Wang, H., & Mitchell, B. G. (2010). Global correlations between winds and ocean chlorophyll. *Journal of Geophysical Research*, *115*, C12040. <https://doi.org/10.1029/2010JC006500>
- Keenlyside, N. S., Ba, J., Mecking, J., Omrani, N.-E., Latif, M., Zhang, R., & Msadek, R. (2015). North Atlantic Multi-decadal Variability—Mechanisms and predictability. In *Climate change: Multidecadal and beyond* (pp. 141). World Scientific Publishing.
- Kempton, W., Pimenta, F. M., Veron, D. E., & Colle, B. A. (2010). Electric power from offshore wind via synoptic-scale interconnection. *Proceedings of the National Academy of Sciences*, *107*(16), 7240–7245. <https://doi.org/10.1073/pnas.0909075107>
- Lalouyax, P., Balmaseda, M., Dee, D., Mogensen, K., & Janssen, P. (2016). A coupled data assimilation system for climate reanalysis. *Quarterly Journal of the Royal Meteorological Society*, *142*(694), 65–78.
- Lalouyax, P., de Boisseson, E., Balmaseda, M., Bidlot, J.-R., Broennimann, S., Buizza, R., et al. (2018). CERA-20c: A coupled reanalysis of the twentieth century. *Journal of Advances in Modeling Earth Systems*, *10*, 1172–1195. <https://doi.org/10.1029/2018MS001273>
- McVicar, T. R., Roderick, M. L., Donohue, R. J., Li, L. T., Van Niel, T. G., Thomas, A., et al. (2012). Global review and synthesis of trends in observed terrestrial near-surface wind speeds: Implications for evaporation. *Journal of Hydrology*, *416–417*, 182–205. <https://doi.org/10.1016/j.jhydrol.2011.10.024>
- Omrani, N.-E., Keenlyside, N. S., Bader, J., & Manzini, E. (2014). Stratosphere key for wintertime atmospheric response to warm Atlantic Decadal Conditions. *Climate Dynamics*, *42*(3–4), 649–663. <https://doi.org/10.1007/s00382-013-1860-3>
- Poli, P., Hersbach, H., Dee, D. P., Berrisford, P., Simmons, A. J., Vitart, F., et al. (2016). ERA-20c: An atmospheric reanalysis of the twentieth century. *Journal of Climate*, *29*(11), 4083–4097. <https://doi.org/10.1175/JCLI-D-15-0556.1>
- Poli, P., & National Center for Atmospheric Research Staff, E. (2017). The Climate Data Guide: ERA-20C: ECMWF's atmospheric reanalysis of the 20th century (and comparisons with NOAA's 20cr). Retrieved from <https://climatedataguide.ucar.edu/climate-data/era-20c-ecmwf-atmospheric-reanalysis-20th-century-and-comparisons-noaa-20cr>
- Reyers, M., Pinto, J. G., & Moemken, J. (2015). Statistical-dynamical downscaling for wind energy potentials: Evaluation and applications to decadal hindcasts and climate change projections. *International Journal of Climatology*, *35*(2), 229–244. <https://doi.org/10.1002/joc.3975>
- Scaife, A. A., Arribas, A., Blockley, E., Brookshaw, A., Clark, R. T., Dunstone, N., et al. (2014). Skillful long-range prediction of European and North American winters: Scaife et al.: Predictability of the NAO. *Geophysical Research Letters*, *41*, 2514–2519. <https://doi.org/10.1002/2014GL059637>
- Schäfer, B., Beck, C., Aihara, K., Witthaut, D., & Timme, M. (2018). Non-gaussian power grid frequency fluctuations characterized by Lévy-stable laws and superstatistics. *Nature Energy*, *3*, 119–126. <https://doi.org/10.1038/s41560-017-0058-z>
- Schlott, M., Kies, A., Brown, T., Schramm, S., & Greiner, M. (2018). The impact of climate change on a cost-optimal highly renewable European electricity network. *Applied Energy*, *230*, 1645–1659. <https://doi.org/10.1016/j.apenergy.2018.09.084>
- Siegmund, F., & Schrum, C. (2001). Decadal changes in the wind forcing over the North Sea. *Climate Research*, *18*(1–2), 39–45.
- Stendel, M., van den Besselaar, E., Hannachi, A., Kent, E. C., Lefebvre, C., Schenk, F., et al. (2016). Recent Change - Atmosphere, *North Sea region climate change assessment* (pp. 55–84). Cham: Springer Nature.
- Taylor, K. E., Stouffer, R. J., & Meehl, G. A. (2011). An overview of CMIP5 and the experiment design. *Bulletin of the American Meteorological Society*, *93*, 485–498.
- The WASA Group (1998). Changing waves and storms in the Northeast Atlantic? *Bulletin of the American Meteorological Society*, *79*(5), 741–760. [https://doi.org/10.1175/1520-0477\(1998\)079<0741:CWASIT>2.0.CO;2](https://doi.org/10.1175/1520-0477(1998)079<0741:CWASIT>2.0.CO;2)
- Thomas, B. R., Kent, E. C., Swail, V. R., & Berry, D. I. (2008). Trends in ship wind speeds adjusted for observation method and height. *International Journal of Climatology*, *28*(6), 747–763. <https://doi.org/10.1002/joc.1570>
- Tobin, I., Jerez, S., Vautard, R., Thais, F., van Meijgaard, E., Prein, A., et al. (2016). Climate change impacts on the power generation potential of a European mid-century wind farms scenario. *Environmental Research Letters*, *11*(3), 34013. <https://doi.org/10.1088/1748-9326/11/3/034013>
- Tokina, H., & Xie, S.-P. (2011). Wave- and anemometer-based sea surface wind (waswind) for climate change analysis*. *Journal of Climate*, *24*(1), 267–285. <https://doi.org/10.1175/2010JCLI3789.1>
- Torralla, V., Doblas-Reyes, F. J., & Gonzalez-Reviriego, N. (2017). Uncertainty in recent near-surface wind speed trends: A global reanalysis intercomparison. *Environmental Research Letters*, *12*(11), 114019. <https://doi.org/10.1088/1748-9326/aa8a58>

- Vautard, R., Cattiaux, J., Yiou, P., Thepaut, J.-N., & Ciais, P. (2010). Northern Hemisphere atmospheric stilling partly attributed to an increase in surface roughness. *Nature Geoscience*, *3*(11), 756–761. <https://doi.org/10.1038/ngeo979>
- Ward, M. N. (1992). Provisionally corrected surface wind data, worldwide ocean-atmosphere surface fields, and Sahelian rainfall variability. *Journal of Climate*, *5*(5), 454–475.
- Ward, M. N., & Hoskins, B. J. (1996). Near-surface wind over the global ocean 1949–1988. *Journal of Climate*, *9*(8), 1877–1895.
- Weisheimer, A., Schaller, N., O'Reilly, C., MacLeod, D. A., & Palmer, T. (2017). Atmospheric seasonal forecasts of the twentieth century: Multi-decadal variability in predictive skill of the winter North Atlantic Oscillation (NAO) and their potential value for extreme event attribution: Atmospheric Seasonal Forecasts of the Twentieth Century. *Quarterly Journal of the Royal Meteorological Society*, *143*(703), 917–926. <https://doi.org/10.1002/qj.2976>
- Williams, P. D., Alexander, M. J., Barnes, E. A., Butler, A. H., Davies, H. C., Garfinkel, C. I., et al. (2017). A census of atmospheric variability from seconds to decades: A census of atmospheric variability. *Geophysical Research Letters*, *44*, 11,201–11,211. <https://doi.org/10.1002/2017GL075483>
- Wohland, J., Meyers, M., Märker, C., & Witthaut, D. (2018). Natural wind variability triggered drop in German redispatch volume and costs from 2015 to 2016. *PLOS One*, *13*(1), e0190707. <https://doi.org/10.1371/journal.pone.0190707>
- Wohland, J., Meyers, M., Weber, J., & Witthaut, D. (2017). More homogeneous wind conditions under strong climate change decrease the potential for inter-state balancing of electricity in Europe. *Earth System Dynamics*, *8*(4), 1047–1060. <https://doi.org/10.5194/esd-8-1047-2017>
- Zubiate, L., McDermott, F., Sweeney, C., & O'Malley, M. (2017). Spatial variability in winter NAO–wind speed relationships in western Europe linked to concomitant states of the East Atlantic and Scandinavian patterns. *Quarterly Journal of the Royal Meteorological Society*, *143*(702), 552–562. <https://doi.org/10.1002/qj.2943>

Supplement

Supplementary Information to: Inconsistent wind speed trends in current 20th century reanalyses

Jan Wohland, Nour-Eddine Omrani, Dirk Witthaut, Noel S. Keenlyside

November 26, 2018

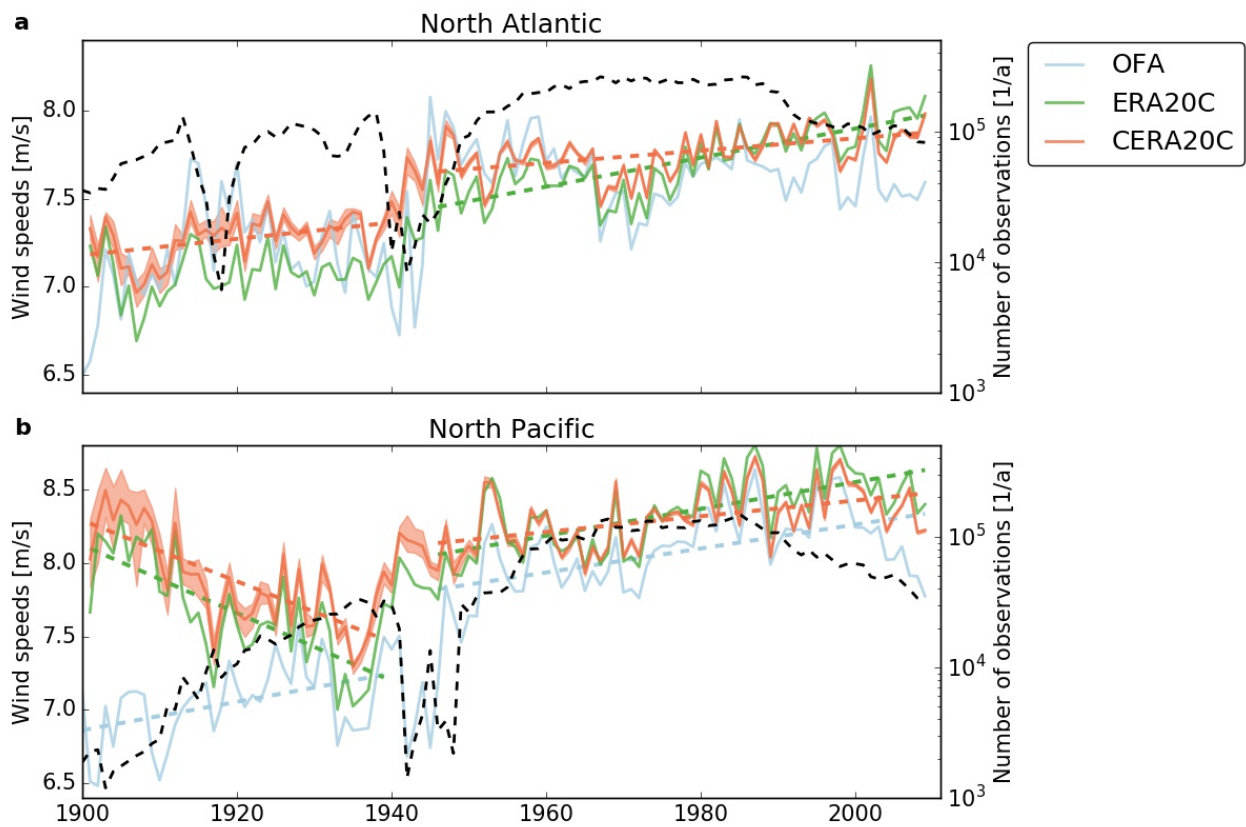


Figure S1: Same as Fig. 2, but trends calculated separately for the periods before and after WW2.

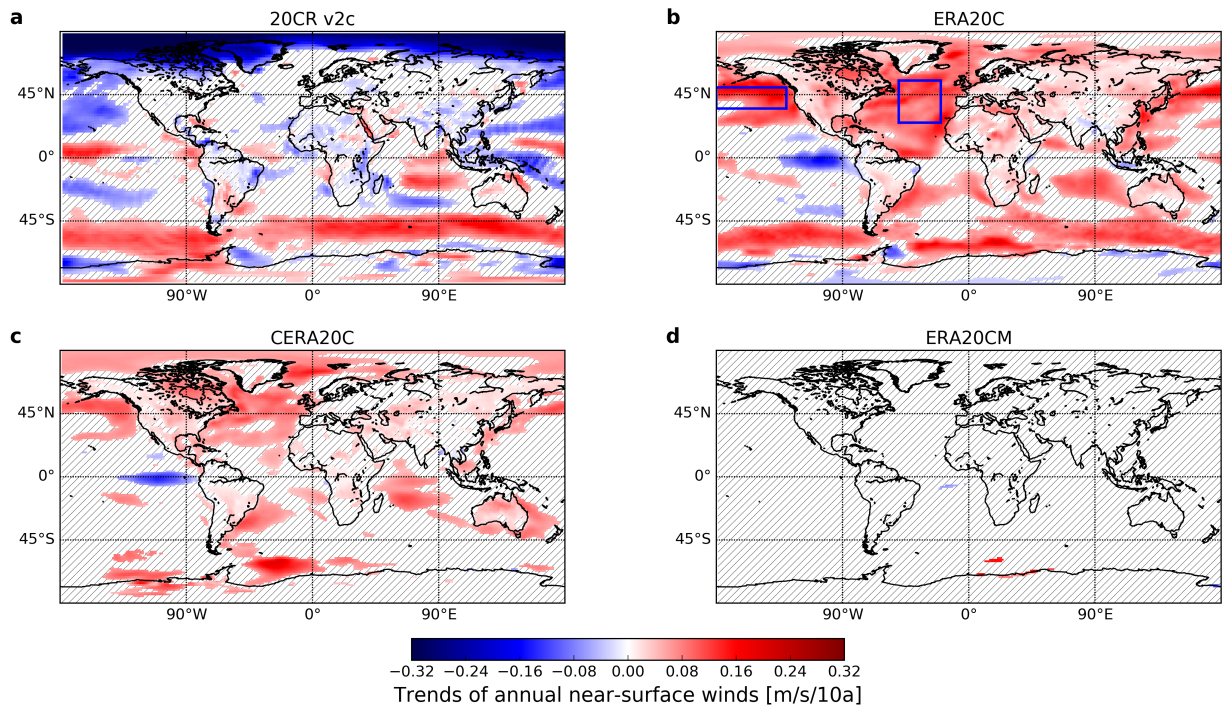


Figure S2: Same as Fig. 1 but MAM for only.

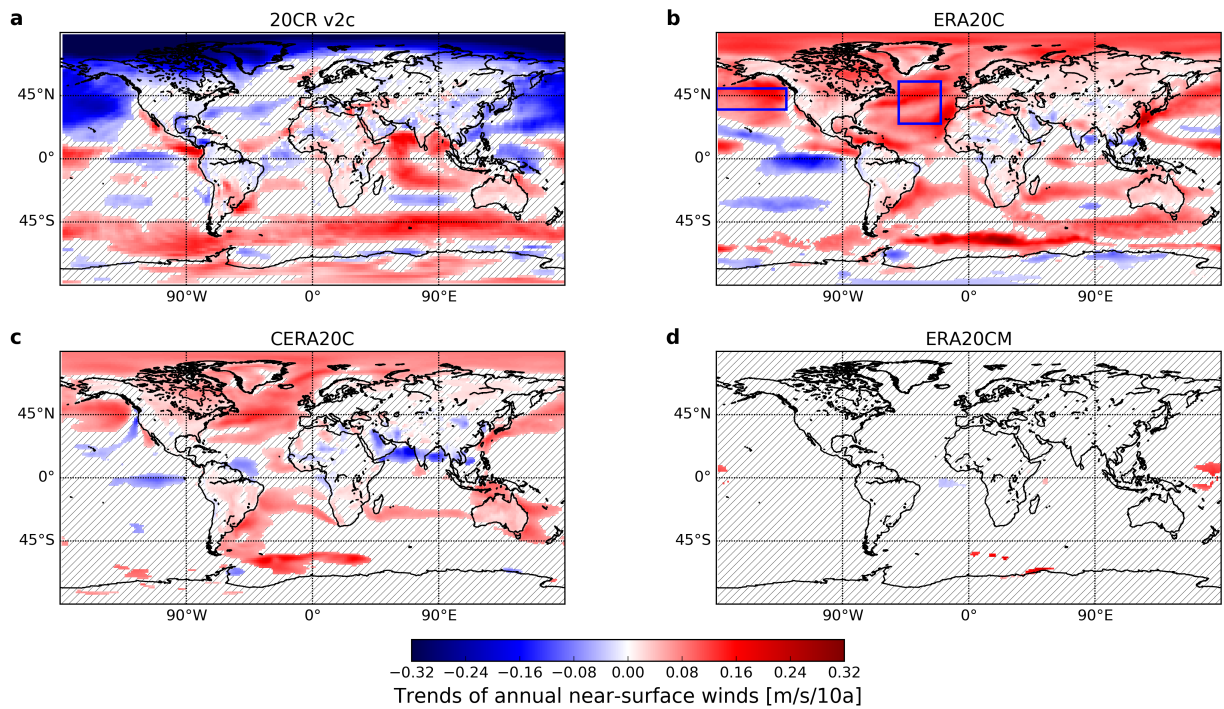


Figure S3: Same as Fig. 1 but for JJA only.

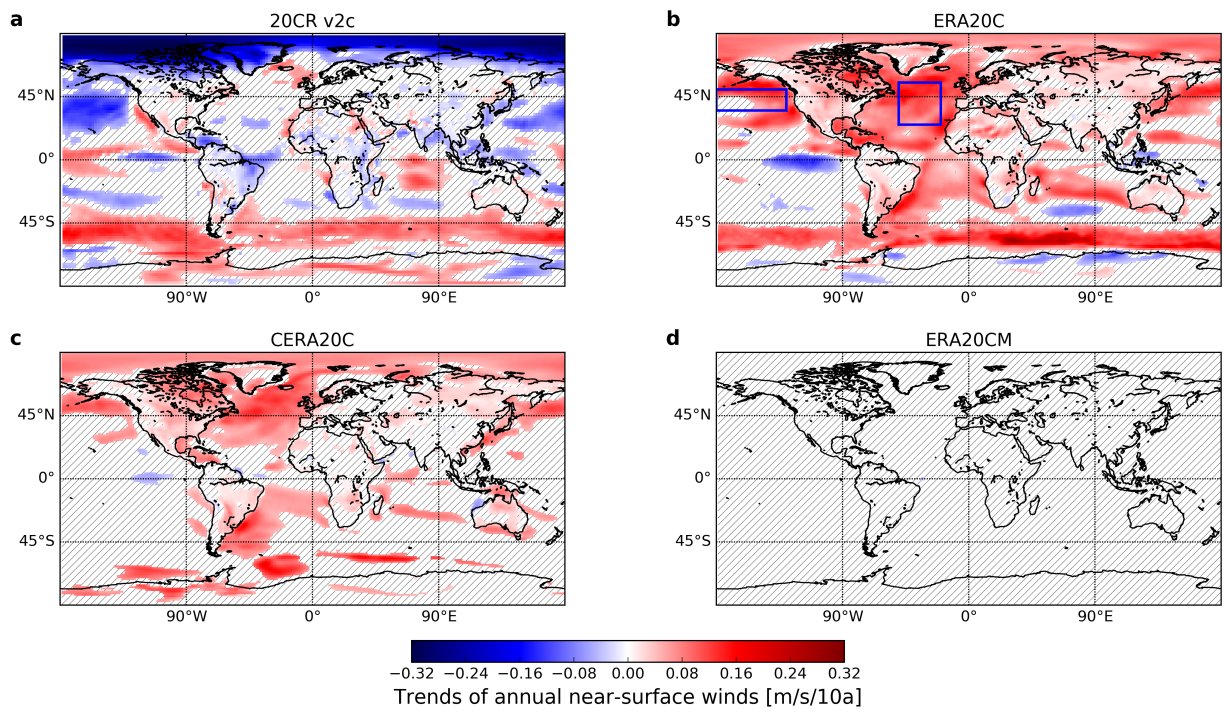


Figure S4: Same as Fig. 1 but for SON only.

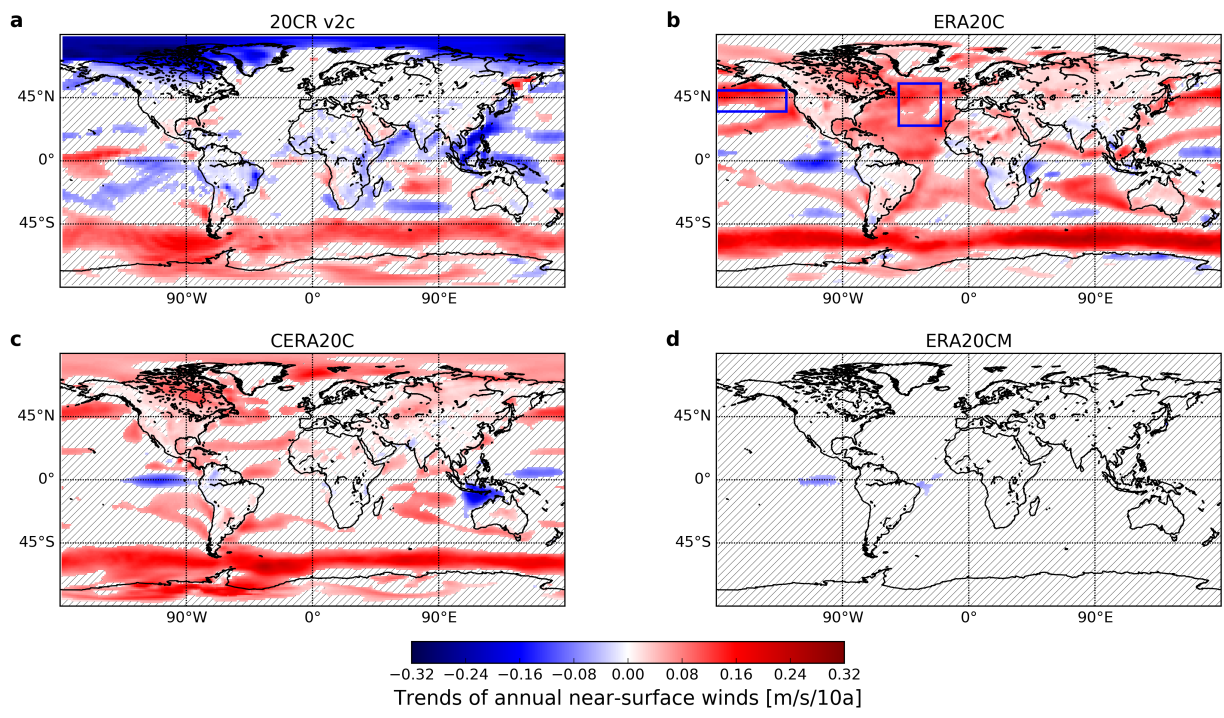


Figure S5: Same as Fig. 1 but for DJF only.

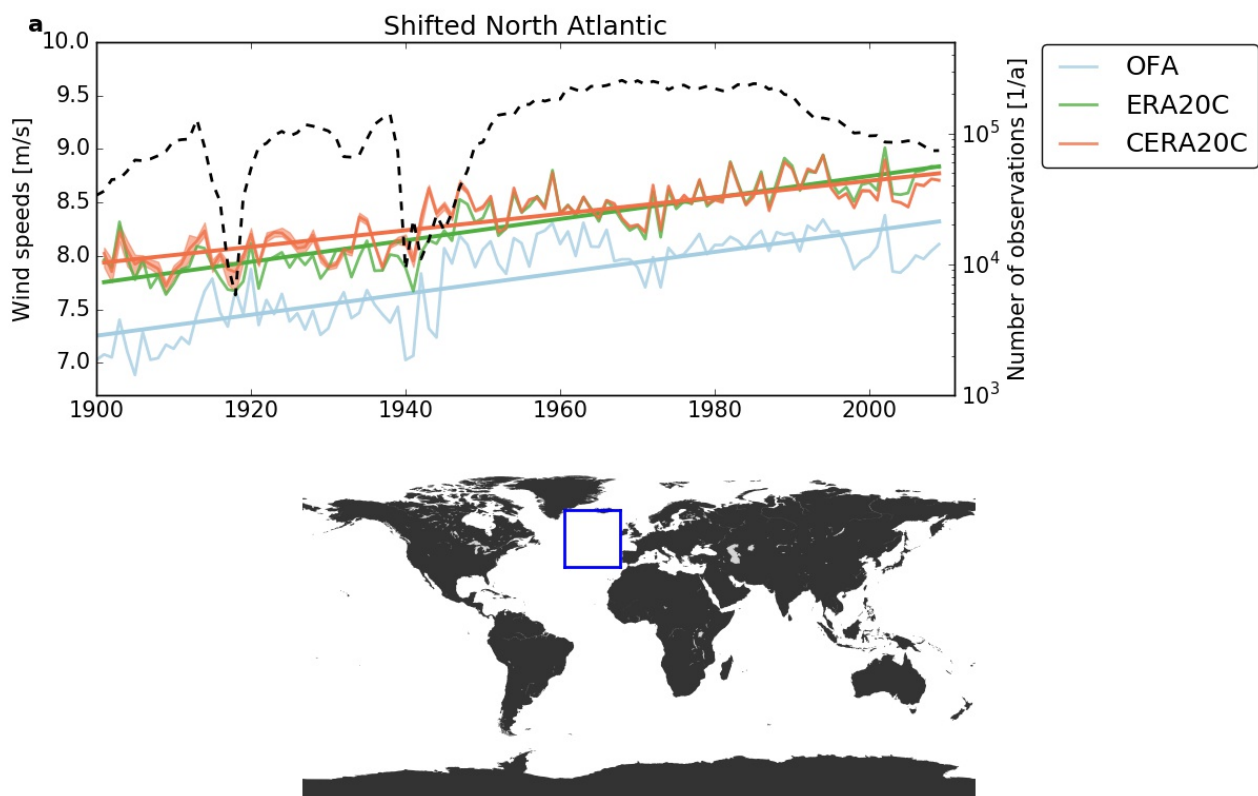


Figure S6: Same as Fig. 2a, but with a North-Easterly shifted box ($35^{\circ}\text{N} - 65^{\circ}\text{N}$, $40^{\circ}\text{W} - 10^{\circ}\text{W}$) as given in the lower subplot.

3.3.2 #4: Multi-decadal wind generation variability



Significant multi-decadal variability of German wind energy generation

Jan Wohland^{1,2}, Nour Eddine Omrani³, Noel Keenlyside³, and Dirk Witthaut^{1,2}

¹Forschungszentrum Jülich, Institute for Energy and Climate Research – Systems Analysis and Technology Evaluation, 52428 Jülich, Germany

²University of Cologne, Institute for Theoretical Physics, 50937 Cologne, Germany

³University of Bergen, Geophysical Institute and Bjerknes Centre for Climate Research, Bergen, Norway

Correspondence: Jan Wohland (j.wohland@fz-juelich.de)

Abstract. Wind energy has seen large deployment and substantial cost reductions over the last decades. Further ambitious upscaling is urgently needed to keep the goals of the Paris Agreement within reach. While the variability of wind power generation poses a challenge to grid integration, much progress in quantifying, understanding and managing it has been made over the last years. Despite this progress, relevant modes of variability in energy generation have been overlooked. Based on long-term reanalyses of the 20th century, we demonstrate that multi-decadal wind variability has significant impact on wind energy generation in Germany. These modes of variability can not be detected in modern reanalyses that are typically used for energy applications due to their short covered timespan of around 40 years. We show that energy generation over a 20y wind park lifetime varies by around $\pm 5\%$ and the summer-to-winter ratio varies by around $\pm 15\%$. Moreover, ERA-interim based annual and winter generations are biased high as the period 1979 - 2010 overlaps with a multi-decadal maximum of wind energy generation. The induced variations of windpark lifetime revenues are at the order of 10% with direct implications for profitability. Our results suggest to rethink energy system design as a perpetual process. Revenues and seasonalities change on a multi-decadal timescale, and so does the optimum energy system layout.

1 Introduction

Wind energy is on the rise. Following a period of high subsidies, drops in wind energy costs have been dramatic. In some places, onshore wind energy outperforms all other types of power generation in terms of levelized costs of electricity (IEA and IRENA, 2017). This economic development, in conjunction with the necessity to eliminate carbon emissions from the electricity sector in the next decades (Schleussner et al., 2016; Rogelj et al., 2015), will most certainly lead to strong investments in wind energy.

Wind parks are costly long-term investments. Since 2000, almost b€ 95 have been invested in wind parks in Germany (BMW, 2018). Compared to current stock exchange values, this figure is higher than the value of Volkswagen and only



marginally lower than that of Germany's most valuable company SAP (PWC, 2018). While planning is typically based on 20 year lifetimes, real-world experiences suggest that turbines can be operated even longer (Ziegler et al., 2018).

Wind power generation is variable which complicates its integration into power systems. This fact is increasingly accounted for in energy system models (a recent overview is provided by Ringkjøb et al., 2018). Underlying wind generation timeseries are typically based on modern reanalysis (e.g., Gonzalez Aparicio et al., 2016; Staffell and Pfenninger, 2016; Moraes et al., 2018). These timeseries cover around 40 years as the observations that they rely on become available in the late 1970s. Many characteristics of renewable generation variability, such as monthly, seasonal and even decadal variability can be investigated using these datasets. But are 40 years sufficient to capture all relevant modes of wind variability?

Some components of the climate system vary on very long timescales and interactions can give rise to low-frequency variability of atmospheric processes. For example, the North Atlantic Oscillation (NAO) has a low-frequency component that is linked to ocean and stratospheric variability (Omrani et al., 2016). The NAO has also been shown to impact the British wind sector (Brayshaw et al., 2011; Ely et al., 2013) and solar generation in Iberia (Jerez et al., 2013). These links suggest that renewable power systems could be affected by low-frequency climate variability. While much attention has been given to the impacts of climate change on renewable power systems (e.g., Pryor and Barthelmie, 2010; Reyers et al., 2016; Tobin et al., 2016; Wohland et al., 2017; Weber et al., 2018; Schlott et al., 2018; Karnauskas et al., 2018; Jerez et al., 2019), little emphasis has been put on the natural low-frequency variability of wind energy (with the notable exception of Bett et al., 2013, 2017). The fact that climate change assessments unanimously report relatively small to negligible impacts of climate change in Europe does not necessarily imply that natural variability is insignificant because climate models exhibit major discrepancies in simulating low-frequency climate variability (e.g., Ba et al., 2014).

In this study, we investigate the long-term evolution of wind energy generation in Germany. We aim to verify if there are relevant modes of variability on timescales of multiple decades. If these modes exist, it is crucially important to incorporate them in long-term decision making with regard to the design and operation of future power systems. Moreover, they would not only matter on a system level but also affect individual investments.

2 Methods and data

Our focus is on the effect of long-term natural climate variability on wind power generation. To isolate the imprint of the climate, we neglect potential changes in technology and deployment of wind parks. Specifically, we freeze the current configuration of wind parks and compute their theoretical energy generation over the 20th century. This approach allows to quantify the importance of climate driven multidecadal variability of wind energy in Germany.

We derive nationally aggregated wind generation timeseries for the period 1901-2010 following the procedure detailed in Wohland et al. (2018a). In short, the method consists of: vertical extrapolation of 10m wind speeds to 80m hub height using a power law followed by the application of a standard turbine power curve at each grid point and finally a multiplication with the installed capacities (from OPSD, 2017). Projections of the installed capacities onto the grids of the 20th century reanalyses are shown in Fig. 1.

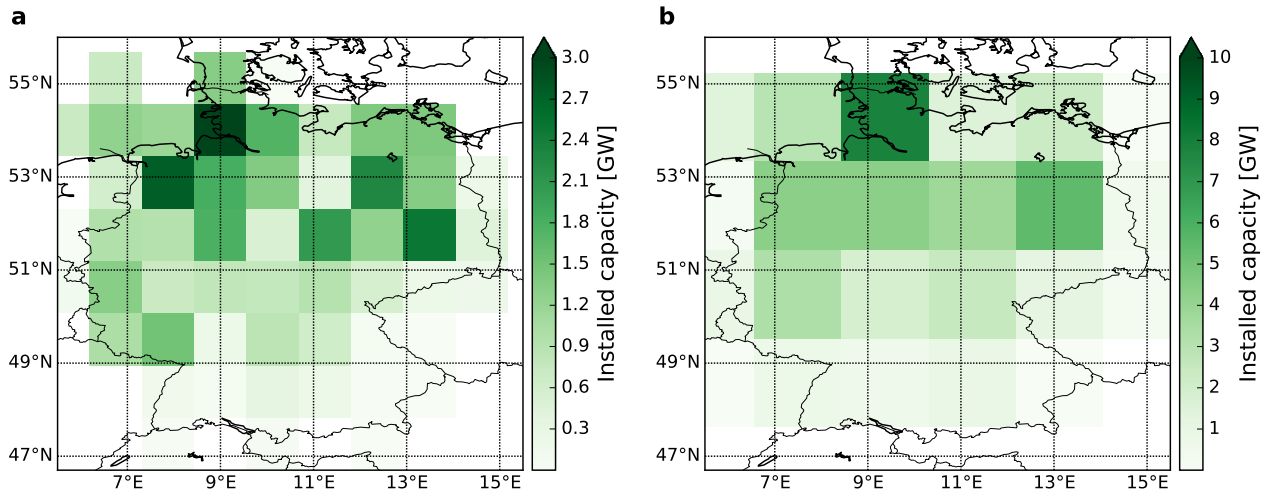


Figure 1. Allocation of turbines based on the Open Power System Database for the end of 2016 (OPSD, 2017). Data is projected on the ERA20CM/ERA20C/CERA20C grid (a) and the 20CR grid (b).

2.1 20th century reanalyses

Wind speeds come from the full set of current 20th century reanalyses and are provided by two different centers: the European Centre for Medium-Range Weather Forecast (ECMWF) and the National Oceanic and Atmospheric Administration (NOAA) from the USA. NOAA provided the first 20th century reanalysis named 20CR (Compo et al., 2011). 20CR is an atmospheric reanalysis that assimilates sea-level pressure observations only. In this study, we use the ensemble mean wind speeds from the version 20CRv2c which has 58 ensemble members. ECMWF followed a different approach and assimilates both sea-level pressure and marine wind observations. This difference in approaches yields substantial disagreement with respect to long-term wind speed trends (Wohland et al., 2019) but, as we show, there is large agreement regarding seasonal to multi-decadal variability after subtraction of the linear trends. ECMWF provides an atmosphere (ERA20C, Poli et al., 2016) and a coupled atmosphere-ocean 20th century reanalysis (CERA20C, Laloyaux et al., 2018). ERA20C is deterministic (i.e., has only one member) and CERA20C comes with a ten member ensemble. Unless otherwise stated, we report the CERA20C ensemble mean as the spread is usually very limited.

The longer temporal coverage comes at the cost of reduced spatial resolution as compared with modern reanalyses such as ERAINT (Dee et al., 2011), MERRA/MERRA2 (Rienecker et al., 2011) or ERA5 (Hennermann, 2018). ERA20C and CERA20C have a spatial resolution of $1.125^\circ \times 1.125^\circ$ and the 20CR resolution is even coarser ($1.875^\circ \times 1.875^\circ$). While the datasets are thus clearly not well suited for site-specific assessments, they are sufficiently detailed for country-level assessments (see also Fig. 1). Temporal resolution is 3h for all datasets and hence allows to capture intra-day effects.



2.2 Trend removal and timescale of interest

There is demonstrated disagreement of the 20th century reanalyses in terms of wind speed trends which originates from the assimilation of marine winds by ECMWF (Wohland et al., 2019). We thus remove the long-term (1901 - 2010) trends by subtraction of the zero-mean trend that is obtained via least-squares fitting of a linear fit function and subsequent subtraction of the trends mean:

$$G(t) = G_{\text{raw}}(t) - (G_{\text{trend}}(t) - \langle G_{\text{trend}}(t) \rangle), \quad (1)$$

where $G_{\text{raw}}(t)$ denotes the raw annual or seasonal timeseries, $G_{\text{trend}}(t)$ denotes the linear fit and $\langle G_{\text{trend}}(t) \rangle$ is its mean value.

We focus on the long term evolution of 20 year generation averages because 20 years are a typical lifetime for wind parks. Moreover, the averaging smooths the pronounced interannual variability which has already been extensively studied elsewhere. Both energy system planning and wind park investment are forward procedures in the sense that infrastructure built today will be operated under the weather conditions of the future. We therefore decided to compute 20 year forward running means of wind power generation G_{20} as

$$G_{20}(t) = \frac{1}{20} \sum_{t'=t}^{t+20y} G(t'), \quad (2)$$

where $G(t')$ denotes the annual wind power generation in year t' . To study the evolution in different seasons (winter DJF, spring MAM, summer JJA, autumn SON), we similarly compute the seasonal 20 year means as

$$G_{20}^{\text{season}}(t) = \frac{1}{20} \sum_{t'=t}^{t+20y} G(t')^{\text{season}}, \quad (3)$$

where $G(t')^{\text{season}}$ denotes the wind power generation in the respective season of year t' . Note that $G_{20}(t)$ and $G_{20}^{\text{season}}(t)$ are ill defined at the end of the dataset when 20 years are not available. We thus only compute them up to 1990. We generally report normalized lifetime generation or normalized seasonal lifetime generation which is obtained by division of $G_{20}(t)$ or $G_{20}^{\text{season}}(t)$ with the 1901-2010 mean $\langle G(t) \rangle$ or $\langle G(t) \rangle^{\text{season}}$, respectively.

2.2.1 Seasonality

In addition to seasonal generation averages, we report the seasonality S , which we define as the ratio of normalized winter to summer generation:

$$S(t) = \frac{G_{20}^{\text{DJF}}(t)}{\langle G \rangle^{\text{DJF}}} \bigg/ \frac{G_{20}^{\text{JJA}}(t)}{\langle G \rangle^{\text{JJA}}}. \quad (4)$$

Seasonality is an important metric for power system design and has a large influence on optimum technology mixes (e.g., Heide et al., 2010). In Germany, wind power generation is generally higher in autumn and winter than in spring and summer.



To ensure stable operation of the power system (i.e., a balance of generation and demand at all timesteps), seasonality has to be accounted for in power system design. For example, the dimensioning of storage or backup infrastructure and optimum wind to solar mixes depend on the seasonality. For completeness, we provide an extended definition of seasonality \hat{S} , which also includes autumn and spring as

$$5 \quad \hat{S}(t) = \frac{G_{20}^{\text{SON+DJF}}(t)}{\langle G \rangle_{\text{SON+DJF}}} \bigg/ \frac{G_{20}^{\text{MAM+JJA}}(t)}{\langle G \rangle_{\text{MAM+JJA}}} \quad (5)$$

2.2.2 Bias

We use the term bias to assess whether the period covered by ERAINT is representative for the longer period covered by the 20th century reanalyses. For example, if the seasonality over 1979 – 2010 is higher than over 1900 – 2010, we call the seasonality estimates of modern reanalyses biased high.

10 2.3 Multi-taper spectral estimation

We test significance of low-frequency components in the annual and seasonal wind generation timeseries using the multi-taper method (MTM, Ghil, 2002). Classical approaches, such as Fourier spectral analysis suffer from spectral leakage when applied to relatively short timeseries, hindering reliable assessments. MTM provides an alternative in that it calculates tapers that are designed to minimize leakage. We use $K = 3$ tapers with a bandwidth of $p = 2y$ as suggested by Ghil (2002) for a comparable
 15 timeseries. Eigentapers are weighted based on their eigenvalues and the computation is performed via the Python package spectrum (Cokelaer and Hasch, 2017)

Significance testing is based on the null hypothesis of red noise. The underlying process that creates a red-noise spectrum is referred to as a autoregressive model of first order or AR(1). The parameters of the red-noise spectrum $S_R(f)$ are fitted to minimize the mismatch between the median smoothed real and the red-noise spectrum (as suggested by Ghil, 2002; Mann and
 20 Lees, 1996). A peak in the real spectrum $S(f)$ at frequency f' is considered significant at the 90% level if

$$S(f') > S_R(f') \cdot \chi^2(90\%, 2K), \quad (6)$$

again following (Ghil, 2002). $\chi^2(90\%, 2K)$ denotes the chi square distribution with $2K$ degrees of freedom at a 90% confidence level. White noise is a special case of red noise and is characterized by a constant spectrum (i.e., $S_W(f) = S_0$, where S_0 is a real positive number). White noise is generated by an autoregressive model of 0th order, AR(0).

25 2.4 Impacts on investments

In an investment decision, the installation and operational costs of an asset have to be compared with expected revenues. Taking into account risks and alternative investments, an investment is made if the expected revenues exceed the total costs by some amount. The expected revenue may be substantially flawed if it is based on only a couple of years of wind data. In contrast, decision makers that are aware of all modes of wind variability gain an advantage through more reliable revenue estimates.



To quantify this impact of low-frequency wind variability on wind park investments, we calculate the discounted lifetime cash inflows as

$$C_{\text{in}}(t) = c \cdot \sum_{t'=t}^{t+\tau} \frac{1}{(1 + \gamma + \Delta\eta)^{t'-t}} G(t'), \quad (7)$$

where $\gamma = 5.5\%/y$ is the discount rate, $\Delta\eta \approx 1.5\%/y$ accounts for the decline in turbine performance (Staffell and Green, 2014), $\tau = 20y$ is the conservatively assumed lifetime, c is the revenue per generated unit of electricity and G is wind power generation. We set c to be constant because the German system is still designed to guarantee prices for wind park operators. Prior to the recent shift towards auctions, the price was determined politically. Since the latest reform of the renewable energy act in 2017, the price is determined via auctions but is still guaranteed over 20 years (BMW, 2017). Both for old and new wind parks it is thus justified to use constant prices, albeit the price will differ dependent on the date of construction and the auction outcome.

2.5 North Atlantic Oscillation

To gain more insight into the co-evolution of wind generation variability and the general circulation of the atmosphere, we include the North Atlantic Oscillation (NAO). The NAO is the leading pattern of climate variability in the North Atlantic Sector affecting weather and climate over Europe, particularly in winter (Marshall et al., 2001). It is here defined as the first principle component of sea-level pressure over the area 20°N to 80°N and 90°W to 40°E as detailed in Omrani et al. (2016). Our NAO index is computed from sea-level pressure data from the Hadley Center (Rayner, 2003) over the winter months December, January, February.

3 Validation

In a recent study, we have shown that ERAINT has skill to reproduce reported wind power generation in Germany (Wohland et al., 2018a). It thus appears logical to test the 20th century reanalyses by comparison with ERAINT over the overlapping period (1979-2009). We also add the widely used Renewables.Ninja wind energy dataset that is based on MERRA-2 (Staffell and Pfenninger, 2016).

The evolution of the normalized lifetime mean generation is similar for all reanalyses under consideration (see Fig. 2a). All start with a period of high values that is followed by roughly five years of low values. Towards the end, the normalized lifetime generation recovers, but not to the same levels as in the first couple of years.

On a finer temporal scale, there is good correlation between the daily generations based on ERAINT and 20CR, ERA20C and CERA20C, respectively (see Fig. 2b–d). 20CR overestimates daily generation (slope < 1 in Fig. 2b). In contrast, ERA20C and CERA20C underestimate daily generation (slopes > 1 in Fig. 2c&d). This systematic over/underestimation of daily wind generations, however, is of minor importance in this study because it is reduced by normalization with the long-term mean. All 20th century reanalyses agree well with ERAINT for very high daily generations larger than around 40GW. Pearson correlation



is high for 20CR ($r = 0.92$) and even higher for the ECMWF products ($r = 0.98$). A similar result is found for the RMSE which is 4.3 GW for 20CR and around 1.3 GW for ERA20C and CERA20C, again indicating larger agreement across the ECMWF reanalyses. This larger agreement could be due to more similar spatial resolutions that allow to capture the same processes in (C)ERA20C as in ERAINT. It may also reflect the common institutional origin as ERAINT and (C)ERA20C have been developed at ECMWF and are based on different versions of the same model. In any case, the substantial agreement of the detrended timeseries on different timescales creates confidence in the 20th century reanalyses.

From visual inspection, there also seems to be a downward trend over the period (1979 - 1990). A trend analysis of the ERAINT data indeed reveals a significant (at the 99% level) downward trend of the normalized lifetime generation, highlighting the relevance of long-term assessments. However, this trend should be interpreted cautiously as it is calculated using only 11 (not independent) values of G_{20} . The remainder of the paper is therefore based on longer timeseries to allow more robust assessments of multi-decadal variability.

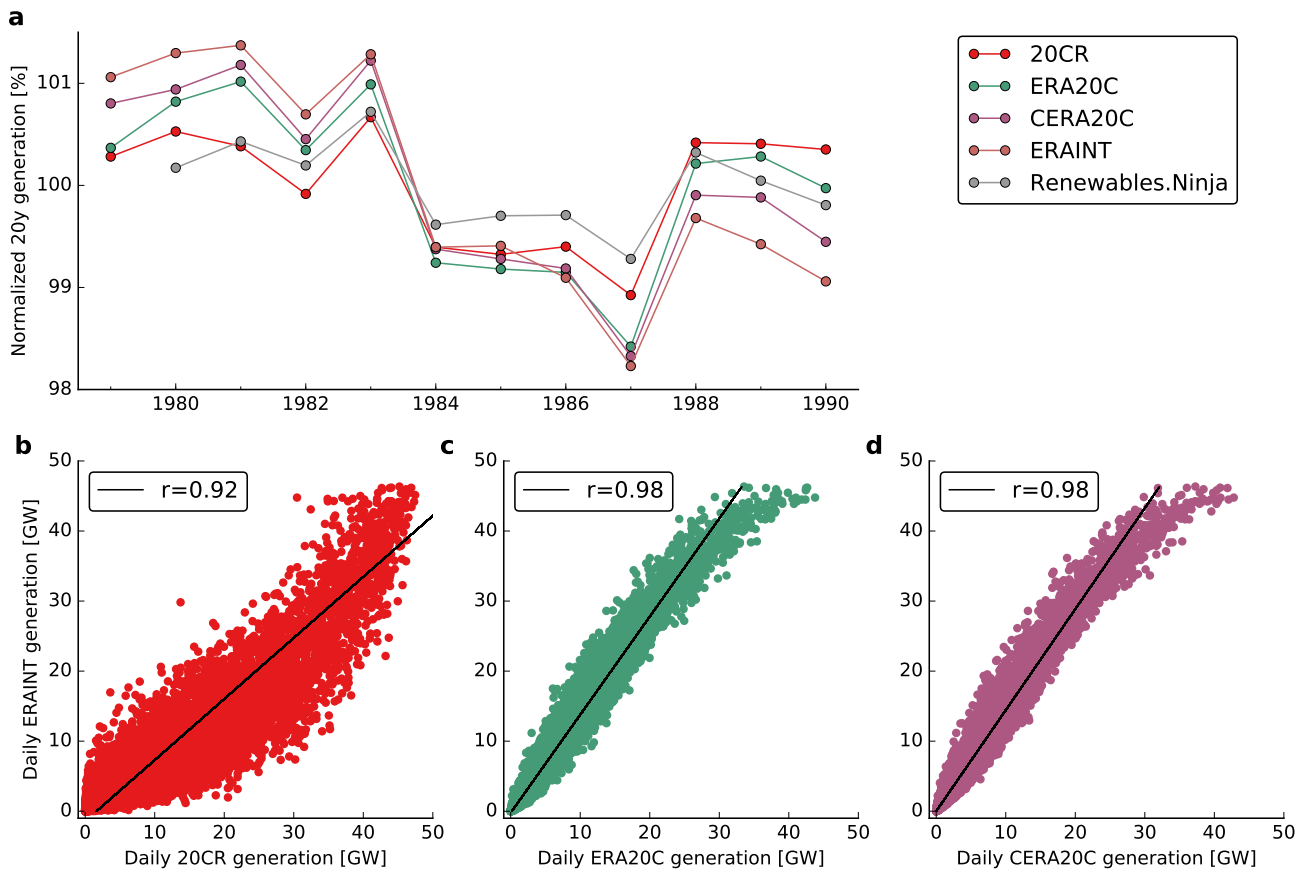


Figure 2. German wind power generation from modern reanalyses (ERAINT, MERRA2) and 20th century reanalyses (20CR, ERA20C, CERA20C) for period of overlap. a) Normalized lifetime generation (i.e., the reported value for 1990 is the average wind power generation of the years 1990-2009 normalized with the long-term mean). Renewables.Ninja is an openly available generation dataset that is based on MERRA2. **b-d)** scatter plots of daily generation from ERAINT versus daily values from 20CR (b), ERA20C (c), CERA20C (d) for the 30y period from 1979 to 2009. The Pearson correlation coefficient r between the daily data is given in the legends. The data is shown prior to long-term trend removal which was performed for the centennial analysis (see Methods).



Table 1. Trend characteristics. Slopes are rounded to integer values and the CERA20C slope corresponds to the mean of the slopes of the individual ensemble members. Significance is tested against the null hypothesis of no trend and using a two-sided t-test. For CERA20C, all streams feature significant trends individually.

dataset	slope [%/100y]	significant at 99.9% level?
20CR version	0	no
ERA20C	28	yes
CERA20C	16	yes

4 Results

4.1 Trends

We find ERA20C and CERA20C to feature statistically highly significant trends (see Table 1). In both datasets, the trends are strong: ERA20C reports 28% higher wind power generation at the end of the 20th century as compared to its beginning. The corresponding increase in CERA20C is substantial (16% increase in a hundred years) but roughly half as large. In contrast, there is no significant trend in 20CR.

The existence of these trends comes as no surprise given strong long-term trends in (C)ERA20C surface wind speeds over large parts of the world (Wohland et al., 2019). In our previous publication, we showed that the trends originate from the assimilated marine wind speeds that also feature very strong long-term trends. They are likely spurious and caused by the evolving measurement technique. In addition to wind speed trends, ERA20C also features trends in marine sea level pressure gradients that are not in line with observations (Bloomfield et al., 2018). All following analyses are therefore based on detrended timeseries.

4.2 Low-frequency variability in normalized lifetime wind generation

After subtraction of the trends, there is large agreement among the datasets regarding multi-decadal variability of normalized lifetime generation (see Fig. 3). Maxima and minima of annual and seasonal timeseries coincide for ERA20C, CERA20C and 20CR. The amplitude of variability is also comparable among the datasets for all seasons and the annual values. Only in September-October-November (SON), there is disagreement from 1960 onwards as 20CR reports values that are 5 to 10% off the (C)ERA20C values. Generally, there is stronger variability of seasonal than annual generation, hinting at compensating effects between seasons. In June-July-August (JJA), for example, the maximum to minimum difference is around 15%. This compares to 5 to 10% maximum to minimum difference for the annual values.

German annual generation is dominated by winter generation due to generally stronger winds in winter. This winter dependence explains the high similarity between the annual and winter timeseries (compare Fig. 3 a with c) and also the high correlation of $r = 0.71$ between them (see Fig. 3 b). On the timescales considered here, there is also a weak anti-correlation between the annual and the summer values ($r = -0.39$) and between the summer and autumn values ($r = -0.46$).



The ratio of winter to summer generation (i.e., seasonality) is characterized by strong multi-decadal variability. While the maximum 20 year seasonality is between 110% and almost 120% (dependent on the dataset), the minimum lies between 80% and 90% (see Fig. 3g). If an extended definition of seasonality is applied, the amplitude of the variability is reduced but the maximum to minimum difference still ranges around 15% to 20% (see Fig. 3h).

5 In winter there is also a good connection between 20 year mean anomalies of the North Atlantic Oscillation (NAO) and normalized lifetime generation as highlighted by correlation coefficients between them that range from $r = 0.7$ to $r = 0.76$ for the different datasets (see Fig. 4a). This relation is consistent with the NAO being the dominant pattern of winter time climate variability in the North Atlantic sector (Marshall et al., 2001). The agreement is strongest on multidecadal timescales and it is particularly high since 1960. However, a peak in normalized lifetime wind generation around mid century is not paralleled by
10 a similar feature in the NAO.

Modern reanalyses, such as ERAINT, are too short to capture these modes of low-frequency variability (see blue arrows in Fig. 3). Unfortunately, ERAINT does not only fail to capture these effects, but also provides biased high estimates in some cases. For example, the seasonality reported by ERAINT, coincides with above average values of seasonality and is hence not representative in general (see Fig. 3g). The same is true for annual and winter generation. Moreover, ERAINT begins at a time
15 of maximum normalized lifetime wind generation. ERAINT based trend assessments can thus misidentify the downward part of reoccurring cycles as trends (as discussed in Sec. 3). Similarly, the decline of autumn generation since the 1970s could be falsely interpreted as a trend.

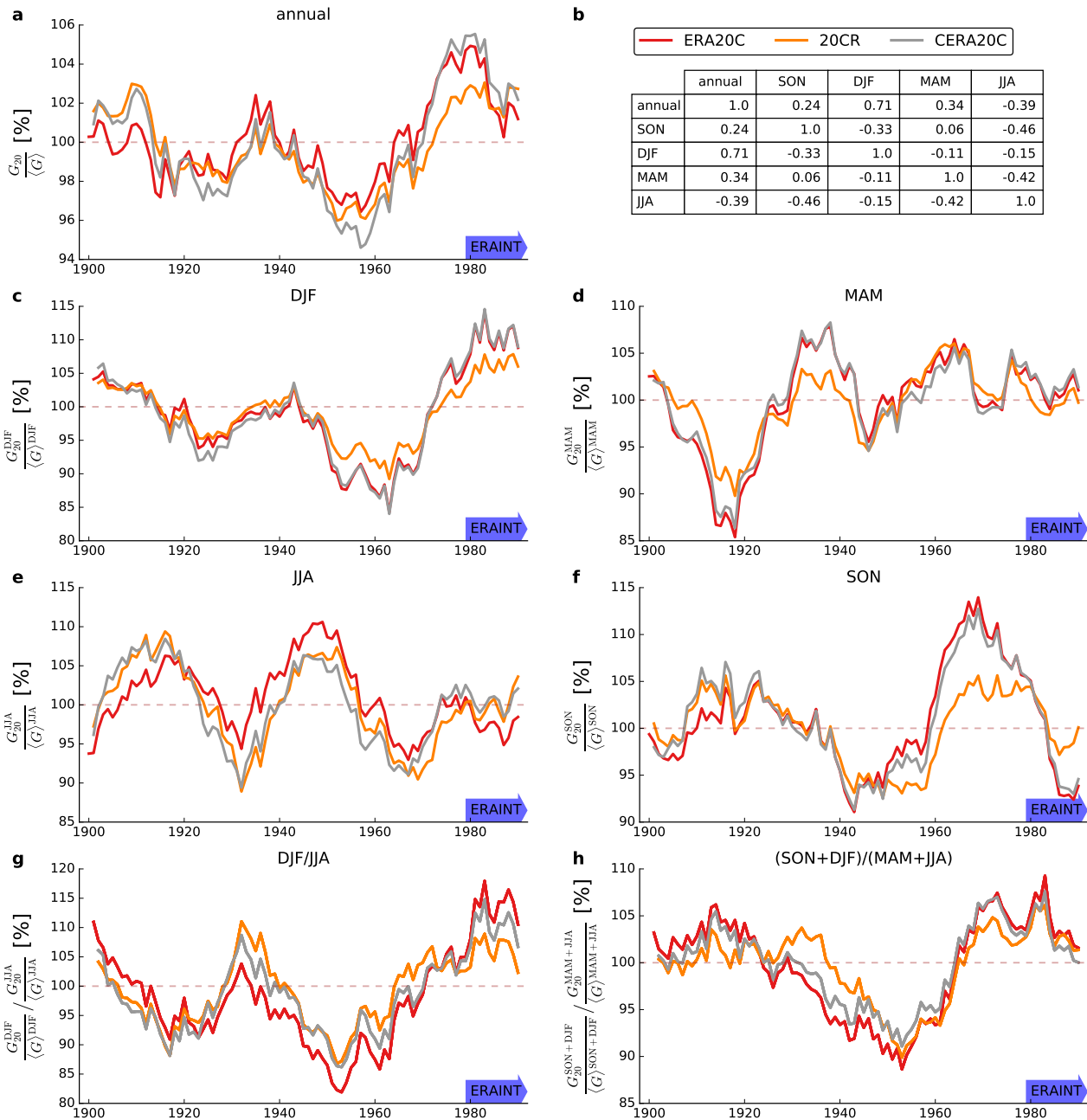


Figure 3. Normalized lifetime generation from German wind parks. Timeseries are based on detrended 20th century reanalyses. The subplots show annual (a) and seasonal (c-f) timeseries. Different versions of the seasonality are also displayed (g-h) and correlations between seasons are reported for ERA20C (b). The data has been smoothed by application of a running mean 20y forward filter (i.e., the reported value for 1900 is the average of the years 1900-1919). The blue arrow highlights the limited coverage of ERAINT.

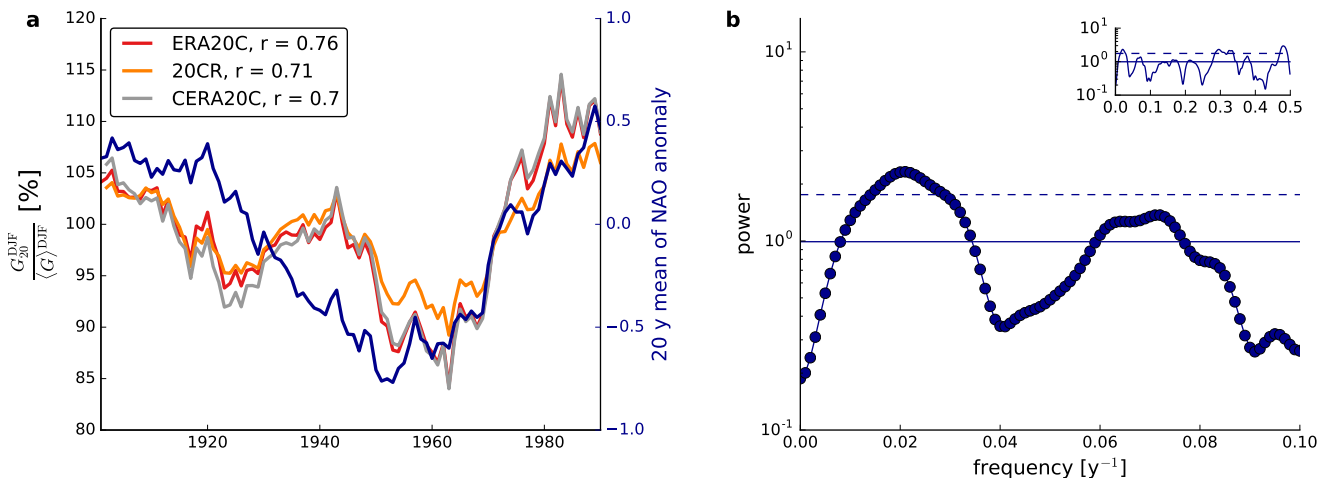


Figure 4. Relation between normalized lifetime winter generation and the winter North Atlantic Oscillation. Timeseries of wind power generation (in red, orange and grey) refer to the left y-axis while the NAO timeseries (in blue) refers to the right y-axis (a). Pearson correlation coefficients r are calculated between the 20y mean NAO anomaly and the 20y mean DJF wind power generation. MTM spectrum of the winter NAO (bullets in b), focusing on the low-frequency interval of the spectrum. Solid lines represent the fitted spectrum of an AR(1) process that is used for significance testing and the dashed lines correspond to the 90% confidence level (see Methods for details).



4.3 Spectral analysis

We perform multi-taper spectral analysis for detrended annual and seasonal German wind power generation for the period 1901-2010 (Fig 5). No prior smoothing or filtering is applied. A focus is given to the low frequency part of the spectrum with frequencies of less than 0.1 y^{-1} , which corresponds to at least 10 year periods. There are statistically significant low frequency peaks in all seasons with different levels of agreement among reanalyses. All reanalyses feature a significant peak in MAM ($f \approx 0.04 \text{ y}^{-1}$ or $f^{-1} \approx 25 \text{ y}$) and JJA ($f \approx 0.03 \text{ y}^{-1}$ or $f^{-1} \approx 33 \text{ y}$) and the latter is also clearly visible in the timeseries (see Fig. 3e). In SON, CERA20C and ERA20C report a clearly significant peak that is also almost significant in 20CR ($f \approx 0.02 \text{ y}^{-1}$ or $f^{-1} \approx 50 \text{ y}$). In winter there is a spectral peak with period of around 50 years ($f \approx 0.02 \text{ y}^{-1}$) that is related to the NAO (see Fig.4b). This connection to a physical pattern of climate variability suggests that the peak is not a statistical artifact, despite its low statistical significance. The generally high agreement among the reanalyses adds confidence to the existence of multi-decadal periodicities during the historical period.

Interestingly, the AR(1) fit to the median-smoothed spectra does not reveal red noise but white noise (except for MAM), in agreement with the understanding of atmospheric variability as a process that is white to first order (Wunsch, 1999). This can be seen by the thin solid lines in Fig. 5, which display the fitted AR(1) spectra: They are virtually flat, i.e. virtually independent of the frequency. For example, in JJA (Fig. 5d), the power of the AR(1) fit is 10^0 (GWh/GWh)^2 for all frequencies. White noise implies that the system does not have relevant memory from one year to the next but rather behaves erratically on year-to-year timescales.

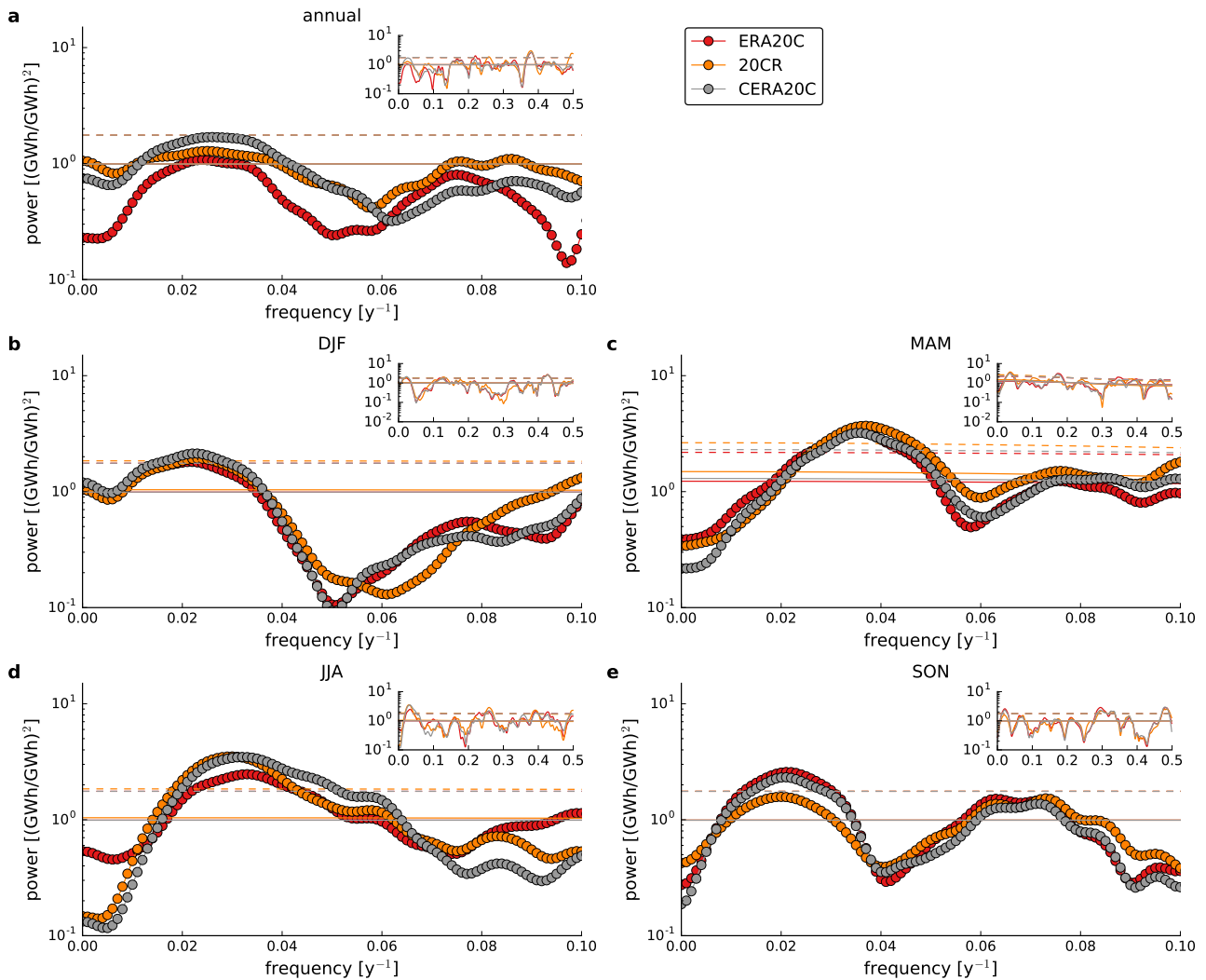


Figure 5. Spectral analysis of the wind generation timeseries using multi-taper method (MTM). Subplots report annual (a) and seasonal spectra (b-e). Focus is given to the low-frequency component with frequencies of less than 0.1 y^{-1} while the full spectrum is shown in the inset of each subplot. Solid lines represent the fitted spectrum of an AR(1) process that is used for significance testing and the dashed lines correspond to the 90% confidence level for each dataset (see Methods for details).



4.4 Relevance for investment decisions

In addition to the relevance of low-frequency variability for system design, the long lifetime of wind parks makes returns on individual investment susceptible to low-frequency variability and not taking this susceptibility into account has substantial economic implications. The effect is illustrated in Fig. 6, where the discounted lifetime cash inflow of a wind park that follows the German mean wind generation is shown. The values are normalized such that 100% refers to the 1901-2010 mean. This graph shows variability of a wind park’s cash inflows between a maximum of 104% to 107% and a minimum of 95% to 97% dependent on the phase of low-frequency climate variability at the commissioning date. In other words, a wind park created in 1955 would produce 7-12% less revenue than one created in 1975. Recall that we abstract from technology innovations throughout the entire manuscript. Dependent on the individual project characteristics, most notably the ratio of the investment to the *expected* lifetime cash inflows, a few per cent more or less on the income side can turn an average project into a very profitable one or might leave a slightly profitable project unprofitable. Roughly between 1960 and 1975, there was a linear increase of cash inflows which has been followed by a decrease since 1980. Assessments based on ERAINT may tend to overestimate discounted lifetime cash inflows as ERAINT coincides with a period of high wind generation.

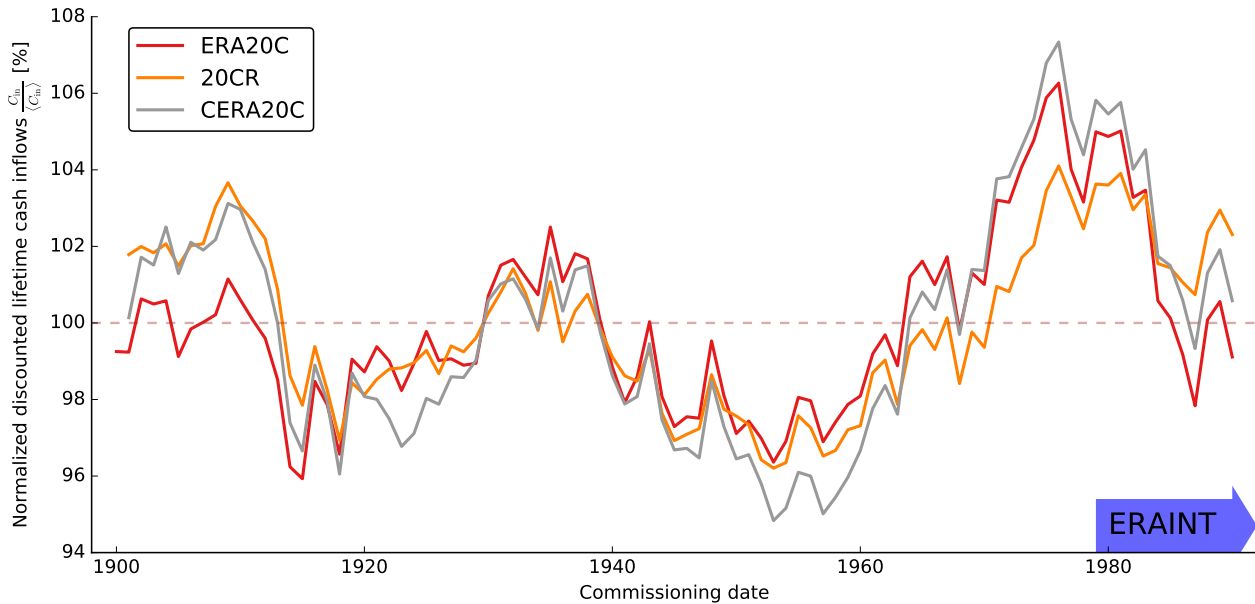


Figure 6. Long-term evolution of normalized discounted lifetime cash inflows of a wind park whose generation follows the German mean. A lifetime of 20y, ageing of 1.5%/y and a discount rate of 5.5%/y are assumed. The timeseries ends in 1990 because the underlying reanalyses end in 2010.



5 Discussion and concluding remarks

Based on the full set of current 20th century reanalyses (20CR, ERA20C, CERA20C), we have shown that multi-decadal variability matters for wind energy in Germany. There are statistically significant modes of generation variability on timescales of 25 to 50 years in spring, summer and autumn. In winter, there is a spectral peak with period of around 50 years that is related to the NAO. This connection to a physical pattern of climate variability suggests that the peak is not a statistical artifact, despite its low statistical significance.

Our results imply that in addition to relatively intuitive timescales (diurnal, seasonal, annual), also slower and less intuitive modes of variability ought to be included in energy assessments. While current modern reanalyses are too short to capture multi-decadal wind generation variability, future products may be better suited due to extended temporal coverage (e.g., ERA5 will start in 1950 and is expected to be entirely published in early 2019).

One of the most relevant results for power system design is the variability of seasonality (defined as the ratio of winter to summer generation here). Far from being constant, 20 year mean seasonality varies by almost up to $\pm 15\%$. As the seasonal evolution of generation is one main factor to determine optimal contributions of wind and photovoltaics (Heide et al., 2010), such optimum shares should also be considered as timeseries that vary on timescales of 50 years or so. This variability calls for a perpetual redesign of power systems to follow climate variability. ERAINT samples a seasonality maximum and therefore reports biased high seasonality. This bias implies that lifetime wind power generation is most often more stable throughout the year than would be expected from ERAINT, facilitating system integration. In the bigger picture, it may be relevant to rethink whether changes in seasonality that were attributed to climate change in earlier studies (e.g., Reyers et al., 2016) may simply reflect natural variability.

There are also implications for individual wind park projects as their profitability is strongly influenced by climate variability on long timescales. The same wind park commissioned in different phases of low-frequency generation variability, can have discounted lifetime cash inflows anywhere between 95% and 107% of the mean value with potentially severe impacts on profitability. To give an impression of scale: As the current German wind park fleet represents a b€ 95 investment, this translates into a lifetime revenue spread at the order of b€ 10 in Germany alone.

The effect of wind variability on revenues obviously depends on the market design. Instead of guaranteeing a constant price for wind energy, adaptive prices that fall in times of high generation and decline in times of low generation could dampen the economic effect of multi-decadal wind variability. We speculate that a higher price of CO₂ emission allowances in combination with an end to guaranteed renewable feed-in might be a possible route forward. The increased CO₂ emission allowance price would guarantee that renewables are favoured over fossils for mere economic reasons and it would also ensure sufficiently high market prices. During decades of high (low) wind generation, the average market price would fall (increase) thereby smoothing the variability of revenues and reducing the risk for investors. However, this strategy would only constitute an interim solution as it relies on a substantial share of non-renewable generation. In a future zero emission energy system, all variability from wind generation needs to be balanced by other means, for example through sector coupling, flexible demands or large scale



storage (Brown et al., 2018). It might become necessary to ponder decadal energy storage systems or to use the atmosphere as a carbon storage (Wohland et al., 2018b).

Our study raises new questions. While Germany was chosen as an exemplary case due to its current high deployment of wind turbines, other and larger areas should also be studied. Are there compensating effects across Europe? If yes, expansion of the transmission network and optimized siting could help mitigate multi-decadal variability in the same fashion that it helps to smooth synoptic generation variability (e.g., Rodriguez et al., 2014; Grams et al., 2017; Santos-Alamillos et al., 2017). This study is restricted to wind energy because we doubt the reanalyses' skill to capture cloud dynamics sufficiently well. Nevertheless, it would be of high interest to investigate low frequency variability of other types of renewable generation: Do similar modes exist for photovoltaics and hydropower? Lastly, climate models are, in theory, an excellent tool to quantify and study natural climate variability as timeseries of arbitrary length can be obtained. Multi-decadal variability can thus be sampled substantially better than in 20th century reanalyses. However, it remains to be shown whether climate models are capable to reproduce multi-decadal variability that is relevant for the energy sector.

Code and data availability. This paper relies on wind speeds from different 20th century reanalysis that are openly available through ECMWF (<https://apps.ecmwf.int/datasets/> and <http://apps.ecmwf.int/datasets/data/era20c-daily/levtype=sfc/type=an/>) and NOAA (https://www.esrl.noaa.gov/psd/data/gridded/data.20thC_ReanV2c.monolevel.html). We also use the end of 2016 wind fleet configuration as reported by the Open Power System Database which is also openly available online (https://data.open-power-system-data.org/renewable_power_plants/). The programming is done in Python and the code is shared upon reasonable request to the authors.

Author contributions. JW initiated the collaboration, developed the methodology, analyzed the data, produced all figures and wrote most of the manuscript. DW contributed to the methodology and interpretation of the data and supervised the research. NEO and NK contributed to the development of the methodology and the interpretation of the results. All authors contributed ideas, gave feedback and helped to improve the manuscript.

Competing interests. The authors declare that they have no conflict of interest.

Acknowledgements. We thank ECMWF for making ERA20C and CERA20C publicly available. We thank NOAA for making 20CRv2c available. JW thanks the Hitec graduate school at Forschungszentrum Jülich for a travel grant. JW and DW are funded by the Helmholtz association through the the joint initiative 'Energy System 2050 – A Contribution of the Research Field Energy' and the grant no. VH-NG-1025 to Dirk Witthaut.



References

- Ba, J., Keenlyside, N. S., Latif, M., Park, W., Ding, H., Lohmann, K., Mignot, J., Menary, M., Otterå, O. H., Wouters, B., Salas y Melia, D., Oka, A., Bellucci, A., and Volodin, E.: A multi-model comparison of Atlantic multidecadal variability, *Climate Dynamics*, 43, 2333–2348, <https://doi.org/10.1007/s00382-014-2056-1>, <http://link.springer.com/10.1007/s00382-014-2056-1>, 2014.
- 5 Bett, P. E., Thornton, H. E., and Clark, R. T.: European wind variability over 140 yr, *Advances in Science and Research*, 10, 51–58, <https://doi.org/10.5194/asr-10-51-2013>, <http://www.adv-sci-res.net/10/51/2013/>, 2013.
- Bett, P. E., Thornton, H. E., and Clark, R. T.: Using the Twentieth Century Reanalysis to assess climate variability for the European wind industry, *Theoretical and Applied Climatology*, 127, 61–80, <https://doi.org/10.1007/s00704-015-1591-y>, <http://link.springer.com/10.1007/s00704-015-1591-y>, 2017.
- 10 Bloomfield, H., Shaffrey, L., Hodges, K. I., and Vidale, P. L.: A critical assessment of the long term changes in the winter-time surface Arctic Oscillation and Northern Hemisphere storminess in the ERA20C reanalysis, *Environmental Research Letters*, <https://doi.org/10.1088/1748-9326/aad5c5>, <http://iopscience.iop.org/article/10.1088/1748-9326/aad5c5>, 2018.
- BMWi: Fragen und Antworten zum EEG 2017, p. 9, 2017.
- BMWi: Zeitreihen zur Entwicklung der erneuerbaren Energien in Deutschland, p. 46, 2018.
- 15 Brayshaw, D. J., Troccoli, A., Fordham, R., and Methven, J.: The impact of large scale atmospheric circulation patterns on wind power generation and its potential predictability: A case study over the UK, *Renewable Energy*, 36, 2087–2096, <https://doi.org/10.1016/j.renene.2011.01.025>, <http://linkinghub.elsevier.com/retrieve/pii/S0960148111000474>, 2011.
- Brown, T., Schlachtberger, D., Kies, A., Schramm, S., and Greiner, M.: Synergies of sector coupling and transmission reinforcement in a cost-optimised, highly renewable European energy system, *Energy*, 160, 720–739, <https://doi.org/10.1016/j.energy.2018.06.222>, <https://linkinghub.elsevier.com/retrieve/pii/S036054421831288X>, 2018.
- 20 Cokelaer, T. and Hasch, J.: 'Spectrum': Spectral Analysis in Python, *The Journal of Open Source Software*, 2, 348, <https://doi.org/10.21105/joss.00348>, <http://joss.theoj.org/papers/10.21105/joss.00348>, 2017.
- Compo, G. P., Whitaker, J. S., Sardeshmukh, P. D., Matsui, N., Allan, R. J., Yin, X., Gleason, B. E., Vose, R. S., Rutledge, G., Bessemoulin, P., Brönnimann, S., Brunet, M., Crouthamel, R. I., Grant, A. N., Groisman, P. Y., Jones, P. D., Kruk, M. C., Kruger, A. C., Marshall, G. J., Mauerer, M., Mok, H. Y., Nordli, O., Ross, T. F., Trigo, R. M., Wang, X. L., Woodruff, S. D., and Worley, S. J.: The Twentieth Century Reanalysis Project, *Quarterly Journal of the Royal Meteorological Society*, 137, 1–28, <https://doi.org/10.1002/qj.776>, <http://doi.wiley.com/10.1002/qj.776>, 2011.
- 25 Dee, D. P., Uppala, S. M., Simmons, A. J., Berrisford, P., Poli, P., Kobayashi, S., Andrae, U., Balmaseda, M. A., Balsamo, G., Bauer, P., Bechtold, P., Beljaars, A. C. M., van de Berg, L., Bidlot, J., Bormann, N., Delsol, C., Dragani, R., Fuentes, M., Geer, A. J., Haimberger, L., Healy, S. B., Hersbach, H., Hólm, E. V., Isaksen, L., Kållberg, P., Köhler, M., Matricardi, M., McNally, A. P., Monge-Sanz, B. M., Morcrette, J.-J., Park, B.-K., Peubey, C., de Rosnay, P., Tavolato, C., Thépaut, J.-N., and Vitart, F.: The ERA-Interim reanalysis: configuration and performance of the data assimilation system, *Quarterly Journal of the Royal Meteorological Society*, 137, 553–597, <https://doi.org/10.1002/qj.828>, <http://doi.wiley.com/10.1002/qj.828>, 2011.
- 30 Ely, C. R., Brayshaw, D. J., Methven, J., Cox, J., and Pearce, O.: Implications of the North Atlantic Oscillation for a UK-Norway Renewable power system, *Energy Policy*, 62, 1420–1427, <https://doi.org/10.1016/j.enpol.2013.06.037>, <http://linkinghub.elsevier.com/retrieve/pii/S0301421513005223>, 2013.



- Ghil, M.: Advanced spectral methods for climatic time series, *Reviews of Geophysics*, 40, <https://doi.org/10.1029/2000RG000092>, <http://doi.wiley.com/10.1029/2000RG000092>, 2002.
- Gonzalez Aparcio, I., Zucker, A., Careri, F., Monforti, F., Huld, T., and Badger, J.: EMHIREs dataset; Part 1: Wind power generation, Tech. Rep. EUR 28171 EN, Joint Research Center, 2016.
- 5 Grams, C. M., Beerli, R., Pfenninger, S., Staffell, I., and Wernli, H.: Balancing Europe's wind-power output through spatial deployment informed by weather regimes, *Nature Climate Change*, <https://doi.org/10.1038/nclimate3338>, <http://www.nature.com/doi/10.1038/nclimate3338>, 2017.
- Heide, D., von Bremen, L., Greiner, M., Hoffmann, C., Speckmann, M., and Bofinger, S.: Seasonal optimal mix of wind and solar power in a future, highly renewable Europe, *Renewable Energy*, 35, 2483–2489, <https://doi.org/10.1016/j.renene.2010.03.012>, <https://linkinghub.elsevier.com/retrieve/pii/S0960148110001291>, 2010.
- 10 Hennermann, K.: ERA5 data documentation, <https://confluence.ecmwf.int/display/CKB/ERA5+data+documentation>, 2018.
- IEA and IRENA: Perspectives for the Energy Transition, Tech. rep., 2017.
- Jerez, S., Trigo, R. M., Vicente-Serrano, S. M., Pozo-Vázquez, D., Lorente-Plazas, R., Lorenzo-Lacruz, J., Santos-Alamillos, F., and Montávez, J. P.: The Impact of the North Atlantic Oscillation on Renewable Energy Resources in Southwestern Europe, *Journal of Applied Meteorology and Climatology*, 52, 2204–2225, <https://doi.org/10.1175/JAMC-D-12-0257.1>, <http://journals.ametsoc.org/doi/abs/10.1175/JAMC-D-12-0257.1>, 2013.
- 15 Jerez, S., Tobin, I., Turco, M., Jiménez-Guerrero, P., Vautard, R., and Montávez, J. P.: Future changes, or lack thereof, in the temporal variability of the combined wind-plus-solar power production in Europe, *Renewable Energy*, p. 21, 2019.
- Karnauskas, K. B., Lundquist, J. K., and Zhang, L.: Southward shift of the global wind energy resource under high carbon dioxide emissions, *Nature Geoscience*, 11, 38–43, <https://doi.org/10.1038/s41561-017-0029-9>, <http://www.nature.com/articles/s41561-017-0029-9>, 2018.
- 20 Laloyaux, P., de Boissesson, E., Balmaseda, M., Bidlot, J.-R., Broennimann, S., Buizza, R., Dalhgren, P., Dee, D., Haimberger, L., Hersbach, H., Kosaka, Y., Martin, M., Poli, P., Rayner, N., Rustemeier, E., and Schepers, D.: CERA-20C: A coupled reanalysis of the Twentieth Century, *Journal of Advances in Modeling Earth Systems*, <https://doi.org/10.1029/2018MS001273>, <http://doi.wiley.com/10.1029/2018MS001273>, 2018.
- 25 Mann, M. E. and Lees, J. M.: Robust estimation of background noise and signal detection in climatic time series, *Climatic Change*, 33, 409–445, <https://doi.org/10.1007/BF00142586>, <http://link.springer.com/10.1007/BF00142586>, 1996.
- Marshall, J., Kushnir, Y., Battisti, D., Chang, P., Czaja, A., Dickson, R., Hurrell, J., McCartney, M., Saravanan, R., and Visbeck, M.: North Atlantic climate variability: phenomena, impacts and mechanisms, *International Journal of Climatology*, 21, 1863–1898, <https://doi.org/10.1002/joc.693>, <http://doi.wiley.com/10.1002/joc.693>, 2001.
- 30 Moraes, L., Bussar, C., Stoecker, P., Jacqué, K., Chang, M., and Sauer, D.: Comparison of long-term wind and photovoltaic power capacity factor datasets with open-license, *Applied Energy*, 225, 209–220, <https://doi.org/10.1016/j.apenergy.2018.04.109>, <https://linkinghub.elsevier.com/retrieve/pii/S0306261918306767>, 2018.
- Omrani, N.-E., Bader, J., Keenlyside, N. S., and Manzini, E.: Troposphere–stratosphere response to large-scale North Atlantic Ocean variability in an atmosphere/ocean coupled model, *Climate Dynamics*, 46, 1397–1415, <https://doi.org/10.1007/s00382-015-2654-6>, <http://link.springer.com/10.1007/s00382-015-2654-6>, 2016.
- 35 OPSD: Renewable power plants, https://data.open-power-system-data.org/renewable_power_plants/ (version 16/02/17), 2017.



- Poli, P., Hersbach, H., Dee, D. P., Berrisford, P., Simmons, A. J., Vitart, F., Laloyaux, P., Tan, D. G. H., Peubey, C., Thépaut, J.-N., Trémolet, Y., Hólm, E. V., Bonavita, M., Isaksen, L., and Fisher, M.: ERA-20C: An Atmospheric Reanalysis of the Twentieth Century, *Journal of Climate*, 29, 4083–4097, <https://doi.org/10.1175/JCLI-D-15-0556.1>, <http://journals.ametsoc.org/doi/10.1175/JCLI-D-15-0556.1>, 2016.
- Pryor, S. and Barthelmie, R.: Climate change impacts on wind energy: A review, *Renewable and Sustainable Energy Reviews*, 14, 430–437, <https://doi.org/10.1016/j.rser.2009.07.028>, <http://linkinghub.elsevier.com/retrieve/pii/S1364032109001713>, 2010.
- PWC: Europas Top 100, 2018.
- Rayner, N. A.: Global analyses of sea surface temperature, sea ice, and night marine air temperature since the late nineteenth century, *Journal of Geophysical Research*, 108, <https://doi.org/10.1029/2002JD002670>, <http://doi.wiley.com/10.1029/2002JD002670>, 2003.
- Reyers, M., Moemken, J., and Pinto, J. G.: Future changes of wind energy potentials over Europe in a large CMIP5 multi-model ensemble, *International Journal of Climatology*, 36, 783–796, <https://doi.org/10.1002/joc.4382>, <http://doi.wiley.com/10.1002/joc.4382>, 2016.
- Rienecker, M. M., Suarez, M. J., Gelaro, R., Todling, R., Bacmeister, J., Liu, E., Bosilovich, M. G., Schubert, S. D., Takacs, L., Kim, G.-K., Bloom, S., Chen, J., Collins, D., Conaty, A., da Silva, A., Gu, W., Joiner, J., Koster, R. D., Lucchesi, R., Molod, A., Owens, T., Pawson, S., Pegion, P., Redder, C. R., Reichle, R., Robertson, F. R., Ruddick, A. G., Sienkiewicz, M., and Woollen, J.: MERRA: NASA’s Modern-Era Retrospective Analysis for Research and Applications, *Journal of Climate*, 24, 3624–3648, <https://doi.org/10.1175/JCLI-D-11-00015.1>, <http://journals.ametsoc.org/doi/abs/10.1175/JCLI-D-11-00015.1>, 2011.
- Ringkjøb, H.-K., Haugan, P. M., and Solbrekke, I. M.: A review of modelling tools for energy and electricity systems with large shares of variable renewables, *Renewable and Sustainable Energy Reviews*, 96, 440–459, <https://doi.org/10.1016/j.rser.2018.08.002>, <https://linkinghub.elsevier.com/retrieve/pii/S1364032118305690>, 2018.
- Rodriguez, R. A., Becker, S., Andresen, G. B., Heide, D., and Greiner, M.: Transmission needs across a fully renewable European power system, *Renewable Energy*, 63, 467–476, <https://doi.org/10.1016/j.renene.2013.10.005>, <http://linkinghub.elsevier.com/retrieve/pii/S0960148113005351>, 2014.
- Rogelj, J., Luderer, G., Pietzcker, R. C., Kriegler, E., Schaeffer, M., Krey, V., and Riahi, K.: Energy system transformations for limiting end-of-century warming to below 1.5 °C, *Nature Climate Change*, 5, 519–527, <https://doi.org/10.1038/nclimate2572>, <http://www.nature.com/doi/10.1038/nclimate2572>, 2015.
- Santos-Alamillos, F. J., Brayshaw, D. J., Methven, J., Thomaidis, N. S., Ruiz-Arias, J. A., and Pozo-Vázquez, D.: Exploring the meteorological potential for planning a high performance European electricity super-grid: optimal power capacity distribution among countries, *Environmental Research Letters*, 12, 114 030, <https://doi.org/10.1088/1748-9326/aa8f18>, <http://stacks.iop.org/1748-9326/12/i=11/a=114030?key=crossref.0952b206a459f113bcf547fd5f08996a>, 2017.
- Schleussner, C.-F., Rogelj, J., Schaeffer, M., Lissner, T., Licker, R., Fischer, E. M., Knutti, R., Levermann, A., Frieler, K., and Hare, W.: Science and policy characteristics of the Paris Agreement temperature goal, *Nature Climate Change*, 6, 827–835, <https://doi.org/10.1038/nclimate3096>, <http://www.nature.com/doi/10.1038/nclimate3096>, 2016.
- Schlott, M., Kies, A., Brown, T., Schramm, S., and Greiner, M.: The impact of climate change on a cost-optimal highly renewable European electricity network, *Applied Energy*, 230, 1645–1659, <https://doi.org/10.1016/j.apenergy.2018.09.084>, <https://linkinghub.elsevier.com/retrieve/pii/S0306261918313953>, 2018.
- Staffell, I. and Green, R.: How does wind farm performance decline with age?, *Renewable Energy*, 66, 775–786, <https://doi.org/10.1016/j.renene.2013.10.041>, <http://linkinghub.elsevier.com/retrieve/pii/S0960148113005727>, 2014.
- Staffell, I. and Pfenninger, S.: Using bias-corrected reanalysis to simulate current and future wind power output, *Energy*, 114, 1224–1239, <https://doi.org/10.1016/j.energy.2016.08.068>, <http://linkinghub.elsevier.com/retrieve/pii/S0360544216311811>, 2016.



- Tobin, I., Jerez, S., Vautard, R., Thais, F., van Meijgaard, E., Prein, A., Deque, M., Kotlarski, S., Maule, C. F., Nikulin, G., Noel, T., and Teichmann, C.: Climate change impacts on the power generation potential of a European mid-century wind farms scenario, *Environmental Research Letters*, 11, 034 013, <https://doi.org/10.1088/1748-9326/11/3/034013>, <http://stacks.iop.org/1748-9326/11/i=3/a=034013?key=crossref.7da88a5a7c6dea354ce58294e3c7482b>, 2016.
- 5 Weber, J., Wohland, J., Reyers, M., Moemken, J., Hoppe, C., Pinto, J. G., and Witthaut, D.: Impact of climate change on backup energy and storage needs in wind-dominated power systems in Europe, *PLOS ONE*, 13, e0201 457, <https://doi.org/10.1371/journal.pone.0201457>, <https://dx.plos.org/10.1371/journal.pone.0201457>, 2018.
- Wohland, J., Reyers, M., Weber, J., and Witthaut, D.: More homogeneous wind conditions under strong climate change decrease the potential for inter-state balancing of electricity in Europe, *Earth System Dynamics*, 8, 1047–1060, <https://doi.org/10.5194/esd-8-1047-2017>, <https://www.earth-syst-dynam.net/8/1047/2017/>, 2017.
- 10 Wohland, J., Reyers, M., Märker, C., and Witthaut, D.: Natural wind variability triggered drop in German redispatch volume and costs from 2015 to 2016, *PLOS ONE*, 13, e0190 707, <https://doi.org/10.1371/journal.pone.0190707>, <http://dx.plos.org/10.1371/journal.pone.0190707>, 2018a.
- Wohland, J., Witthaut, D., and Schleussner, C.-F.: Negative Emission Potential of Direct Air Capture Powered by Renewable Excess Electricity in Europe, *Earth's Future*, 6, 1380–1384, <https://doi.org/10.1029/2018EF000954>, <https://agupubs.onlinelibrary.wiley.com/doi/abs/10.1029/2018EF000954>, 2018b.
- 15 Wohland, J., Omrani, N.-E., Witthaut, D., and Keenlyside, N. S.: Inconsistent Wind Speed Trends in Current Twentieth Century Reanalyses, *Journal of Geophysical Research: Atmospheres*, <https://doi.org/10.1029/2018JD030083>, <http://doi.wiley.com/10.1029/2018JD030083>, 2019.
- 20 Wunsch, C.: The Interpretation of Short Climate Records, with Comments on the North Atlantic and Southern Oscillations, *Bulletin of the American Meteorological Society*, 80, 245–255, [https://doi.org/10.1175/1520-0477\(1999\)080<0245:TIOSCR>2.0.CO;2](https://doi.org/10.1175/1520-0477(1999)080<0245:TIOSCR>2.0.CO;2), <http://journals.ametsoc.org/doi/abs/10.1175/1520-0477%281999%29080%3C0245%3ATIOSCR%3E2.0.CO%3B2>, 1999.
- Ziegler, L., Gonzalez, E., Rubert, T., Smolka, U., and Melero, J. J.: Lifetime extension of onshore wind turbines: A review covering Germany, Spain, Denmark, and the UK, *Renewable and Sustainable Energy Reviews*, 82, 1261–1271, <https://doi.org/10.1016/j.rser.2017.09.100>, <https://linkinghub.elsevier.com/retrieve/pii/S1364032117313503>, 2018.
- 25

3.4 Negative emissions

3.4.1 #5: Direct Air Capture



Earth's Future

COMMENTARY

10.1029/2018EF000954

Key Points:

- As part of a highly renewable power system, Direct Air Capture (DAC) has substantial carbon dioxide removal potential
- DAC can complement volatile renewable power generation by providing flexibility
- Assessments of cobenefits of different technologies for negative emission, flexibility provision, and sector coupling are needed

Supporting Information:

- Supporting Information S1

Correspondence to:

J. Wohland,
j.wohland@fz-juelich.de

Citation:

Wohland, J., Witthaut, D., Schlessner, C.-F. (2018). Negative emission potential of Direct Air Capture powered by renewable excess electricity in Europe. *Earth's Future*, 6, 1380–1384. <https://doi.org/10.1029/2018EF000954>

Received 8 JUN 2018

Accepted 17 SEP 2018

Accepted article online 19 SEP 2018

Published online 15 OCT 2018

©2018. The Authors.

This is an open access article under the terms of the Creative Commons Attribution-NonCommercial-NoDerivs License, which permits use and distribution in any medium, provided the original work is properly cited, the use is non-commercial and no modifications or adaptations are made.

Negative Emission Potential of Direct Air Capture Powered by Renewable Excess Electricity in Europe

Jan Wohland^{1,2}, Dirk Witthaut^{1,2}, and Carl-Friedrich Schlessner^{3,4,5}

¹Institute for Energy and Climate Research - Systems Analysis and Technology Evaluation, Forschungszentrum Jülich, Jülich, Germany, ²Institute for Theoretical Physics, University of Cologne, Cologne, Germany, ³Climate Analytics, Berlin, Germany, ⁴Potsdam Institute for Climate Impact Research, Potsdam, Germany, ⁵Integrative Research Institute on Transformations of Human-Environment Systems, Humboldt University of Berlin, Berlin, Germany

Abstract The mitigation of climate change requires fast reductions in greenhouse gas emissions and calls for fundamental transitions of energy systems. In most places, the increased exploitation of variable renewable sources (wind and solar) forms the backbone of these transitions. To remain consistent with the Paris Agreement temperature goals, negative emission technologies will likely be needed to achieve net zero emissions in the second half of the century. In integrated assessment models, negative emissions are typically realized through land-based approaches. However, due to their coarse temporal and spatial resolution, such models might underestimate the potential of decentrally deployable and flexible technologies such as Direct Air Capture (DAC). Based on validated high-resolution power generation time series, we show that DAC can extract CO₂ from the atmosphere and facilitate the integration of variable renewables at the same time. It is a promising flexibility provider as it can be ramped within minutes. Our results show that negative emissions of up to 500 Mt CO₂/year in Europe may be achievable by using renewable excess energy only. Electricity systems with high shares of volatile renewables will induce excess generation events during which electricity is cheap thereby lowering the operational costs of DAC. If investment costs can be sufficiently reduced, this may render very energy intensive but highly flexible technologies such as DAC viable.

Plain Language Summary There is a finite amount of greenhouse gases that humankind can emit into the atmosphere before the 1.5 and 2 °C climate targets are exceeded. This calls for emission reductions in all sectors of human activity, in particular in the energy sector. In many countries, energy transitions have already led to the expansion of variable renewable energy technologies that depend strongly on weather such as wind and solar. In addition to the expansion of renewable energy, scenarios that achieve the 1.5 or 2 °C target require negative carbon emissions later in the century to make up for insufficient emission reductions so far. In this study, we investigate the cobenefits of a negative emission technology called Direct Air Capture (DAC) and a high share of wind and solar energy. The advantage of DAC is that it can in principle be deployed decentrally and it can be switched on and off very quickly. It is thus possible to use DAC to smooth the variability of renewable power generation while achieving negative emissions. Our study focuses on the technical aspects of including DAC in the power system and does not provide a thorough assessment of the economic viability of DAC deployment.

1. Introduction

The achievement of the Paris Agreement climate goals is difficult to impossible without the availability of negative carbon emissions, as the reduction of greenhouse gas emissions to date is insufficient (Schlessner et al., 2016). Halving global CO₂ emissions every decade from 2020 onward as well as upscaling of negative emission technologies is required to reach global net zero CO₂ emissions by midcentury (Rockström et al., 2017). The exact amount of required negative CO₂ emissions depends on a range of scenario assumptions, first and foremost the stringency of near-term emission reductions (van Vuuren et al., 2018). Implementing negative emissions at the scale demanded by energy economic models requires large-scale investments (Fuss et al., 2014). While substantial progress in the deployment of renewable energies has been seen over recent years, progress on negative emission falls behind expectations (Peters et al., 2017).

A multitude of negative emission technologies exists. Minx et al. (2018) provide an overview and distinguish seven different technologies: afforestation and reforestation, soil carbon sequestration, biochar, bioenergy in combination with carbon capture and storage (BECCS), enhanced weathering, ocean fertilization, and Direct Air Capture (DAC). Among them, BECCS features most prominently (Minx et al., 2017). Along with other land-based approaches, it requires substantial amounts of land and water raising sustainability concerns (Smith et al., 2015). The focus on BECCS or afforestation and reforestation in energy economic models may be partly linked to outdated assumptions about the development of renewable energy costs that lead to overly conservative deployment (Creutzig et al., 2017). As recently argued by van Vuuren et al. (2017), an open discussion of negative emission technologies is urgently needed. For completeness, this discussion has to include DAC.

2. DAC May Complement Volatile Renewables

The availability of very cheap renewable energy, including occasional negative prices (Kyritsis et al., 2017), provides an opportunity to implement negative emission technologies that were previously uneconomic. For example, DAC has been assessed to be of limited applicability due to high costs (two-thirds capital and one-third operational) and energy demand at least in the near term (Smith et al., 2015). However, substantial amounts of excess energy are available in highly renewable power systems due to temporal and spatial volatility of these energy sources (e.g., Rodriguez et al., 2014). To ensure system stability and to avoid wasting electricity, flexibility options that harmonize generation and loads are needed (Kondziella & Bruckner, 2016; Schäfer et al., 2018). Various technologies can provide this flexibility (e.g., power-to-gas/heat, dispatchable renewables, and demand-side-management), and all of them will compete in a real-world market situation. Without touching the intricate and uncertain economic comparison between the different flexibility providers, we want to expand this list by DAC that can also provide this system service, as it can be ramped within minutes (Climeworks, 2017). Moreover, it can be deployed in decentral units, which may alleviate transmission grid congestions and corresponding costs (Wohland et al., 2018). DAC could thus in principle be complementary to the fast expansion of renewables.

Here we explore the potential of negative emissions by integrating DAC in a stylized simulation of the European electricity system. We follow an optimistic scenario for European cooperation in assuming that all benefits from interstate balancing are implemented. This scenario provides a lower bound for the usage of DAC because grid limitations increase the amount of excess energy. Based on validated long-term time series for photovoltaics and wind power generation in 28 states (Pfenninger & Staffell, 2016; Staffell & Pfenninger, 2016), we run a simple energy balance model that accounts for storage but neglects other flexibility options (e.g., sector coupling and demand-side management). The storage strategy is based on the filling level and a day-ahead forecast of residual loads (see the supporting information). DAC is assumed to become available at scale and is modeled for different second-order efficiencies as proposed by House et al. (2011). Unless explicitly stated, we conservatively assume that the heat needed for DAC is electricity based. During shortfall in the generation of renewable energy, we assume open-cycle gas power plants will provide backup energy. Although such a stylized experimental design does not allow for robust projections of technology deployment, it yields interesting insights into fundamental cobenefits of DAC and highly renewable systems.

3. System Requirements for Net Negative Emissions

DAC contributes relevant amounts of negative emissions only if at least 80% of the electricity are renewable, independent on the installed DAC capacity (see Figure 1). DAC contributes significantly earlier in smaller power systems but backup emissions are also higher (see Figure S2). This indicates potential for early deployment in conjunction with progressing grid extensions. Current national renewable contributions are still substantially smaller. For example, in 2017 the German power system generated 28% from wind and solar although some of its federal states already exceeded 100%. As expected, large negative emissions require large DAC capacities and renewable penetrations. Net negative emissions at very high penetrations can exceed 500 Mt CO₂ although the viability of such high penetrations is unclear. For a DAC capacity of 300 GW, net emissions roughly become a linear function of the penetration. For comparison, the European net generating capacity was about 1,000 GW in late 2015 (ENTSOE, 2018).

Storage technologies and DAC are not competing but complementary: Increases in storage size allow for reductions of remaining carbon emissions and enable more efficient usage of DAC units. Their codependency

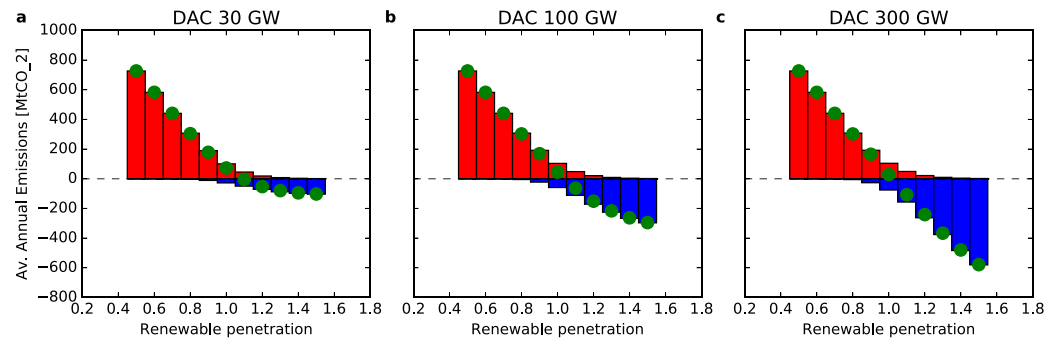


Figure 1. European CO₂ emissions versus renewable penetration for different DAC capacities at a storage size of one average load day. Red bars denote emissions from open-cycle gas turbines that are used for backup. Blue indicates negative emissions from DAC. Green circles denote net emissions. DAC = Direct Air Capture.

in order to reach a hypothetical negative emission target of 500 Mt CO₂ is shown in Figure 2. Below a DAC capacity of roughly 130 GW, the target is infeasible. Above that limit, necessary penetrations generally decrease with increasing DAC capacities and storage sizes.

Our DAC energy estimates are based on the upper bounds provided by a producer named Climeworks (Lozanovski et al., 2014). They are consistent with other reports (Keith et al., 2018; Socolow et al., 2011) and the Climeworks second-order efficiency (5.5%) is slightly lower than in the two other studies (6.3% and 6.9%, respectively). We refer to supporting information Text S1.4 for more details. Since we also assume that heat is entirely generated from electricity, our estimates can be seen as conservative. Energy requirements could be substantially lowered if the technology advances or if the heat partly comes from sources other than electricity. For example, the second-order efficiency would increase from $\eta = 5.5\%$ to $\eta = 9.7\%$, and energy needs drop by more than 40%, if half the heat came from other sources (see Figure S3). Similarly, inclusion of dispatchable renewables such as bioenergy, hydro power and concentrated solar (Pfenninger et al., 2014) would allow parts of the backup to be carbon neutral and thereby facilitating net negative emissions.

4. DAC Merits Thorough Assessments

Our results suggest that DAC has the potential to fully complement highly renewable power systems. This is due to its flexibility and decentrality, which can be advantageous for system integration of high shares of volatile renewables. DAC also requires less land and water resources than BECCS. We thus argue that

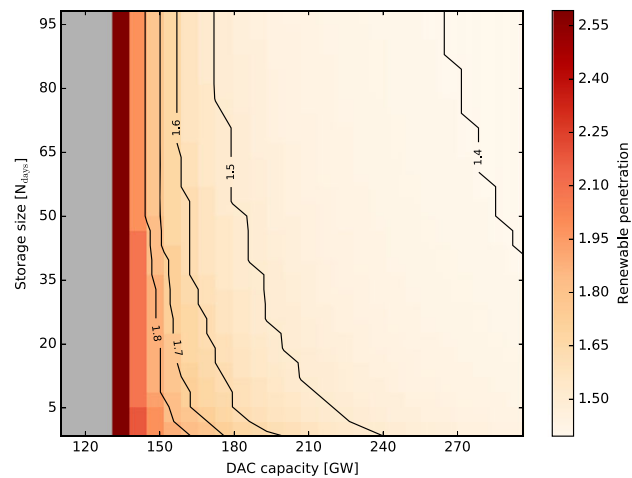


Figure 2. Codependency of storage size, DAC capacity, and renewable penetration to reach a negative emission target of 500 Mt CO₂/year. Colors and contours denote the necessary renewable penetration. Gray denotes infeasibility given the combination of storage size and DAC capacity. The storage size is given in units of the average daily load. DAC = Direct Air Capture.

DAC should be intensively researched. In addition to the technological development of DAC, more realistic energy system simulations that quantify cobenefits and competitions of different technologies are needed. For instance, coupling the heating and transport sector to the electricity system can also provide flexibility (Brown et al., 2018; Connolly et al., 2016) and power to hydrogen may help to decarbonize the industrial sector (Welder et al., 2018). Present-day global energy economic integrated assessment models are not necessarily well suited, because they do not resolve the high-frequency generation dynamics explicitly and hence may underestimate the potential of DAC. Currently high investment costs for DAC are not prohibitive as there will likely be massive potentials for cost reductions as the technology matures and is scaled up (Keith et al., 2018; Lackner et al., 2012). Scenario studies should consider steep learning curves as highlighted by the recent development in the photovoltaics sector (Creutzig et al., 2017). While the investment costs may thus be brought down, potential revenues might increase substantially. For instance, Brown et al. (2018) report CO₂ shadow prices of at least 400 Euro/t_{CO₂} to reach a 95% emission reduction in the electricity, heating, and land-based transport sector. Current prices of EU emission allowances are more than 1 order of magnitude lower.

We have mapped out energy needs and system requirements of a 500 Mt CO₂/year DAC contribution for Europe. If extended globally, DAC could contribute substantially to required end of century negative emissions of 7–22 Gt CO₂/year under Paris Agreement compatible mitigation scenarios (Smith et al., 2015). The system requirements to achieve such rates are very ambitious under our conservative estimates, but substantial potential for increased DAC efficiency exists (see Figure S3). However, discussions of system integration potential of negative emission technologies should not divert attention from the need of very stringent emission reductions in the near term (Schleussner et al., 2016).

Acknowledgments

We are grateful to two anonymous reviewers and to the Editor for critical and useful comments. We want to thank Tom Brown for stimulating discussions. The authors do not have any conflict of interest or potential economic gain to be made through association with Climeworks, a company that provided estimates of DAC energy requirements. J. W. and D. W. are funded through the Helmholtz Association (via the joint initiative 'Energy System 2050—A Contribution of the Research Field Energy' and the grant VH-NG-1025 to Dirk Witthaut). C. F. S. acknowledges support by the German Federal Ministry of Education and Research (01LS1613A) and by the German Federal Ministry for the Environment, Nature Conservation and Nuclear Safety (16_II_148_Global_A_IMPACT). Input data are publicly available. Electricity consumption is from the European Network of Transmission System operators (<https://www.entsoe.eu/db-query/consumption/mhlv-all-countries-for-a-specific-month>.) and renewable generation from the Renewables.ninja project (<https://www.renewables.ninja/downloads>). Version numbers and further details are given in the supporting information.

References

- Brown, T., Schlachtberger, D., Kies, A., Schramm, S., & Greiner, M. (2018). Synergies of sector coupling and transmission reinforcement in a cost-optimised, highly renewable European energy system. *Energy*, *160*, 720–739. <https://doi.org/10.1016/j.energy.2018.06.222>
- Climeworks (2017). Personal communication with Valentin Gutknecht (Marketing & Communications).
- Connolly, D., Lund, H., & Mathiesen, B. (2016). Smart Energy Europe: The technical and economic impact of one potential 100% renewable energy scenario for the European Union. *Renewable and Sustainable Energy Reviews*, *60*, 1634–1653. <https://doi.org/10.1016/j.rser.2016.02.025>
- Creutzig, F., Agoston, P., Goldschmidt, J. C., Luderer, G., Nemet, G., & Pietzcker, R. C. (2017). The underestimated potential of solar energy to mitigate climate change. *Nature Energy*, *2*(9), 17140. <https://doi.org/10.1038/nenergy.2017.140>
- ENTSOE (2018). Net generating capacity on december 31st 2015 (Database: 05.02.2018).
- Fuss, S., Canadell, J. G., Peters, G. P., Tavoni, M., Andrew, R. M., Ciais, P., et al. (2014). Betting on negative emissions. *Nature Climate Change*, *4*(10), 850–853.
- House, K. Z., Baclig, A. C., Ranjan, M., van Nierop, E. A., Wilcox, J., & Herzog, H. J. (2011). Economic and energetic analysis of capturing CO₂ from ambient air. *Proceedings of the National Academy of Sciences*, *108*(51), 20,428–20,433. <https://doi.org/10.1073/pnas.1012253108>
- Keith, D. W., Holmes, G., Angelo, D. S., & Heidel, K. (2018). A process for capturing CO₂ from the atmosphere. *Joule*, *2*, 1–22. <https://doi.org/10.1016/j.joule.2018.05.006>
- Kondziella, H., & Bruckner, T. (2016). Flexibility requirements of renewable energy based electricity systems – a review of research results and methodologies. *Renewable and Sustainable Energy Reviews*, *53*, 10–22. <https://doi.org/10.1016/j.rser.2015.07.199>
- Kyrtsis, E., Andersson, J., & Serletis, A. (2017). Electricity prices, large-scale renewable integration, and policy implications. *Energy Policy*, *101*, 550–560. <https://doi.org/10.1016/j.enpol.2016.11.014>
- Lackner, K. S., Brennan, S., Matter, J. M., Alissa Park, A. H., Wright, A., & Van Der Zwaan, B. (2012). The urgency of the development of CO₂ capture from ambient air. *Proceedings of the National Academy of Sciences*, *33*(109), 13,156–13,162.
- Lozanovski, A., Gebald, C., Brandstetter, C. P., Lindner, J. P., & Albrecht, S. (2014). Direct Air Capture of CO₂, University of Stuttgart and Climeworks. <https://oc1.mainbase.ch/index.php/s/1aCEkJP0n3kwxP#pdfviewer> (accessed on August 9th, 2018), Archived at, <http://www.webcitation.org/71XYICfS5> on August 9th, 2018.
- Minx, J. C., Lamb, W. F., Callaghan, M. W., Bornmann, L., & Fuss, S. (2017). Fast growing research on negative emissions. *Environmental Research Letters*, *12*(3), 035007. <https://doi.org/10.1088/1748-9326/aa5ee5>
- Minx, J. C., Lamb, W. F., Callaghan, M. W., Fuss, S., Hilaire, J., Creutzig, F., et al. (2018). Negative emissions—Part 1: Research landscape and synthesis. *Environmental Research Letters*, *13*(6), 063001. <https://doi.org/10.1088/1748-9326/aabf9b>
- Peters, G. P., Andrew, R. M., Canadell, J. G., Fuss, S., Jackson, R. B., Korsbakken, J., et al. (2017). Key indicators to track current progress and future ambition of the Paris Agreement. *Nature Climate Change*, *7*(1), 118–122. <https://doi.org/10.1038/nclimate3202>
- Pfenninger, S., Gauché, P., Lilliestam, J., Damerau, K., Wagner, F., & Patt, A. (2014). Potential for concentrating solar power to provide baseload and dispatchable power. *Nature Climate Change*, *4*(8), 689–692. <https://doi.org/10.1038/nclimate2276>
- Pfenninger, S., & Staffell, P. (2016). Long-term patterns of European PV output using 30 years of validated hourly reanalysis and satellite data. *Energy*, *114*, 1251–1265. <https://doi.org/10.1016/j.energy.2016.08.060>
- Rockström, J., Gaffney, O., Rogelj, J., Meinshausen, M., Nakicenovic, N., & Schellnhuber, H. J. (2017). A roadmap for rapid decarbonization. *Science*, *355*(6331), 1269–1271. <https://doi.org/10.1126/science.aah3443>
- Rodriguez, R. A., Becker, S., Andresen, G. B., Heide, D., & Greiner, M. (2014). Transmission needs across a fully renewable European power system. *Renewable Energy*, *63*, 467–476. <https://doi.org/10.1016/j.renene.2013.10.005>
- Schäfer, B., Beck, C., Aihara, K., Witthaut, D., & Timme, M. (2018). Non-Gaussian power grid frequency fluctuations characterized by Lévy-stable laws and superstatistics. *Nature*, *3*(2), 119–126. <https://doi.org/10.1038/s41560-017-0058-z>
- Schleussner, C.-F., Rogelj, J., Schaeffer, M., Lissner, T., Licker, R., Fischer, E. M., et al. (2016). Science and policy characteristics of the Paris Agreement temperature goal. *Nature Climate Change*, *6*(9), 827–835. <https://doi.org/10.1038/nclimate3096>

- Smith, P., Davis, S. J., Creutzig, F., Fuss, S., Minx, J., Gabrielle, B., et al. (2015). Biophysical and economic limits to negative CO₂ emissions. *Nature Climate Change*, *6*(1), 42–50. <https://doi.org/10.1038/nclimate2870>
- Socolow, R., Desmond, M., Aines, R., Blackstock, J., Bolland, O., Kaarsberg, T., et al. (2011). Direct air capture of CO₂ with chemicals: A technology assessment for the APS Panel on Public Affairs (Tech. rep.). American Physical Society.
- Staffell, I., & Pfenninger, S. (2016). Using bias-corrected reanalysis to simulate current and future wind power output. *Energy*, *114*, 1224–1239. <https://doi.org/10.1016/j.energy.2016.08.068>
- van Vuuren, D. P., Hof, A. F., van Sluisveld, M. A., & Riahi, K. (2017). Open discussion of negative emissions is urgently needed. *Nature Energy*, *2*(12), 902–904. <https://doi.org/10.1038/s41560-017-0055-2>
- van Vuuren, D. P., Stehfest, E., Gernaat, D. E. H. J., van den Berg, M., Bijl, D. L., de Boer, H. S., et al. (2018). Alternative pathways to the 1.5°C target reduce the need for negative emission technologies. *Nature Climate Change*, *8*(5), 391–397. <https://doi.org/10.1038/s41558-018-0119-8>
- Welder, L., Ryberg, D., Kotzur, L., Grube, T., Robinius, M., & Stolten, D. (2018). Spatio-temporal optimization of a future energy system for power-to-hydrogen applications in Germany. *Energy*, *158*, 1130–1149. <https://doi.org/10.1016/j.energy.2018.05.059>
- Wohland, J., Reyers, M., Maerker, C., & Witthaut, D. (2018). Natural wind variability triggered drop in German redispatch volume and costs from 2015 to 2016. *PLOS ONE*, *13*(1), e0190707. <https://doi.org/10.1371/journal.pone.0190707>

Supplement

Supplementary Information

Negative emission potential of Direct Air Capture powered by renewable excess electricity in Europe

Jan Wohland, Dirk Witthaut, Carl-Friedrich Schleussner
August 14, 2018

1 Data

1.1 Temporal and spatial coverage

In order to capture the relevant dynamics of wind and solar generation, appropriate input data for the model is needed. In order to account for low-frequency generation variability, we cover the longest possible period. It is constrained by the PV data to start in 1985 and ends in 2016. To account for positive effects of European integration (Schlachtberger et al., 2017; Rodriguez et al., 2015, 2014; Andresen et al., 2012), we use a large set of European countries. Inclusion in our assessment, however, requires generation and load data to be available for any particular country. The included countries along with their respective annual electricity consumption are given in Table S1.

1.2 Renewable generation

We use the publicly available renewables.ninja datasets (version 1.1) as inputs to our model (Staffell and Pfenninger, 2016; Pfenninger and Staffell, 2016). The datasets are bias corrected and validated with measured generation timeseries. They come at hourly resolution and thus capture intra-day effects that are crucial for power system operation. The dataset is based on the MERRA2 reanalysis (Rienecker et al., 2011)

1.3 Electricity consumption

We use 2015 hourly load data from the European Network of Transmission System Operators for Electricity (2015) which is publicly available online. In order to construct a multi-year time series of the same length as the climate input data, the load data is looped. This allows to include the mismatch variability that stems from climate variability while it mutes variations in electricity consumption.

Table S1: Annual sums of country electricity consumption based on hourly 2015 data provided by the European Network of Transmission System Operators for Electricity (2015).

country	country code	Annual load [TWh]
Austria	AT	69.62
Belgium	BE	85.22
Bulgaria	BG	38.62
Switzerland	CH	62.06
Czech Republic	CZ	63.53
Germany	DE	505.27
Denmark	DK	33.9
Estonia	EE	7.93
Spain	ES	248.5
Finland	FI	82.5
France	FR	471.26
Great Britain	GB	282.19
Greece	GR	51.4
Croatia	HR	17.19
Hungary	HU	40.75
Ireland	IE	26.57
Italy	IT	314.35
Lithuania	LT	10.86
Latvia	LV	7.07
Macedonia	MK	7.84
Netherlands	NL	113.25
Norway	NO	128.65
Poland	PL	149.96
Portugal	PT	48.93
Romania	RO	52.31
Sweden	SE	135.93
Slovenia	SI	13.65
Slovakia	SK	28.21
Total		3097.52

23 1.4 CO₂ intensities

24 Schematic decomposition of the DAC process

25 In order to quantify how much carbon dioxide can be extracted from the atmosphere using
26 a certain amount of energy, we follow the approach of House et al. (2011). They decompose
27 the DAC process into two parts. The first part is an ideal, reversible thermodynamic process
28 that separates a stream of 400 ppm CO₂ into on stream of high purity (99%) CO₂ and another
29 stream of 200 ppm CO₂. This process sets a lower bound for the energy requirement of any
30 industrial process because real-world processes will never be ideal. The deviation from the ideal
31 process is accounted for by including a second process.

32 The carbon intensity I_{DAC} , defined as

$$I_{\text{DAC}} = \frac{dm_{\text{CO}_2}}{dE}, \quad (\text{S1})$$

33 where m_{CO_2} denotes the mass of CO₂ extracted using the electric energy E , can thus be
34 expressed in terms of the carbon intensity of the ideal process I_{id} and a second-order efficiency
35 η

$$I_{\text{DAC}} = I_{\text{id}} \cdot \eta. \quad (\text{S2})$$

36 House et al. report $I_{\text{id}} = (20\text{kJ}/(\text{mol CO}_2))^{-1} = 7920 \frac{\text{tCO}_2}{\text{GWh}}$. According to them, typical
37 values for η in real-world separation processes, lie in between 0.05 and 0.4.

38 The Climeworks second order efficiency

39 The company Climeworks reports heat requirements Q of 1500...2000 kWh/tCO₂ and electricity
40 requirements W of 200...300 kWh/tCO₂ for their DAC modules (Lozanovski et al.). We use
41 the upper values here to derive conservative estimates. The heat is needed at 105°C and can be
42 obtained from a multitude of different processes. In the worst case, the entire heat is generated
43 from electricity such that the total electricity demand per ton CO₂ is $E_{\text{worst}} = W + Q = 2300$
44 kWh/tCO₂. In the best case, the heat comes as waste heat or is generated from solar radiation
45 such that total electricity needs would be $E_{\text{best}} = W = 300$ kWh/tCO₂. We also consider
46 intermediate cases where only a fraction α of the heat comes from electricity $E_{\alpha} = W + \alpha \cdot Q$,
47 where $0 < \alpha < 1$. In the case where half of the heat comes from electricity, it follows that
48 $E_{0.5} = W + 0.5 \cdot Q = 1300$ kWh/tCO₂. The corresponding second order efficiencies are $\eta_{\text{worst}} =$
49 0.06 , $\eta_{\text{best}} = 0.42$, $\eta_{0.5} = 0.10$.

50 Comparison with other energy estimates

51 In Table S2, we provide a comparison of the climeworks estimates with estimates reported in
52 the scientific literature. We restrict the discussion to the upper-end estimates of the climeworks
53 process, because they were used in our energy simulation.

54 The reported work requirements show little variation indicating large agreement between the
55 different studies. Socolow et al. (2011) and climeworks report the same work requirements,
56 while Keith et al. (2018) report slightly higher values (around 20%). The heat requirements in
57 the climeworks process are the highest reported and lie approximately 15% above the Socolow
58 et al. (2011) and 35% above the Keith et al. (2018) estimates. As a consequence, the second
59 order efficiency η is lowest for the climeworks process (5.5%) and slightly higher for the other
60 two (6.3% and 6.9%). All second order efficiencies lie within the plausible range of second order
61 efficiencies reported by House et al. (2011).

62 We conclude that the climeworks estimates are in agreement with the other studies. If
 63 anything, they overestimate the heat requirements and thus serve well as conservative estimates
 64 of a maturing technology.

Table S2: Comparison of work and heat requirements for DAC processes as reported in different studies. We also list the corresponding second order efficiencies as defined in Eq. S2.

	climeworks	Sokolov et al.	Keith et al.	House et al.
Work E	$300 \frac{\text{kWh}}{t_{\text{CO}_2}}$	$1.08 \frac{\text{GJ}}{t_{\text{CO}_2}} = 300 \frac{\text{kWh}}{t_{\text{CO}_2}}$	$366 \frac{\text{kWh}}{t_{\text{CO}_2}}$	
Heat Q	$2000 \frac{\text{kWh}}{t_{\text{CO}_2}}$	$6.1 \frac{\text{GJ}}{t_{\text{CO}_2}} = 1700 \frac{\text{kWh}}{t_{\text{CO}_2}}$	$5.25 \frac{\text{GJ}}{t_{\text{CO}_2}} = 1460 \frac{\text{kWh}}{t_{\text{CO}_2}}$	
η [%]	5.5	6.3	6.9	5 .. 40

65 **Open-cycle gas turbines**

66 We assume that backup energy is provided by open-cycle gas turbines with a carbon intensity
 67 of $I_{\text{Gas}} = 469 \frac{t_{\text{CO}_2}}{\text{GWh}}$ (see 50th percentile value in Table A.II.4, Moomaw et al., 2011). Gas
 68 turbines have high ramping rates and are thus ideally suited to complement volatile renewables.
 69 Moreover, their carbon intensity is distinctly lower than the one of coal fired power plants
 70 allowing less interference with stringent emission reductions. A perfect DAC process coupled to
 71 one of these turbines would hence extract roughly 17 times the amount of CO_2 that is emitted
 72 by burning gas. For real processes, net neutrality of the coupled system would be achieved
 73 at a second-order efficiency of $\eta = \frac{469}{7920} \approx 0.06$ which is close to the reported efficiency of the
 74 Climeworks plants if heat is electricity based.

2 Methods

We adopt a schematic modeling framework aiming to illustrate the fundamental co-benefits of flexible Direct Air Capture and volatile renewable generation. We include the major strategies to cope with variable renewable generation, namely transmission, storage and fast backup. At the same time, we neglect many other flexibility providers such as demand side management, power-to-X and sector coupling. We furthermore restrict our analysis to the power sector even though it is evident that all other sectors need to be included in more realistic assessments. Some sectors may alleviate issues of electricity system management (e.g., storage in batteries of future electric vehicle fleets) and others may continue to emit carbon long after the Paris goals urge us to reach net neutrality (e.g., aviation).

2.1 Model equations

Let $P_{PV,i}(t)$ and $P_{Wind,i}(t)$ denote the photovoltaic (PV) and wind power generation timeseries of country i , respectively. Moreover, $L_i(t)$ is the load (i.e. electricity consumption) of country i . We construct a load time series of the same length as the PV and wind timeseries by repeating the measured 1-year time series of 2015. Following Rodriguez et al. (2014), we calculate the renewable generation as

$$P_i(t) = q \cdot (c_1 \cdot P_{PV,i}(t) + (1 - c_1) \cdot P_{Wind,i}(t)), \quad (\text{S3})$$

where q is a scaling parameter, c_1 denotes the share of PV and $(1 - c_1)$ is the wind share. We choose $c_1 = 0.3$ uniformly in all countries, which is close to the optimum value reported by Rodriguez et al. (2014). We scale the renewable generation $P(t)$ as

$$\langle P_i(t) \rangle \stackrel{!}{=} c \cdot \langle L_i(t) \rangle \quad (\text{S4})$$

where $\langle L_i(t) \rangle$ gives the average load of country i . c is the renewable penetration and describes which share of the load is met by renewables on average. Eqs. S4 and S3 allow to calculate q as a function of c .

We define a nodal mismatch between generation and load as

$$\Delta_i(t) = P_i(t) - L_i(t). \quad (\text{S5})$$

2.1.1 Copper plate

We now assume that all countries are perfectly connected using lossless transmission lines (copper plate):

$$\Delta(t) = \sum_i \Delta_i(t) \quad (\text{S6})$$

Summing over large areas is known to reduce volatility of renewable generation and the copper plate assumption provides an upper bound for the achievable benefits of large transmission systems. Systems on smaller spatial scales yield higher values of curtailment and hence still higher potential for DAC (see Fig. S2).

105 2.1.2 Balance equation

106 For all timesteps there needs to be a balance between the European mismatch $\Delta(t)$, the conven-
 107 tional backup $B(t)$, the power used for Direct Air Capture $DAC(t)$, the energy fed into/taken
 108 from the storage ΔS and the curtailment $C(t)$ as:

$$\Delta(t) + B(t) = DAC(t) + \Delta S(t) + C(t). \quad (S7)$$

109 We assume that backup comes from open-cycle gas turbines without ramping constraints.
 110 There is a maximum amount of power the DAC system can handle $DAC(t) \in [0, DAC_{\max}]$.

111 When energy flows into the storage, it evolves according to $S(t+1) = S(t) + \eta_S \Delta S(t)$, where
 112 $S(t)$ is the storage filling level at time t and $\eta_S = 0.9$ is the storage efficiency. In turn, when
 113 energy is taken from the storage, it evolves as $S(t+1) = S(t) + \eta_S^{-1} \Delta S(t)$. This translates into
 114 a round-trip efficiency of 0.81 which is typical for pumped hydro according to Schlachtberger
 115 et al. (2017). The storage is constrained: $S(t) \in [0, S_{\max}]$. The storage strategy is explained
 116 in Sec. 2.1.3. We define the storage size S_{\max} in units of the duration T that the average load
 117 $\langle \sum_i L_i \rangle$ could be met by storage:

$$S_{\max} = T \cdot \left\langle \sum_i L_i \right\rangle. \quad (S8)$$

118 Curtailment has to be non-negative and is avoided whenever possible.

119 2.1.3 Storage strategy

120 We choose a storage strategy that is based on the current filling level $S(t)$ as well as the
 121 forecasted mismatch evolution for the 24 hours ahead (day ahead). In light of relatively high
 122 precision forecasts for such short time intervals, we use the real evolution as forecast.

123 Excess generation ($\Delta(t) > 0$)

124 We differentiate three different states of the storage:

- 125 1. **Low** ($S(t) \leq 25\% \cdot S_{\max}$): Positive mismatches are used to fill the storage ($\Delta S = \Delta$),
 126 regardless of expected future mismatch evolution. If this leads to an overfull storage (i.e.
 127 $S(t) + \eta_S \Delta S > S_{\max}$), the storage is filled to its maximum and the remaining energy is
 128 used for DAC and is otherwise curtailed.
- 129 2. **Medium** ($25\% \cdot S_{\max} < S(t) \leq 75\% \cdot S_{\max}$): Decisions are based on the future mismatch
 130 evolution. If the expected positive mismatch of the next day allows to fill the storage
 131 beyond the desired 75% level, only the fraction that fills it to exactly 75% after 24 hours
 132 is stored. This maintains more flexibility as the storage less often hits its maximum limit
 133 and DAC is already used earlier in comparison to storage strategies that rely on the filling
 134 level only. Otherwise, if the expected mismatches do not suffice to reach a filling level
 135 beyond 75%, the energy is entirely stored.

We also give the explicit formula for the sake of reproducibility. We calculate an ancilla
 variable

$$\chi(t) = \frac{\int_t^{t+w} \eta_S \Delta_{\text{pred}}(t') dt'}{0.75 S_{\max} - S(t)}, \quad (S9)$$

136 where w denotes the forecast window (here: 24 hours) and $\Delta_{\text{pred}}(t')$ is the predicted
 137 mismatch at timestep t' . If $\chi \leq 1$, everything is stored ($\Delta S = \Delta$). However, if $\chi > 1$

138 only a fraction of the available energy is stored ($\Delta S = \frac{1}{\chi}\Delta$) and the rest goes to DAC
 139 ($DAC = (1 - \frac{1}{\chi})\Delta$).

140 3. **High** ($S(t) > 75\% \cdot S_{\max}$): Positive mismatches are used to drive DAC ($DAC = \Delta$),
 141 regardless of the future mismatch evolution. If the DAC capacity limit is hit ($\Delta >$
 142 DAC_{\max}), energy is stored (if possible) and otherwise curtailed.

143 **Generation shortfall** ($\Delta(t) < 0$)

144 In times of generation shortfall ($\Delta(t) < 0$), energy is firstly taken from the storage ($\Delta S = \Delta$)
 145 in order to minimize usage of backup plants. If the storage filling level after subtraction of the
 146 mismatch is still higher than the desired filling level, energy is used for DAC:

$$\begin{aligned} & \text{If } \left(S + \frac{\Delta}{\eta_S} > 0.75S_{\max} \right) \\ & \text{then } DAC = \begin{cases} \eta_S \cdot \left(S + \frac{\Delta}{\eta_S} - 0.75S_{\max} \right), & \text{if term} < DAC_{\max} \\ DAC_{\max}, & \text{otherwise} \end{cases} \\ & \text{and } \Delta S = \Delta - \frac{DAC}{\eta_S}. \end{aligned}$$

147 **2.2 Alternative approach: Minimizing carbon emissions**

148 Instead of running the model iteratively, the problem could have also been treated as an op-
 149 timization problem. We could have defined the time series of the storage, the DAC process
 150 and the backup such that net emissions are minimal. Although this alternative approach may
 151 seem appealing, we argue that it is not well suited here for a couple of reasons. First, such an
 152 optimization assumes that the evolution of both generation and load are perfectly known be-
 153 forehand ("perfect foresight"), which is not the case for fundamental reasons (complexity, chaos
 154 etc.). Second, a minimization can easily be misleading since carbon emissions are not the only
 155 reason for concern. For example, air quality issues and sustainable land use call for a minimum
 156 usage of fossil power plants, even if their carbon emissions were entirely compensated for by
 157 DAC. Since the absolute carbon intensities of open-cycle gas turbines and the DAC process are
 158 close, a small increase in DAC efficiency might turn the coupled gas-DAC system slightly CO₂
 159 negative. A minimization of emissions would then potentially schedule the gas plants to run
 160 nonstop.

161 **Carbon transportation infrastructure and geological storage**

162 As this study aims to quantify the potential of DAC to net negative emissions in Europe, a
 163 couple of further simplifications are made. We neglect the entire post-capture aspect of DAC,
 164 namely the transportation and storage of high purity CO₂. We consider this simplification
 165 appropriate since the transportation of CO₂ in pipes comes with relatively little energy require-
 166 ments as compared to the separation from a low-purity stream. Nevertheless, future engineering
 167 assessments aiming to answer questions related to the actual system design, have to take these
 168 steps into account.

169 **3 Additional results**

170 **Europe**

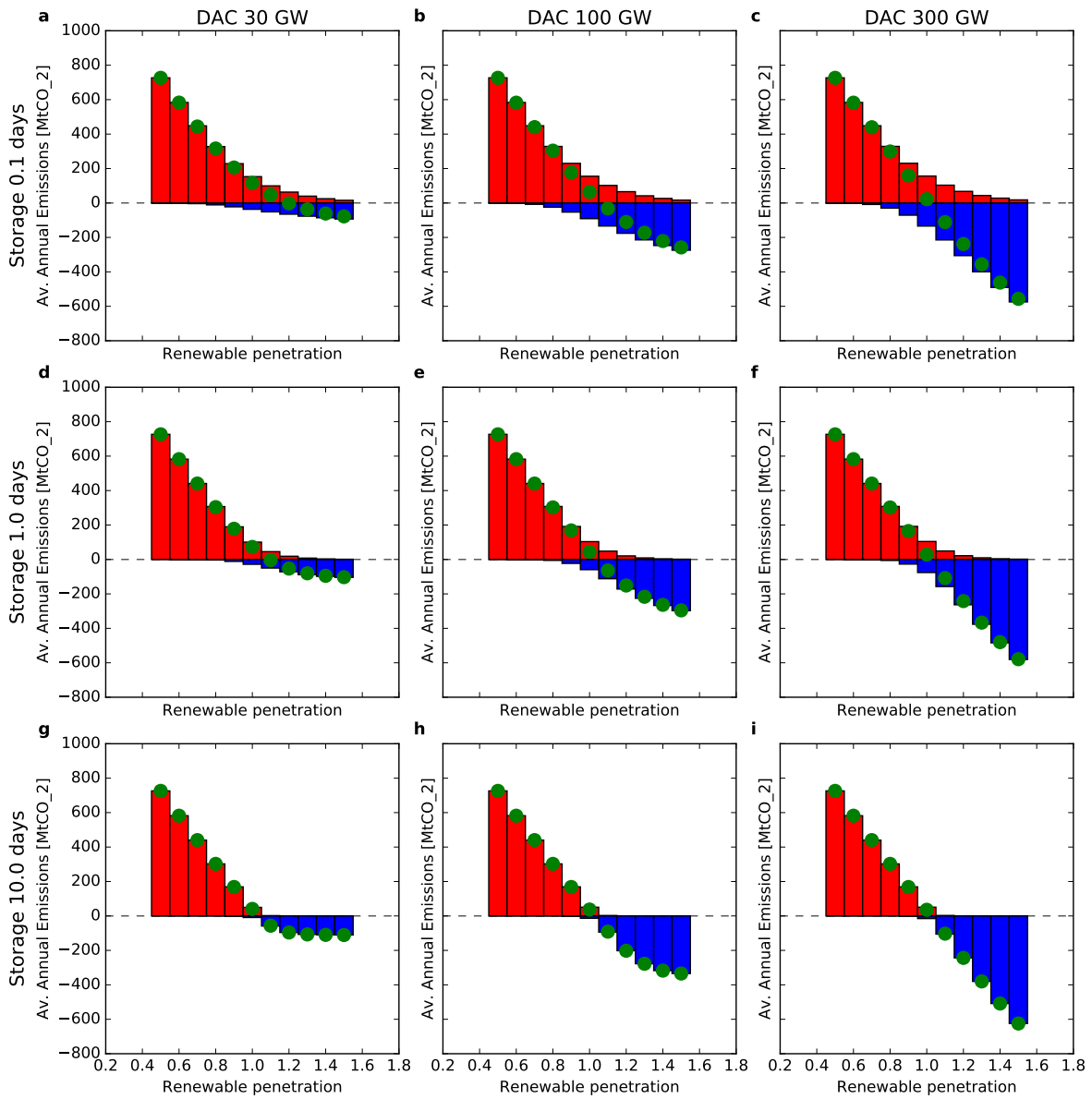


Figure S1: **European CO_2 emissions versus renewable penetration for different DAC capacities (columns) and storage sizes (rows) using a 24 hour forecast window for storage dispatching.** Red bars denote emissions from open-cycle gas turbines that are used for backup. Blue indicates negative emissions from DAC. Green circles denote total emissions.

172 In addition to the scenario of unlimited transmission capacity in Europe, we also modeled a
 173 single individual country. We arbitrarily picked France as one country that contributes substan-
 174 tially to European electricity consumption. As expected, Fig. S2 reveals that backup energies
 175 and associated emissions decrease slower with renewable penetration as compared to the sce-
 176 nario with an extensive European grid. This is linked to more frequent and stronger phases of
 177 generation shortfall and can be compensated for by large storage assets. We furthermore report
 178 that DAC is substantially used at relatively low penetrations since overgeneration also occurs
 179 more frequently.

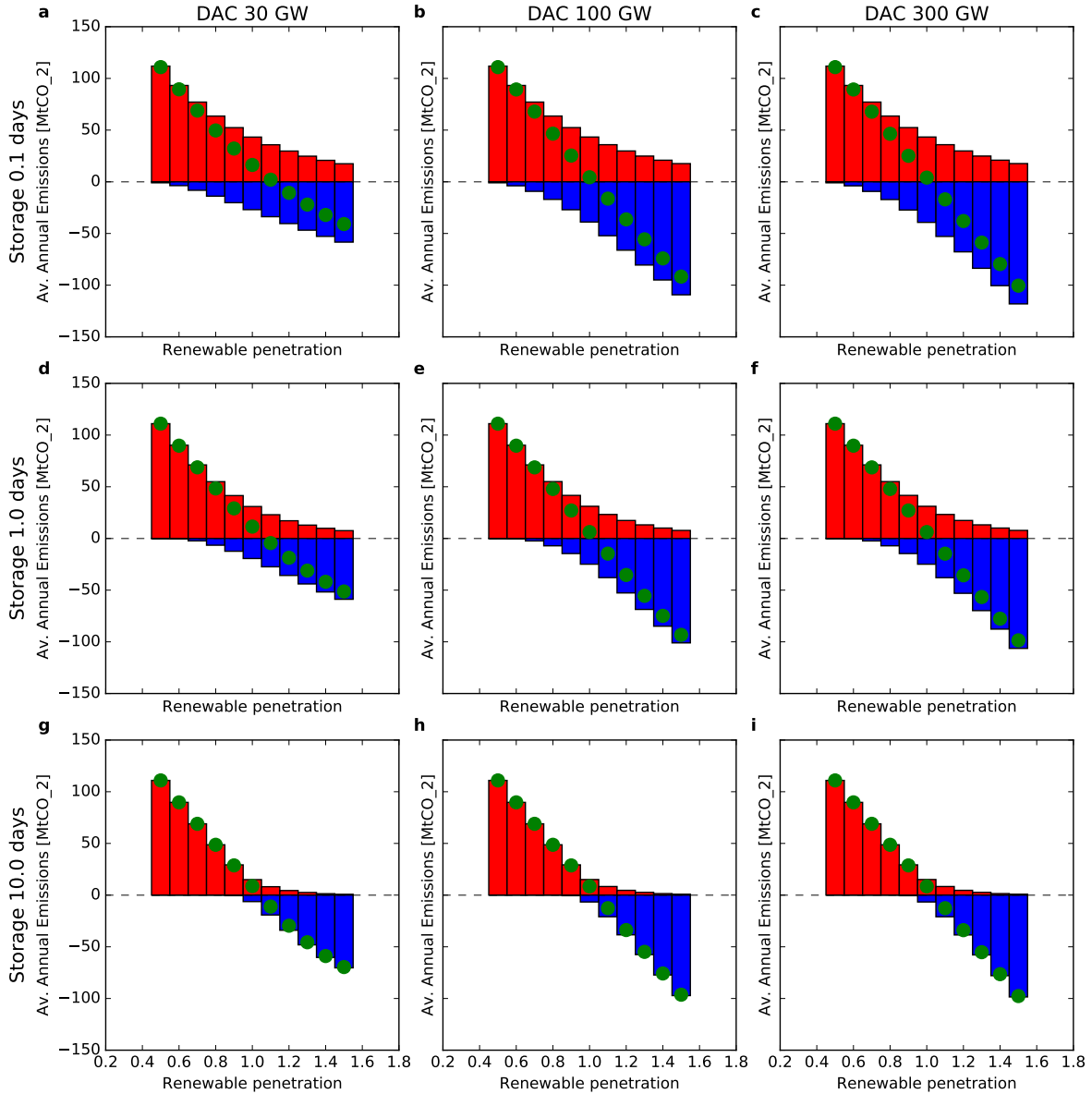


Figure S2: **French CO_2 emissions versus renewable penetration for different DAC capacities (columns) and storage sizes (rows) using a 24 hour forecast window for storage dispatching.** Red bars denote emissions from open-cycle gas turbines that are used for backup. Blue indicates negative emissions from DAC. Green circles denote total emissions.

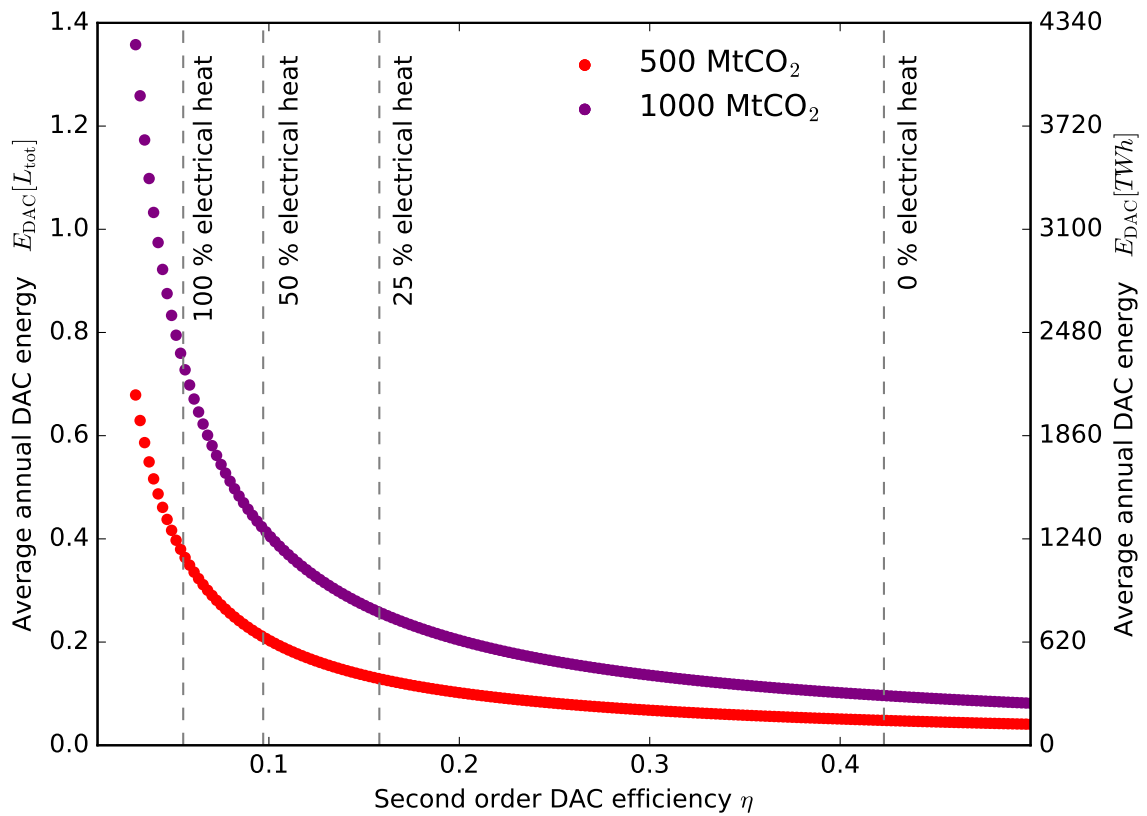


Figure S3: **DAC energy requirement to reach negative emission targets.** Vertical dashed lines correspond to today's second order efficiency of the Climeworks DAC unit for different shares of electrical heat. For an electrical share of less than 100%, heat is supplied from other sources such as industrial waste or renewable heat.

References

- 180
- 181 G.B. Andresen, M.G. Rasmussen, R.A. Rodriguez, S. Becker, and M. Greiner. Fundamental
182 Properties of and Transition to a Fully Renewable Pan-European Power System. *EPJ Web*
183 *of Conferences*, 33:04001, 2012. ISSN 2100-014X. doi: 10.1051/epjconf/20123304001. URL
184 <http://www.epj-conferences.org/10.1051/epjconf/20123304001>.
- 185 . European Network of Transmission System Operators for Electricity. Hourly load values for
186 all countries for a specific month (last accessed on 21/11/2016), 2015. URL [https://www.](https://www.entsoe.eu/db-query/consumption/mhlv-all-countries-for-a-specific-month)
187 [entsoe.eu/db-query/consumption/mhlv-all-countries-for-a-specific-month](https://www.entsoe.eu/db-query/consumption/mhlv-all-countries-for-a-specific-month).
- 188 Kurt Zenz House, Antonio C. Baclig, Manya Ranjan, Ernst A. van Nierop, Jennifer Wilcox,
189 and Howard J. Herzog. Economic and energetic analysis of capturing CO₂ from ambient air.
190 *Proceedings of the National Academy of Sciences*, 108(51):20428–20433, 2011. doi: 10.1073/
191 [pnas.1012253108](http://www.pnas.org/content/108/51/20428.abstract). URL <http://www.pnas.org/content/108/51/20428.abstract>.
- 192 David W. Keith, Geoffrey Holmes, David St. Angelo, and Kenton Heidel. A Process for Captur-
193 ing CO₂ from the Atmosphere. *Joule*, June 2018. ISSN 25424351. doi: 10.1016/j.joule.2018.
194 05.006. URL <https://linkinghub.elsevier.com/retrieve/pii/S2542435118302253>.
- 195 Aleksandar Lozanovski, Christoph Gebald, Christian Peter Brandstetter, Jan Paul Lindner,
196 and Stefan Albrecht. Direct Air Capture of CO₂. Climeworks and University of Stuttgart.
- 197 William Moomaw, Peter Burgherr, Gavin Heath, Manfred Lenzen, John Nyboer, and Aviel
198 Verbruggen. Annex II: Methodology. In *In IPCC Special Report on Renewable Energy Sources*
199 *and Climate Change Mitigation [O. Edenhofer, R. Pichs-Madruga, Y. Sokona, K. Seyboth,*
200 *P. Matschoss, S. Kadner, T. Zwickel, P. Eickemeier, G. Hansen, S. Schlmer, C. von Stechow*
201 *(eds)]*. Cambridge University Press, Cambridge, 2011.
- 202 Stefan Pfenninger and Iain Staffell. Long-term patterns of European PV output using 30 years
203 of validated hourly reanalysis and satellite data. *Energy*, 114:1251–1265, November 2016.
204 ISSN 03605442. doi: 10.1016/j.energy.2016.08.060. URL [http://linkinghub.elsevier.](http://linkinghub.elsevier.com/retrieve/pii/S0360544216311744)
205 [com/retrieve/pii/S0360544216311744](http://linkinghub.elsevier.com/retrieve/pii/S0360544216311744).
- 206 Michele M. Rienecker, Max J. Suarez, Ronald Gelaro, Ricardo Todling, Julio Bacmeister,
207 Emily Liu, Michael G. Bosilovich, Siegfried D. Schubert, Lawrence Takacs, Gi-Kong Kim,
208 Stephen Bloom, Junye Chen, Douglas Collins, Austin Conaty, Arlindo da Silva, Wei Gu,
209 Joanna Joiner, Randal D. Koster, Robert Lucchesi, Andrea Molod, Tommy Owens, Steven
210 Pawson, Philip Pegion, Christopher R. Redder, Rolf Reichle, Franklin R. Robertson, Al-
211 bert G. Ruddick, Meta Sienkiewicz, and Jack Woollen. MERRA: NASAs Modern-Era
212 Retrospective Analysis for Research and Applications. *Journal of Climate*, 24(14):3624–
213 3648, July 2011. ISSN 0894-8755, 1520-0442. doi: 10.1175/JCLI-D-11-00015.1. URL
214 <http://journals.ametsoc.org/doi/abs/10.1175/JCLI-D-11-00015.1>.
- 215 Rolando A. Rodriguez, Sarah Becker, Gorm B. Andresen, Dominik Heide, and Martin Greiner.
216 Transmission needs across a fully renewable European power system. *Renewable Energy*,
217 63:467–476, March 2014. ISSN 09601481. doi: 10.1016/j.renene.2013.10.005. URL [http:](http://linkinghub.elsevier.com/retrieve/pii/S0960148113005351)
218 [//linkinghub.elsevier.com/retrieve/pii/S0960148113005351](http://linkinghub.elsevier.com/retrieve/pii/S0960148113005351).
- 219 Rolando A. Rodriguez, Sarah Becker, and Martin Greiner. Cost-optimal design of a simpli-
220 fied, highly renewable pan-European electricity system. *Energy*, 83:658–668, April 2015.
221 ISSN 03605442. doi: 10.1016/j.energy.2015.02.066. URL [http://linkinghub.elsevier.](http://linkinghub.elsevier.com/retrieve/pii/S0360544215002212)
222 [com/retrieve/pii/S0360544215002212](http://linkinghub.elsevier.com/retrieve/pii/S0360544215002212).

- 223 D.P. Schlachtberger, T. Brown, S. Schramm, and M. Greiner. The benefits of cooperation
224 in a highly renewable European electricity network. *Energy*, 134:469–481, September 2017.
225 ISSN 03605442. doi: 10.1016/j.energy.2017.06.004. URL [http://linkinghub.elsevier.](http://linkinghub.elsevier.com/retrieve/pii/S0360544217309969)
226 [com/retrieve/pii/S0360544217309969](http://linkinghub.elsevier.com/retrieve/pii/S0360544217309969).
- 227 Robert Socolow, Michael Desmond, Roger Aines, Jason Blackstock, Olav Bolland, Tina Kaars-
228 berg, Nathan Lewis, Marco Mazzotti, Allen Pfeffer, Karma Sawyer, and others. Direct air
229 capture of CO2 with chemicals: a technology assessment for the APS Panel on Public Affairs.
230 Technical report, American Physical Society, 2011. URL [https://infoscience.epfl.ch/](https://infoscience.epfl.ch/record/200555/files/dac2011.pdf)
231 [record/200555/files/dac2011.pdf](https://infoscience.epfl.ch/record/200555/files/dac2011.pdf).
- 232 Iain Staffell and Stefan Pfenninger. Using bias-corrected reanalysis to simulate current and
233 future wind power output. *Energy*, 114:1224–1239, November 2016. ISSN 03605442.
234 doi: 10.1016/j.energy.2016.08.068. URL [http://linkinghub.elsevier.com/retrieve/](http://linkinghub.elsevier.com/retrieve/pii/S0360544216311811)
235 [pii/S0360544216311811](http://linkinghub.elsevier.com/retrieve/pii/S0360544216311811).

Chapter 4

Common discussion

This chapter provides a discussion of the results in a wider context. In the first part, it addresses similarities, differences and links between the contributions and aims to distill overarching topics. A repetition of the discussion sections of the individual publications is avoided on purpose for the sake of conciseness. Later on, new publications by other authors that are relevant in the context of publications #1 to #5 are presented and discussed.

Humankind has established remarkable independence of weather since the beginning of the industrialization. While in the earlier days, many processes relied on favourable weather conditions, progress in engineering has weakened or completely erased this dependency. For example, the international cargo shipping system that once relied on sailing vessels which required fair winds, is now fueled by fossil resources and can go more or less everywhere regardless of the weather. Wind mills used to grain cereals by transforming the kinetic energy of the air masses to rotational kinetic energy of stones. Nowadays, grinding is powered by electricity and has lost its wind dependence. Modern agriculture provides food to those who can afford it, irrespective of the season in the country of consumption. In the International Space Station, humans survive in an artificial atmosphere. While this list could be extended a lot further, it is interesting to realize that renewable power generation inverts this general tendency because it increases the weather dependency of energy systems. After the energy sector had gained independence from weather conditions with the invention of thermal power plants (ignoring some minor details such as the availability of cooling water), this independence is now lost again as systems are redesigned to more strongly rely on renewables. This u-turn in the overall development requires new (or in fact old) thinking that incorporates the fluctuations of the weather and the climate. It requires to understand and communicate variability as a normal feature that has to be taken care of in planning processes. We therefore require reliable and accurate statistical information of societally relevant climate variability.

4.1 The need for climate information in energy assessments

One main message of this dissertation is to substantiate the claim that renewable power systems are affected by the weather and its long-term statistics. This has been shown on different temporal and spatial scales and across different climate data types. Inter-annual climate variability relevantly impacts current power system operation in Germany (Sec. 3.2.1). On longer timescales, both multi-decadal climate variability (Sec. 3.3) and anthropogenic climate change (Sec. 3.1.1) lead to modifications of the boundary conditions under which power systems are operated. Shorter-term climate variability opens an opportunity space for flexible negative emission technologies (Sec. 3.4.1). Consequently, understanding and quantification of climate

variability and change is essential for planning, financing and operating renewable power systems.

4.1.1 Uncertainties of climate data sources

The climate of the earth is an interconnected system of complex systems and our information about it is incomplete. Uncertainty therefore is an integral part of any climate assessment. Consideration of the uncertainty is of utmost importance in the context of power systems where relationships are often non-linear. Different sources of climate information exist and have been used in this dissertation. All of them combine strengths and weaknesses and their appropriateness has to be verified for each particular research question. Contrasting observations and model results, observations are generally considered as the ground truth. This assumption is often correct and has proven its value numerous over the history of modern science. However, systematic evolution of the measurement technique can induce incorrect trends in the observations as was shown for marine wind speed measurements over the last century (Sec. 3.3.1). Consequently, data sets that rely on marine wind observations, such as the ECMWF's 20th century reanalyses have to be interpreted carefully when it comes to trends. A similar effect is known for surface wind speeds over land which feature decreases over the last decades (Vautard et al., 2010). This decrease is largely attributed to increasing surface roughness and can not be meaningfully extrapolated to heights that are relevant for wind energy without explicitly accounting for the evolution of the vertical wind profile. Every data source, including observations, therefore has to be checked for consistency.

Modern reanalyses have been the starting point of the assessments in Sec. 3.2.1 and 3.4.1. In Sec. 3.2.1, results based on two different reanalyses (ERA-interim and MERRA2) were compared to quantify agreement. Given that they are calculated by two different data centers, using different computer codes, their comparison is a meaningful indicator for model uncertainty. We showed that results based on both datasets largely agree in terms of inter-annual wind generation variability, thus building trust in the findings. A second verification of the suitability of the approach is that it reproduces measured wind generation over the years 2016 and 2017. While modern reanalyses are thus well suited to quantify inter-annual wind generation variability in Germany, their usefulness for long-term assessments seems less. The chosen start date in 1979 is due to pragmatic considerations (good data availability thereafter) and does not necessarily lead to representative estimates for renewable energy generation. For example, the lifetime wind energy generation of an average wind park in Germany shows a statistically significant downward trend in ERA-interim (see Sec. 3.3.2). Extrapolation of this trend into the future would, however, be misleading as closer inspection reveals that 1979 coincides with a maximum of multi-decadal wind generation variability (again Sec. 3.3.2). The trend thus only represents the downward sloping fraction of longer-term variability. This exemplifies that modern reanalyses, such as ERA-interim, are sufficiently short to only sample parts of multi-decadal climate variability. Any estimate and trend assessment can thus be compromised by the start date, which has been chosen fairly randomly. A high stakes, huge investments project like the energy transition thus has to be complemented by long-term assessments.

Such long-term assessments were performed in this dissertation for the historical period that is likely mainly affected by climate variability (Sec. 3.3.2) and for a high emissions climate change scenario in the future in which forced changes are expected to dominate (Sec. 3.1.1). Assessments of climate change impacts add an

additional layer of uncertainty, namely future atmospheric greenhouse gas concentrations. As human activity is not captured in climate models, the GHG emissions are not modeled. Instead, the evolution of GHG concentration is prescribed following different scenarios. The uncertainty that stems from choosing the 'wrong' scenario is named scenario uncertainty. In choosing the representative concentration pathway 8.5, which is currently the highest emission scenario, the scenario uncertainty is circumvented here as we aim for a sensitivity analysis rather than a prediction. However, instead of addressing *likely* wind energy changes due to climate change, we thereby restrict the analysis to a particular climate change scenario. In focusing on the most extreme scenario, forced changes are expected to be larger in magnitude than internal variability. Confidence in the results stems from agreement across a five member climate model ensemble that unanimously reports changes of the same sign in backup energy. Moreover, a large fraction of the CMIP5 ensemble also supports the underlying effect of more homogeneous winds in Europe. The agreement across the climate model ensemble weighs even more than the agreement between different reanalyses. This is because the reanalyses are synchronized owing to the assimilation of observations while climate models are not synchronized. This means that natural variability in the climate models is out of phase. Agreement of the climate model ensemble with respect to the sign of change therefore implies that the forced changes plus a randomly offset component of natural variability yields changes in the same direction in all cases.

4.1.2 Suitable metrics depend on context

In a discussion about the impacts of climate variability and change on renewable power generation, it should be mentioned that many metrics are of potential relevance. This is because different sectors and stakeholders are interested in different aspects. A wind park planner in Germany, for example, may be mostly interested in the discounted lifetime revenues of an asset. Given guaranteed feed-in tariffs, this translates into an interest in weighted wind energy yields (see Sec. 3.3.2). A Transmission System Operator, in contrast, cares less for the returns/energy yields of individual parks over 20 years, but needs information on generation variability on shorter timescales as his/her job is to ensure a balance of electricity generation and demand at all time steps. A civil engineer in charge of dimensioning large storage infrastructure may care most about seasonal differences. This multitude of perspectives is reflected in this dissertation by focusing on different metrics.

For instance, inspired by a public debate about seemingly escalating grid management costs, we investigated redispatch. Redispatch is a short-term measure implemented by a Transmission System Operator to mitigate congestion in the transmission grid. Redispatch is scheduled to last a few hours up to a couple of days and depends on the combined generation of all technologies, the demand pattern and ex-/imports. The multi-decadal assessment, in contrast, focused entirely on the generation side and did not take grid integration into account. However, the results found are relevant for the sizing of infrastructure components that are needed to integrate wind energy (e.g., storage and other types of power generation). Our contribution to the field of climate change impacts on power systems highlighted the vulnerability of spatial balancing via continental transmission. We put the emphasis on changes in the spatial co-variability of wind energy generation rather than wind energy yields as mitigating this variability is a key challenge in building renewable power systems. These results are therefore relevant for robust transmission system design in Europe.

4.1.3 The relative importance of forced changes versus multi-decadal climate variability for wind energy

The separation of climate variability and climate change is a simple task from a conceptual point of view. Climate variability happens without anthropogenic forcing, climate change is a response to the forcing. In practice, however, this separation proves much more difficult. The climate has been subject to forced changes over the course of the 20th century, implying that 20th century reanalyses do not only contain climate variability but also climate change. Similarly, climate models feature both forced changes and climate variability in transient model runs. Owing to the large interest in understanding risk from climate change, most effort, for example in the EUROCORDEX downscaling initiative, has been put in providing transient runs. Runs with prescribed and unaltered GHG concentrations could be used to study climate variability in the absence of climate change. However, such simulations could then not necessarily be meaningfully compared with 20th century reanalyses or observations.

In the context of disentangling change and variability of wind and wind energy, a couple of aspects are worth to be highlighted. The range of 20y average wind power generation variability estimated from 20th century reanalysis (Sec. 3.3.2) and the impact of climate change on European wind energy yields (Tobin et al., 2016) are both around $\pm 5\%$. This similarity in magnitude could imply that both findings reflect the same mechanism. If climate models capture multi-decadal wind variability, the alterations reported by Tobin et al. (2016) could be independent of climate change. However, it remains to be shown whether climate models capture multi-decadal wind variability and it would be a huge coincidence if the models reported the same variation synchronously. If they are unable to capture multi-decadal variability, their results are independent of climate variability on this timescale. The real climate system will feature a compound effect (multi-decadal as inferred from 20th century reanalyses plus climate change as inferred from climate models). The combined change can be substantially more important than the individual contributors. A similar argument can be made for the changes in seasonality that are found both in the 20th century reanalysis and in climate change assessments (Reyers, Moemken, and Pinto, 2016). It is thus a key question for future investigations to test the ability of climate models to capture multi-decadal variability of climatic variables that are relevant for the energy sector, such as wind.

4.2 Beyond wind

Most parts of this dissertation focus on wind energy even though it is obvious that the diversity of renewables can help to mitigate generation variability. The reason for the focus is simple. It is reliability of the data as already discussed, for example, in the Introduction of publication #1 in the context of climate models. Given the large uncertainties that are already present in long-term wind trends (see Sec. 3.3.2), it is equally unclear whether radiation and precipitation data from 20th century reanalyses is any good. While winds are directly constrained by the assimilated pressure and marine wind observations, radiation is fairly independent of these observations. Based on the standard assumption that the assimilation of observations adds realism, it appears thus justified to question the reliability of radiation estimates. However, this assumption has been proven wrong for marine winds and it may well be that the model provides useful radiation and precipitation estimates.

Given the importance of technology diversification and the fact that others use climate models for PV and CSP assessments (e.g., Jerez et al., 2015; Patt, Pfenninger, and Lilliestam, 2013; Müller et al., 2019), the skill of 20th century reanalysis to provide radiation and precipitation estimates should be tackled in the future.

4.3 Multi-disciplinary approaches

In addition to more holistic approaches in terms of technologies, cross-disciplinarity is needed to grasp all relevant dimensions. In Sec. 3.2.1, the public and political debate around redispatch motivated our statistical analysis and we have complemented our work with a review of public uptake and changes in jurisdiction. While this is a first step towards more holistic energy system assessments, the study still clearly stems from a physics background (e.g., regarding its methods). The inclusion of social and societal aspects is of high importance in understanding energy transitions. It is not only about proper resource assessments as cultural norms, biases and public perception play vital roles. The ethical dimension is reflected, for example, in a study that assesses justice in energy efficiency (Snell, Bevan, and Gillard, 2018).

Connections between different sectors, such as the interconnections between energy and water (Konadu et al., 2017), are increasingly accounted for. In a study about the governance of the coupled food-energy-water system, Märker, Venghaus, and Hake (2018) investigate the necessary changes in policy structures and processes. They investigate multiple approaches that differ in the extent to which the coupling between the sectors is included and the level of interaction between the actors active in each sector. In addition to these system-level assessments, also the individual scale is investigated. Roberts, Hope, and Skelton (2017) built a typology of regretted consumption because understanding the reasons why people make such purchases bears the potential to avoid them. Avoiding regretted consumption would mean personal and ecological benefits as the usage of scarce resources is reduced.

The fact that the current academic system is still strictly subdivided into different disciplines enforces, or at least incentivizes, disciplinary approaches. In light of large-scale challenges such as sustainability, old boundaries between disciplines may have to be revised. Physics alone will not sufficiently inform the transition to a sustainable society, nor will any other discipline, including engineering and the social sciences.

4.4 Generation variability and the likely need for negative emissions

Net zero emissions from all sectors of human activity is an ambitious goal that directly follows the adoption of a long-term temperature target in international climate policy. Reaching exactly zero will be cumbersome and the results of publications #1 - #4 underline this statement in highlighting the variability on unexpected timescales and the vulnerability of wind energy. Unless the variability, including on very long timescales of multiple decades, and vulnerability is perfectly accounted for in energy system design, dispatchable power generation will always be needed. Moreover, dispatchable power generation may still be associated with GHG emissions in the near-to-medium future as dispatchable renewables face deployment limitations. In theory, storage of electricity could solve this issue. In light of the timescales involved (at least up to multi-decadal), however, energy storage alone will likely not

solve the problem owing to size limitations and losses. In such a situation, it might be relevant to consider the atmosphere as a giant quasi-battery.

While a battery allows to store electricity, the atmosphere can be filled with CO₂ while generating electricity in a gas-fired power station. At a later stage, the CO₂ can theoretically be removed again using renewable excess electricity for DAC. As the current efficiency of open cycle gas turbines and DAC units is comparable (see Sec. 3.4.1), the entire process is neutral in terms of electricity and CO₂. As long as the stored amount of CO₂ is small in comparison to the total net emissions since pre-industrial times, for example the equivalent of one year of current GHG emissions, the effect on the planet's energy balance is limited. However, both the economic viability and the technological readiness for deployment at scale remain to be shown for DAC.

4.5 New literature

The scientific literature around the topics addressed in this thesis evolves rapidly. Albeit only around one year has elapsed since the publication of paper #1, some important additions have been made to the body of literature in the fields of climate change impacts on the power system, redispatch and DAC. They are reviewed and discussed in the following.

4.5.1 Climate change impacts on the power system

Karnauskas, Lundquist, and Zhang (2018)

A general decrease of wind energy potentials in Northern hemisphere mid-latitudes, including most of Europe, is found by Karnauskas, Lundquist, and Zhang (2018) using a 10 member GCM ensemble and two emission scenarios (RCP4.5 and RCP8.5). This decrease is accompanied by increases in the tropics and the Southern Hemisphere, such that the authors refer to the changes as a southward shift of the wind energy resource. GCM performance is validated by comparison with wind speed measurements at a tower in Boulder, USA. The change is explained by means of arctic amplification that reduces the meridional temperature gradient in the Northern Hemisphere and enhanced land-sea gradients in the tropics and Southern Hemisphere. The magnitude of the changes varies by region and can be as high as +41% in Northern Australia and -15% in Central USA.

The authors use monthly mean wind speeds from CMIP5 to compute monthly mean wind power generation. However, due to the non-linear dependence of wind power generation on wind speeds (see eq. S2 in Sec. 3.1.1), the computed value of wind power generation depends on the time resolution of the input data. In particular, the wind power generation of monthly mean wind speed is not the same as the monthly mean wind power generation because

$$\langle v^3 \rangle \neq \langle v \rangle^3.$$

The authors are aware of this potential weakness of their approach and use measured mast data to justify it. Comparing monthly wind power generation computed from hourly measured wind speeds and wind power generation from monthly mean wind speeds, they report a very high correlation ($r = 0.94$). Based on this high correlation, they argue that monthly mean wind speeds are a suitable input parameter

for their analysis. However, one should note that this line of reasoning depends on the specifics of the wind distribution that (i) need not be the same everywhere on the planet and (ii) could be altered in a changing climate.

To illustrate this argument, let v be the wind speed at a certain grid point. We can rewrite it as

$$v = \langle v \rangle - \langle v \rangle + v = \langle v \rangle + \Delta v, \quad (4.1)$$

where $\langle v \rangle$ denotes the mean of v and $\Delta v = v - \langle v \rangle$ denotes the deviation from its mean which is often referred to as anomaly in the climate sciences.

It follows that

$$\begin{aligned} \langle v^3 \rangle &= \langle (\langle v \rangle + \Delta v)^3 \rangle \\ &= \langle \langle v \rangle^3 + 3\langle v \rangle(\Delta v)^2 + 3\langle v \rangle^2\Delta v + (\Delta v)^3 \rangle \\ &= \langle v \rangle^3 + 3\langle v \rangle\langle (\Delta v)^2 \rangle + 3\langle v \rangle^2 \underbrace{\langle \Delta v \rangle}_{=0 \text{ by definition}} + \langle (\Delta v)^3 \rangle \\ &= \langle v \rangle^3 + 3\langle v \rangle\langle (\Delta v)^2 \rangle + \langle (\Delta v)^3 \rangle, \end{aligned} \quad (4.2)$$

which can be rewritten as

$$\langle v^3 \rangle - \langle v \rangle^3 = 3\langle v \rangle\langle (\Delta v)^2 \rangle + \langle (\Delta v)^3 \rangle. \quad (4.3)$$

Recall that the wind energy density WED is proportional to the cube of wind speeds ($WED \propto v^3$) and that the wind energy density sets an upper limit to wind power generation (see Sec. 3.1.1). Eq. 4.3 thus implies that the error in the wind energy density that is introduced by substituting the high resolution wind speed data v with the mean wind speeds $\langle v \rangle$ depends on multiple factors. To be precise, it depends on the mean wind speed $\langle v \rangle$ itself, the mean of the squared wind speed anomaly $\langle (\Delta v)^2 \rangle$ and the mean of the cubed wind speed anomaly $\langle (\Delta v)^3 \rangle$.

The potential issue with the approach is that there is no a priori reason for the right hand side of eq. 4.3 not to change. One could even suspect that changes in $\langle (\Delta v)^2 \rangle$ and $\langle (\Delta v)^3 \rangle$ are likely if the mean wind speed changes. In fact, in publication #1, we demonstrated that the spatial co-variability of wind power generation across Europe changes under strong climate change. This might be pointing towards changes in other statistical properties of wind speeds. Moreover, just because the right hand side is proportional to $\langle v \rangle$ in one particular location in the past does not safely imply that this relationship holds everywhere and at any time (as assumed by Karnauskas, Lundquist, and Zhang (2018)).

In any case, the main finding is neither in contrast to publication #1 nor does it support it. This is because we focus on the spatial co-variability of wind power generation to assess the vulnerability of transmission infrastructure. To do so, we mute all changes in wind power generation potentials by the assumption of a fully renewable power system. If wind power potentials in a country decrease in the future, this would be compensated by a larger number of wind parks in our article.

Schlott et al. (2018)

Schlott et al. (2018) aim at a more holistic assessment of climate change impacts on the power system. Also drawing from EUROCORDEX (3 members), they include

different renewable technologies (PV, wind and hydro) and they optimize generation technology deployment and transmission infrastructure. To this end, they use 6 (sometimes 8) year intervals over the 21st century during which an optimum system is computed. They find that climate change has an impact on power system costs which generally increase over the course of the 21st century by around 5%. This can be largely attributed to an increased share of PV following increasing correlation lengths of wind power generation.

Increasing correlation lengths are in line with our result of more homogeneous winds and dominantly increasing correlations (see also paper #1). However, the concept of a correlation *length* might be somewhat misleading because correlation decay does not necessarily feature rotational symmetry due to, for example, complex topography such as mountains or land-sea transitions.

Peter (2019)

Peter (2019) tests whether strategies that anticipate climate change can help to reduce power system vulnerability. The analysis is based on a single GCM-RCM combination, thereby neglecting model uncertainty. His modeling approach follows a two-step procedure. First, he runs the model with perfect foresight to determine the cost optimum system design. In a second step, this system is operated without any further modification of infrastructures under perturbed conditions. Peter distinguishes a set of scenarios in which climate change is anticipated (i.e., included in the optimum design in step one) or ignored. Moreover, he disentangles the effect of individual components (wind and solar, cooling water for conventional power generation, hydropower, electricity demand) on the overall change. The combined effect of climate change on the non-anticipation system is €24, which is a 12% cost increase. Anticipation of climate change reduces the economic damages by around €4. This is achieved by more offshore wind and reduced onshore wind and solar. As climate change impacts on the offshore wind resource are found to be positive, more offshore wind parks allow higher capacity factors and consequently less fuel and CO₂ allowance costs. While this study adds many layers of realism and thereby contributes relevantly to the literature, its results may be compromised by two methodological weaknesses. A single GCM-RCM combination does not allow to draw robust conclusions and the approach is based on individual representative weather years, which implies that interannual variability and climate change are not effectively separated.

Jerez et al. (2019)

In continuation of their previous isolated works on climate change impacts on wind (Tobin et al., 2016) and solar (Jerez et al., 2015), Jerez et al. (2019) study the combined effect on a system that contains both wind and solar power generation. Through changes in their co-variability, the reaction of the combined system can be different from the individual components. Based on an EUROCORDEX ensemble and RCP8.5, the authors find that projected changes by the end of the century are at the order of 5%. Even though they are mostly negative, the limited magnitude leads Jerez et al. to conclude that the effects can be neglected. Confirming earlier results, mean power generation from wind, solar and wind + solar is reduced by only around 2% at the continental scale. Nevertheless, the standard deviation of the combined timeseries and the wind or solar timeseries individually increases almost everywhere. The increase of the standard deviation of the combined system is found

to be smaller than the increase of the individual components in some regions (e.g., Benelux-Germany and France). The authors argue that this hints to increased complementarity between wind and solar which weakens the effect on the combined system. It remains to be shown, however, if the standard deviation is a useful indicator for power system operation. This might not be necessarily the case as, for example, dispatching storage infrastructure critically depends on the sequencing of generation events while the standard deviation does not.

Tobin et al. (2018)

While most studies that tackle climate change impacts on renewables use strong climate change scenarios and focus on long-term changes at the end of the 21st century, Tobin et al. (2018) follow a different approach. They adopt a framing that is often used in the climate impact community and investigate impacts at different warming levels, namely 1.5°C, 2°C and 3°C. The climate state associated with these thresholds is defined as the first 30 year interval that features an average global mean temperature increase higher than the threshold. The period studied consequently varies from model to model owing to different reactions to external forcing (i.e., climate sensitivity). Data is taken from EUROCORDEX and the ensemble consists of 3 different GCMs and RCMs, respectively. In most cases RCP8.5 is used, which implies that none of the temperature thresholds is close to the thermodynamic equilibrium and transient effects are expected to play a considerable role. Tobin et al. find negative impacts of climate change on electricity production in most locations and for most technologies (wind, solar, hydro and conventional). The magnitude of the changes is small for 1.5°C and roughly doubles with a doubling of the temperature threshold to 3°C. Moreover, impacts are distributed unevenly across Europe and Southern Europe is a hot spot, implying inequity within the EU. As in our paper #1, Greece shows a different evolution, here indicated by an increase of wind power potential. By also including risks for conventional generation due to lacking cooling water, they report that the overall system becomes more resilient with an increasing share of renewables.

Behrens et al. (2017)

In a spatially detailed analysis, Behrens et al. (2017) assess the impact of insufficient and too warm cooling water availability on the operation of conventional power plants in greater detail. They include a sophisticated database of power plants, including additions and retirements over time. The authors conclude that more basins are affected by water stresses that enforce a reduction of power generation in 2030 (54 basins) as compared to 2014 (47 basins). The impacts are strongest in the Mediterranean but are also visible in highly used basins in Central Europe.

From a climatic point of view, however, the interpretation of the results is not convincing. The main methodological issue is that the temporal offset between the years studied (2014, 2020, 2030) is likely insufficient to yield a meaningful signal-to-noise ratio such that the changes can not be safely attributed to climate change rather than climate variability (or other reasons such as consumption changes and capacity additions). It is known that precipitation changes are often uncertain and agreement in the CMIP5 ensemble is sparse. For example, the latest IPCC report documents that the change in 20 year mean precipitation averaged over 1986-2005 and 2081-2100 is small compared to natural internal variability over the Mediterranean using RCP2.6 and a 32 member GCM ensemble (see Fig. SPM.8 b in IPCC, 2013). Only in

the stronger RCP8.5 a consistent large scale decrease in the Mediterranean develops. Even though the authors use relatively strong climate change scenarios (RCP4.5 and RCP 8.5), the expected impact over a timespan as short as around 15 years is small. In particular, it is a lot smaller than the impacts over a 100 year period as reported by the IPCC. Moreover, the authors seem to intermingle also interannual variability as individual years are compared. In such a situation, the attribution of any alteration to a forced change is speculative. The negligible relevance of the climatic forcing is even documented by the authors who report that there is "very little variation between scenarios by 2030".

Kozarcenin, Liu, and Andresen (2018)

In contrast to most other studies, Kozarcenin, Liu, and Andresen (2018) argue that the effects of climate change on power system design can likely be ignored. They compare the effect of changes in the solar-to-wind ratio with climate change impacts and conclude that the former outweigh the latter. Using the solar-to-wind ratio effect as a benchmark for the comparison appears interesting, but also fairly random. This is because the authors want to investigate whether climate change has a discernible effect on major power system metrics. It would appear more straightforward to keep the system parameters fixed or optimize the system following the same logic in all cases. Moreover, the impact of climate change on a solar dominated power system, interestingly, is close to non-existent. While this could imply that solar-powered systems are indeed less vulnerable, it could also reflect the climate model's incapability to capture changes in cloud formation and atmospheric chemistry. In conclusion, there does not seem to be sufficient evidence for the author's claim that climate change impacts on the power system can be neglected.

4.5.2 Redispatch

As argued in publication #2, redispatch is partially rooted in the design of the power market: The working hypothesis of the German market is that all feed-in patterns are generally consistent with the physical limitations of the transmission network. Following this hypothesis, a cost optimum overall solution is derived by dispatching a set of generators that minimize the operational costs. The validity of the assumption is under pressure given frequent interventions of Transmission System Operators via, for example, redispatch. Moreover, the potential to forecast redispatch with high accuracy opens a possibility for power plant operators to try to take advantage of the redispatch mechanism as explained in the following.

Using a conceptual two node model that can be solved graphically, Hirth and Schlecht (2018) investigate the effect of strategic bidding of agents who anticipate redispatch. This means that a power plant operator could underbid to ensure that his plant is dispatched if he/she knows that the plant will be redispatched down eventually. Underbidding here signifies that the bid is less than the operational cost of running the power plant. Similarly, a plant operator who knows that his/her plant will be needed to increase generation in the redispatch and who anticipates higher prices in the redispatch, could increase its bid to the price that is expected to be the outcome of the redispatch. Both strategies maximize profits of individual agents and lead to higher system costs. More specifically, Hirth and Schlecht focus on a two step procedure that sequentially (1) dispatches power plants following the merit order and (2) redispatches based on a redispatch market. They argue that a

redispatch market yields incentives that deteriorate overall performance as reflected in higher than necessary total costs and aggravated congestion.

Staudt et al. (2018) show that redispatch on a power plant level can be predicted with high precision one day ahead. They use forecasts of load, solar generation, wind generation, total generation and electricity price as inputs to an extra-tree and an artificial neural network. Focusing on the 25 member subset of plants that were redispatched most frequently in Germany in 2015 - 2017, they calculate the average precision

$$p = \frac{TP}{TP + FP} \quad (4.4)$$

where TP is the number of true positives (i.e., plant is correctly predicted to be redispatched) and FP is the number of false positives (i.e., plant is not redispatched in disarray with the prediction). Using the extra-tree method, an average precision $p = 0.72$ is obtained, which can be further increased to $p = 0.94$ if regional input data is used. The latter comes at a relatively high computational cost. Given that large electric utilities companies such as Innogy, Vattenfall and EnBW, have access to additional information that is not available for research purposes (most importantly the bids of their various plants), it appears highly likely that such players can predict redispatch with an even higher precision. Staudt et al. conclude that the low risk of strategic bidding that comes with the chance to realize extra-profits for individual companies leads to non-optimum system wide decisions. Thereby, system costs and carbon emissions are increased.

It appears worthwhile to contemplate the implications of these results. Let π_m be the marginal price of electricity generation of a plant, π_{bid} be its bid into the spot market and π_{cl} be the market clearance price. For simplicity, we assume that all bids have the same volume (e.g., 1 MWh of electricity). The plant operator could underbid to ensure that his/her plant is dispatched if he/she assumes that it is redispatched eventually. Such behaviour induces gains if the anticipated redispatch occurs (case 1) and creates losses if it doesn't (case 2). In case 1, the price difference is positive

$$\Delta\pi_1 = \pi_{cl} - \pi_{bid} \geq 0, \quad (4.5)$$

because the market clearance price is determined via the merit order¹ and can not be smaller than any individual bid that is dispatched. In contrast, in case 2, the price difference will generally be negative

$$\Delta\pi_2 = \pi_{cl} - \pi_m < 0, \quad (4.6)$$

because of the underbidding ($\Delta\pi_2 \geq 0$ is also conceivable if the clearance price is high enough. However, this case is trivial as both cases would be beneficial for the plant operator. It will thus not be further discussed here). The total effect of both cases depends on the frequency of their occurrence. That is, it depends on the

¹The merit order is simply a sorted list of all bids that starts with the cheapest and ends with the most expensive one. In the dispatch, power plants are activated following the merit order until there is a balance between electricity consumption and electricity generation. The price of the last unit that is dispatched is referred to as the market clearance price. All power plants that are dispatched receive the market clearance price, irrespective of their own bid.

precision p with which redispatch can be predicted on a power plant level and also on the number of redispatch predictions N . The total effect reads

$$\Delta\pi_{\text{tot}} = N \cdot [p\Delta\pi_1 + (1 - p)\Delta\pi_2]. \quad (4.7)$$

Using the high precision $p = 0.94$ reported in (Staudt et al., 2018), this means that $\Delta\pi_{\text{tot}} \geq 0$ if $\Delta\pi_1 \geq -0.06 \cdot \Delta\pi_2$. Note that $\Delta\pi_2$ is negative. In other words, strategic bidding pays off for the plant operator if the per case-1 event gain is at least 6% of the case-2 event loss. It appears very plausible that this is the case. However, the bids are not made public such that further verification of this plausibility would require indirect reasoning and is beyond the scope of this discussion. Nevertheless, this simple calculation in conjunction with the results of Hirth and Schlecht (2018) and Staudt et al. (2018) indicates that the design of the redispatch system deserves further attention.

Following a more general approach, Niet et al. (2018) model the effect of explicitly accounting for curtailment related costs. Based on the poor temporal resolution of models used for long-term planning, curtailment is often overlooked, leading to an underestimation of the benefits of infrastructure that reduces curtailment. They quantify the effect to be highly significant: the value of storage and dispatchable loads is increased by up to 60% if curtailment is included in the model. This finding highlights that economically reasonable, or even optimum, systems need to be specifically designed to cope with renewable generation variability.

4.5.3 DAC

Breyer, Fasihi, and Aghahosseini (2019) assess Direct Air Capture with the techno-economic Lappeenranta-Lahti University of Technology (LUT) Energy System model. They focus on the Maghreb region which features high potential for solar energy and large unused areas and report relatively low levelized costs of DAC of around €55 per ton CO₂ in 2050 with additional potential for cost reduction. Their assessment is similar to publication #5 in that it explicitly includes the sub-daily renewable generation variability. However, there are also major differences, for example, the different region of interest, the cost analysis and the methodology. As a consequence of high DAC investment cost and their cost-minimizing modeling approach, Breyer, Fasihi, and Aghahosseini report that DAC units are used in near baseload mode and thus do not provide much flexibility.

4.5.4 Multi-decadal aspects

Owing to the short timespan between the time of writing and publication of articles #4 and #5, no additions to the relevant literature were made in this field (to the best knowledge of the author). That said, I intend to deepen the analysis of multi-decadal effects on renewable power systems in future work. This will include studying a larger geographical domain and multiple renewable technologies.

Moreover, new datasets are about to become available. ECMWF has already published parts of the new ERA-5 reanalysis that covers the years 1979 to 2019 (Hennermann, 2018). In contrast to ERA-Interim, ERA-5 will include wind speeds at 100m height which fits better to the needs of renewable energy modeling. An extended version of ERA-5 that dates back until 1950 is scheduled to be published in late 2019. Future work will reveal whether it features discontinuities and/or spurious trends prior to the satellite era as were found in ERA20C and CERA20C (see Sec. 3.3.1).

In addition, a new round of global climate model results is currently underway for CMIP6 (Eyring et al., 2016). Some of the model outputs are tailored to the needs of the renewable energy community, for example, the contribution from the PRIMAV-ERA project.

4.6 Conclusion

The publications presented in this dissertation add to our knowledge about climate-energy interactions. The research field evolves rapidly which is evidenced by a large number of publications and a widening of the research focus through the integration of other sectors and disciplines. My publications emphasize the need for targeted and robust climatic information in order to build future zero emission power and energy systems. Relevant metrics depend on the stakeholder and evolve in time, thereby requiring sound understanding of the context. While climate variability already has a distinct impact on operational costs in the German power system, stronger impacts are to be expected in the future as the share of renewables increases. The impacts of anthropogenic climate change as well as multi-decadal climate variability ought to be included in designing future power systems. Strong climate change reduces the efficacy of a European transmission system due to more homogeneous winds by a few per cent. Multi-decadal wind variability impacts investment decisions and system design, for example, through time-varying winter-to-summer generation ratios with considerable amplitude.

Bibliography

- Andresen, G.B. et al. (2012). “Fundamental Properties of and Transition to a Fully Renewable Pan-European Power System”. In: *EPJ Web of Conferences* 33, p. 04001. DOI: [10.1051/epjconf/20123304001](https://doi.org/10.1051/epjconf/20123304001).
- Bank, World (2012). “Turn Down the Heat: Why a 4 degree C Warmer World Must Be Avoided”. In: URL: <http://citeseerx.ist.psu.edu/viewdoc/download?doi=10.1.1.374.6046&rep=rep1&type=pdf> (visited on 08/03/2016).
- Beaudin, Marc et al. (2010). “Energy storage for mitigating the variability of renewable electricity sources: An updated review”. In: *Energy for Sustainable Development* 14.4, pp. 302–314. DOI: [10.1016/j.esd.2010.09.007](https://doi.org/10.1016/j.esd.2010.09.007).
- Becker, S. et al. (2014). “Transmission grid extensions during the build-up of a fully renewable pan-European electricity supply”. In: *Energy* 64, pp. 404–418. DOI: [10.1016/j.energy.2013.10.010](https://doi.org/10.1016/j.energy.2013.10.010).
- Behrens, Paul et al. (2017). “Climate change and the vulnerability of electricity generation to water stress in the European Union”. In: *Nature Energy* 2.8. ISSN: 2058-7546. DOI: [10.1038/nenergy.2017.114](https://doi.org/10.1038/nenergy.2017.114).
- Bierkandt, R, M Auffhammer, and A Levermann (2015). “US power plant sites at risk of future sea-level rise”. In: *Environmental Research Letters* 10.12, p. 124022. DOI: [10.1088/1748-9326/10/12/124022](https://doi.org/10.1088/1748-9326/10/12/124022).
- Breyer, Christian, Mahdi Fasihi, and Arman Aghahosseini (2019). “Carbon dioxide direct air capture for effective climate change mitigation based on renewable electricity: a new type of energy system sector coupling”. In: *Mitigation and Adaptation Strategies for Global Change*. DOI: [10.1007/s11027-019-9847-y](https://doi.org/10.1007/s11027-019-9847-y).
- Brown, T. et al. (2018a). “Response to ‘Burden of proof: A comprehensive review of the feasibility of 100% renewable-electricity systems’”. In: *Renewable and Sustainable Energy Reviews* 92, pp. 834–847. DOI: [10.1016/j.rser.2018.04.113](https://doi.org/10.1016/j.rser.2018.04.113).
- Brown, T. et al. (2018b). “Synergies of sector coupling and transmission reinforcement in a cost-optimised, highly renewable European energy system”. In: *Energy* 160, pp. 720–739. DOI: [10.1016/j.energy.2018.06.222](https://doi.org/10.1016/j.energy.2018.06.222).
- Buckley, Martha W. and John Marshall (2016). “Observations, inferences, and mechanisms of the Atlantic Meridional Overturning Circulation: A review”. In: *Reviews of Geophysics* 54.1, pp. 5–63. DOI: [10.1002/2015RG000493](https://doi.org/10.1002/2015RG000493).
- Caesar, L. et al. (2018). “Observed fingerprint of a weakening Atlantic Ocean overturning circulation”. In: *Nature* 556.7700, pp. 191–196. DOI: [10.1038/s41586-018-0006-5](https://doi.org/10.1038/s41586-018-0006-5).
- Coumou, Dim and Stefan Rahmstorf (2012). “A decade of weather extremes”. In: *Nature Climate Change* 2.7, pp. 491–496. DOI: [10.1038/nclimate1452](https://doi.org/10.1038/nclimate1452).
- Creutzig, Felix et al. (2017). “The underestimated potential of solar energy to mitigate climate change”. In: *Nature Energy* 2.9, p. 17140. DOI: [10.1038/nenergy.2017.140](https://doi.org/10.1038/nenergy.2017.140).
- Díaz-González, Francisco et al. (2012). “A review of energy storage technologies for wind power applications”. In: *Renewable and Sustainable Energy Reviews* 16.4, pp. 2154–2171. DOI: [10.1016/j.rser.2012.01.029](https://doi.org/10.1016/j.rser.2012.01.029).

- EFD (2012). "Fusion Electricity - A roadmap to the realisation of fusion energy". In: URL: https://www.euro-fusion.org/fileadmin/user_upload/EUROfusion/Documents/Roadmap.pdf (visited on 03/15/2019).
- Eyring, Veronika et al. (2016). "Overview of the Coupled Model Intercomparison Project Phase 6 (CMIP6) experimental design and organization". In: *Geoscientific Model Development* 9.5, pp. 1937–1958. DOI: [10.5194/gmd-9-1937-2016](https://doi.org/10.5194/gmd-9-1937-2016).
- Favier, L. et al. (2014). "Retreat of Pine Island Glacier controlled by marine ice-sheet instability". en. In: *Nature Climate Change* 4.2, pp. 117–121. DOI: [10.1038/nclimate2094](https://doi.org/10.1038/nclimate2094).
- Feldmann, Johannes and Anders Levermann (2015). "Collapse of the West Antarctic Ice Sheet after local destabilization of the Amundsen Basin". In: *Proceedings of the National Academy of Sciences* 112.46, pp. 14191–14196. DOI: [10.1073/pnas.1512482112](https://doi.org/10.1073/pnas.1512482112).
- Figueres, Christiana et al. (2018). "Emissions are still rising: ramp up the cuts". In: *Nature* 564, pp. 27–30. DOI: [10.1038/d41586-018-07585-6](https://doi.org/10.1038/d41586-018-07585-6).
- Ghil, M. (2002). "Advanced spectral methods for climatic time series". en. In: *Reviews of Geophysics* 40.1. DOI: [10.1029/2000RG000092](https://doi.org/10.1029/2000RG000092).
- Giorgi, Filippo and William J. Gutowski (2015). "Regional Dynamical Downscaling and the CORDEX Initiative". In: *Annual Review of Environment and Resources* 40.1, pp. 467–490. DOI: [10.1146/annurev-environ-102014-021217](https://doi.org/10.1146/annurev-environ-102014-021217).
- Grams, Christian M. et al. (2017). "Balancing Europe's wind-power output through spatial deployment informed by weather regimes". In: *Nature Climate Change*. DOI: [10.1038/nclimate3338](https://doi.org/10.1038/nclimate3338).
- Hawkins, Ed and Rowan Sutton (2009). "The potential to narrow uncertainty in regional climate predictions". In: *Bulletin of the American Meteorological Society*. DOI: [10.1175/2009BAMS2607.1](https://doi.org/10.1175/2009BAMS2607.1).
- Hennermann, Karl (2018). *ERA5 data documentation*. URL: <https://confluence.ecmwf.int/display/CKB/ERA5+data+documentation> (visited on 11/22/2018).
- Hewitson, B. C. et al. (2014). "Interrogating empirical-statistical downscaling". In: *Climatic Change* 122.4, pp. 539–554. DOI: [10.1007/s10584-013-1021-z](https://doi.org/10.1007/s10584-013-1021-z).
- Hewitson, Bruce et al. (2017). "Climate information websites: an evolving landscape: Climate information websites". In: *Wiley Interdisciplinary Reviews: Climate Change* 8.5, e470. DOI: [10.1002/wcc.470](https://doi.org/10.1002/wcc.470).
- Hirth, Lion and Ingmar Schlecht (2018). "Inc-dec gaming as a consequence of inconsistent power market design". en. In: *USAE Working Paper No. 18-369*, p. 26. URL: <https://www.econstor.eu/bitstream/10419/194292/1/Market-Based-Redispatch-in-Zonal-Electricity-Markets.pdf> (visited on 03/27/2019).
- Hoegh-Guldberg, O. et al. (2007). "Coral Reefs Under Rapid Climate Change and Ocean Acidification". In: *Science* 318.5857, pp. 1737–1742. DOI: [10.1126/science.1152509](https://doi.org/10.1126/science.1152509).
- Huber, Matthias, Desislava Dimkova, and Thomas Hamacher (2014). "Integration of wind and solar power in Europe: Assessment of flexibility requirements". In: *Energy* 69, pp. 236–246. DOI: [10.1016/j.energy.2014.02.109](https://doi.org/10.1016/j.energy.2014.02.109).
- IEA (2017a). *CO2 Emissions from Fuel Combustion 2017 - Highlights*. en. Tech. rep.
- (2017b). *Renewables Information: Overview*. Tech. rep. International Energy Agency.
- IEA and IRENA (2017). *Perspectives for the Energy Transition*. Tech. rep. URL: <https://www.iea.org/publications/insights/insightpublications/PerspectivesfortheEnergyTransition.pdf> (visited on 03/27/2019).
- Imbrie, John et al. (1992). "On the structure and origin of major glaciation cycles 1. Linear responses to Milankovitch forcing". In: *Paleoceanography* 7.6, pp. 701–738. DOI: [10.1029/92PA02253](https://doi.org/10.1029/92PA02253).

- IPCC (2013). *Climate Change 2013: The Physical Science Basis. Contribution of Working Group I to the Fifth Assessment Report of the Intergovernmental Panel on Climate Change* [Stocker, T.F., D. Qin, G.-K. Plattner, M. Tignor, S.K. Allen, J. Boschung, A. Nauels, Y. Xia, V. Bex and P.M. Midgley (eds.)] Cambridge, United Kingdom and New York, NY, USA: Cambridge University Press. URL: <https://www.ipcc.ch/report/ar5/wg1/> (visited on 03/27/2019).
- (2014). “Energy Systems”. In: *Climate Change 2014: Mitigation of Climate Change. Contribution of Working Group III to the Fifth Assessment Report of the Intergovernmental Panel on Climate Change*. Cambridge, United Kingdom and New York, NY, USA: Cambridge University Press. URL: https://www.ipcc.ch/site/assets/uploads/2018/02/ipcc_wg3_ar5_chapter7.pdf (visited on 03/27/2019).
- (2018). “Technical Summary”. In: *Global warming of 1.5 degree C. An IPCC Special Report on the impacts of global warming of 1.5 degree C above pre-industrial levels and related global greenhouse gas emission pathways, in the context of strengthening the global response to the threat of climate change, sustainable development, and efforts to eradicate poverty* [V. Masson-Delmotte, P. Zhai, H. O. Pörtner, D. Roberts, J. Skea, P.R. Shukla, A. Pirani, W. Moufouma-Okia, C. Péan, R. Pidcock, S. Connors, J. B. R. Matthews, Y. Chen, X. Zhou, M. I. Gomis, E. Lonnoy, T. Maycock, M. Tignor, T. Waterfield (eds.)] In Press. URL: <https://www.ipcc.ch/sr15/> (visited on 03/27/2019).
- Jacob, Daniela et al. (2014). “EURO-CORDEX: new high-resolution climate change projections for European impact research”. In: *Regional Environmental Change* 14.2, pp. 563–578. DOI: [10.1007/s10113-013-0499-2](https://doi.org/10.1007/s10113-013-0499-2).
- James, Rachel et al. (2017). “Characterizing half-a-degree difference: a review of methods for identifying regional climate responses to global warming targets: Characterizing half-a-degree difference”. In: *Wiley Interdisciplinary Reviews: Climate Change* 8.2, e457. DOI: [10.1002/wcc.457](https://doi.org/10.1002/wcc.457).
- Jerez, S et al. (2019). “Future changes, or lack thereof, in the temporal variability of the combined wind-plus-solar power production in Europe”. In: *Renewable Energy* 139, pp. 251–260. DOI: [10.1016/j.renene.2019.02.060](https://doi.org/10.1016/j.renene.2019.02.060).
- Jerez, Sonia et al. (2015). “The impact of climate change on photovoltaic power generation in Europe”. In: *Nature Communications* 6, p. 10014. DOI: [10.1038/ncomms10014](https://doi.org/10.1038/ncomms10014).
- Karnauskas, Kristopher B., Julie K. Lundquist, and Lei Zhang (2018). “Southward shift of the global wind energy resource under high carbon dioxide emissions”. In: *Nature Geoscience* 11.1, pp. 38–43. DOI: [10.1038/s41561-017-0029-9](https://doi.org/10.1038/s41561-017-0029-9).
- Keenlyside, Noel S. et al. (2015). “North Atlantic multi-decadal variability-mechanisms and predictability”. In: *Climate Change: Multidecadal and Beyond*, p. 141. URL: [http://books.google.com/books?hl=en&lr=&id=1wC3CgAAQBAJ&oi=fnd&pg=PA141&dq=%221964%3B+Deser+and+Blackmon,+%22+%22this+book+and+references+therein\).+The%22+%22in+observed+global+mean%22+%221.+0bserved+AMV+\(a\)+index+and+\(b\)+pattern,+computed+by+regressing+the+index+on+to+SST+in+North%22+%22&ots=emoWQ9R4Gq&sig=rYFj4fnIkBi9AIIKqF0wddnSRc](http://books.google.com/books?hl=en&lr=&id=1wC3CgAAQBAJ&oi=fnd&pg=PA141&dq=%221964%3B+Deser+and+Blackmon,+%22+%22this+book+and+references+therein).+The%22+%22in+observed+global+mean%22+%221.+0bserved+AMV+(a)+index+and+(b)+pattern,+computed+by+regressing+the+index+on+to+SST+in+North%22+%22&ots=emoWQ9R4Gq&sig=rYFj4fnIkBi9AIIKqF0wddnSRc) (visited on 04/26/2017).
- Kittner, Noah, Felix Lill, and Daniel M. Kammen (2017). “Energy storage deployment and innovation for the clean energy transition”. In: *Nature Energy* 2, p. 17125. DOI: [10.1038/nenergy.2017.125](https://doi.org/10.1038/nenergy.2017.125).
- Konadu, Daniel Dennis et al. (2017). “UK water-energy nexus under climate change: Key issues and priorities”. In: URL: <https://www-csd.eng.cam.ac.uk/news/wholesem-report-uk-water-energy-report>.

- Kondziella, Hendrik and Thomas Bruckner (2016). "Flexibility requirements of renewable energy based electricity systems – a review of research results and methodologies". In: *Renewable and Sustainable Energy Reviews* 53, pp. 10–22. DOI: [10.1016/j.rser.2015.07.199](https://doi.org/10.1016/j.rser.2015.07.199).
- Kozarcenin, S, H Liu, and G B Andresen (2018). "Climate change impacts on large-scale electricity system design decisions for the 21st Century". en. In: *arXiv preprint, arXiv:1805.01364v1*, p. 16. URL: <https://arxiv.org/abs/1805.01364> (visited on 01/13/2019).
- Luo, Xing et al. (2015). "Overview of current development in electrical energy storage technologies and the application potential in power system operation". In: *Applied Energy* 137, pp. 511–536. DOI: [10.1016/j.apenergy.2014.09.081](https://doi.org/10.1016/j.apenergy.2014.09.081).
- Mann, Michael E. and Jonathan M. Lees (1996). "Robust estimation of background noise and signal detection in climatic time series". In: *Climatic Change* 33.3, pp. 409–445. DOI: [10.1007/BF00142586](https://doi.org/10.1007/BF00142586).
- Marzeion, Ben and Anders Levermann (2014). "Loss of cultural world heritage and currently inhabited places to sea-level rise". In: *Environmental Research Letters* 9.3, p. 034001. DOI: [10.1088/1748-9326/9/3/034001](https://doi.org/10.1088/1748-9326/9/3/034001).
- Mecking, Jennifer V., Noel S. Keenlyside, and Richard J. Greatbatch (2015). "Multiple timescales of stochastically forced North Atlantic Ocean variability: A model study". In: *Ocean Dynamics* 65.9-10, pp. 1367–1381. DOI: [10.1007/s10236-015-0868-0](https://doi.org/10.1007/s10236-015-0868-0).
- Mengel, M. and A. Levermann (2014). "Ice plug prevents irreversible discharge from East Antarctica". en. In: *Nature Climate Change* 4.6, pp. 451–455. DOI: [10.1038/nclimate2226](https://doi.org/10.1038/nclimate2226).
- Mengel, Matthias et al. (2018). "Committed sea-level rise under the Paris Agreement and the legacy of delayed mitigation action". In: *Nature Communications* 9.1. DOI: [10.1038/s41467-018-02985-8](https://doi.org/10.1038/s41467-018-02985-8).
- Messner, Dirk et al. (2010). "The budget approach: A framework for a global transformation toward a low-carbon economy". In: *Journal of Renewable and Sustainable Energy* 2.3, p. 031003. DOI: [10.1063/1.3318695](https://doi.org/10.1063/1.3318695).
- Millar, Richard J. et al. (2017). "Emission budgets and pathways consistent with limiting warming to 1.5 degree C". In: *Nature Geoscience* 10.10, pp. 741–747. DOI: [10.1038/ngeo3031](https://doi.org/10.1038/ngeo3031).
- Märker, Carolin, Sandra Venghaus, and Jürgen-Friedrich Hake (2018). "Integrated governance for the food–energy–water nexus – The scope of action for institutional change". In: *Renewable and Sustainable Energy Reviews* 97, pp. 290–300. DOI: [10.1016/j.rser.2018.08.020](https://doi.org/10.1016/j.rser.2018.08.020).
- Müller, Johannes et al. (2019). "CMIP-5 models project photovoltaics are a no-regrets investment in Europe irrespective of climate change". In: *Energy* 171, pp. 135–148. DOI: [10.1016/j.energy.2018.12.139](https://doi.org/10.1016/j.energy.2018.12.139).
- Niet, T. et al. (2018). "Valuing infrastructure investments to reduce curtailment". In: *Energy Strategy Reviews* 22, pp. 196–206. DOI: [10.1016/j.esr.2018.08.010](https://doi.org/10.1016/j.esr.2018.08.010).
- Omrani, N.-E. et al. (2016). "Troposphere–stratosphere response to large-scale North Atlantic Ocean variability in an atmosphere/ocean coupled model". In: *Climate Dynamics* 46.5-6, pp. 1397–1415. DOI: [10.1007/s00382-015-2654-6](https://doi.org/10.1007/s00382-015-2654-6).
- Patt, Anthony, Stefan Pfenninger, and Johan Lilliestam (2013). "Vulnerability of solar energy infrastructure and output to climate change". In: *Climatic Change* 121.1, pp. 93–102. DOI: [10.1007/s10584-013-0887-0](https://doi.org/10.1007/s10584-013-0887-0).
- Pehl, Michaja et al. (2017). "Understanding future emissions from low-carbon power systems by integration of life-cycle assessment and integrated energy modelling". In: *Nature Energy* 2.12, pp. 939–945. DOI: [10.1038/s41560-017-0032-9](https://doi.org/10.1038/s41560-017-0032-9).

- Peter, Jakob (2019). "How Does Climate Change Affect Optimal Allocation of Variable Renewable Energy?" en. In: *EWI Working Paper* 03.19, p. 38. URL: https://www.ewi.uni-koeln.de/cms/wp-content/uploads/2019/02/EWI_WP_19-03_How_Does_Climate_Change_Affect_Optimal_Allocation_of_VRE.pdf (visited on 01/18/2019).
- Pfenninger, Stefan et al. (2014). "Potential for concentrating solar power to provide baseload and dispatchable power". In: *Nature Climate Change* 4.8, pp. 689–692. DOI: [10.1038/nclimate2276](https://doi.org/10.1038/nclimate2276).
- Pleißmann, Guido et al. (2014). "Global Energy Storage Demand for a 100% Renewable Electricity Supply". In: *Energy Procedia* 46, pp. 22–31. DOI: [10.1016/j.egypro.2014.01.154](https://doi.org/10.1016/j.egypro.2014.01.154).
- Rahmstorf, Stefan et al. (2015). "Exceptional twentieth-century slowdown in Atlantic Ocean overturning circulation". In: *Nature Climate Change* 5.5, pp. 475–480. DOI: [10.1038/nclimate2554](https://doi.org/10.1038/nclimate2554).
- Reuß, M. et al. (2017). "Seasonal storage and alternative carriers: A flexible hydrogen supply chain model". In: *Applied Energy* 200, pp. 290–302. DOI: [10.1016/j.apenergy.2017.05.050](https://doi.org/10.1016/j.apenergy.2017.05.050).
- Reyers, Mark, Julia Moemken, and Joaquim G. Pinto (2016). "Future changes of wind energy potentials over Europe in a large CMIP5 multi-model ensemble". In: *International Journal of Climatology* 36.2, pp. 783–796. DOI: [10.1002/joc.4382](https://doi.org/10.1002/joc.4382).
- Reyers, Mark, Joaquim G. Pinto, and Julia Moemken (2015). "Statistical-dynamical downscaling for wind energy potentials: evaluation and applications to decadal hindcasts and climate change projections". en. In: *International Journal of Climatology* 35.2, pp. 229–244. ISSN: 08998418. DOI: [10.1002/joc.3975](https://doi.org/10.1002/joc.3975). URL: <http://doi.wiley.com/10.1002/joc.3975> (visited on 07/13/2016).
- Riahi, Keywan et al. (2011). "RCP 8.5—A scenario of comparatively high greenhouse gas emissions". In: *Climatic Change* 109.1-2, pp. 33–57. DOI: [10.1007/s10584-011-0149-y](https://doi.org/10.1007/s10584-011-0149-y).
- Roberts, T., A. Hope, and A. Skelton (2017). "Why on earth did I buy that? A study of regretted appliance purchases". In: *Philosophical Transactions of the Royal Society A: Mathematical, Physical and Engineering Sciences* 375.2095, p. 20160373. DOI: [10.1098/rsta.2016.0373](https://doi.org/10.1098/rsta.2016.0373).
- Rockstroem, Johan et al. (2017). "A roadmap for rapid decarbonization". In: *Science* 355.6331, p. 1269. DOI: [10.1126/science.aah3443](https://doi.org/10.1126/science.aah3443).
- Rodriguez, A. Rolando (2014). "Weather-driven power transmission in a highly renewable European electricity network". PhD thesis. Aarhus University.
- Rodriguez, Rolando A., Sarah Becker, and Martin Greiner (2015). "Cost-optimal design of a simplified, highly renewable pan-European electricity system". In: *Energy* 83, pp. 658–668. DOI: [10.1016/j.energy.2015.02.066](https://doi.org/10.1016/j.energy.2015.02.066).
- Rodriguez, Rolando A. et al. (2014). "Transmission needs across a fully renewable European power system". In: *Renewable Energy* 63, pp. 467–476. DOI: [10.1016/j.renene.2013.10.005](https://doi.org/10.1016/j.renene.2013.10.005).
- Rogelj, Joeri et al. (2015). "Energy system transformations for limiting end-of-century warming to below 1.5 degree C". In: *Nature Climate Change* 5.6, pp. 519–527. DOI: [10.1038/nclimate2572](https://doi.org/10.1038/nclimate2572).
- Rogelj, Joeri et al. (2016). "Paris Agreement climate proposals need a boost to keep warming well below 2 degree C". In: *Nature* 534.7609, pp. 631–639. DOI: [10.1038/nature18307](https://doi.org/10.1038/nature18307).
- Santos-Alamillos, Francisco J et al. (2017). "Exploring the meteorological potential for planning a high performance European electricity super-grid: optimal power

- capacity distribution among countries". In: *Environmental Research Letters* 12.11, p. 114030.
- Schellnhuber, Hans Joachim, Stefan Rahmstorf, and Ricarda Winkelmann (2016). "Why the right climate target was agreed in Paris". In: *Nature Climate Change* 6. DOI: [10.1038/nclimate3013](https://doi.org/10.1038/nclimate3013).
- Schlachtberger, D.P. et al. (2016). "Backup flexibility classes in emerging large-scale renewable electricity systems". In: *Energy Conversion and Management* 125, pp. 336–346. DOI: [10.1016/j.enconman.2016.04.020](https://doi.org/10.1016/j.enconman.2016.04.020).
- Schlachtberger, D.P. et al. (2017). "The benefits of cooperation in a highly renewable European electricity network". In: *Energy* 134, pp. 469–481. DOI: [10.1016/j.energy.2017.06.004](https://doi.org/10.1016/j.energy.2017.06.004).
- Schleussner, Carl-Friedrich et al. (2016a). "Differential climate impacts for policy-relevant limits to global warming: the case of 1.5 degree C and 2 degree C". In: *Earth System Dynamics* 7.2, pp. 327–351. DOI: [10.5194/esd-7-327-2016](https://doi.org/10.5194/esd-7-327-2016).
- Schleussner, Carl-Friedrich et al. (2016b). "Science and policy characteristics of the Paris Agreement temperature goal". In: *Nature Climate Change* 6.9, pp. 827–835. DOI: [10.1038/nclimate3096](https://doi.org/10.1038/nclimate3096).
- Schlott, Markus et al. (2018). "The impact of climate change on a cost-optimal highly renewable European electricity network". In: *Applied Energy* 230, pp. 1645–1659. DOI: [10.1016/j.apenergy.2018.09.084](https://doi.org/10.1016/j.apenergy.2018.09.084).
- Snell, Carolyn Jane, Mark Alistair Bevan, and Ross Gillard (2018). "Policy Pathways to Justice in Energy Efficiency". In: URL: <http://www.ukerc.ac.uk/asset/74213192%2D7D80%2D4FFF%2DAF6ABBE492D56AB7/>.
- Staudt, Philipp et al. (2018). "Predicting Redispatch in the German Electricity Market using Information Systems based on Machine Learning". In: *The Ninth International Conference on Information Systems, San Francisco*, p. 17. URL: <https://aisel.aisnet.org/icis2018/green/Presentations/7/> (visited on 03/27/2019).
- Storch, H. v and Francis W. Zwiers (1999). *Statistical analysis in climate research*. Cambridge ; New York: Cambridge University Press. ISBN: 978-0-521-45071-3.
- Taylor, Karl E., Ronald J. Stouffer, and Gerald A. Meehl (2011). "An Overview of CMIP5 and the Experiment Design". In: *Bulletin of the American Meteorological Society*, pp. 485–498. DOI: [10.1175/BAMS-D-11-00094.1](https://doi.org/10.1175/BAMS-D-11-00094.1).
- Tobin, Isabelle et al. (2016). "Climate change impacts on the power generation potential of a European mid-century wind farms scenario". In: *Environmental Research Letters* 11.3, p. 034013. DOI: [10.1088/1748-9326/11/3/034013](https://doi.org/10.1088/1748-9326/11/3/034013).
- Tobin, Isabelle et al. (2018). "Vulnerabilities and resilience of European power generation to 1.5 degree C, 2 degree C and 3 degree C warming". In: *Environmental Research Letters*. DOI: [10.1088/1748-9326/aab211](https://doi.org/10.1088/1748-9326/aab211).
- Toledo, Olga Moraes, Dely Oliveira Filho, and Antônia Sônia Alves Cardoso Diniz (2010). "Distributed photovoltaic generation and energy storage systems: A review". In: *Renewable and Sustainable Energy Reviews* 14.1, pp. 506–511. DOI: [10.1016/j.rser.2009.08.007](https://doi.org/10.1016/j.rser.2009.08.007).
- UNFCCC (2015). "Adoption of the Paris Agreement". In: FCCC/CP/2015/10/Add.1. URL: <https://unfccc.int/resource/docs/2015/cop21/eng/l09r01.pdf> (visited on 03/27/2019).
- UNFCCC, COP 1 (1992). *United Nations framework convention on climate change*. United Nations New York. URL: <https://unfccc.int/resource/docs/convkp/conveng.pdf> (visited on 03/27/2019).
- Vautard, Robert et al. (2010). "Northern Hemisphere atmospheric stilling partly attributed to an increase in surface roughness". In: *Nature Geoscience* 3.11, pp. 756–761. DOI: [10.1038/ngeo979](https://doi.org/10.1038/ngeo979).

- Vuuren, Detlef P. van et al. (2011). "The representative concentration pathways: an overview". In: *Climatic Change* 109.1-2, pp. 5–31. DOI: [10.1007/s10584-011-0148-z](https://doi.org/10.1007/s10584-011-0148-z).
- Weaver, Andrew J. et al. (2012). "Stability of the Atlantic meridional overturning circulation: A model intercomparison". In: *Geophysical Research Letters* 39.20. DOI: [10.1029/2012GL053763](https://doi.org/10.1029/2012GL053763).
- Weber, Juliane et al. (2018). "Impact of climate change on backup energy and storage needs in wind-dominated power systems in Europe". In: *PLOS ONE* 13.8. Ed. by Vanesa Magar, e0201457. ISSN: 1932-6203. DOI: [10.1371/journal.pone.0201457](https://doi.org/10.1371/journal.pone.0201457).
- Welder, Lara et al. (2018). "Spatio-temporal optimization of a future energy system for power-to-hydrogen applications in Germany". In: *Energy*. DOI: [10.1016/j.energy.2018.05.059](https://doi.org/10.1016/j.energy.2018.05.059).
- Wergen, G., A. Hense, and J. Krug (2014). "Record occurrence and record values in daily and monthly temperatures". In: *Climate Dynamics* 42.5-6, pp. 1275–1289. DOI: [10.1007/s00382-013-1693-0](https://doi.org/10.1007/s00382-013-1693-0).
- Wergen, G. and J. Krug (2010). "Record-breaking temperatures reveal a warming climate". In: *EPL (Europhysics Letters)* 92.3, p. 30008. DOI: [10.1209/0295-5075/92/30008](https://doi.org/10.1209/0295-5075/92/30008).
- Williams, Paul D. et al. (2017). "A Census of Atmospheric Variability From Seconds to Decades: A Census of Atmospheric Variability". In: *Geophysical Research Letters* 44.21, pp. 11,201–11,211. DOI: [10.1002/2017GL075483](https://doi.org/10.1002/2017GL075483).
- Winkelmann, R. et al. (2015). "Combustion of available fossil fuel resources sufficient to eliminate the Antarctic Ice Sheet". In: *Science Advances* 1.8, e1500589–e1500589. DOI: [10.1126/sciadv.1500589](https://doi.org/10.1126/sciadv.1500589).
- Wohland, Jan, Dirk Witthaut, and Carl-Friedrich Schleussner (2018). "Negative Emission Potential of Direct Air Capture Powered by Renewable Excess Electricity in Europe". In: *Earth's Future* 6.10, pp. 1380–1384. DOI: [10.1029/2018EF000954](https://doi.org/10.1029/2018EF000954).
- Wohland, Jan et al. (2017). "More homogeneous wind conditions under strong climate change decrease the potential for inter-state balancing of electricity in Europe". In: *Earth System Dynamics* 8.4, pp. 1047–1060. DOI: [10.5194/esd-8-1047-2017](https://doi.org/10.5194/esd-8-1047-2017).
- Wohland, Jan et al. (2018). "Natural wind variability triggered drop in German re-dispatch volume and costs from 2015 to 2016". In: *PLOS ONE* 13.1. Ed. by Bruno Merk, e0190707. DOI: [10.1371/journal.pone.0190707](https://doi.org/10.1371/journal.pone.0190707).
- Wohland, Jan et al. (2019a). "Inconsistent wind speed trends in current 20th century reanalyses". In: *Journal of Geophysical Research: Atmospheres* 124.4, pp. 1931–1940. DOI: [10.1029/2018JD030083](https://doi.org/10.1029/2018JD030083).
- Wohland, Jan et al. (2019b). "Significant multi-decadal variability of German wind energy yields". In: *Wind Energy Science Discussions (in review)*. DOI: <https://doi.org/10.5194/wes-2019-8>.
- Wunsch, Carl (1999). "The Interpretation of Short Climate Records, with Comments on the North Atlantic and Southern Oscillations". In: *Bulletin of the American Meteorological Society* 80.2, pp. 245–255. DOI: [10.1175/1520-0477\(1999\)080<0245:TIOSCR>2.0.CO;2](https://doi.org/10.1175/1520-0477(1999)080<0245:TIOSCR>2.0.CO;2).
- Zickfeld, Kirsten et al. (2009). "Setting cumulative emissions targets to reduce the risk of dangerous climate change". In: *Proceedings of the National Academy of Sciences* 38, pp. 16129–16134. DOI: [10.1073/pnas.0805800106](https://doi.org/10.1073/pnas.0805800106).

Appendix A

Appendix

A.1 Own contribution

I was by far the dominant contributor to all five publications that form the basis of this dissertation. This is documented in the author contributions section of papers #1 - #4 which have been copied to the list below for simpler accessibility. Publication #5 does not include an author contribution section due to the journal policy such that the contributions are detailed below.

- #1 "JaW performed the simulations, analyzed the data, produced all figures and wrote most of the manuscript" (Wohland et al., 2017).
- #2 I was in charge of or contributed to "Conceptualization", "Formal analysis", "Investigation", "Methodology", "Software", "Visualization", "Writing – original draft" and "Writing – review & editing" (Wohland et al., 2018).
- #3 I was in charge of or contributed to "Conceptualization", "Funding Acquisition", "Methodology", "Formal Analysis", "Investigation", "Writing – Original Draft" and "Writing - review & editing" (Wohland, Witthaut, and Schleussner, 2018).
- #4 "JW initiated the collaboration, developed the methodology, analyzed the data, produced all figures and wrote most of the manuscript (...) All authors contributed ideas, gave feedback and helped to improve the manuscript." (Wohland et al., 2019b)
- #5 : JW developed the model, performed all simulations, produced all figures, wrote the manuscript draft, revised and edited the draft taking the co-authors feedback into account. (Wohland, Witthaut, and Schleussner, 2018)

A.2 Erklärung (gemäß §4 Abs 1 Punkt 9 der Promotionsordnung)

Ich versichere,

- dass ich die von mir vorgelegte Dissertation selbständig angefertigt, die benutzten Quellen und Hilfsmittel vollständig angegeben und die Stellen der Arbeit – einschließlich Tabellen, Karten und Abbildungen –, die anderen Werken im Wortlaut oder dem Sinn nach entnommen sind, in jedem Einzelfall als Entlehnung kenntlich gemacht habe;
- dass diese Dissertation noch keiner anderen Fakultät oder Universität zur Prüfung vorgelegen hat;
- dass sie – abgesehen von den fünf in Kapitel 1.5 angegebenen Teilpublikationen – noch nicht veröffentlicht worden ist, sowie, dass ich eine solche Veröffentlichung vor Abschluss des Promotionsverfahrens nicht vornehmen werde.

Die Bestimmungen der Promotionsordnung sind mir bekannt.

Die von mir vorgelegte Dissertation ist von JProf. Dr. Dirk WITTHAUT betreut worden.

Unterschrift:

Datum:
